Dynamic uplift, recycling, and climate control on the petrology of passive-margin sand (Angola)

Eduardo Garzanti[1*], Pedro Dinis[2], Pieter Vermeesch[3], Sergio Andò[1], Annette Hahn[4], João Huvi[5], Mara Limonta[1], Marta Padoan[1], Alberto Resentini[1], Martin Rittner[3], Giovanni Vezzoli[1]

[1] *Laboratory for Provenance Studies, Department of Earth and Environmental Sciences, University of Milano-Bicocca, 20126 Milano, Italy*

[2] *MARE - Marine and Environmental Sciences Centre, Department of Earth Sciences, University of Coimbra, Portugal*

[3] *London Geochronology Centre, Department of Earth Sciences, University College London, London WC1E 6BT, UK*

[4] *MARUM Center for Marine Environmental Sciences, University of Bremen, Bremen, Germany*

[5] *Marine and Environmental Sciences Centre, University Katyavala Bwila, Benguela, Angola*

* Corresponding author. E-mail: eduardo.garzanti@unimib.it . Tel.: +39-02-64482088

E-mail addresses: eduardo.garzanti@unimib.it (E. Garzanti), pdinis@dct.uc.pt (P. Dinis), p.vermeesch@ucl.ac.uk (P.Vermeesch), sergio.ando@unimib.it (S. Andò), ahahn@marum.de (A.Hahn), hjoaobaptistahuvi@yahoo.com.br (J.Huvi), mara.limonta@unimib.it (M.Limonta), marta.padoan@unimib.it (M.Padoan), alberto.resentini@unimib.it (A. Resentini), m.rittner@ucl.ac.uk (M. Rittner), giovanni.vezzoli@unimib.it (G. Vezzoli)

ABSTRACT

The subequatorial Angolan continental margin offers excellent conditions to test textbook theories on the composition of passive-margin sediments generated in different climatic and tectonic regimes. We use here comprehensive petrographic, heavy-mineral, geochemical and zircon-geochronology datasets on modern fluvial, beach, shelfal, and deep-marine sands and muds collected from hyperarid northern Namibia to hyperhumid Congo to investigate and assess: a) how faithfully sand mineralogy reflects the lithological and time structures of source rocks in a tectonically active rifted margin; b) in what climatic and geomorphological conditions the mark of chemical weathering becomes strong and next overwhelming; and, c) to what extent the effect of weathering can be isolated from quartz dilution by recycling of older siliciclastic strata and other physical controls including hydraulic sorting and mechanical wear. A new refined classification of feldspatho-quartzose and quartzose sands and sandstones is proposed.

First-cycle quartzo-feldspathic to feldspar-rich feldspatho-quartzose sand eroded from mid-crustal granitoid gneisses of the Angola Block exposed in the dynamically uplifted Bié-Huila dome is deposited in arid southern Angola, whereas quartz-rich feldspatho-quartzose to quartzose sand characterizes the lower-relief, less deeply dissected, and more intensely weathered rifted margin of humid northern Angola. Pure quartzose, largely recycled sand is generated in the vast, low-lying hyperhumid continental interiors drained by the Congo River. The progressive relative increase of durable minerals toward the Equator results from three distinct processes acting in accord: active tectonic uplift in the arid south, and progressively stronger weathering coupled with more extensive recycling in the humid north. The quartz/feldspar ratio increases and the plagioclase/feldspar ratio decreases rapidly in first-cycle sand generated farther inland in the Catumbela catchment, reflecting stronger weathering in wet interior highlands. Discriminating weathering from recycling control is difficult in northern Angola. Although textural features including deep etch pits even on relatively resistant minerals such as quartz and microcline or rounded outline and abraded overgrowths provide valuable independent information, recycling remains as a most elusive problem in provenance analysis of terrigenous sediments.

Keywords: Provenance analysis; Classification of feldspatho-quartzose sands; Raman-counting of deep-water silt; U-Pb zircon geochronology; Weathering of detrital minerals; Quartzarenite problem.

"*The present is the key to the past*"
Archibald Geikie, The Founders of Geology

"*From this gateway Moment a long eternal lane stretches backward: behind us lies an eternity. Must not what ever can happen, already have happened, been done, passed by before? And if everything has already been here before, what do you think of this moment, dwarf?* "
Friedrich Nietzsche, Thus Spoke Zarathustra, On the Vision and the Riddle.

1. Introduction

Paleotectonic and paleoclimatic interpretations based on the composition of ancient sandstone suites often rely on assumptions seldom verified in a sufficient number of modern case studies (Basu, 1985). The effect of chemical weathering in the weathering-prone climatic conditions found in equatorial and subequatorial settings has been investigated extensively in South America (Franzinelli and Potter, 1983; Johnsson et al., 1988, 1991; Potter, 1994), but less so in Africa (e.g. Dupré et al., 1996; Schneider et al., 2016), which is an excellent location in which to test classic textbook theories on passive-margin sediments generated at diverse latitudes and in diverse climatic and tectonic regimes.

Sand deposited along passive margins is generally viewed as characterized by feldspatho-quartzose composition, with quartz/feldspar ratio controlled on the one hand by tectonic activity favoring rapid erosion of exhumed basement rocks and preservation of less stable detrital components, and on the other hand by chemical weathering that determines instead their progressive alteration and final breakdown (Folk, 1980; Dickinson, 1985). Passive margins can be distinguished into volcanic (magma-rich) and magma-poor (Franke, 2013). Sediment sources in the latter are ancient crystalline basements exposed on rifted-margin shoulders and their cover strata including pre-rift, syn-rift and post-rift siliciclastic and carbonate rocks. Volcanic detritus derived from continental flood basalts and associated felsic products may be common and locally dominant in the former (Garzanti et al., 2014a).

Coastal Angola, located at subequatorial latitudes, is characterized by hyperarid climate in the south passing progressively northward to semiarid, humid, and eventually hyperhumid in the Congo (Fig.

1). The geology of the Angolan rifted margin is relatively simple and homogeneous, with the Angola Block consisting of largely mid-Paleoproterozoic granitoid basement in the southern and central parts and the metamorphic West Congo Belt of Neoproterozoic age in the north. After Early Cretaceous rifting leading to the opening of the southern Atlantic Ocean, the region has undergone successive and also recent stages of dynamic uplift (Giresse et al., 1984; Hudec and Jackson, 2004; Al-Hajri et al., 2009; Guiraud et al., 2010; MacGregor, 2013;White, 2016; Green and Machado, 2017). Coastal Angola represents therefore an exceptionally suitable natural laboratory in which to investigate how the detrital signature of daughter sand may respond to the lithological and time structures (i.e., the diverse age patterns of source areas obtained by different geochronological methods) of parent rocks, and to assess to what extent sand mineralogy can be modified during the sedimentary cycle by chemical weathering as well as by diverse physical factors (i.e., mechanical breakdown, hydraulic sorting, and recycling).

This study illustrates an integrated petrographic, mineralogical, geochemical and geochronological dataset on modern sands collected along the entire Angolan continental margin, which complements data obtained with the same methods and following the same criteria during previous studies on sediment generation in southwestern Africa (Vermeesch et al., 2010; Garzanti et al., 2012a, 2014a, 2014b, 2014c, 2015, 2017; Dinis et al., 2016, 2017), to which the reader is referred as aspects specific to adjacent regions are concerned.

2. The Angolan rifted margin

2.1. Basement rocks

The oldest rocks of subequatorial Africa belong to the Archean to Paleoproterozoic Kalahari and Congo cratons, welded together by a series of orogenies including the major Namaqua arc–accretion and continent–collision event between ~ 1.1 and 1.05 Ga (De Waele et al., 2008; Jacobs et al., 2008). West Gondwana was finally amalgamated during the Neoproterozoic to Cambrian

Damara ("Pan-African") orogeny (Gray et al., 2008; Heilbron et al., 2008; Vaughan and Pankhurst, 2008; Frimmel et al., 2011).

In western Africa, the Congo craton is represented by the Angola Block, the core of which consists of felsic Eburnean (~ 2 Ga) plutonic and metamorphic rocks (Fig. 1D; De Carvalho et al., 2000; McCourt et al., 2013). Along its northeastern limit, Neoarchean granites, gneisses and migmatites occur together with gabbros, norites and charnockites (Liberian-Limpopo massifs; Delhal et al., 1976; De Carvalho et al., 2000). In southern Angola to northernmost Namibia, where it is represented by the Epupa metamorphic unit, the Angola Block is intruded by one of the largest anorthosite bodies on Earth, dated at 1.37-1.38 Ga and including norite and gabbro (Mayer et al., 2004; Drüppel et al., 2007).

The West Congo and Kaoko belts were formed during the Neoproterozoic-Cambrian orogeny and both display progressively increasing metamorphic grade from only mildly deformed Neoproterozoic foreland units in the east to medium-grade or even high-grade rocks in the west. The West Congo Belt, stretching from southwestern Gabon to northwestern Angola, comprises Paleoproterozoic basement gneisses intruded by ~ 2 Ga granites and thrust NE-ward onto a Neoproterozoic succession beginning with a thick volcano-sedimentary unit including a bimodal magmatic suite dated between 1.0 and 0.9 Ga (Tack et al., 2001). The overlying West Congolian Group, only gently folded and unmetamorphosed in the east, includes siliciclastic strata with intercalated pillow-basalts and diamictites, capped by a stromatolite-bearing carbonate platform followed in turn by siliciclastic syn-orogenic to post-orogenic sediments (Frimmel et al., 2006). The Kaoko Belt, located at the southwestern tip of the Congo craton and representing the transpressive northern arm of the Damara orogen, comprises the Epupa Paleoproterozoic basement and an arc terrane with high-grade metasediments and granitoids close to the coast (Goscombe et al., 2003; Goscombe and Gray, 2007).

2.2. Syn-rift to post-rift sedimentary successions

Rifting and initial sea-floor spreading in the South Atlantic progressed northward during the Early Cretaceous (Moulin et al., 2010). Tectonic evolution was controlled by oceanic fracture zones extending through continental crust commonly along Precambrian structures and locally leaking mantle-derived magmas (Mohriak and Rosendhal, 2003). The conjugate Brazilian and African rifted margins were thus segmented into transform, oblique and normal-rifted tracts separated by transverse fault zones (Guiraud et al., 2010). Along the Angolan coast, Precambrian basement is non-conformably overlain by a several km-thick Lower Cretaceous to Neogene succession accumulated in distinct depocenters (Lower Congo, Inner and Outer Cuanza, Benguela, and Namibe basins) and subdivided into syn-rift continental deposits followed by evaporites and post-rift marine sediments (Hudec and Jackson, 2002; Chaboureau et al., 2013).

The up to 5 km-thick pre-salt strata of Neocomian to Aptian age include feldspar-rich fluvio-lacustrine conglomerates, sandstones and shales, lacustrine carbonates, and interbedded lava flows and ash deposited during tectonic extension (Bate et al., 2001; Sabato-Ceraldi and Green, 2017). Salt deposits mostly consisting of massive halite were deposited at mid-Aptian times from north of the Walvis Ridge to Gabon. Some tens of m-thick onshore, evaporites reach up to 1.4 km offshore and overstep the underlying pre-salt wedge both landward and seaward, suggesting direct deposition onto oceanic crust formed close to sea-level (Marton et al., 2000). Halokynesis impacted greatly sedimentation at subsequent stages and determined the structural style of the Angolan passive margin (Fort et al., 2004). The post-salt succession is up to 5 km-thick. Fully marine conditions returned in the Albian, with deposition of platform carbonates passing to deep-water mudstones offshore. Siliciclastic sedimentation, mainly confined to the Benguela and Namibe basins in the Albian (Quesne et al., 2009; Gindre-Chanu et al., 2015), became dominant in the Upper Cretaceous and Cenozoic (Séranne and Anka, 2005). Prograding clastic wedges and repeated erosional gaps in the coastal plain and shelf document several phases of inner-margin uplift during the Neogene (Jackson et al., 2005). In the vast Kalahari basin, stretching ~ 2200 km in the hinterland from the Congo to South Africa, up to 450 m-thick largely fluvial sediments were deposited possibly since the Late Cretaceous, and a huge sand sea was formed by eolian reworking during drier periods of the Plio-Pleistocene to early Holocene (Haddon and McCarthy, 2005).

2.3. Syn-rift to post-rift volcanic rocks

Syn-rift volcanism reaching climax around 132 Ma is best represented by the Etendeka continental flood basalts and quartz latites of northern Namibia, situated landward of the Walvis Ridge (Renne et al., 1996; Ewart et al., 2004). The Angolan margin is instead mainly volcanic-poor (Séranne and Anka, 2005; Péron-Pinvidic et al., 2017), although Lower to Upper Cretaceous tholeiitic to alkaline bimodal volcanic products are found in several localities of the Namibe and Cuanza basins (Fig. 1D; Masse and Laurent, 2016). In the Namibe basin, tholeiitic basalts overlain by felsic stratoid flows and travertine rest unconformably on Precambrian basement or pre-rift Karoo sandstones, whereas basaltic flows overlying ammonite-bearing strata are dated as Santonian (84.6 ± 1.5 Ma; Alberti et al., 1992; Strganac et al. 2014; Gindre-Chanu et al., 2016). In the Sumbe area of central Angola, ~ 100 m-thick tholeiitic lavas dated at ~ 132 Ma and altered pyroclastic rocks directly overlie the Precambrian basement, which is intruded by tholeiitic dykes subparallel to the coast. Sodic alkaline and transitional products dated at ~ 91 Ma are intercalated with Upper Cretaceous marine strata (Marzoli et al., 1999). Volcanism took place at the landward extension of the Cuanza seamount chain built on oceanic crust, which acted as a sedimentary barrier between the Benguela and Cuanza basins (Hudec and Jackson, 2002). Reactivation of deep lithospheric faults during Early Cretaceous rifting was associated with kimberlite and carbonatite magmatism concentrated along the 50-90 km-wide Lucapa tectonic corridor extending to the NE of the Namibe basin (Comin-Chiaramonti et al., 2011; Castillo-Oliver et al., 2016).

2.4. Climatic gradients and weathering conditions

Angola is situated between ~ 17°30'S and ~ 6°S, roughly at the same distance from the Tropic of Capricorn and the Equator and thus right in the middle of the subequatorial belt. The coastal zone, stretching N/S for ~ 1450 km between the mouths of the Cunene and Congo rivers, experiences a latitudinal climatic gradient. Conditions change progressively from hot desert in coastal Namibia and southern Angola to hot semi-arid in the coastal Benguela region, and next to tropical savanna northward toward the humid Congo (Fig. 1C). The aridity of the southern region results from the influence of quasi-stationary anticyclonic conditions on most austral Africa coupled with the Benguela upwelling system responsible for low sea-surface temperatures and low-humidity southerly winds (Shannon and Nelson, 1996; Lancaster, 2002). The cold and nutrient-rich Benguela Current flows equatorward all along the Atlantic coast of southern Africa as the eastern branch of the subtropical gyre, until it converges with the warm and nutrient-poor southward-flowing Angola Current representing the eastern part of the Angola gyre (Lass and Mohrholz, 2008). Aridity decreases progressively north of the Angola-Benguela Front, located between 20°S and 14°S and moving northward in July-September and southward in January-March (Kostianoy and Lutjeharms, 1999; Hardman-Mountford et al., 2003). Along the coast, average annual precipitation varies from < 100 mm in the hyperarid south, where rainfall is rare and exceeded by water generated from condensation and fog (locally called "*cassimbo*"), to 400-600 mm north of Luanda. Rainfall increases more rapidly up to ~1500 mm inland, where climate becomes humid subtropical or temperate-highland tropical with dry winters at high elevation. The isohyets trend approximately E/W in the continental interior, where the latitudinal gradient is much stronger than along the coast (Fig. 1C).

Average annual temperatures vary little through much of coastal Angola, from 21-27ºC north of 10ºS to 20-24ºC in the south, and drop to ~ 15ºC only in the Moçamedes Desert and in the highlands, which reach 2619 m a.s.l. at Mount Moco in the headwaters of the Balombo River (Diniz, 2006). The warm rainy season, longer at lower latitudes and in the highlands, starts between September and November and lasts until March to May depending on the region, with rainfall peak in February to March. Weak southerly to south-westerly winds prevail all over the year in the coastal region, where north of Namibe eolian sand transport becomes negligible.

Different weathering conditions controlled by the two broadly perpendicular N/S and E/W climatic gradients, and consequently different intensities of pedogenic processes, are reflected by clay-mineral assemblages and chemical-weathering proxies in river muds (Dinis et al., 2017). Kaolinite, supplied in abundance to the coast by most major Angolan rivers, is largely generated in the wet hinterland, and particularly on ancient flat surfaces decreasing in elevation westward and separated by escarpments of variable relief. Expansive clays, instead, are mainly formed in Meso-Cenozoic basins located in dryer areas along the coast. As a consequence, the smectite/kaolinite ratio is ~ 1 in arid southern Angola, decreases rapidly in the semiarid Benguela region, and is very low in the more humid north with the exception of muds carried by the Longa, Cuanza, and Bengo rivers cutting across the Meso-Cenozoic Cuanza basin in their lower course.

2.5. River systems

Apart for the Congo (4,000,000 km^2, length 4700 km), the largest Angolan rivers draining into the Atlantic Ocean are the Cunene (~ 110,000 km^2, ~ 1050 km) and the Cuanza (~ 150,000 km^2, ~ 960 km). The Longa, Queve, Curoca, and Mebridege are ~ 300 km-long and drain ~ 20,000 km^2 each; the Catumbela and Coporolo are 200-250 km-long and drain ~ 15,000 km^2 (Fig. 1B). Of similar length are the Loge, Dande, Bengo, and Bero, which also drain more than 10,000 km^2 each, and another dozen ephemeral rivers draining between 2000 and 7000 km^2. Three major rivers are sourced in the very same area between the cities of Huambo and Katchiungo at ~ 1800 m a.s.l. on the dynamically uplifted Bié-Huila dome: the Queve draining northward, the Cunene draining southward, and the Cubango branch of the Okavango draining southeastwards across the Kalahari (Fig. 1). The Cuanza is instead sourced in the Kalahari and flows northwards around the Angola Block. These river courses may have formed soon after opening of the South Atlantic, although the modern configuration with radial drainage of the Biè-Huila dome was acquired much more recently in response to dynamic uplift, as documented by morphometric analysis (Pritchard et al., 2009; Anka et al. 2010). Few rivers have regular concave equilibrium profiles. Most display youthful, staircase profiles with long flat segments separated by very steep tracts, reflecting the stepped remnant plateaus typical of the African landscape (Diniz, 2006). Convex profiles indicative of retrogressive erosion characterize rivers draining the Kalahari plateau or coastal uplifts (Leturmy et al., 2003).

Sizeable dams or weirs were built on the Cunene (Matala 1954, Gove 1975, Calueque 1976, Ruacana 1980), Cuanza (Cambambe 1963, Capanda 2004), and Catumbela rivers (Lomaum 1965). Several were abandoned, damaged severely or destroyed during the civil war (1975-2002), and have been rehabilitated recenty. Others include the Mabubas Dam on the Dande and the Kiminha Dam on the Bengo. Based on sediment volumes stored in the Cambambe reservoir and measured in the late Eighties, the Cuanza solid load amounts to 620 ± 100 10^3 ton/a (43% mostly fine sand with some gravel, 44% coarse silt, 13% clay to medium silt; Holisticos, 2012). This corresponds to low sediment yields and erosion rates (4 ± 1 ton/km^2 a, < 0.002 mm/a).

2.6. Coastal geomorphology and marine processes

The Atlantic coast of Angola is wave-dominated and microtidal (maximum significant wave height ~ 1.75 m; mean tide amplitude ~ 1 m). A powerful southerly swell, originated by persistent stormy winds far away in the Southern Ocean between 40°S and 60°S, causes periodic high-energy wave events called "*calema*" and extensive northward sand transport all along the Atlantic shore of southern Africa. Scarcely affected by either local winds or the Benguela Current, the direction of littoral transport is controlled by the oblique incidence of the wave front to the coast, which determines the asymmetry of deltas and the formation of sand spits in proximity of coastal re-entrants were waves are refracted and sand accumulates offshore (Guilcher et al., 1974).

Shelf topography and width exert a major role on sediment transport. The southern Angola oblique-rifted to transform-rifted margin has a narrow coastal plain delimited offshore by a steep continental slope and inland by a high-elevation escarpment with relief up to 1.5 km (Feio, 1981; Lopes et al., 2016). The normal-rifted margin of northern Angola is much wider and has gentler continental slope and hinterland relief without a major escarpment. Such a marked topographic difference reflects both the tectonic structure inherited from Lower Cretaceous rifting and prominent recent uplift of the Bié-Huila dome in southwestern Angola (Moulin et al., 2005; Pritchard et al., 2009; Guiraud et al., 2010).

The continental shelf, 25-30 km-wide to the -150 m isobath offshore of the Cunene mouth, narrows rapidly north of the Baia dos Tigres spit to < 10 km along most of the coast from Tombua to Benguela. Shelf width is reduced to ~ 1 km at the head of submarine canyons offshore of the Curoca and Bero river mouths, which intercept littoral drifting sand thus terminating the ~ 1800 km-long Orange littoral cell (Garzanti et al., 2017), as well as between north of the Coporolo mouth and the Baia Farta spit. The shelf widens again to ≥ 20 km north of Benguela, and widens further north of Luanda to ~ 70 km south of the Congo river mouth.

3. Sampling and analytical methods

All along the coast of Angola, in June 2015 we have sampled 26 fluvial sand bars exposed at low-water level from all major rivers draining into the Atlantic Ocean, 43 beaches, and 2 dunes. Sediment samples collected offshore of the Congo, Tapado, Balombo, Coporolo and Cunene mouths as well as south of the Cuanza seamount chain and on the Walvis Ridge at water depths between -30 and -3000 m b.s.l. were retrieved from the MARUM repository in Bremen. Offshore samples were collected a few dm below seafloor during Meteor expeditions M6/6, M20/2, and M41/1 (Wefer et al, 1988; Schulz et al., 1992, 1998), or represent the upper meters of cores drilled during DSDP Leg 40 and ODP Leg 175 (Fig. 1A). Numerous other river, beach, and dune samples were collected in various years along the coast of Namibia, in the Cunene catchment and southern Moçamedes Desert, in central Angola, in the terminal tract of the Congo River, and in the Republic of Congo. This extensive set of 136 samples overall allowed us to monitor detrital signatures in response to changing lithology and age of source terranes along the Atlantic passive margin of southern Africa, as well as compositional trends controlled not only by latitudinal climatic zonation from hyperarid Namibia to hyperhumid Congo but also by the sharp inland rainfall gradient. Full information on sampling sites is provided in Appendix Table A1 and Google Earth™ file

Angolamargin.kmz. Main parameters characterizing river catchments are given in Appendix Table A2.

3.1. Petrography and heavy minerals

Petrographic composition of each sand sample was determined by counting 400 to 450 points in thin section by the Gazzi-Dickinson method (Ingersoll et al., 1984). Sands are classified by their main components exceeding 10%QFL (e.g., in a feldspatho-quartzose sand Q > F > 10%QFL > L; Garzanti, 2016). An adjective reflecting the dominant rock-fragment type may be added freely (e.g., plutoniclastic). Among feldspatho-quartzose sands, feldspar-rich (Q/F < 2; plagioclase-rich if plagioclase/K-feldspar > 2, K-feldspar-rich if K-feldspar/plagioclase > 2) and quartz-rich (Q/F > 4) compositions are here formally distinguished (Fig. 2A). Cross-hatched microcline and untwinned K-feldspar including perthite are called for simplicity microcline and orthoclase throughout the text. Metamorphic grains were classified by protolith composition and metamorphic rank; average rank for each sample was expressed by the Metamorphic Indices MI and MI*, ranging respectively from 0 (detritus from sedimentary and volcanic rocks) and 100 (detritus from very low-grade metamorphic rocks) to 500 (detritus from high-grade metamorphic rocks; Garzanti and Vezzoli 2003).

From the widest possible size-range obtained by wet sieving (mostly < 500 μm for clean beach and dune sands and 15-500 μm for positively skewed river sands), heavy minerals were separated by centrifuging in Na-polytungstate (2.90 g/cm^3) and recovered by partial freezing with liquid nitrogen; 200 to 250 transparent heavy minerals were point-counted at suitable regular spacing on grain mounts to obtain real volume percentages (Galehouse, 1971). On finer-grained offshore samples, heavy-mineral analyses were carried out by Raman point-counting (Andò et al., 2011) on the > 5 μm (silty clays) or >15 μm fraction (sandy silts and silty sands) obtained by wet sieving. The ZTR index, expressing the "chemical durability" of the suite (Garzanti, 2017), is the sum of zircon, tourmaline and rutile over total transparent heavy minerals (Hubert, 1962). The hornblende colour index (HCI) varies from 0 in detritus from greenschist-facies and lowermost amphibolite-facies rocks to 100 in detritus from granulite-facies rocks (Andò et al., 2014). Heavy-mineral concentration, calculated as the volume percentage of total (HMC) and transparent (tHMC) heavy minerals, ranges from extremely poor (HMC < 0.1), poor (0.5 ≤ HMC < 1) and moderately poor (1 ≤ HMC < 2), to rich (5 ≤ HMC < 10), very rich (10 ≤ HMC < 20) and extremely rich (20 ≤ HMC < 50); placer sands are defined by HMC ≥ 50. The Source Rock Density (SRD) index, defined as the weighted average density of extrabasinal terrigenous grains, was used to detect hydraulic-controlled concentration of denser minerals (Garzanti and Andò, 2007). In all analysed samples corrosion features were assessed systematically by three different operators on ~ 25,000 transparent heavy-mineral grains, following the classification of surface textures in Andó et al. (2012). Significant minerals are listed in order of abundance throughout the text. Key compositional parameters are summarized in Table 1. The complete petrographic, heavy-mineral and surface-texture datasets are provided in Appendix Tables A3, A4, and A5.

3.2. Geochemistry

Chemical analyses of 26 river, 23 beach and 2 dune sands were carried out at ACME Laboratories (Vancouver) mostly on a quartered aliquot of the 63-2000 μm class obtained by wet-sieving. Following a lithium metaborate/tetraborate fusion and nitric acid digestion, major oxides and several minor elements were determined by ICP-ES and trace elements by ICP-MS (see Appendix A for specific information on the adopted analytical protocol).

To estimate weathering we used several chemical indices, including the Chemical Index of Alteration [CIA = $100 \cdot Al_2O_3 / (Al_2O_3 + CaO + Na_2O + K_2O)$; Nesbitt and Young, 1982] and the Weathering Index [WIP = $100 \cdot (CaO/0.7 + 2Na_2O/0.35 + 2K_2O/0.25 + MgO/0.9)$; Parker, 1970], calculated using molecular proportions of mobile alkali and alkaline earth metals corrected for CaO in apatite. Instead of correcting the CIA for CaO in carbonates based on mineralogical data, which may result in significant error (Garzanti and Resentini, 2016), we preferred to use the CIX, a simple modification of the CIA not considering CaO [CIX = $100 \cdot Al_2O_3 / (Al_2O_3 + Na_2O + K_2O)$; Garzanti et al., 2013]. Weathering intensities were also calculated for each single mobile element by comparing its concentration to that of non-mobile Al in our samples and in the Upper Continental Crust standard: $\alpha^{Al}E = (Al/E)_{sample}/(Al/E)_{UCC}$ (Garzanti et al., 2013, modified after α values of Gaillardet et al. 1999; UCC standard after Taylor and McLennan, 1995; Rudnick and Gao, 2003). Rare earth elements (REE) were normalized to CI carbonaceous chondrites (McDonough and Sun 1995). Main weathering indices are shown in Table 1. The complete geochemical dataset is provided in Appendix Table A6.

3.3. Detrital geochronology

Detrital zircons were identified by Automated Phase Mapping with a QEMSCAN® WellSite™ instrument (Vermeesch et al., 2017) on the heavy-mineral separates (mostly < 500 or 15-500 μm class) of 50 selected samples. U-Pb ages were determined at the London Geochronology Centre using an Agilent 7700x LA-ICP-MS (laser ablation-inductively coupled plasma-mass spectrometry) system, employing a NWR193 Excimer Laser operated at 11 Hz with a 20 μm spot size and 2.5-3.0 J/cm^2 fluence.

No cathodo-luminescence (CL) imaging was done, and the laser spot was always placed "blindly" in the interior of zircon grains. Textural information acquired by CL-imaging can be useful for detrital geochronology. For example, the presence of oscillatory zoning in zircon may indicate an igneous origin, whereas the presence of complex patterns indicates a multi-phase growth history. This knowledge can be very useful for studies whose aim is to identify specific igneous or metamorphic sediment sources. But in other studies the textural information provided by CL-imaging creates additional challenges. If one's main goal is to compare different age distributions with each other like fingerprints, then it is important that all samples are treated in exactly the same way. The availability of textural information makes it more difficult to decide which part of a grain should be analysed: core, rim, or both? In such cases, it is better to always place the ablation spots in the middle of the grain. A "blind dating strategy" is the easiest way to ensure consistency between samples. Data reduction was peformed using GLITTER 4.4.2 software (Griffin et al., 2008). We used $^{206}Pb/^{238}U$ and $^{207}Pb/^{206}Pb$ ages for zircons younger and older than 1100 Ma, respectively. No common Pb correction was applied. Grains with > +5/-15% age discordance were discarded, and 2967 concordant ages were obtained overall. The complete geochronological dataset is provided in Appendix B.

4. Detrital signatures of river sands

4.1. Cunene River

The Cunene River, sourced in Bié-Huila highlands, flows across the fossil Kalahari dunefield and once drained towards the Etosha Pan of northern Namibia as the Okavango River drains today into the Makgadikgadi Pan of Botswana (Fig. 1B). Captured only recently by a coastal stream (Haddon and McCarthy, 2005), the lower Cunene cuts deeply across the rifted-margin shoulder where the Paleoproterozoic Epupa basement, the Mesoproterozoic Cunene anorthosite, and finally the Kaoko northern branch of the Damara orogen are exposed (Becker et al., 2006). In the terminal tract the river marks the northern limit of the Cunene coastal dunefield and eventually reaches the Atlantic Ocean south of the Moçamedes Desert. Sand mineralogy changes repeatedly downstream (Fig. 2E), which implies higher erosion rates in the lower tract than in the upper to middle course. At Ruacana Falls at the end of the middle course, sand composition is quartz-rich feldspatho-quartzose with dominant monocrystalline quartz, orthoclase > plagioclase ≥ microcline and a poor amphibole-epidote heavy-mineral suite. Quartz grains recycled from Kalahari dunes (e.g., supplied by the Caculuvar tributary and Mucope subtributary) are about twice as abundant as first-cycle detritus from basement rocks. At Epupa Falls, sand is plagioclase-rich feldspatho-quartzose and markedly enriched in polycrystalline quartz, clinopyroxene and hypersthene, revealing dominant supply from crystalline basement including the Cunene anorthosite and associated mafic rocks (e.g., drained by the Omuhongo tributary; Fig. 3). Sand composition changes again in the terminal tract because of extensive mixing with dune sand windblown from the coast and mostly derived ultralong-distance from the Orange River (Garzanti et al., 2014c). In Cunene sand at Epupa Falls, zircon-age spectra are unimodal with broad slightly asymmetric Mesoproterozoic peak centered at ~ 1.4 Ga and most ages ranging between 1 and 2 Ga.

4.2. Rivers of southern Angola (Curoca to Cangala)

The Curoca River marks the northern boundary of the Moçamedes coastal dunefield, and in its terminal tract — as in the terminal tract of the Cunene — mixing with windblown sand is so extensive that composition becomes indistinguishable from littoral sand largely derived ultralong-distance from the Orange River (Fig. 2E). A fossil dune collected upstream of the mouth contains more K-feldspar and less heavy minerals including mainly staurolite and tourmaline, and no pyroxene. Zircon-age spectra in both Curoca mouth and fossil-dune samples display a polymodal distribution undistinguishable from that of Moçamedes desert sand, with the Damaran (Cambrian-late Neoproterozoic) and Namaqua (late Mesoproterozoic) clusters typical of Orange sand associated with subordinate Eburnean (late Paleoproterozoic) ages.

All rivers to the north drain the Angola Block, consisting of Eburnean granitoid rocks and subordinate metasediments with an overlying volcano-sedimentary sequence and younger bimodal magmatic products exposed in the "coastal polyorogenic belt" (De Carvalho et al., 2000; Pereira et al., 2011; Ernst et al., 2013). Sand composition ranges from quartzo-feldspathic to feldspar-rich feldspatho-quartzose with plagioclase > orthoclase > microcline (Fig. 2B). Granitoid rock fragments and polycrystalline quartz are very common, associated with a few metamorphic (quartz-mica, quartz-epidote, low-grade metabasite, rare schist, and amphibolite) and rare sedimentary (sparite and quartz siltstone) lithics. Muscovite and biotite occur sporadically. Moderately rich heavy-mineral suites range from amphibole-epidote in Bero and Giraul sands in the south, to epidote-amphibole in the north (Fig. 3). Clinopyroxene and hypersthene in Bero sand may be supplied by the Cunene intrusive complex drained in the headwaters. Provenance from chiefly granitoid rocks is reflected by very strong depletion in Mg and enrichment in K, Rb, and especially Ba relative to the UCC standard (α^{Al}Mg 8 ± 2, α^{Al}K 0.6 ± 0.1, α^{Al}Ba 0.4 ± 0.0 for Giraul, Bentiaba, Inamangando, and Cangala sands, Bero sand being slightly more mafic) (Fig. 4E). The Eu anomaly is only slightly negative (Eu* 0.88 ± 0.06). Bero sand yielded few Mesoproterozoic zircon ages, whereas spectra in Giraul and Inamangando sands are unimodal with peak centered around 2 Ga (Fig. 5).

4.3. Rivers of southern central Angola (Coporolo to Catumbela)

Composition ranges from quartzo-feldspathic (Cavaco sand) to feldspatho-quartzose (Catumbela sand) with plagioclase ≥ microcline ≥ orthoclase (Fig. 2B). Common granitoid and metaigneous rock fragments occur. Biotite prevails over muscovite. Heavy-mineral suites are moderately poor and epidote-dominated with amphibole in Coporolo and Cavaco sands. A richer epidote-amphibole-clinopyroxene suite with minor zircon and olivine characterizes Catumbela sand. Mafic igneous detritus in the Catumbela catchment is supplied by the lowermost-course Capilongo tributary draining gabbroic rocks of possible Mesoproterozoic age intruded in the "coastal polyorogenic belt" (Ernst et al., 2013) (Fig. 3). Geochemical signatures are similar to river sands of southern Angola but somewhat depleted in alkali and alkaline-earth metals. Zircon-age spectra are unimodal with sharp peak centered around 2 Ga (Fig. 5).

4.4. Rivers of northern central Angola (Culango to Longa)

The quartz/feldspar (Q/F) ratio increases progressively northward, composition ranging from feldspar-rich feldspatho-quartzose in the south to quartz-rich feldspato-quartzose in Longa sand (Fig. 2B,D). K-feldspar mainly prevails over plagioclase. Granitoid and a few metamorphic rock fragments occur. Limestone grains with marine fossils (echinoderm plates), and a few felsic volcanic grains are present in Longa sand, where monocrystalline quartz locally showing rounded outline or abraded overgrowths is dominant. Quicombo sand includes a few carbonate grains. Biotite prevails over muscovite. Poor to moderately rich, epidote-dominated to epidote ≈ amphibole suites include zircon. Cambongo sand contains a few mafic volcanic and clinopyroxene grains. Silica concentration is highest in Longa sand, with consequent dilution of most other elements. Zircon-age spectra are unimodal with sharp peak centered around 2 Ga (Fig. 5). Late Neoarchean to early Paleoproterozoic ages are represented in Queve sand. A few zircon grains with Early

Cretaceous age occur in Quicombo sand, indicating additional supply from local syn-rift volcanic rocks.

4.5. Rivers of northern Angola (Cuanza to Luculu)

Composition is mainly quartz-rich feldspatho-quartzose with orthoclase + microcline ≥ plagioclase. Lifune, Mebridege, and Luculu sands are quartzose (Fig. 2B,D). Monocrystalline quartz is dominant in most samples, with well rounded grains most common in Cuanza, Bengo, and Luculu sands. Granitoid and metasedimentary rock fragments occur. Micas (muscovite > biotite) and medium-rank schist and quartz-mica lithics are most common in Dande sand. Quartz-siltstone to metasiltstone/metasandstone rock fragments are associated with quartz displaying abraded overgrowths or subrounded outline in Mebridege sand. Micrite to sparite grains are most common in Bengo sand and occur in Cuanza and Dande sand, where they may contain Cenozoic planktonic foraminifera. Very poor to rich heavy-mineral suites include mainly amphibole, epidote, garnet, and kyanite (ZTR 6 ± 5). River sands are progressively enriched northward in SiO_2, with stronger and stronger dilution of most other elements. Zircon-age spectra display a peak around 2 Ga and ages ranging mostly between ~ 0.5 and ~ 3 Ga. Loge sand yielded a sharper unimodal Eburnean peak. Luculu sand yielded ~ 10% of zircon grains with mid-Permian to mid-Triassic ages, which occur rarely in Cuanza and Bengo sands as well (Fig. 5).

4.6. Rivers of the Congo

Sands are dominated by subrounded to well rounded monocrystalline quartz; SiO_2 reaches above 98%. The Congo River carries to the mouth a few K-feldspar (orthoclase > microcline) and quartzose siltstone grains (Fig. 2D). The very poor heavy-mineral suite includes zircon, tourmaline, epidote, staurolite, kyanite, and minor rutile, amphibole, garnet, sillimanite, and andalusite (ZTR 51 ± 16). Sands in the Republic of Congo to the north also contain a few quartzose siltstone grains and very poor suites dominated by zircon and tourmaline, with rutile, staurolite, kyanite, epidote, and garnet (ZTR 74 ± 4).

5. Detrital signatures of coastal and offshore sediments

5.1. The Orange littoral cell

Dune and beach sands between the Cunene mouth and south of Namibe are feldspatho-quartzose with lathwork volcanic rock fragments and moderately poor to extremely rich garnet-clinopyroxene-epidote-amphibole suites including hypersthene and staurolite. Higher Fe, Mg, Ca, Ti, P, Mn, Sc, Y, HREE, V, Cr, Co, and Ni than most other Angolan sands reflect the presence of common volcanic rocks fragments, pyroxene, and garnet. Zircon-age spectra show broad Cambrian/late Neoproterozoic, late Mesoproterozoic, and late Paleoproterozoic peaks, with a few younger (as young as Early Cretaceous) and older ages (as old as late Neoarchean; Fig. 5). Such petrographic, mineralogical, geochemical, and geochronological fingerprints resemble closely those of the Skeleton Coast Erg, pointing to ultralong-distance littoral transport from the Orange mouth with subordinate contributions from the Cunene River and ephemeral rivers draining the Damara orogen in Namibia (Garzanti et al., 2014c, 2017).

Sediments collected on the Walvis Ridge and offshore of the Cunene mouth are dominated by planktonic foraminifers and green glaucony grains, respectively (Fig. 6). The sandy-silt to silty-sand feldspatho-quartzose terrigenous fraction contains mafic volcanic rock fragments and a rich, clinopyroxene-dominated heavy-mineral suite with subordinate epidote, amphibole and garnet, indicating provenance mostly from the Orange mouth. Deep-sea silty clays offshore of Baia dos Tigres contain diatom tests and siliceous sponge spicules with minor radiolaria, silicoflagellates, glaucony, plant debris, and organic matter. The subordinate feldspar-rich feldspatho-quartzose terrigenous fraction yielded either the same clinopyroxene-dominated suite as Walvis Ridge and offshore Cunene samples, or a clinopyroxene-epidote-amphibole-garnet suite comparing closely with beaches and dunes of the southernmost Moçamedes Desert, thus revealing additional contribution from the Cunene River.

5.2. From Namibe beach to Coporolo mouth

Beaches in the oblique Namibe rifted-margin segment bear the same feldspar-rich quartzo-feldspathic composition and epidote-amphibole suites of local river sand, reflecting dominant supply from largely granitoid rocks exposed in adjacent Angolan highlands. Chemical composition is also similar, with higher Fe, Mg, Ti, P, Mn, Sc, U, V, Cr, Co, Ni, and Cu in Namibe beach reflecting the abundance of heavy minerals including pyroxenes fed from the Bero River. Zircon-age spectra are mostly unimodal with peak centered around 2 Ga (Fig. 5). Mesoproterozic ages are significant in Namibe beach. In Equimina beach, 22% of zircon grains yielded ages between 84 and 104 Ma, indicating provenance from mid-Cretaceous trachytic lavas exposed locally (Neto, 1960). Supply from Meso-Cenozoic strata of the Namibe basin is revealed in Chapeu Armado beach by microcline ≈ plagioclase, occurrence of a few carbonate and mafic volcanic lithics, and poor suites with common durable heavy minerals (ZTR 24). Carbonate, quartz-siltstone, and basaltic grains occur also at Mariquita and Bentiaba beaches. Beach sand is derived dominantly from basement rocks in the north where the Namibe basin tapers out, as documented by abundant feldspar, metabasite rock fragments and up to very rich epidote-amphibole suites, although a few carbonate rock fragments also occur. Presence of carbonate grains is reflected in locally high CaO and LOI (e.g., Baia Binga beach). Local differences in sand composition along this coastal stretch, where the shelf width is reduced to only some kilometers thus limiting the possibility of longshore sand drift, indicate that pocket beaches are largely independent sediment systems fed from the associated stream and coastal cliffs.

5.3. The Coporolo and Catumbela littoral cells

The perennial Coporolo and Catumbela Rivers represent the major source of beach sand along the Benguela transform rifted-margin sement (Dinis et al., 2016). Beaches north of the Coporolo mouth display the same feldspar-rich feldspatho-quartzose signature with moderately poor to moderately rich epidote-dominated suites with amphibole as Coporolo river sand. A few carbonate and quartz-bearing siltstone and sandstone grains are however added along the coast, and quartz increases in the Baia Farta sand spit indicating additional supply from local streams and coastal cliffs. The shelf is very narrow offshore of the Baia Farta promontory, where a submarine canyon may capture longshore-drifting sand thus hampering northward elongation of the spit. The silty clay collected in the deep sea is quartzo-feldspathic with the same epidote-dominated suite as beach sand in the Coporolo cell. North of Benguela the continental shelf widens again to ~ 25 km, and northward littoral drift is renewed. Beach sand between the Cavaco and Catumbela mouths is nearly as feldspar-rich as Cavaco river sand. Sand with the same feldspatho-quartzose signature as Catumbela river sand with a rich epidote-dominated suite including amphibole and clinopyroxene is carried northward of the strongly asymmetric Catumbela delta to build prograding beach ridges culminating in the 5 km-long Lobito spit. Zircon-age spectra are unimodal with sharp Eburnean peak. Beach sand north of Coporolo mouth yielded a few zircon grains with younger ages, one of which mid-Cretaceous (Fig. 5).

5.4. From Lobito to Cabo Ledo

Beach sand along the oblique-rifted Cuanza margin segment is invariably feldspatho-quartzose, and thus richer in quartz than local river sands suggesting either additional supply from coastal cliffs or northward longhsore drift from the Catumbela mouth. The moderately poor to rich epidote-amphibole-clinopyroxene heavy-mineral suite may include rare olivine. Clinopyroxene, notably more abundant than in river sands, is derived from volcanic rocks best exposed in the Sumbe area (Marzoli et al., 1999) and/or longshore from the Catumbela mouth. Local enrichment in heavy minerals is revealed by higher Fe, Mg, Ti, Sc, REE, Zr, Hf, V, Nb, Ta, and Cr than in river sands. Beach sand at Cabo Ledo, containing carbonate grains as reflected by locally high CaO and LOI, yielded a unimodal zircon-age spectrum with sharp Eburnean peak as beach sand at Porto Amboim. A few mid-Cretaceous ages confirm additional detritus from syn-rift igneous rocks along the coast.

Silty sands collected offshore of the Tapado mouth include mostly benthic foraminifers, which become dominant beyond the shelfbreak (Fig. 6). The quartzo-feldspathic to feldspar-rich feldspatho-quartzose terrigenous fraction yielded a rich, epidote-dominated heavy-mineral suite with subordinate amphibole. Feldspar is more abundant than in beach sand and clinopyroxene minor, indicating provenance directly from the Balombo and/or Tapado river mouths rather than from longshore drifting sand. The silty clay collected in the deep sea south of the Cuanza seamounts (Fig. 1A), dominated by planktonic and subordinately benthic foraminifers, yielded a similar epidote-amphibole suite with no clinopyroxene.

5.5. The Cuanza littoral cell

Beach sand from the Cuanza mouth to Ilha de Luanda is quartz-rich feldspatho-quartzose with plagioclase ≈ microcline ≈ orthoclase. The poor to moderately rich epidote-amphibole-clinopyroxene heavy-mineral suite includes minor garnet, kyanite, staurolite, andalusite, and rare olivine. Feldspar is more common and ZTR indices lower than in Cuanza river sand. Clinopyroxene increases along the littoral cell where polycrystalline quartz is also more abundant, suggesting mixing with northward drifting sand along the broad littoral zone. Chemical data confirm significant differences between Cuanza river sand and the Mussulo and Ilha de Luanda spits, which have less Si, higher alkali and alkaline earth metals (and hence systematically lower weathering indices), lower Zr and Hf, and much steeper REE patterns with no Eu anomaly.

5.6. From Luanda to the Congo

Beach sands along the orthogonal to oblique-rifted Congo-margin segment vary from mainly quartz-rich feldspatho-quartzose in the south to quartzose north of N'Zeto, with a progressive northward decrease in feldspar (orthoclase ≥ plagioclase ≥ microcline). The heavy-mineral concentration of epidote-amphibole-garnet-kyanite suites tends to decrease from mainly rich in the south to moderately rich and finally poor in the north, where staurolite becomes significant and zircon, tourmaline, and rutile increase (ZTR up to 13). Beach sand in the Republic of Congo consists almost entirely of commonly rounded monocrystalline quartz grains displaying deep etch pits, with only a few microcline grains and a very poor suite with zircon, rutile, tourmaline, staurolite, kyanite, and rare andalusite (ZTR 66). SiO_2 increases progressively northward, reflecting increasing and finally overwhelming quartz dilution.

Zircon grains in Ambriz sand yielded a sharp unimodal Eburnean peak along with 5% of Upper Permian ages. The Eburnean peak becomes broader north of the Loge mouth, where Permian ages also occur. The zircon-age spectrum is multimodal in beach sand south of the Congo mouth with Pan-African (0.5-0.7 Ga), Namaqua (~ 1 Ga), Eburnean (~ 2 Ga) and Neoarchean (2.5-2.7 Ga) clusters. A similar spectrum characterizes Congo estuary sand (Fig. 5).

Fine-grained quartzose sand collected on the inner shelf just south of the Congo mouth includes common brown goethite ooids (Fig. 6), a few plagioclase and K-feldspar grains, and a moderately rich heavy-mineral suite including epidote, garnet, amphibole, zircon, rutile, kyanite, minor andalusite, tourmaline, apatite and staurolite, indicating provenance form northward longshore drift rather than from the Congo River. Very fine-grained shelfal sediment north of the Congo mouth consists of brown pellets and foraminifers (Fig. 6).

6. Provenance control on sand composition

The geology of Angola includes two main domains, the Paleoproterozoic Angola Block with the prominent Mesoproterozoic Cunene intrusive complex in the south, and the Pan-African West Congo Belt in the north. The dual time structure of source rocks is best reflected by U-Pb ages of detrital zircons, characterized by unimodal spectra with sharp Eburnean peak at ~ 2 Ga from north of Namibe to south of the Cuanza mouth, and by multimodal distributions in northern Angola with Cambrian-Neoproterozoic, latest Mesoproterozoic, and Neoarchean clusters best defined in Congo estuary sand. The Mesoproterozoic peak with Eburnean shoulder displayed by detrital zircons in Cunene sand at Epupa Falls reflects contribution from the Cunene intrusive complex, documented as far north as Namibe beach fed by the Bero River. To the south, sharply different detrital modes, heavy-mineral suites, and zircon-age clusters characterize dunes and beaches of the Moçamedes Desert, documenting ultralong-distance provenance mainly from the Orange River.

Detrital modes, heavy minerals, and concentration of chemical elements reflect local source-rock distribution as faithfully as zircon age-spectra only in dry southern Angola north of the Orange littoral cell, where abundance of feldspar and granitoid rock fragments among main framework grains and of epidote and amphibole among transparent heavy minerals indicate the Angola Block as the dominant source ("basement uplift subprovenance" of Dickinson, 1985; "dissected continental block subprovenance" of Garzanti, 2016). Metamorphic rock fragments of mainly medium to high rank (MI* 312 ± 50), epidote/hornblende ratio mostly > 1 and dominantly blue/green amphiboles (HCI mostly ≤ 10) point to mainly greenschist-facies to lower amphibolite-facies source rocks. Scarcity of garnet, lack of kyanite, andalusite and sillimanite, and only sporadic occurrence of metasedimentary rock fragments reflect predominance of granitoid and metagranitoid source rocks, as confirmed by geochemical signatures. Metabasite rock fragments and higher heavy-mineral concentration indicate more significant supply from mafic greenschist-facies rocks in beach sand from Lucira to the Coporolo mouth. Meso-Cenozoic strata and intercalated lavas of the Namibe basin supply minor amounts of sedimentary and volcanic detritus to pocket beaches locally. Lower Cretaceous mafic rocks contribute a few basaltic fragments and clinopyroxene, whereas more felsic younger products provide zircon grains with mid-Cretaceous ages (e.g., Equimina beach).

Provenance is dominantly from the Angola Block also in central Angola, as reflected by the same unimodal Eburnean zircon-age spectra and epidote-amphibole suites. Sand is however characterized by higher quartz/feldspar (Q/F; Fig. 2B) and lower plagioclase/feldspar (P/F) ratios, chiefly reflecting increasing weathering conditions (as discussed in section 8 below) rather than different provenance. Mafic igneous detritus documented by gabbroic rock fragments and clinopyroxene is most significant in Catumbela sands. In beaches from the Catumbela mouth to Luanda, clinopyroxene is invariably much more common than in local rivers (Fig. 3), indicating coastal dispersal of mafic igneous detritus derived from either the Catumbela mouth or Cretaceous syn-rift tholeiitic to post-rift alkaline basalts exposed at the landward termination of the Cuanza volcanic line ("anorogenic volcanic provenance" of Garzanti, 2016). Heavy-mineral concentration tends to be higher in beach sands than in river sands, but differences in heavy-mineral suites cannot be ascribed to hydrodynamic processes, because clinopyroxene is only slighly less dense than epidote and none of our samples show markedly anomalous SRD indices. Offshore samples are pyroxene-poor, which argues against longshore drift from the Catumbela mouth.

In northern Angola, the provenance signal is dimmed further by progressively stronger weathering effects. Mainly low-grade to lower medium-grade metasedimentary detritus from the West Congo Belt is documented by medium-rank schist and quartz-mica lithics, muscovite, biotite, and common garnet and kyanite; staurolite increases in relative abundance from northernmost Angola to the Congo. Quartz and durable heavy minerals recycled largely from Meso-Cenozoic coastal basins, but also partly from Neoproterozoic successions, are common in sands of rivers cutting across the Cuanza basin in their terminal tract, including the Longa, Bengo, and especially the Cuanza (as discussed in subection 7.3 below).

In the Congo, the provenance signal is largely obliterated by extreme weathering conditions, which coupled with extensive recycling produce pure quartzose sand with high ZTR (Figs. 2D, 4A,C; "craton interior provenance" of Dickinson, 1985; "recycled clastic provenance" of Garzanti, 2016).

7. Physical processes controlling sand composition

In this section we discuss the compositional modifications associated with physical processes in the depositional environment, namely hydraulic sorting, mechanical breakdown, and recycling.

7.1. Hydraulic sorting

Sorting of detrital grains based on their size, density, and shape occurs in all three stages of the sedimentary cycle, during erosion by selective entrainment, during transport by vertical partitioning of particles carried in suspension, and eventually during deposition according to their settling velocity (Komar 2007). Erosive processes may lead to extreme modifications of sand composition, as documented by common formation of garnet and magnetite beach placers in southern Angola

(Garzanti et al., 2017). These lag deposits are generated during storm events when tectosilicate grains — having smaller pivoting angles and projecting higher above the bed than smaller settling-equivalent dense minerals and thus experiencing greater flow velocities and drag forces (Komar and Li 1988) — are selectively removed offshore. These phenomena are readily revealed by the anomalous concentration of dense and ultradense minerals, as reflected by bulk-sediment grain densities notably higher or lower than the estimated weighted average density of source rocks (ranging from ~ 2.65 g/cm^3 for quartzarenites, quartzites and granites to 2.8-3.0 g/cm^3 for mafic igneous and metamorphic rocks; Garzanti et al., 2009). Among our samples, anomalously high grain densities are estimated for the Inamangando outer berm and for the Equimina and Cabo Ledo beaches (SRD between 2.77 and 2.94 g/cm^3), all notably enriched in opaque Fe-Ti-Cr oxides and zircon relative to adjacent beaches derived from similar source rocks. Placer lags rich in Fe-Ti-Cr oxides and zircon were sampled at the Catumbela mouth and sporadically observed in northern Angolan beaches (e.g., garnet-rich Ambriz sample). Such strong selective-entrainment effects are revealed readily by the anomalous concentration of elements hosted preferentially in ultradense minerals (e.g., Ti, REE, Zr, Hf, Nb, Ta, Cr), as well as by highly negative Eu anomalies (Garzanti et al., 2010). Zr and Hf concentrations reach 2474 and 49 ppm in Equimina beach (Eu/Eu* 0.45), reflecting zircon abundance. The Eu anomaly is most strongly negative in the Inamangando outer berm (Eu/Eu* 0.28). Such hydrodynamic effects were not observed in river sands.

7.2. Mechanical breakdown

Mechanical wear is scarcely effective during even long-distance fluvial and longshore transport in acqueous media (Russell, 1937; Shukri, 1950; Breyer and Bart, 1978). Although feldspar is softer than quartz and has good cleavage, no significant decrease in the Q/F ratio or in feldspar size is observed over a distance of eighteen hundred kilometers from the Orange mouth to southern Angola. We thus concluded that mechanical breakdown cannot modify the composition of passive-margin sand significantly (Garzanti et al., 2015).

The Q/F ratio, however, decreases in offshore silts. In northern Namibia to southern Angola, tectosilicate modes are very close in fine to medium Skeleton Coast and Moçamedes desert sands (Q 78±4 K 8±2 P 14±3 and Q 74±4 K 10±3 P 16±3) and in very fine shelfal sand offshore of the Cunene mouth (Q 77±1 K 8±0 P 15±1), but do change in deep-sea silt from the Walvis Ridge (Q 57 K 12 P 31). Cleavable feldspar thus concentrates in the silt fraction. In central Angola, feldspar increases with grain size from Coporolo medium sand (Q 63±2 K 21±3 P 16±2) to deep-sea silty clay (Q 39 K 25 P 36), but only slightly from fine to medium Balombo and Tapado river sands (Q 55±2 K 27±0 P 18±3) to very fine sand offshore (Q 49±6 K 29±0 P 23±5). Fine sand offshore of the Congo mouth is richer in feldspar than beach sand, but chiefly because of longshore transport from the south.

North of Namibe, where eolian dunefields are lacking, most silicates are observed to remain mainly subangular in beach sand, indicating that mechanical wear during fluvial and longshore transport has a limited influence on both composition and texture of sand-sized sediment.

7.3. Recycling

Recycling represents the most elusive problem by far in provenance analysis of modern sands (Blatt, 1967). The presence of recycled detritus is qualitatively revealed by the occurrence of quartz grains with abraded overgrowths or well-rounded outline and of shale, siltstone or sandstone rock fragments, together with a series of parameters, including high Q/F and ZTR indices and low P/F and heavy-mineral concentration (Fig. 4C). All of these features characterize river and beach sands in northern Angola, and become extreme from northernmost Angola to the Congo (Fig. 7F,G).

Any attempt to quantify precisely the amount of recycled versus first-cycle detritus is however unrobust, because mineralogical parameters indicative of recycling are generally affected by weathering as well (Garzanti, 2017). In southern Angola north of the Orange littoral cell, where climate is arid and weathering negligible, detritus recycled locally from Meso-Cenozoic strata of the Namibe basin is estimated by forward compositional modelling (Garzanti et al., 2012b) to be ≥ 15%

in the Mariquita and Chapeu Armado pocket beaches, and very minor elsewhere. In central Angola, beach sands tend to be richer in quartz than river sands, suggesting that detritus recycled from coastal outcrops of sedimentary strata may reach up to ~ 30%, a percentage estimated tentatively to increase to ~ 40% for Longa sand and to ≥ 50% for Cuanza sand. The recycled component, estimated to be ~ 30% for Bengo sand and ~ 15% for Dande sand, is prominent in beaches of northern Angola and overwhelming in the Congo, but an accurate estimate cannot be made because of strong superposed weathering effects. Recycled monocrystalline quartz is dominant in rivers draining Kalahari fossil dunes including middle Cunene tributaries as well as the uppermost Cuanza, the endorheic Okavango, the Cuando, and the upper Zambezi draining into the Indian Ocean. Detritus recycled from quartzose sandstones and metasandstones of the Neoproterozoic West Congo Belt occurs in all major rivers from the Cuanza to the Congo and it is most evident in Mebridege sand. Quartzose detritus recycled from siliciclastic strata of the Meso-Cenozoic Cuanza basin is most significant in Longa, Cuanza and Bengo sands, whereas Luculu sand and beach sand in northernmost Angola are recycled from Lower Congo basin strata (Fig. 1D).

Rivers of southern and central Angola carry very few garnet grains (< 3% of transparent heavy minerals), reflecting virtual lack of garnet in granitoid rocks of the Angola Block. Garnet represents 8 %tHM in Chapeau Armado beach, indicating recycling of sandstones in the coastal Namibe basin. In northern Angola, garnet is significant (5-13 %tHM) in rivers between the Cuanza and the Onzo draining the northern part of the Cuanza basin, and it is common in Luculu sand draining the Lower Congo basin (33 %tHM) and in all beach sands between the Dande and Congo mouths (20±10 %tHM). The areal distribution of garnet along the Angolan rifted margin thus reveals that it is mostly recycled from siliciclastic strata of Meso-Cenozoic basins ─ ultimately derived from metasedimentary rocks of the West Congo Belt in northern Angola and of the Kaoko Belt in southern Angola ─ rather than first-cycle from basement rocks.

Interpretation of chemical data also suffers from the superposed effects of weathering and recycling. In river and beach sands from southern Angola to the Congo, Si increases markedly (corr. coeff. r =

0.88, sign. lev. 0.1%), whereas most other elements decrease, non-mobile Al most evidently (r = -0.92). The sharp northward decrease in aluminum results from the superposed effects of selective feldspar breakdown by paleoweathering during previous sedimentary cycle(s), by intrastratal dissolution between successive cycle(s), and only last by hydrolisis in the present subequatorial climate. Because of such strong multiphase depletion in Al, chemical-weathering proxies including the CIA, PIA, CIX, and α^{Al} may give unexpectedly low values in sand generated in hyper-humid equatorial climates (e.g., Congo sand; Table 1). The Eu anomaly is more strongly negative in sands containing more recycled quartz as suggested independently by detrital modes and textural features (Eu/Eu* 0.45-0.50 for Cuanza and Longa sands, Eu/Eu* 0.50-0.70 for Mebridege and Congo river sands and all beaches north of 6°30'S). In order to single out the recycling effect we may calculate the ratio between the CIX (a truer indicator of weathering unaffected by the addition of biogenic, pedogenic, or extrabasinal carbonate grains) and the WIP (strongly influenced by quartz dilution; Garzanti et al., 2013). The CIX/WIP ratio does increase northward (Fig. 4), but the correlation (r = 0.49) is barely significant.

8. Weathering control and relative durability of detrital minerals

The effect of weathering on Angolan continental-margin sediments, associated with both latitudinal climatic zonation and strong inland rainfall gradients, has been discussed in detail in a previous study focusing on clay minerals and sediment geochemistry (Dinis et al., 2017). Here we focus instead on sand composition, and discuss specifically the effects of subequatorial weathering on detrital modes and surface textures of quartz, feldspar, and heavy minerals (Fig. 7).

8.1. Main framework grains

In order to consider a homogeneous population of sediment samples, we have selected 23 river sands lacking clues of polycyclic origin (e.g., quartz grains with abraded overgrowths or well rounded outline, arenaceous rock fragments) and thus held to be derived dominantly first-cycle from crystalline basement. In this sample set, the quartz/feldspar ratio is ≥ 1 in southern Angola, ~ 2 in central Angola, and ~ 7 in northern Angola (Figs. 2B and 4A). The plagioclase/K-feldspar ratio is > 1 in southern Angola and ≤ 1 in central and northern Angola; cross-hatched microcline represents ~ 30% of K-feldspar grains in southern Angola and ~ 45% in central and northern Angola (Fig. 4B). Because source rocks are broadly homogeneous in southern and central Angola, these trends are interpreted as chiefly weathering-controlled. Plagioclase disappears in the Congo, where microcline may be the only detrital feldspar present. Quartz is thus inferred to resist chemical dissolution far better than feldspars, K-feldspar somewhat better than plagioclase, and microcline somewhat better than orthoclase, confirming earlier observations (e.g., Blatt, 1967; James et al., 1981; McBride, 1985).

The same set of selected river sands were photographed, and the degree of weathering evaluated on both thin sections and microphotographs by two different operators, based on the presence and depth of etch pits, and on the degree of replacement of quartz and feldspar lattice by clay plasma (Fig. 7). We subdivided the samples in groups with similar frequency and extent of alteration features, and then ranked them — from the apparently least weathered to the apparently most weathered — in five independent trials. A trend of increasing weathering with decreasing southern latitude was obtained in all trials, with a median of Spearman rank correlation coefficients of 0.76 ± 0.25 (sign. lev. 0.1%); the rather large standard deviation reflects the considerable degree of subjectivity involved in qualitative judgments.

The compositional change associated with the strong W/E climatic gradient was investigated in the Catumbela catchment, where we studied sands carried by three tributaries draining progressively more humid areas farther from the coast. The Q/F ratio is observed to increase rapidly and the P/F ratio to decrease in sands derived from more humid areas of the interior. Highest Q/F and lowest P/F ratios characterize trunk-river sand derived largely from humid headwater highlands (Fig. 2C). These samples, although limited in number, display a much sharper weathering-controlled compositional trend than the one associated with latitudinal climatic zonation.

8.2. Heavy minerals

Pyroxene and amphibole grains are mostly corroded, and show a higher degree of weathering relative to all other heavy minerals in most samples. Epidote and staurolite are commonly corroded and occasionally deeply etched or skeletal. Andalusite, garnet, kyanite, titanite, and apatite are also corroded, but etched or deeply etched only locally. Tourmaline is corroded more commonly than rutile, and rutile more commonly than zircon. Etch pits do not appear to increase remarkably in frequency or depth with decreasing latitude. A latitudinal trend is best displayed by clinopyroxene, and specifically by deeply etched to skeletal clinopyroxene grains, which are most common north of Luanda where etched garnet is also recorded. Garnet, widely considered as relatively resistant during diagenesis (Morton and Hallsworth, 2007), resulted to be very unstable in hyperhumid equatorial rift highlands (fig. 9 in Garzanti et al., 2013) and yet it is common in all beach samples between Luanda and the Congo mouth, and most abundant in Ambriz beach and Luculu river sands. Garnet becomes rare only in rivers and beaches of the Congo, indicating stronger weathering conditions than in northern Angola.

8.3. Chemical proxies

Among chemical indices of weathering, only the WIP correlates very well with latitude (r = 0.91). This is simply because it reflects the combined effects of weathering and recycling, which both increase notably in northern Angola and very markedly in the Congo (Fig. 4). Among indices unaffected by quartz dilution but sensitive to source-rock lithology, only the CIX correlates with latitude relatively well (r = 0.62, sign. lev. 0.1%); α^{Al}Na, α^{Al}K and α^{Al}Rb correlate poorly (r = 0.42-0.49; sign. lev. 1%). Indices considering Ca (CIA, PIA, α^{Al}Ca) are uncorrelated with latitude, being low to even very low in Bengo, Cuanza, and Longa river sands of northern Angola containing carbonate rock fragments derived from Meso-Cenozoic basins (Fig. 8). Relative to aluminum and with reference to the UCC standard, depletion in Na, Ca, and K is not particularly strong in northern Angolan sands, suggesting that plagioclase is not much less durable than K-feldspar and that recycling is more responsible than weathering for feldspar depletion (Nesbitt et al., 1997) (Fig. 4). A markedly negative Eu anomaly produced by plagioclase breakdown (McLennan, 1993; Condie et al., 1995) is not observed in river sands of northermost Angola (e.g., Eu/Eu* 0.89 in Loge sand), where plagioclase is as abundant as K-feldspar. Final plagioclase breakdown is indicated by the sharp increase of the CIA, CIX, and especially of α^{Al}Na in the Congo (Table 1).

9. Passive-margin sand and the arkose-quartzarenite problem

The traditional view in sedimentary petrology is that passive-margin sands are generated from the adjacent cratonic block — held to consist of gneissic-granitoid basement with cover strata — and thus contain quartz and feldspar with few lithic fragments ("continental block provenance" of Dickinson, 1985). Such sand suites are basically distinguished by their Q/F ratio, which may be ≤ 1 ("ideal arkose" of Dickinson, 1985) either where tectonic activity is particularly intense ("tectonic arkose" of Folk, 1980; "basement uplift subprovenance" of Dickinson, 1985) and/or in arid climatic conditions ("climatic arkose" of Folk, 1980). Instead, in case of tectonic quiescence favoring prolonged weathering in low-relief shield areas, quartz would dominate over mainly K-feldspar ("craton interior subprovenance" of Dickinson, 1985).

As a first approximation, this case study on sediment generation along the magma-poor Angolan passive margin represents a neat confirmation of such a simplified conceptual framework. First-cycle quartzo-feldspathic to feldspar-rich feldspatho-quartzose sand eroded from mid-crustal granitoid gneisses of the Angola Block exposed in the dynamically uplifted Bié-Huila dome is deposited in arid southern Angola, whereas quartz-rich feldspatho-quartzose to quartzose sand characterizes the lower-relief and more intensely weathered rifted margin of humid northern Angola, where sedimentary and metasedimentary rocks are more common. Pure quartzose, largely recycled sand is generated in the vast, low-lying hyperhumid Congo basin (Giresse, 2005). Sand composition in these three segments of the African passive margin thus reflects northward decreasing dissection of the Congo craton (i.e., dissected, transitional, and undissected stages of continental block provenance; Garzanti, 2016).

Such an apparently simple scenario stems from three distinct processes acting in accord. Stronger tectonic uplift in the arid south, and stronger weathering coupled with extensive recycling in the humid north determine a progressive northward increase of more durable quartz and heavy minerals such as zircon, tourmaline and rutile, relative to less durable minerals such as plagioclase, amphibole and pyroxene. The superposition of such partly interrelated effects makes it difficult to quantify the relative importance of each, which has always represented a major drawback in the paleotectonic and paleoclimatic interpretation of ancient passive-margin sandstones (e.g., Johnsson, 1993). Particularly hard to infer from detrital modes is the importance of recycling, because chemical dissolution during diagenesis of parent sandstones may produce similar effects as weathering of daughter sands (Velbel and Saad, 1991). One key, although chiefly qualitative, is provided by the shape of quartz grains, rounded in the case of recycling especially of eolian parent sandstones, deeply etched in the case of subequatorial weathering (Fig. 7).

Angolan sands present a relatively simple case also because this tract of the Atlantic rifted margin is essentially non-volcanic, with limited syn-rift to post-rift magmatic activity confined to a few coastal areas. Basaltic detritus derived from as far as Lesotho highlands represents 4 ± 2% of dune and beach sands of the Moçamedes Desert, where it provides the most distinctive trace of ultralong-distance littoral transport from the Orange river mouth. North of the Moçamedes Desert, basaltic rocks fragments, clinopyroxene and detrital zircons with mid-Cretaceous U-Pb ages occur in a few river sands (e.g., Cambongo, Quicombo) and in several beaches from southern to central Angola, where volcanic detritus represents ≤ 2 % of bulk sand. Anorogenic volcanic provenance is thus minor, which is not the case for many other regions of southern Africa still widely preserving remnants of the widespread Jurassic Karoo and Cretaceous Etendeka flood basalts (Garzanti et al., 2014a).

10. Conclusion

The N/S trending Angolan continental margin, located in the subequatorial belt of the Southern Hemisphere where climate changes progressively with latitude from hyperarid in tropical Namibia to hyperhumid in equatorial Congo, offers an exceptionally suitable natural laboratory in which to study the effects of climatic-induced weathering on sediment composition. Excepting the Moçamedes Desert in the south, where sand is mainly supplied by ultralong littoral transport from the Orange river mouth, Angolan sand suites consist chiefly of quartz and feldspar derived first-cycle from granitoid Precambrian basement but also partly recycled from Meso-Cenozoic basins formed during initial rifting of the South Atlantic. Sand samples were thus formally classified by their quartz/feldspar ratio as quartzo-feldspathic ($Q/F < 1$), feldspar-rich ($1 < Q/F < 2$) to quartz-rich ($4 < Q/F < 9$) feldspatho-quartzose, and quartzose ($Q/F > 9$; pure quartzose if $Q\%QFL > 95$; Fig. 2A).

Quartzo-feldspathic to feldspar-rich feldspatho-quartzose sands characterize the arid south adjacent to dynamically uplifted highlands. Moving toward the humid equator, river and beach sands pass from feldspatho-quartzose in central Angola to mostly quartz-rich feldspatho-quartzose in northern Angola, quartzose in northernmost Angola, and eventually pure quartzose in the Congo. Sharper compositional trends are associated with the steep E/W climatic gradient, reflecting much stronger chemical weathering in humid highlands than along the arid coast. Minor volcanic detritus is supplied locally by Cretaceous lavas exposed close to the coast. Heavy-mineral suites are generally dominated by epidote and amphibole. North of the Moçamedes Desert, clinopyroxene is present in a few pocket beaches of southern Angola and widespread in beaches of central Angola. Garnet associated with kyanite is common in beaches of northern Angola, where it is largely recycled from sandstone strata of the Cuanza and Lower Congo basins and ultimately derived from metasedimentary rocks of the West Congo Belt (Fig. 3). The dual time structure of Angolan source rocks is best reflected by U-Pb ages of detrital zircons, characterized by unimodal spectra with sharp Eburnean peak at ~ 2 Ga from north of Namibe to south of the Cuanza mouth, and by broader multimodal distributions in northern Angola, with a few Permo-Triassic ages locally and additional clusters at 0.5-0.7 Ga, ~ 1 Ga, and 2.5-2.7 Ga best defined in Congo estuary sand (Fig. 5). Among chemical indices of weathering, the WIP correlates well with latitude because it reflects the superposed effects of weathering and recycling. Other indices correlate poorly because they are largely affected by source-rock lithology as well (Fig. 4). Depletion in Ca, Na, and K is not very strong even in northern Angola, where plagioclase results to be not much less durable than K-feldspar and recycling is more responsible than weathering for feldspar depletion. Feldspar and garnet are weathered out only in the hyperhumid climate of the Congo.

This modern study of Angolan sands shows how extracting the climatic signal from sediment composition is not straightforward, because multiple controlling factors operate in nature simultaneously, and because mineralogical and geochemical proxies do not respond to weathering only but are affected by other variables, including source-rock lithology, hydraulic sorting, and recycling as well.

ACKNOWLEDGMENTS

Fundamental logistic support by the University of Katyavala Bwila and the Instituto Superior Politécnico da Tundavala, and kind help by Manuel Bandeira, Silvano Levy, Margarida Ventura, and Carlos Ribeiro are very warmly appreciated. Additional samples from Angola and the Congo were kindly provided by Edson Baptista, Francesca Bolognesi, Daniela Dell'Era, Raffaele Giardini, Maurizio Orlando, Alcides Pereira, Afonso Sampaio, and Armanda Trindade. Ethan Petrou helped with geochronological analyses and Elisa Malinverno with determination of fossil assemblages. Constructive reviews by two anonymous reviewers and Editor Sebastien Bertrand were gratefully received.

SUPPLEMENTARY MATERIAL

Supplementary data associated with this article, to be found in the online version at http://dx.doi.___________, include information on sampling sites (Table A1) and river catchments

(Table A2), together with the complete datasets on bulk-sand petrography (Table A3), heavy minerals (Table A4), surface textures (Table A5), sand geochemistry (Table A6) and detrital-zircon geochronology (Appendix B). Figure A1 illustrating river profiles, and the Google-Earth™ map of sampling sites *Angolamargin.kmz* are also provided.

FIGURE CAPTIONS

Figure 1. Topography, climate, and geology of Angola. **A**) Google Earth™ image showing the recently uplifted Bié-Huila plateau of southwestern Angola, lying largely at altitudes above 1500 m and delimited by very steep scarps cleaved by deep narrow gorges in the northwest (Lopes et al., 2016). Location of river (green), dune (orange), beach (yellow), and offshore samples (white; MARUM sites GeoB 1000->1008, 1011->1014, 1019->1022, 1702, 1704->1706, and 4918; DSDP Leg 40 site 365 and ODP Leg 175 sites 1078->1080 in *italics*) is indicated. **B**) Location and river map. **C**) Rainfall map (annual precipitation in mm; Hijmans et al., 2005). **D**) Geological sketch map (redrawn after Schlüter, 2008 and various sources cited in the text).

Figure 2. Petrographic classification and effects of weathering and recycling in subequatorial passive-margin sands. Data points: intensity of blue color increases with increasing rainfall at decreasing southern latitude; outline ranges from black to light grey with increasing estimated proportion of recycled component. **A**) The proposed refined classification of lithic-poor sands and sandstones. **B**) River sands chiefly derived first-cycle from basement rocks display a latitudinal trend of quartz enrichment controlled by climatic zonation. Latitude and average rainfall are indicated for Mebridege River in the north and Bero River in the south. **C**) The W/E inland trend of weathering-controlled quartz enrichment is well displayed in the Catumbela catchment. The Q/F ratio increases systematically in sand of tributaries draining progressively farther from the coast, being highest in trunk-river sand derived largely from humid interior highlands. The opposite trend is displayed by the P/F ratio, indicating selective dissolution of plagioclase. Longitude of headwaters and average rainfall are indicated for each catchment. **D**) River sands containing a significant recycled component as revealed by textural and mineralogical parameters are enriched further in quartz, reaching pure quartzose compositions in hyperhumid Congo. **E**) Cunene sands are a mixture of pure quartzose sand recycled from the fossil Kalahari Desert in the middle reaches and unweathered first-cycle quartzo-feldspathic sand eroded from crystalline basement in the dry lower

reaches (Fig 1C). Sand composition in the terminal tract of the Curoca River reflects extensive mixing with eolian coastal sand derived mainly from the Orange mouth.

Figure 3. Heavy-mineral suites of Angolan passive-margin sands. Moçamedes desert sands are richer than Skeleton Coast sands in amphibole and epidote contributed by the Cunene River; offshore sands are hydrodynamically depleted in garnet. Angolan basement chiefly supplies epidote and amphibole. From the Catumbela mouth to Luanda, beach sand is richer in clinopyroxene than river sand. From northern Angola to the Congo, beach sand is enriched in garnet, next in kyanite, and finally in staurolite, all largely recycled from Meso-Cenozoic strata of the northern Cuanza and Lower Congo basin and ultimately derived from metasedimentary rocks of the West Congo Belt. Both multivariate observations (points) and variables (rays) are displayed in the compositional biplot (Gabriel, 1971). The length of each ray is proportional to the variance of the corresponding element in the data set. If the angle between two rays is close to 0°, 90°, or 180°, then the corresponding elements are directly correlated, uncorrelated, or inversely correlated, respectively.

Figure 4. Latitudinal variation of key compositional parameters in river sands. Three-point-centered moving averages of all indices reflect extensive recycling of fossil Kalahari dunes in the middle Cunene catchment (right end of panels) and the combined effects of weathering and recycling in the Congo (left end of panels). **A)** The quartz/feldspar (Q/F) ratio shows the same trend as the CIX/WIP ratio, indicating the overwhelming effect of recycling. **B)** Metamorphic rank of rock fragments (MI) reflects mainly first-cycle provenance of Angolan sands from low to medium-grade basements; mixing with detritus from siliciclastic covers is major in rivers draining the Kalahari (right end), the Cuanza basin (center left), and the Congo basin (left end). Plagioclase (P) tends to decrease slighly with decreasing latitude relative to K-feldspar (KF; $r = 0.60$), and microcline (Mic) to increase imperceptibly relative to orthoclase ($r = 0.37$). **C)** The anticorrelation between the relative concentration of durable minerals (ZTR) and the absolute concentration of transparent heavy minerals (tHMC) is chiefly a recycling effect. **D)** Among the variants of the CIA

unaffected by quartz dilution, the CIX proves to be the most accurate indicator of weathering. The WIP, markedly affected by quartz dilution, decreases sharply in northern Angola. **E)** Among alfa indices: $\alpha^{Al}Na$ is the best indicator of weathering, although affected by recycling as well; $\alpha^{Al}Ca$ is affected by local occurrence of carbonate grains (e.g., Bengo sand); $\alpha^{Al}Mg$ and $\alpha^{Al}K$ show opposite behaviour, increasing in sands derived from felsic and mafic sources, respectively.

Figure 5. U-Pb age spectra of detrital zircons (age vs. frequencies plotted as Kernel Density Estimates using the *provenance* package of Vermeesch et al., 2016). Moçamedes desert sand in the south displays the same Damara and Namaqua peaks as Skeleton Coast sand mostly derived from the Orange River. Unimodal distributions with sharp Eburnean peak characterize sands of central Angola. Zircons from Cretaceous magmatic rocks are most common in Equimina beach. Spectra become broader and finally markedly multimodal in northern Angola, with prominent Pan-African, Namaqua, Eburnean, and Neoarchean clusters best displayed in Congo estuary sands.

Figure 6. Petrography of offshore sediments sampled during DSDP, ODP and Meteor expeditions. Shelfal sands to deep-sea sandy silts are variously enriched in planktonic foraminifers (Walvis Ridge), green glaucony (offshore Cunene mouth), benthic foraminifers (offshore Tapado mouth), and brown goethite ooids or pellets (offshore Congo mouth). Skeleton Coast dunes include basaltic rock fragments and clinopyroxene derived from the Orange River; the Congo River carries pure quartzose sand. Water depths are indicated; white circle for scale = 250 μm.

Figure 7. The effects of weathering and recycling on surface textures of sand grains. A,B) Numerous etch pits and re-entrants commonly filled with clay "plasma" testify to intense weathering even of quartz and other durable grains in river sands of northern Angola. Note strong leaching and deep penetration of iron-stained clay in: C) monocrystalline quartz; D) polycrystalline quartz; E) microcline. F,G) Abundance of rounded quartz grains testifies to extensive recycling of

Meso-Cenozoic siliciclastic units in the Cuanza and Congo catchments. All photos with crossed polars; blue bar for scale = 250 μm.

Figure 8. Inability of chemical indices to effectively single out weathering control from the effects of provenance, recycling, and hydraulic sorting in Angolan river sands. Both multivariate observations (points) and variables (rays) are displayed in the compositional biplot (Gabriel, 1971). Mobile alkali and alkaline earth elements largely reflect their original concentration in source-rock lithologies, and thus the CIA and its variants correlate poorly with latitude; α^{Al}Mg, α^{Al}Ca and α^{Al}Sr (higher for felsic sources) anticorrelate with α^{Al}K, α^{Al}Rb and α^{Al}Ba (higher for mafic sources). Being affected by quartz dilution, the WIP decreases markedly toward the equator reflecting the combined effect of recycling and weathering. The more reliable indicator of weathering is α^{Al}Na. The Eu anomaly tends to become more negative with weathering, but also with recycling and in sands derived from more felsic source rocks or in placer lags. The hydraulic-sorting effect is displayed by placer and semiplacer deposits formed at the Catumbela and Inamangando mouths (symbols with purple outline). Some beaches and a few river sands (e.g., Bengo, Longa; symbols with yellow outline) contain intrabasinal or extrabasinal carbonate grains and thus plot lower in the diagram because of their very low α^{Al}Ca (and low α^{Al}Sr).

Table 1. Key petrographic, heavy-mineral, and geochemical parameters of Angolan passive-margin sands. N° = number of samples; Qz = quartz; KF = K-feldspar; Pl = plagioclase; L = aphanitic lithic grains (Lvm = volcanic and metavolcanic; Lsm = sedimentary and metasedimentary; Lm = high-rank metamorphic); MI* = metamorphic index; HM = heavy minerals; tHMC = transparent heavy-mineral concentration; ZTR = zircon + tourmaline + rutile; Ep = epidote; Grt = garnet; St = staurolite; Ky = kyanite; Amp = amphibole; Px = pyroxene; &tHM = other transparent heavy minerals (apatite, titanite, and rare sillimanite, andalusite, olivine, barite, monazite, allanite, or scheelite). Chemical weathering indices cannot be calculated reliably for offshore sediments

containing abundant intrabasinal grains and authigenic minerals, including calcareous and non-calcareous allochems, glaucony, phosphates, sulphates, or iron ooids.

REFERENCES

Al-Hajri, Y., White, N., Fishwick, S., 2009. Scales of transient convective support beneath Africa. Geology, 37, 883-887.

Alberti, A., Piccirillo, E.M., Bellieni, G., Civetta, L., Comin-Chiaramonti, P., Morais, E.A.A., 1992. Mesozoic acid volcanics from southern Angola: petrology, Sr-Nd isotope characteristics and correlation with acid stratoid volcanic suites of the Paranà basin (southeastern Brazil). European Journal of Mineralogy, 4, 597-604.

Andò, S., Vignola, P., Garzanti, E., 2011. Raman counting: a new method to determine provenance of silt Rendiconti Lincei Scienze Fisiche e Naturali, 22, 327-347.

Andò, S., Garzanti, E., Padoan, M., Limonta, M., 2012. Corrosion of heavy minerals during weathering and diagenesis: a catalog for optical analysis. In: von Eynatten, H., Critelli, S., Ingersoll, R.V., Weltje, G.J. (Eds.), Actualistic Models of Sediment Generation. Sedimentary Geology, 280, 165-178.

Andò, S., Morton, A., Garzanti, E. 2014. Metamorphic grade of source rocks revealed by chemical fingerprints of detrital amphibole and garnet. In: Scott, R.A., Smyth. H.R., Morton, A.C., Richardson, N. (Eds.), Sediment provenance studies in hydrocarbon exploration and production. Geological Society London, Special Publication 386, 351-371.

Anka, Z., Seranne, M., Di Primio, R., 2010. Evidence of a large upper-Cretaceous depocentre across the continent-ocean boundary of the Congo-Angola basin. Implications for palaeo-drainage and potential ultra-deep source rocks. Marine and Petroleum Geology, 27, 601-611.

Basu, A., 1985. Influence of climate and relief on compositions of sands released at source areas. In: Zuffa, G.G. (Ed.), Provenance of arenites. Reidel, Dordrecht, NATO ASI Series, 148, pp. 1-18.

Bate, R.H., Cameron, N., Brandão, M.G.P., 2001. Lower Cretaceous (pre-salt) lithostratigraphy of the Kwanza Basin, Angola. Newsletters on Stratigraphy, 38, 117-127.

Becker, T., Schreiber, U., Kampunzu, A.B., Armstrong, R., 2006. Mesoproterozoic rocks of Namibia and their plate tectonic setting. Journal of African Earth Sciences, 46, 112-140.

Blatt, H. 1967. Provenance determinations and recycling of sediments. Journal of Sedimentary Petrology, 37, 1031-1044.

Breyer, J.A., Bart, H.A., 1978. The composition of fluvial sands in a temperate semiarid region. Journal of Sedimentary Petrology, 48, 1311-1320.

Castillo-Oliver, M., Galí, S., Melgarejo, J.C., Griffin, W.L., Belousova, E., Pearson, N.J., Watangua, M., O'Reilly, S.Y., 2016. Trace-element geochemistry and U–Pb dating of perovskite in kimberlites of the Lunda Norte province (NE Angola): petrogenetic and tectonic implications. Chemical Geology, 426, 118-134.

Chaboureau, A.C., Guillocheau, F., Robin, C., Rohais, S., Moulin, M., Aslanian, D., 2013. Paleogeographic evolution of the central segment of the South Atlantic during Early Cretaceous times: paleotopographic and geodynamic implications. Tectonophysics, 604, 191-223.

Comin-Chiaramonti, P., De Min, A., Girardi, V.A.V., Ruberti, E., 2011. Post-Paleozoic magmatism in Angola and Namibia: a review. In: Beccaluva, L., Bianchini, G., Wilson, M. (Eds.), Volcanism and Evolution of the African Lithosphere. Geological Society of America, Special Paper 478, pp. 223-247.

Condie, K.C., Dengate, J., Cullers, R.L., 1995. Behavior of rare earth elements in a paleoweathering profile on granodiorite in the Front Range, Colorado, USA. Geochimica ec Cosmochimica Acta, 59, 279-294.

De Carvalho, H., Tassinari, C., Alves, P.H., Guimarães, F., Simões, M.C., 2000. Geochronological review of the Precambrian in western Angola: links with Brazil. Journal of African Earth Sciences, 31, 383-402.

Delhal, J., Ledent, D., Torquato, J.R., 1976. Nouvelles données géochronologiques relatives au complexe gabbro-noritique et charnockitique du bouclier du Kasai et à son prolongement en Angola. Ann. Société Géologique Belgique, 99, 211-226.

De Waele, B., Johnson, S.P., Pisarevsky, S.A., 2008. Palaeoproterozoic to Neoproterozoic growth and evolution of the eastern Congo Craton: its role in the Rodinia puzzle. Precambrian Research, 160, 127-141.

Dickinson, W.R. 1985. Interpreting provenance relations from detrital modes of sandstones. In: Zuffa, G.G. (Ed.), Provenance of arenites. Dordrecht, Reidel, NATO ASI Series, 148, pp. 333-361.

Dinis, P., Huvi, J., Cascalho, J., Garzanti, E., Vermeesch, P., Callapez, P., 2016. Sand-spits systems from Benguela region (SW Angola). An analysis of sediment sources and dispersal from textural and compositional data. Journal of African Earth Sciences, 117, 171-182.

Dinis, P., Garzanti, E., Vermeesch, P., Huvi, J., 2017. Climatic zonation and weathering control on sediment composition (Angola). Chemical Geology, 467, 110-121.

Diniz, A.C., 2006. Características mesológicas de Angola : descrição e correlação dos aspectos fisiográficos, dos solos e da vegetação das zonas agrícolas angolanas. Lisboa, Instituto Português de Apoio ao Desenvolvimento, 546 p.

Drüppel, K., Littmann, S., Romer, R.L., Okrusch, M., 2007. Petrology and isotope geochemistry of the Mesoproterozoic anorthosite and related rocks of the Kunene Intrusive Complex, NW Namibia. Precambrian Research, 156, 1-31.

Dupré, B., Gaillardet, J., Rousseau, D., Allègre, C.J., 1996. Major and trace elements of river-borne material: the Congo Basin. Geochimica et Cosmochimica Acta, 60, 1301-1321.

Ernst, R.E., Pereira, E., Hamilton, M.A., Pisarevsky, S.A., Rodriques, J., Tassinari, C.C.G., Teixeira, W., Van-Dunem, V., 2013. Mesoproterozoic intraplate magmatic 'barcode' record of the Angola portion of the Congo Craton: newly dated magmatic events at 1505 and 1110 Ma and implications for Nuna (Columbia) supercontinent reconstructions. Precambrian Research, 230, 103-118.

Ewart, A., Marsh, J.S., Milner, S.C., Duncan, A.R., Kamber, B.S., Armstrong, R.A., 2004. Petrology and geochemistry of Early Cretaceous bimodal continental flood volcanism of the NW Etendeka, Namibia. Journal of Petrology, 45, 59-138.

Feio, M., 1981. O relevo do sudoeste de Angola; estudo de geomorfologia. Memórias da Junta de Investigações Científicas do Ultramar, 67, 1-67.

Folk, R.L., 1980. Petrology of sedimentary rocks. Hemphill, Austin. 185 p.

Fort, X., Brun, J.P., Chauvel, F., 2004. Salt tectonics on the Angolan margin, synsedimentary deformation processes. American Association of Petroleum Geologists Bulletin, 88, 1523-1544.

Franke, D., 2013. Rifting, lithosphere breakup and volcanism: comparison of magma-poor and volcanic rifted margins. Marine and Petroleum Geology, 43, 63-87.

Franzinelli, E., Potter, P.E. 1983. Petrology, chemistry, and texture of modern river sands, Amazon River system. The Journal of Geology, 91, 23-39.

Frimmel, H.E., Tack, L., Basei, M.S., Nutman, A.P., Boven, A., 2006. Provenance and chemostratigraphy of the Neoproterozoic West Congolian Group in the Democratic Republic of Congo. Journal of African Earth Sciences, 46, 221-239.

Frimmel, H.E., Basei, M.S., Gaucher, C., 2011. Neoproterozoic geodynamic evolution of SW-Gondwana: a southern African perspective. Interanational Journal of Earth Sciences, 100, 323-354.

Gabriel, K.R., 1971. The biplot graphic display of matrices with application to principal component analysis.

Biometrika, 58, 453-467.

Gaillardet, J., Dupré, B., Allègre, C.J., 1999. Geochemistry of large river suspended sediments: silicate weathering or recycling tracer? Geochimica et Cosmochimica Acta, 63, 4037-4051.

Galehouse, J.S., 1971. Point counting. In: Carver, R.E. (Ed.), Procedures in sedimentary petrology. Wiley, New York, pp. 385-407.

Garzanti, E., 2016. From static to dynamic provenance analysis – Sedimentary petrology upgraded. In: Caracciolo, L., Garzanti, E., von Eynatten, H., Weltje, G.J. (Eds.), Sediment generation and provenance: processes and pathways. Sedimentary Geology, 336, 3-13.

Garzanti E., 2017. The maturity myth in sedimentology and provenance analysis. Journal of Sedimentary Research, 87, 353-365.

Garzanti, E., Andò, S., 2007. Heavy-mineral concentration in modern sands: implications for provenance interpretation. In: Mange, M.A., Wright, D.T. (Eds.), Heavy minerals in use. Elsevier, Amsterdam, Developments in Sedimentology Series, 58, 517-545.

Garzanti, E., Resentini, A., 2016. Provenance control on chemical indices of weathering (Taiwan river sands). In: Caracciolo, L., Garzanti, E., von Eynatten, H., Weltje, G.J. (Eds.), Sediment generation and provenance: processes and pathways.Sedimentary Geology, 336, 81-95.

Garzanti, E., Vezzoli, G. 2003. A classification of metamorphic grains in sands based on their composition and grade. Journal of Sedimentary Research, 73, 830-837.

Garzanti, E., Andò, S., Vezzoli, G., 2009. Grain-size dependence of sediment composition and environmental bias in provenance studies. Earth and Planetary Science Letters, 277, 422-432.

Garzanti, E., Andó, S., France-Lanord, C., Vezzoli, G., Najman, Y., 2010. Mineralogical and chemical variability of fluvial sediments. 1. Bedload sand (Ganga-Brahmaputra, Bangladesh). Earth and Planetary Science Letters, 299, 368-381.

Garzanti, E., Andò, S., Vezzoli, G., Lustrino, M., Boni, M., Vermeesch, P., 2012a. Petrology of the Namib sand sea: long-distance transport and compositional variability in the wind-displaced Orange Delta. Earth-Science Reviews, 11, 173-189.

Garzanti, E., Resentini, A., Vezzoli, G., Andò, S., Malusà, M., Padoan, M., 2012b. Forward compositional modelling of Alpine orogenic sediments. In: von Eynatten, H., Critelli, S., Ingersoll, R.V., Weltje, G.J., Actualistic Models of Sediment Generation. Sedimentary Geology, 280, 149-164.

Garzanti, E., Padoan, M., Andò, S., Resentini, A., Vezzoli, G., Lustrino, M., 2013. Weathering and relative durability of detrital minerals in equatorial climate: sand petrology and geochemistry in the East African Rift. The Journal of Geology, 121, 547-580.

Garzanti, E., Vermeesch, P., Padoan, M., Resentini, A., Vezzoli, G., Andò, S., 2014a. Provenance of passive-margin sand (southern Africa). The Journal of Geology, 122, 17-42.

Garzanti, E., Padoan, M., Setti, M., López-Galindo, A., Villa, I.M., 2014b. Provenance versus weathering control on the composition of tropical river mud (southern Africa). Chemical Geology, 366, 61-74.

Garzanti, E., Vermeesch, P., Andò, S., Lustrino, M., Padoan, M. and Vezzoli, G., 2014c. Ultra-long distance littoral transport of Orange sand and provenance of the Skeleton Coast Erg (Namibia). Marine Geology, 357, 25-36.

Garzanti, E., Resentini, A., Andò, S., Vezzoli, G., Vermeesch, P., 2015. Physical controls on sand composition and relative durability of detrital minerals during long-distance littoral and eolian transport (coastal Namibia). Sedimentology, 62, 971-996.

Garzanti, E., Dinis, P., Vermeesch, P., Andò, S., Hahn, A., Huvi, J., Limonta, M., Padoan, M., Resentini, A., Rittner, M., Vezzoli, G., 2017. Sedimentary processes controlling ultralong cells of littoral transport : placer formation and termination of the Orange sand highway in southern Angola. Sedimentology, doi: 10.1111/sed.12387.

Gindre-Chanu, L., Warren, J.K., Puigdefabregas, C., Sharp, I.R., Peacock, D.C.P., Swart R., Poulsen, R., Ferreira, H., Henrique, L., 2015. Diagenetic evolution of Aptian evaporites in the Namibe Basin (south-west Angola). Sedimentology, 62, 204-233

Gindre-Chanu, L., Perri E., Sharp, I.R., Peacock, D.C.P., Swart, R., Poulsen R., Ferreira, H., Machado, V., 2016. Origin and diagenetic evolution of gypsum and microbialitic carbonates in the Late Sag of the Namibe Basin (SW Angola). Sedimentary Geology, 342, 133-153.

Giresse, P., Hoang, C.T., Kouyoumontzakis, G., 1984. Analysis of vertical movements deduced from a geochronological study of marine Pleistocene deposits, southern coast of Angola. Journal of African Earth Sciences, 2, 177-187.

Giresse, P., 2005. Mesozoic–Cenozoic history of the Congo Basin. Journal of African Earth Sciences, 43, 301-315.

Goscombe, B., Gray, D.R., 2007. The Coastal Terrane of the Kaoko Belt, Namibia: outboard arc-terrane and tectonic significance. Precambrian Research, 155, 139-158.

Goscombe, B., Hand, M., Gray, D., Mawby, J., 2003. The metamorphic architecture of a transpressional orogen, the Kaoko belt, Namibia. Journal of Petrology, 44, 679-711.

Gray, D.R., Foster, D.A., Meert, J.G., Goscombe, B.D., Armstrong, R., Trouw, R.A.J., Passchier, C.W., 2008. A Damara Orogen perspective on the assembly of southwestern Gondwana. In: Pankhurst, R.J., Trouw, R.A.J., Brito Neves, B.B., De Wit, M.J. (Eds.), West Gondwana: pre-Cenozoic correlations across the South Atlantic region. Geological Society of London, Special Publication 294, 257-278.

Green, P.F., Machado, V., 2017. Pre-rift and synrift exhumation, post-rift subsidence and exhumation of the onshore Namibe Margin of Angola revealed from apatite fission track analysis. In: Sabato-Ceraldi, T., Hodgkinson, R.A., Backe, G. (Eds.), Petroleum Geoscience of the West Africa Margin. Geological Society London, Special Publication 438, 99-118.

Griffin, W.L., Powell, W.J., Pearson, N.J., O'Reilly, S.Y., 2008. GLITTER: data reduction software for laser ablation ICP-MS. Laser Ablation-ICP-MS in the earth sciences. Mineralogical association of Canada short course series, 40, 204-207

Guilcher, A., Medeiros, C.A., Matos, J.E., Oliveira, J.T., 1974. Les restingas (fléches littorales) d'Angola, spécialment celles du sud et du centre. Finisterra, 9, 117-211.

Guiraud, M., Buta-Neto, A., Quesne, D., 2010. Segmentation and differential post-rift uplift at the Angola margin as recorded by the transform-rifted Benguela and oblique-to-orthogonal-rifted Kwanza basins. Marine and Petroleum Geology, 27, 1040-1068.

Haddon, I.G., McCarthy, T.S., 2005. The Mesozoic–Cenozoic interior sag basins of Central Africa: the Late-Cretaceous–Cenozoic Kalahari and Okavango basins. Journal of African Earth Sciences, 43, 316-333.

Hardman-Mountford, N.J., Richardson, A.J., Agenbag, J.J., Hagen, E., Nykjaer, L., Shillington, F.A., Villacastin, C., 2003. Ocean climate of the South East Atlantic observed from satellite data and wind models. Progress in Oceanography, 59, 181-221.

Heilbron, M., Valeriano, C.M., Tassinari, C.C.G., Almeida, J., Tupinambá, M., Siga, O., Trouw, R., 2008. Correlation of Neoproterozoic terranes between the Ribeira Belt, SE Brazil and its African counterpart: comparative tectonic evolution and open questions. In: Pankhurst, R.J., Trouw, R.A.J., Brito Neves, B.B., Wit, M.J. (Eds.), West Gondwana: Pre-Cenozoic Correlations Across the South Atlantic Region. Geological Society London, Special Publication 294, pp. 211-237.

Hijmans, R.J., Cameron, S.E., Parra, J.L., Jones, P.G., Jarvis, A., 2005. Very high resolution interpolated climate surfaces for global land areas. International Journal of Climatology, 25, 1965-1978.

Holisticos, 2012. Environmental impact study for the rehabilitation and expansion of the Cambambe hydroelectric power plant. https://www.miga.org/documents/Angola_Cambambe_HPP_EIS.pdf

Hubert, J.F., 1962. A zircon–tourmaline–rutile maturity index and the interdependence of the composition of heavy mineral assemblages with the gross composition and texture of sandstones. Journal of Sedimentary Petrology, 32, 440-450.

Hudec, M.R., Jackson, M.P.A., 2002. Structural segmentation, inversion, and salt tectonics on a passive margin: evolution of the Inner Kwanza Basin, Angola. Geological Society of America Bulletin, 114, 1222-1244.

Hudec, M.R., Jackson, M.P.A., 2004. Regional restoration across the Kwanza Basin, Angola: salt tectonics triggered by repeated uplift of a metastable passive margin. American Association of Petroleum Geologists Bulletin, 88, 971-990.

Ingersoll, R.V., Bullard, T.F., Ford, R.L., Grimm, J.P., Pickle, J.D., Sares, S.W., 1984. The effect of grain size on detrital modes: a test of the Gazzi-Dickinson point-counting method. Journal of Sedimentary Petrology, 54, 103-116.

Jackson, M.P.A, Hudec, M.R., Hegarty, K.A., 2005. The great West African Tertiary coastal uplift: fact or fiction? A perspective from the Angolan divergent margin. Tectonics, 24, TC6014, doi:10.1029/2005TC001836.

Jacobs, J., Pisarevsky, S., Thomas, R.J., Becker, T., 2008. The Kalahari Craton during the assembly and dispersal of Rodinia. Precambrian Research, 160, 142-158.

James, C.W., Mack, G.H., Suttner, L.J., 1981. Relative alteration of microcline and sodic plagioclase in semi-arid and humid climates. Journal of Sedimentary Petrology, 51, 151-164.

Johnsson, M.J., 1993. The system controlling the composition of clastic sediments. In: Johnsson, M.J., Basu, A. (Eds.), Processes controlling the composition of clastic sediments. Geological Society of America, Special Paper 284, pp. 1-19.

Johnsson, M.J., Stallard, R.F., Meade, R.H., 1988. First-cycle quartz arenites in the Orinoco River basin: Venezuela and Colombia. The Journal of Geology, 96, 263-277.

Johnsson, M.J., Stallard, R.F., Lundberg, N., 1991. Controls on the composition of fluvial sands from a tropical weathering environments: sands of the Orinoco River drainage basin, Venezuela and Colombia. Geological Society of America Bulletin, 103, 1622-1647.

Köhn, M., 1928. Bemerkungen zur mechanischen Bodenanalyse. III. Ein neuer Pipettapparat. Zeitschrift für Pflanzenernährung, Düngung, Bodenkunde, 11, 50-54.

Komar, P.D., 2007. The entrainment, transport and sorting of heavy minerals by waves and currents In: Mange, M.A., Wright, D.T. (Eds.), Heavy minerals in use. Elsevier, Amsterdam, Developments in Sedimentology Series, 58, pp. 3-48.

Komar, P.D., Li, Z., 1988. Application of grain-pivoting and sliding analyses to selective entrainment of gravel and to flow-competence evaluations. Sedimentology, 35, 681-695.

Kostianoy, A.G., Lutjeharms, J.R.E., 1999. Atmospheric effects in the Angola-Benguela frontal zone. Journal of Geophysical Research: Oceans, 104, 20963-20970.

Lancaster, N., 2002. How dry was dry? Late Pleistocene palaeoclimates in the Namib desert. Quaternary Science Reviews, 21, 769-782.

Lass, H.U., Mohrholz, V., 2008. On the interaction between the subtropical gyre and the Subtropical Cell on the shelf of the SE Atlantic. Journal of Marine Systems, 74, 1-43-

Leturmy, P., Lucazeau, F., Brigaud, F., 2003. Dynamic interactions between the Gulf of Guinea passive margin and the Congo River drainage basin: 1. Morphology and mass balance. Journal of Geophysical Research, 108(B8), 2383, doi:10.1029/2002JB001927.

Lopes, F.C., Pereira, A.J., Mantas, V.M., Mpengo, H.K., 2016. Morphostructural characterization of the western edge of the Huila Plateau (SW Angola), based on remote sensing techniques. Journal of African Earth Sciences, 117, 114-123.

Macgregor, D.S., 2013. Late Cretaceous–Cenozoic sediment and turbidite reservoir supply to South Atlantic margins. Geological Society London, Special Publications, 369, 109-128.

Marton, G.L., Tari, G.C., Lehmann, C.T., 2000. Evolution of the Angolan passive margin, West Africa, with emphasis on post-salt structural styles. In: Mohriak, W., Talwani, M. (Eds.), Atlantic Rifts and Continental Margins. American Geophysical Union, Geophysical Monograph Series, 115, pp. 129-149.

Marzoli, A., Melluso, L., Morra, V., Renne, P.R., Sgrosso, I., D'Antonio, M., Morais, L.D., Morais, E.A.A., Ricci, G., 1999. Geochronology and petrology of Cretaceous basaltic magmatism in the Kwanza basin (western Angola), and relationships with the Paranà-Etendeka continental flood basalt province. Journal of Geodynamics , 28, 341-356.

Masse, P., Laurent, O., 2016. Geological exploration of Angola from Sumbe to Namibe: a review at the frontier between geology, natural resources and the history of geology. Comptes Rendus Geoscience, 348, 80-88.

Mayer, A., Hofmann, A.W., Sinigoi, S., Morais, E., 2004. Mesoproterozoic Sm–Nd and U–Pb ages for the Kunene Anorthosite Complex of SW Angola. Precambrian Research, 133, 187-206.

McBride, E.F., 1985, Diagenetic processes that affect provenance determinations in sandstones. In: Zuffa, G.G. (Ed.), Provenance of Arenites. Reidel, Dordrecht, NATO ASI Series, 148, 95-113.

McCourt, S., Armstrong, R.A., Jelsma, H., Mapeo, R.B.M, 2013. New U–Pb SHRIMP ages from the Lubango region, SW Angola: insights into the Palaeoproterozoic evolution of the Angolan Shield, southern Congo Craton, Africa. Journal of the Geological Society London, 170, 353-363.

McDonough, W.F., Sun, S.S., 1995. The composition of the Earth. Chemical Geology, 120, 223-253.

Mohriak W.U., Rosendahl, B.R., 2003. Transform zones in the South Atlantic rifted continental margins. In: Storti, F., Holdsworth, R.E., Salvini, F. (Eds), Intraplate Strike-Slip Deformation Belts. Geological Society London, Special Publication 210, pp. 211-228.

Morton, A.C., Hallsworth, C., 2007. Stability of detrital heavy minerals during burial diagenesis. In: Mange, M.A., Wright, D.T. (Eds.), Heavy Minerals in Use. Developments in Sedimentology Series, 58, 215-245.

Moulin, M., Aslanian, D., Olivet, J.L., Contrucci, I., Matias, L., Géli, L., Klingelhoefer, F., Nouzé, H., Réhault, J.P., Unternehr, P., 2005. Geological constraints on the evolution of the Angolan margin based on reflection and refraction seismic data (ZaïAngo project). Geophysical Journal International, 162, 793-810.

Moulin, M., Aslanian, D., Unternehr, P., 2010. A new starting point for the South and Equatorial Atlantic Ocean. Earth-Science Reviews, 98, 1-37.

Nesbitt, H.W., Young, G.M., 1982. Early Proterozoic climates and plate motions inferred from major element chemistry of lutites. Nature, 299, 715-717.

Neto, M.M.G.N., 1960. Estratigrafia da região de entre Benguela e o Cabo de S.^{ta} Maria (Angola). Revista do Museu e Laboratorio Mineralogico e Geologico, Faculdade de Ciencias de Coimbra, 19 p.

Parker, A. 1970. An index of weathering for silicate rocks. Geological Magazine, 107, 501-504.

Pereira, E., Tassinari, C.C.G., Rodrigues, J.F., Van-Dúnem, M.V., 2011. New data on the deposition age of the volcano-sedimentary Chela Group and its Eburnean basement: implications to post-Eburnean crustal evolution of the SW of Angola. Comunicações Geológicas, 98, 29-40.

Péron-Pinvidic, G., Manatschal, G., Masini, E., Sutra, E., Flament J.M., Haupert, I., Unternehr, P., 2017. Unravelling the along-strike variability of the Angola–Gabon rifted margin: a mapping approach. In: Sabato-Ceraldi, T., Hodgkinson, R.A., Backe, G. (Eds.), Petroleum Geoscience of the West Africa Margin. Geological Society London, Special Publication 438, 49-76.

Potter, P.E., 1994. Modern sands of South America: composition, provenance and global significance. Geologische Rundschau, 83, 212-232.

Pritchard, D., Roberts, G.G., White, N.J., Richardson, C.N., 2009. Uplift histories from river profiles. Geophysical research letters, 36, L24301, doi:10.1029/2009GL040928.

Quesne, D., Buta-Neto, A., Benard, D., Guiraud, G., 2009. Distribuition of Albian clastic deposits in the Benguela basin (Angola): evidence of a Benguela palaeocurrent? Bulletin de la Société Géologique de France, 180, 117-129.

Renne, P.R., Glen, J.M., Milner, S.C., Duncan, A.R., 1996. Africa age of Etendeka flood volcanism and associated intrusions in southwestern Africa. Geology, 24, 659-662.

Roberts, G.G., White, N., 2010. Estimating uplift rate histories from river profiles using African examples. Journal of Geophysical Research, 115, B02406. doi:10.1029/2009JB006692.

Rudnick, R.L., Gao, S., 2003. Composition of the continental crust. In: Rudnick, R.L., Holland, H.D., Turekian, K.K. (Eds.), Treatise on geochemistry, 3, The crust. Elsevier Pergamon, Oxford, pp. 1-64.

Russell, R.D., 1937. Mineral composition of Mississippi River sands. Geological Society of America Bulletin, 48, 1307-1348.

Sabato-Ceraldi, T., Green, D., 2017. Evolution of the South Atlantic lacustrine deposits in response to Early Cretaceous rifting, subsidence and lake hydrology. In: Sabato-Ceraldi, T., Hodgkinson, R.A., Backe, G. (Eds.), Petroleum Geoscience of the West Africa Margin. Geological Society, London, Special Publication 438, 77-98.

Schlüter, T. 2008. Geological Atlas of Africa. Springer, Heidelberg, 307 p.

Schneider, S., Hornung, J., Hinderer, M., Garzanti, E., 2016. Petrography and geochemistry of modern river sediments in an equatorial environment (Albertine Rift, Uganda) – Implications for weathering and provenance. In: Caracciolo, L., Garzanti, E., von Eynatten, H., Weltje, G.J. (Eds.), Sediment generation and provenance: processes and pathways. Sedimentary Geology, 336, 106-119.

Schulz, H.D., Beese, D., Breitzke, M., Brück, L., Brügger, B., Dahmke, A., Dehning, K., Diekamp, V., Dünner, B., Ehrhardt, I., Gerlach, H., Giese, M., Glud, R., Gumprecht, R., Gundersen, J., Henning, R., Hinrichs, S., Petermann, H., Richter, M., Sagemann, J., Schmidt, W., Schneider, R., Scholz, M., Segl, M., Werner, U., Zabel, M., 1992. Bericht und erste Ergebnisse über die Meteor-Fahrt M20/2, Abidjan-Dakar, 27.12.1991-3.2.1992. Berichte aus dem Fachbereich Geowissenschaften der Universität Bremen, 025. Department of Geosciences, Bremen University, 25, 175 p.

Schulz, H.D., Adegbie, A.T., Boehme, S., Brune, A., Däumler, K., Dehning, K. …., Funk, J., 1998. Report and preliminary results of METEOR-Cruise M 41/1, Málaga - Libreville, 13.2.-15.3.1998 with partial results of METEOR CRUISE 41/2 Libreville-Vitoria, 18.03.1998-15.4.1998. Berichte aus dem Fachbereich Geowissenschaften der Universität Bremen, 114, 124 p.

Séranne, M., Anka, Z., 2005. South Atlantic continental margins of Africa: a comparison of the tectonic vs climate interplay on the evolution of equatorial west Africa and SW Africa margins. Journal of African

Earth Sciences, 43, 283-300.

Shannon, L.V., Nelson, G., 1996. The Benguela: large scale features and processes and system variability. In: Wefer, G., Berger, W.H., Siedler, G., Webb, D.J. (Eds.), The South Atlantic: past and present circulation. Springer, Berlin, pp. 163-210.

Shukri, N.M., 1950. The mineralogy of some Nile sediments. Quarterly Journal of the Geological Society London, 105, 511-534.

Strganac, C., Salminen, J., Jacobs, L.L., Polcyn, M.J., Ferguson, K.M., Mateus, O., Schulp, A.S., Morais, M.L., Tavares; T. da S., Gonçalves, A.O., 2014. Carbon isotope stratigraphy, magnetostratigraphy, and ^{40}Ar/^{39}Ar age of the Cretaceous South Atlantic coast, Namibe Basin, Angola. Journal of African Earth Sciences, 99, 452-462.

Tack, L., Wingate, M.T.D., Liégeois, J.P., Fernandez-Alonso, M., Deblond, A., 2001. Early Neoproterozoic magmatism (1000–910 Ma) of the Zadinian and Mayumbian Groups (Bas-Congo): onset of Rodinia rifting at the western edge of the Congo craton. Precambrian Research, 110, 277-306.

Taylor, S.R., McLennan, S.M., 1995. The geochemical evolution of the continental crust. Reviews of Geophysics, 33, 241-265.

Vaughan, A.P., Pankhurst, R.J., 2008. Tectonic overview of the West Gondwana margin. Gondwana Research, 13, 150-162.

Velbel, M.A., Saad, M.K., 1991. Palaeoweathering or diagenesis as the principal modifier of sandstone framework composition? A case study from some Triassic rift-valley redbeds of eastern North America. Geological Society London, Special Publication 57, 91-99.

Vermeesch, P., Fenton, C.R., Kober, F., Wiggs, G.F.S., Bristow, C.S., Xu, S., 2010. Sand residence times of one million years in the Namib Sand Sea from cosmogenic nuclides. Nature Geosciences, 3, 862-865.

Vermeesch, P., Resentini, A., Garzanti, E., 2016. An R package for statistical provenance analysis. Sedimentary Geology, 336, 14-25.

Vermeesch, P., Rittner, M., Petrou, E., Omma, J., Mattinson, C, Garzanti, E., 2017. High throughput petrochronology and sedimentary provenance analysis by automated phase mapping and LAICPMS. Geochemistry, Geophysics, Geosystems, 18, doi.org/10.1002/2017GC007109.

Wefer, G., Bleil, U., Müller, P.J., Schulz, H.D., Berger, W.H., Brathauer, U., Brück, L., Dahmke, A., Dehning, K., Durate-Morais, M.L., Fürsich, F., Hinrichs, S., Klockgeter, K., Kölling, A., Kothe, C., Makaya, J.F., Oberhänsli, H., Oschmann, W., Posny, J., Rostek, F., Schmidt, H., Schneider, R.R., Segl, M., Sobiesiak, M., Soltwedel, T., Spieß, V., 1988. Bericht über die Meteor-Fahrt M6-6, Libreville - Las Palmas, 18.2.1988 - 23.3.1988. Berichte aus dem Fachbereich Geowissenschaften der Universität Bremen, 003. Department of Geosciences, Bremen University, 3, 97 p.

White, N., 2016. Geodynamics: surface sculpting by hidden agents. Nature Geoscience, 9, 867-869.

Figure 1

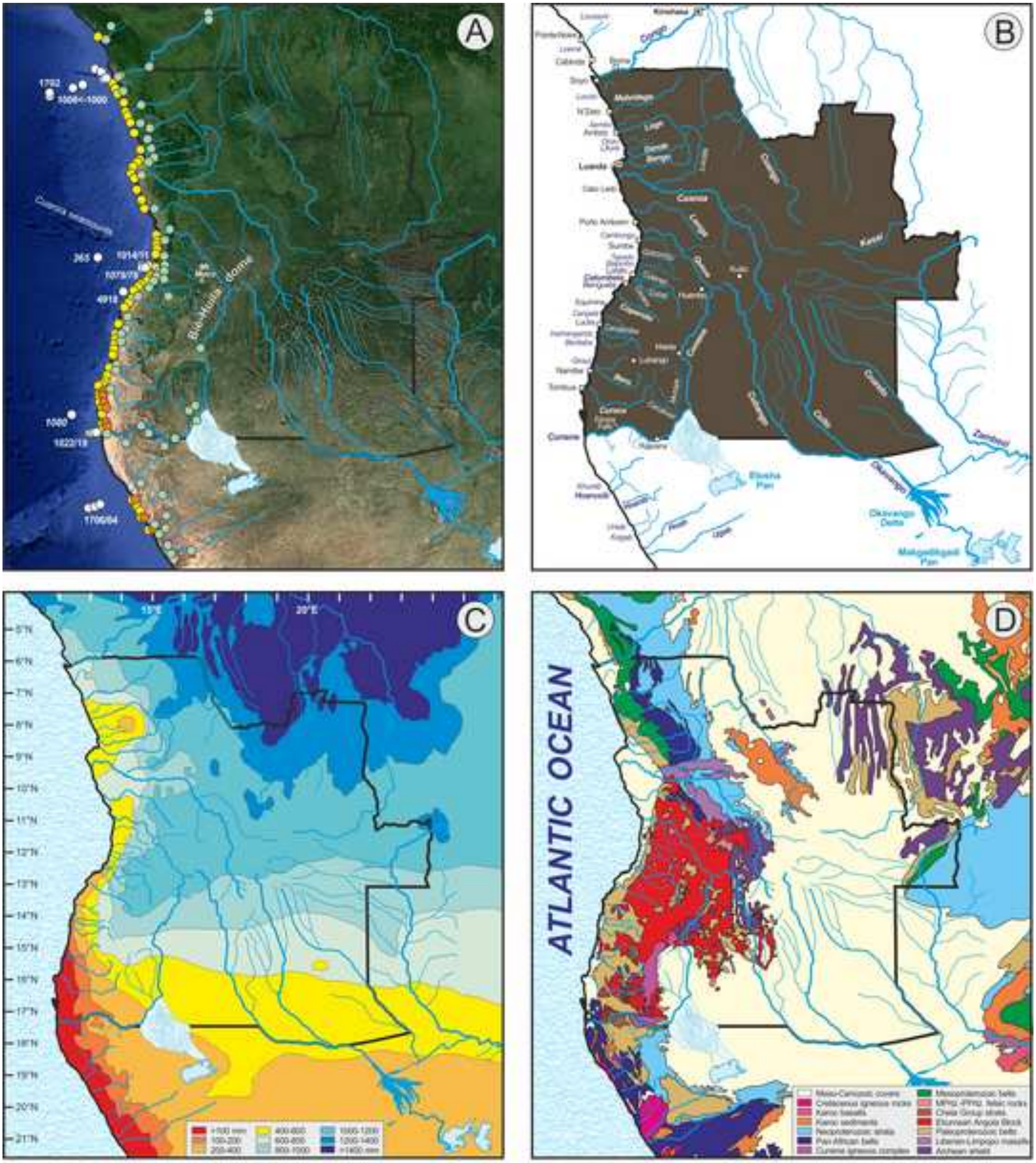

Figure 1 Angola

Figure 2

Click here to download high resolution image

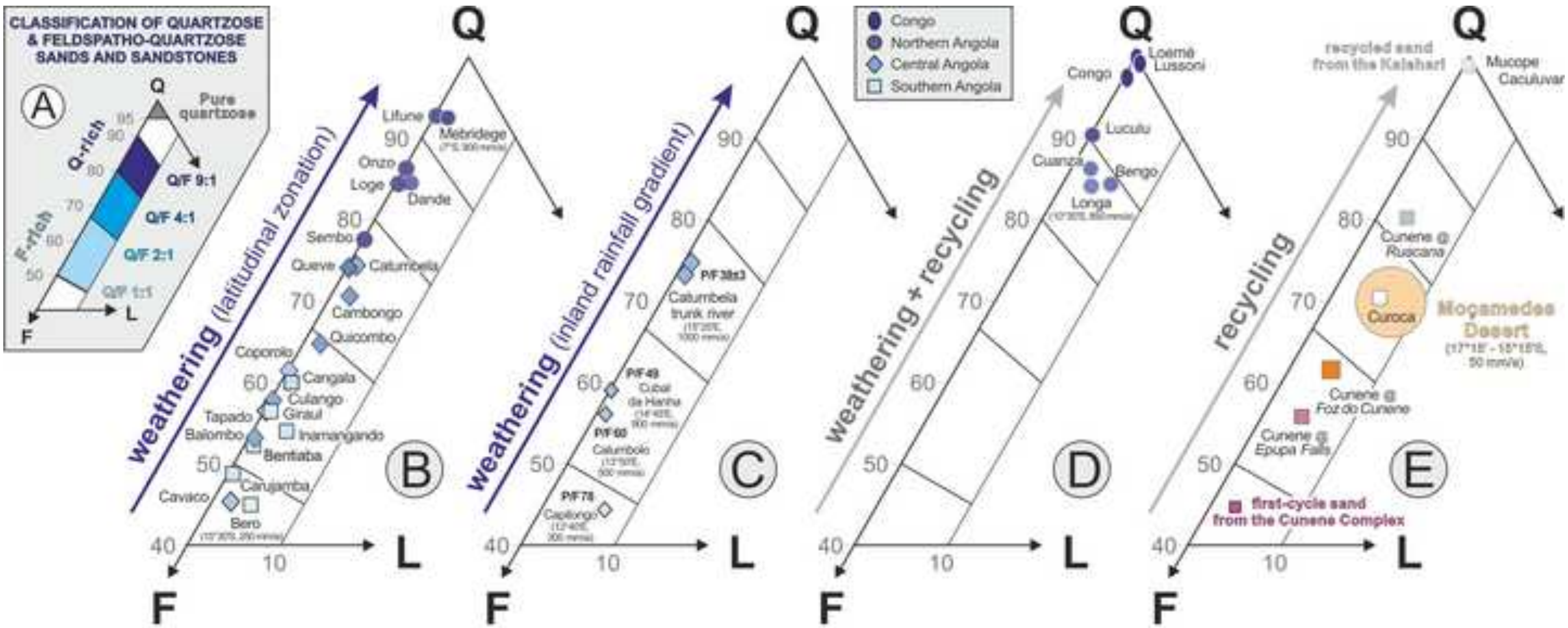

Figure 2 Angola

Figure 3
Click here to download high resolution image

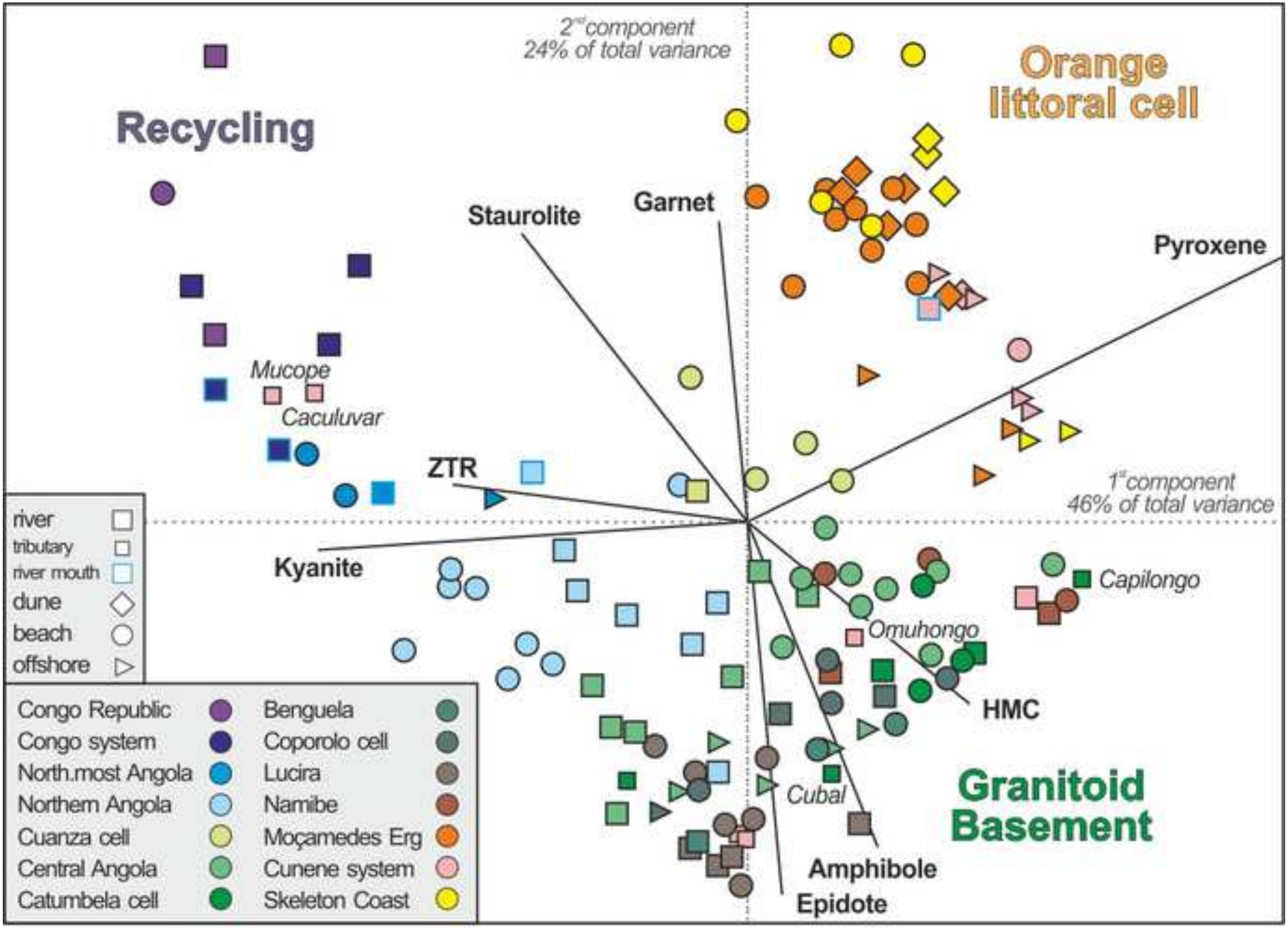

Figure 3 Angola

Figure 4

Click here to download high resolution image

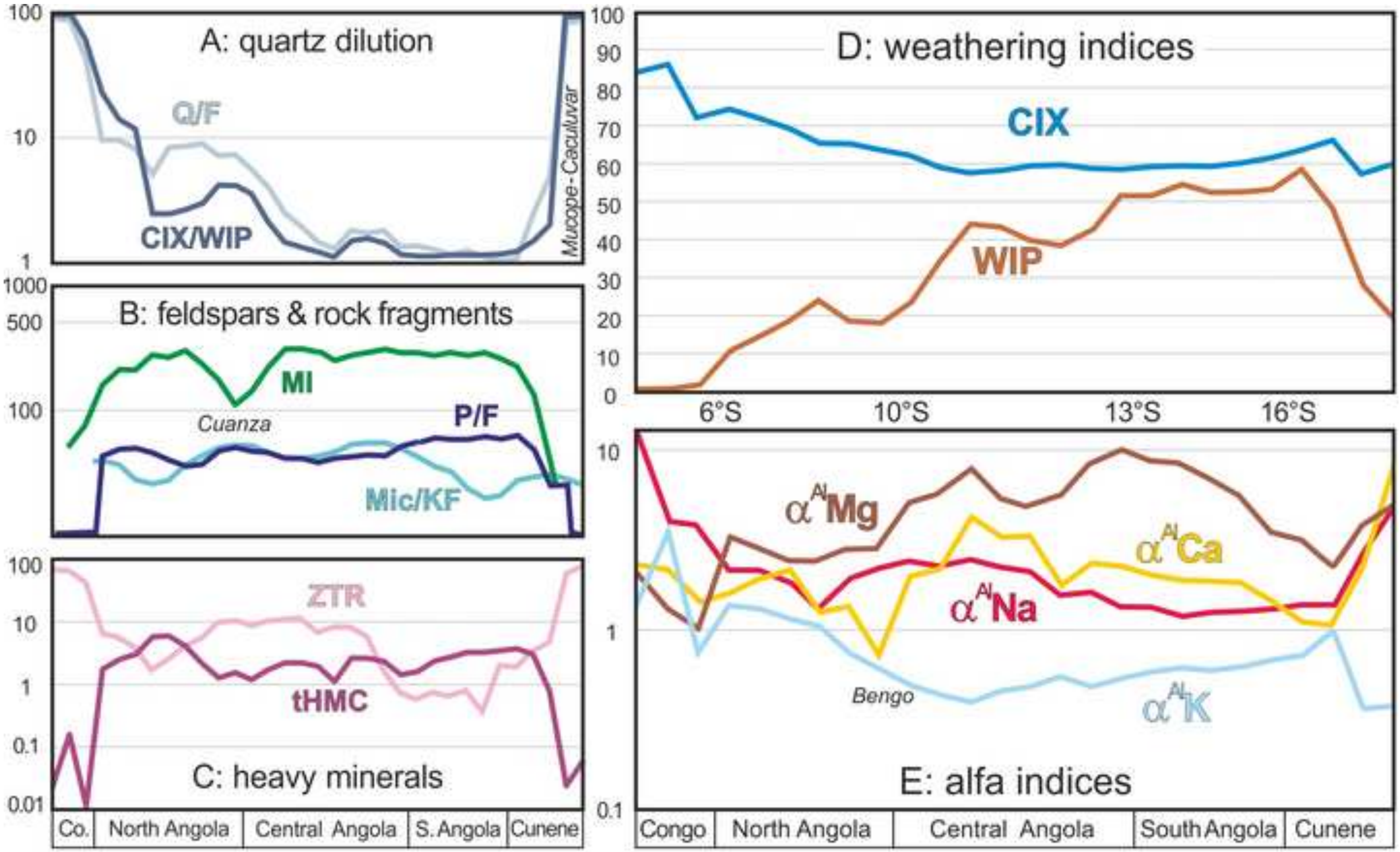

Figure 4 Angola

Figure 5

Click here to download high resolution image

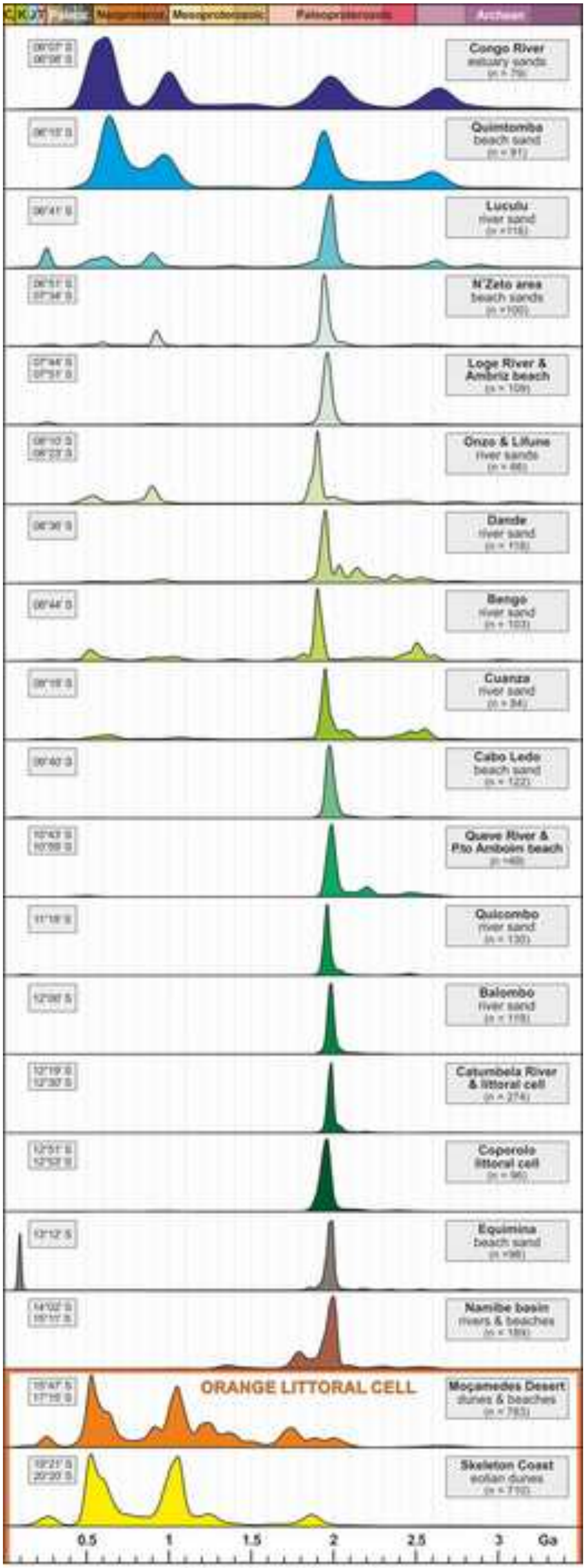

Figure 5 Angola

Figure 6
Click here to download high resolution image

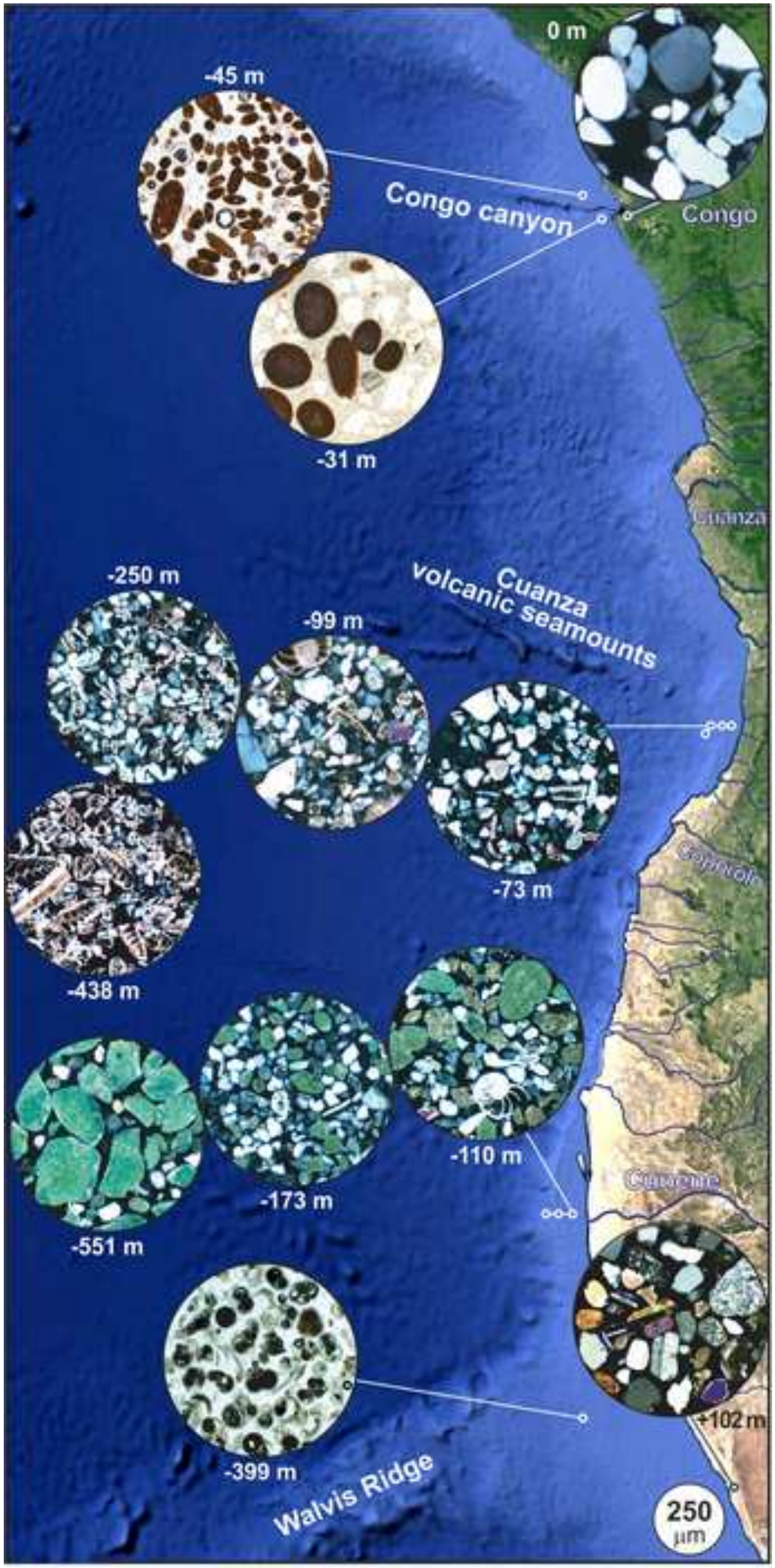

Figure 6 Angola

Figure 7
Click here to download high resolution image

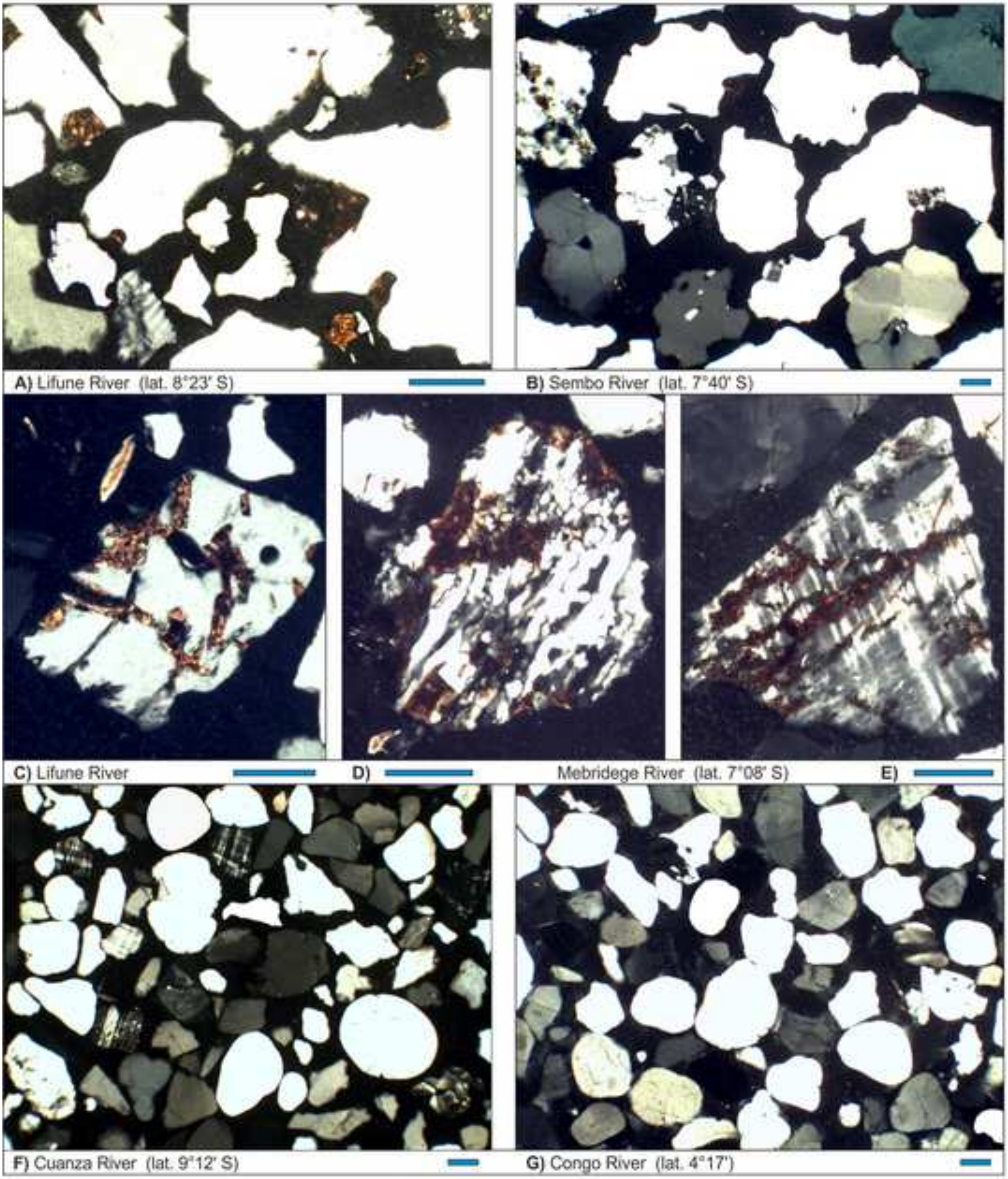

Figure 7 Angola

Figure 8

Click here to download high resolution image

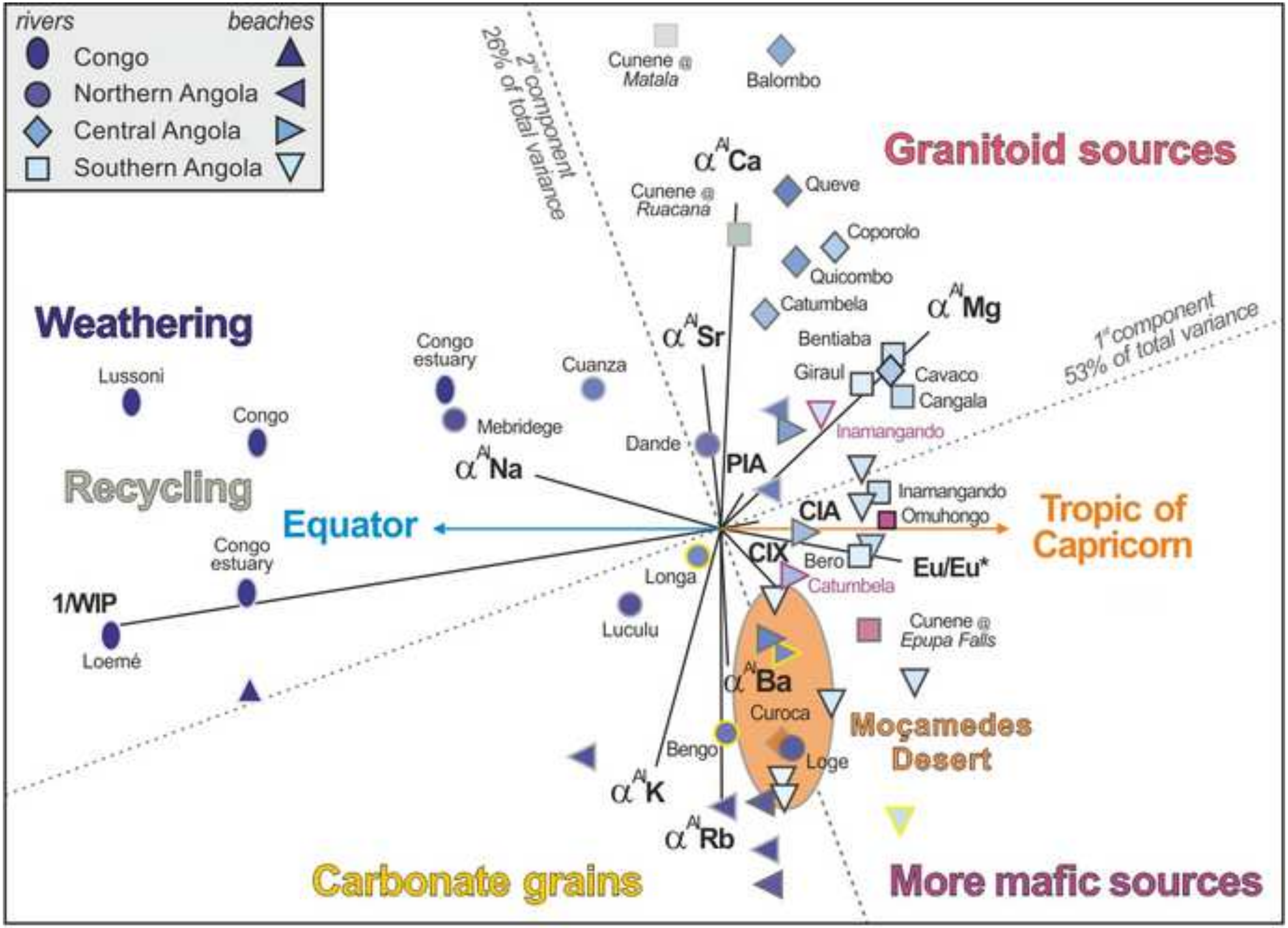

Figure 8 Angola

Table 1
Click here to download Table: Table 1 Angola PTHMCHI.pdf

Table 1. Angola Margin

	N°	Qz	KF	Pl	Lvm	Lsm	Lm	mica	HM		MI*	tHMC	ZTR	Ep	Grt	St	Ky	Amp	Px	&tHM		CIA	CIX	WIP	$\alpha^{Al}Na$
RIVER SANDS																									
Repubblic of Congo	2	99	0	0	0	0	0	0	1	100.0		0.2	74	5	4	8	6	0	0	3	100.0	87	86	0.3	6.2
		0	0	0	0	0	0	0	0			0.2	4	4	6	3	6	0	0	2		10	6	0.3	0.2
Congo	3	98	1	0	0	0	0	0	1	100.0		0.2	57	13	2	14	7	3	0	3	100.0	63	72	1	3.9
		1	1	0	0	0	0	0	1			0.2	18	7	1	4	4	2	0	2					
Congo Estuary	2	98	1	1	0	0	0	0	0	100.0		0.1	41	14	3	7	20	12	0	4	100.0	81	85	2	7.8
		0	0	0	0	0	0	0	0			0.1	8	8	0	2	18	2	0	3		12	13	2	7.0
Luculu	1	86	4	5	0	0	0	0	5	100.0		3.8	7	30	33	2	15	13	0	1	100.0	62	74	11	2.2
Mebridege	1	93	3	3	0	1	1	0	0	100.0	183	0.02	9	8	1	0	3	71	1	7	100.0	70	75	4	3.2
Sembo	1	77	14	8	0	0	0	0	0	100.0		1.1	2	21	2	0	1	72	1	0	100.0				
Loge	1	76	6	8	0	0	0	0	10	100.0		7.3	1	70	2	0	0	26	0	2	100.0	50	67	27	1.1
Onzo	1	81	7	6	0	0	0	0	6	100.0	325	5.8	1	27	7	0	6	57	2	0	100.0				
Lifune	1	87	5	1	0	0	0	2	5	100.0		3.3	7	35	11	0	11	34	1	0	100.0				
Dande	1	80	8	6	0	0	1	4	2	100.0	275	1.3	6	48	6	0	4	36	1	1	100.0	58	65	24	1.3
Bengo	1	82	6	5	0	4	0	0	4	100.0		2.1	6	30	13	1	10	37	1	1	100.0	33	64	20	1.5
Cuanza	1	87	5	6	0	1	0	0	0	100.0		0.3	18	52	5	0	2	15	7	1	100.0	54	66	10	2.9
Longa	1	82	6	6	1	2	0	0	3	100.0		2.1	8	85	0	0	0	6	0	1	100.0	38	62	23	2.3
Queve	1	73	16	9	0	0	0	1	1	100.0		0.6	1	43	2	0	0	51	0	2	100.0	55	59	37	2.1
Cambongo	1	68	13	14	2	0	0	1	2	100.0	425	1.4	22	51	1	0	0	18	6	1	100.0				
Quicombo	1	60	21	10	0	1	1	2	5	100.0	340	3.2	10	64	3	0	0	15	2	6	100.0	51	57	43	2.3
Tapado	1	56	27	16	0	0	0	1	0	100.0		0.4	3	78	1	0	0	17	0	0	100.0				
Balombo	1	53	26	19	0	0	0	1	0	100.0		0.5	8	89	0	0	0	3	1	0	100.0	55	57	52	3.1
Culango	1	57	23	18	0	0	0	1	1	100.0		0.9	14	71	0	0	0	14	0	1	100.0				
Catumbela	2	69	15	9	0	0	0	0	6	100.0	317	2.2	4	59	0	0	0	18	14	4	100.0	54	59	32	1.9
		5	2	0	0	0	0	0	7			1.8	3	14	0	0	0	4	11	5					
Cavaco	1	43	26	24	0	0	1	1	3	100.0	350	1.9	1	71	0	0	0	24	0	3	100.0	52	59	48	1.3
Coporolo	2	61	20	16	0	0	0	1	2	100.0	300	1.2	2	67	0	0	0	28	3	1	100.0	53	58	48	1.7
		1	4	2	0	0	0	0	1			0.7	1	0	0	0	0	0	3	1					
Cangala	1	59	13	25	0	0	1	0	2	100.0	267	1.8	0	76	0	0	0	22	0	2	100.0	52	58	57	1.1
Carujamba	1	48	21	29	0	0	0	0	2	100.0		1.5	0	63	0	0	0	35	0	1	100.0				
Inamangando	1	52	18	22	1	1	2	0	5	100.0	275	3.1	1	78	0	0	0	18	0	3	100.0	51	61	49	1.2
Bentiaba	1	52	19	28	0	0	1	0	1	100.0	317	2.0	0	62	0	0	0	36	0	2	100.0	52	58	56	1.2
Giraul	1	53	17	23	0	0	1	0	5	100.0	250	3.2	1	42	3	0	0	52	1	2	100.0	52	59	51	1.3
Bero	1	42	16	32	0	1	2	1	5	100.0	350	3.2	0	21	0	0	0	60	16	2	100.0	51	62	51	1.2
Cunene@Matala	1	75	19	6	0	0	0	0	0	100.0		0.1	93	2	0	1	1	1	1	3	100.0	58	60	20	4.7
Cunene@Ruacana	1	79	12	4	1	3	0	0	1	100.0		0.7	5	32	1	0	0	55	0	7	100.0	51	57	28	2.7
Cunene@Epupa F.	1	54	13	26	1	1	1	0	3	100.0	295	3.0	1	27	1	0	0	44	23	6	100.0	51	66	48	1.4
Cunene@Foz	1	57	12	20	3	1	1	0	6	100.0	256	4.2	1	19	10	4	0	33	28	4	100.0				
BEACH SANDS																									
Repubblic of Congo	1	99	1	0	0	0	0	0	0	100.0		0.1	67	1	0	13	18	0	0	1	100.0	>59	>89	<0.9	>11
North.most Angola	2	96	2	1	0	0	0	0	1	100.0		0.6	9	35	13	7	16	19	0	1	100.0	42	72	7	1.8
		2	1	0	0	0	0	0	1			0.1	5	6	0	3	2	5	0	0					
Northern Angola	8	83	6	3	0	1	0	0	6	100.0	425	4.4	4	43	19	1	6	24	1	2	100.0	39	67	23	1.2
		7	2	1	0	0	0	0	5			3.0	3	12	12	1	3	9	2	1		5	2	4	0.2
Cuanza cell	4	81	11	6	0	0	0	0	1	100.0		0.9	4	51	3	1	1	22	14	4	100.0	39	55	27	1.5
		2	1	2	0	0	0	0	1			0.5	3	4	2	1	1	5	7	1		2	0	3	0.1
Central Angola	9	71	13	11	0	1	0	0	5	100.0	325	3.7	7	54	1	0	0	19	14	4	100.0	38	60	38	1.7
		3	2	2	0	1	0	0	3			2.3	5	8	1	0	1	4	9	4		9	2	5	0.1
Catumbela cell	3	61	14	13	0	0	1	1	10	100.0	374	6.2	4	63	1	0	0	19	13	1	100.0	47	61	43	1
		13	3	4	0	0	1	1	6		66	4.4	2	6	1	0	0	6	5	0					
Benguela	1	64	11	18	0	2	1	1	4	100.0	260	4.0	2	71	0	0	0	18	4	6	100.0				
Coporolo cell	4	65	19	12	0	0	0	0	3	100.0		2.1	1	72	0	0	0	22	2	2	100.0				
		4	6	3	0	0	0	0	3			1.7	1	7	0	0	0	7	1	0					
Southern Angola	10	50	16	23	0	1	1	0	9	100.0	319	5.4	5	55	2	0	0	32	3	3	100.0	47	62	52	1.1
		6	5	7	0	1	1	0	8		55	4.0	8	16	2	0	0	16	6	3		4	2	6	0.2
Moçamedes Desert	13	67	9	13	3	0	0	0	7	100.0	282	4.7	4	14	35	4	0	15	26	2	100.0	49	66	28	1.3
		6	3	2	1	1	0	0	7		87	4.1	2	3	21	2	0	7	14	1		3	2	2	0.1
Skeleton Coast Erg	3	70	7	12	3	1	0	0	6	100.0	360	4.6	4	6	18	2	0	6	61	3	100.0	48	62	28	1.1
		1	1	3	1	0	0	0	1			0.5	2	2	8	1	0	2	3	3		3	1	2	0.0
OFFSHORE SEDIMENTS																									
Congo mouth	1	82	5	3	0	0	0	0	10	100.0		3.3	19	29	23	0	8	19	0	3	100.0				
Tapado mouth	4	44	26	20	0	2	0	1	6	100.0		5.2	3	74	0	0	0	19	1	3	100.0				
		5	0	5	0	1	0	2	1			1.0	1	7	0	0	0	6	1	1					
Coporolo mouth	1	36	23	33	0	1	0	0	6	100.0		3.1	0	78	1	0	0	15	0	5	100.0				
Baia dos Tigres	3												4	19	3	0	0	15	50	8	100.0				
													2	4	4	0	1	6	16	4					
Cunene mouth	4	69	7	13	1	3	0	0	5	100.0	146	5.8	3	13	3	0	0	8	65	7	100.0				
		1	0	1	0	0	0	0	1		5	1.4	2	3	2	0	0	3	4	1					
Walvis Ridge	4												1	18	2	0	0	14	60	5	100.0				
													1	4	1	0	0	6	12	0					

APPENDIX

" Dynamic uplift, recycling, and climate control on the petrology of passive-margin sand (Angola)"

by Garzanti E., Dinis P., Vermeesch P., Andò S., Hahn A., Huvi J., Limonta M., Padoan, M., Resentini, A., Rittner M., Vezzoli, G.

APPENDIX A

Figure A1. Channel profiles of Angolan rivers draining into the Atlantic Ocean (same horizontal and vertical scale for all profiles). The alternation of subhorizontal and very steep tracts along the course of major rivers reflects the presence of stepped planation surfaces separated by escarpments, a characteristic feature of the dynamically uplifted landscapes of southwestern Angola. Fluvial network delineated in TecDEM (software shell implemented in MATLAB; Shahzad and Gloaguen, 2011) from a 30 m resolution digital elevation model provided by ASTER GDEM (http://www.gdem.aster.ersdac.or.jp). Channel concavity θ and steepness k_s (referenced to a fixed concavity 0.45 to compare gradients in channels with different drainage areas; Korup and Schlunegger, 2009) are defined by a power-law relationship between the local channel slope *S* and the contributing drainage area *A* used as a proxy for discharge ($S = k_s A^{-\theta}$; Flint 1974).

Table A1. Sample information. Location of the studied river, beach, shelfal and deep-sea sediment samples with year of sampling (see also the Google Earth file *Angolamargin.kmz*).

Table A2. Geomorphology and hydrology of Angolan river systems (data after National Directorate of Water, 2005). Sediment loads of Congo, Cuanza and Cunene rivers after Hay (1998), Holisticos (2012), and Bremner and Willis (1993), respectively.

Table A3. Sand petrography. GSZ= grain size. Q= quartz (Qp= polycrystalline); F= feldspars (KF= K-feldspar; P= plagioclase; Mic= cross-hatched microcline); L= aphanitic lithic grains (Lv= volcanic and subvolcanic; Ls= sedimentary; Lc= carbonate; Lh= chert; Lp= shale/siltstone; Lm= metamorphic; Lms= low-rank metasedimentary; Lmv= low-rank metavolcanic; Lmf= high-rank metapelite/metapsammite/metafelsite; Lmb= high-rank metabasite; Lu= ultramafic). HM= heavy minerals. Rock fragments: V= volcanic; Vm= intermediate and mafic volcanic; M= metamorphic; Mb= mafic metamorphic; n.d. = not determined. The Metamorphic Indices MI and MI* express the average metamorphic rank of rock fragments in each sample. MI varies from 0 (detritus shed by exclusively sedimentary and volcanic cover rocks) to 500 (very-high-rank detritus shed by exclusively high-grade basement rocks). MI* considers only metamorphic rock fragments, and thus varies from 100 (very-low-rank detritus shed by exclusively very low-grade metamorphic rocks) to 500 (Garzanti and Vezzoli, 2003).

Table A4. Heavy minerals. GSZ= grain size. HM= heavy minerals; tHM= transparent heavy minerals; HMC and tHMC = total and transparent-heavy-mineral concentration indices (Garzanti and Andò, 2007); RF= rock fragments; n.d. = not determined. The ZTR index (sum of zircon, tourmaline and rutile over total transparent heavy minerals) evaluates the “chemical durability” of the detrital assemblage (Hubert 1962). The HCI (Hornblende Colour Index) and MMI (Metasedimentary Minerals Index) vary from 0 in detritus from greenschist-facies to lowermost amphibolite-facies rocks yielding exclusively blue/green amphibole and chloritoid, to 100 in detritus from granulite-facies rocks yielding exclusively brown hornblende and sillimanite, and are used to estimate the average metamorphic grade of metaigneous and metasedimentary source rocks, respectively (Andò et al. 2014).

Table A5. Surface textures of heavy minerals in Angolan sediment samples. Determination of corrosion features on transparent heavy-mineral grains by three operators, following the classification of Andó et al. (2012). Q= quartz; F= feldspar; L= aphanitic lithic grains; n.d.= not determined.

Table A6. Geochemistry of Angolan sands (analyses made at ACME Laboratories, Vancouver). Following a lithium metaborate/tetraborate fusion and nitric acid digestion, major oxides and several minor elements were determined by inductively coupled plasma emission spectroscopy, and trace elements by ICP-MS. Discrepancies in replicate analyses are ≤ 1% for major elements and ≤ 5% for most trace elements (for further information on adopted procedures, geostandards used, and precision for various elements of group 4A-4B and code LF200 see http://acmelab.com). A separate split was digested in aqua regia and analyzed by ICP-MS for Mo, Ni, Cu, Ag, Au, Zn, Cd, Hg, Tl, Pb, As, Sb, Bi, and Se. Elements analysed by aqua regia digestion (a.r.d.) are commonly underestimated because of only partial leaching of refractory minerals. Chemical weathering indices are defined in Nesbitt and Young (1982; CIA), Harnois (1988; CIW), Fedo et al. (1995; PIA), Parker (1970; WIP), and Garzanti et al. (2014; CIX). In order to avoid bias caused by hydraulic concentration of heavy minerals hosting Ti, REE and Th, α^{Al} values were normalized to non-mobile Al (Garzanti et al., 2014). The Eu anomaly is the measured chondrite-normalized Eu value over the value that Eu would have in a linear extrapolation between chondrite-normalized values of Sm and Gd. The Ce anomaly, indicative of redox state, is the measured PAAS-normalized Ce value over the value that Ce would have in a linear extrapolation between PAAS-normalized values of La and Pr. MREE is the average of Eu, Gd, Tb and Dy normalized to PAAS, MREE* the average of LREE (La, Ce, Pr, Nd) and HREE (Er, Tm, Yb, Lu) values (Haley et al., 2004). The chondrite-normalized La_N/Yb_N, La_N/Sm_N, Gd_N/Ho_N, and Ho_N/Yb_N ratios are also given. GSZ= grain size; D.L. = detection limit; n.d.= not determined.

APPENDIX B

U-Pb detrital zircon geochronology of modern sands from northern Namibia and southern Angola (analyses made at the London Geochronology Centre, University College London). We used $^{206}Pb/^{238}U$ and $^{207}Pb/^{206}Pb$ ages for zircons younger and older than 1100 Ma, respectively; grains with >10% age discordance were discarded. No common Pb correction was applied. Grains with +5/-15% age discordance were discarded.

CITED REFERENCES

Andò, S., Garzanti, E., Padoan, M., Limonta, M., 2012. Corrosion of heavy minerals during weathering and diagenesis: a catalog for optical analysis. Sedimentary Geology, 280, 165-178.

Andó, S., Morton, A., Garzanti, E., 2014. Metamorphic grade of source rocks revealed by chemical fingerprints of detrital amphibole and garnet. In: Scott, R., Smyth. H., Morton, A., Richardson, N. (Eds.), Sediment provenance studies in hydrocarbon exploration and production. Geological Society London, Special Publications 386, pp. 351-371.

Bremner, J.M.,Willis, J.P., 1993. Mineralogy and geochemistry of the clay fraction of sediments from the Namibian continental margin and the adjacent hinterland. Marine Geology, 115, 85-116.

Fedo, C.M., Nesbitt, H.W., Young, G.M., 1995. Unraveling the effects of potassium metasomatism in sedimentary rocks and paleosols, with implications for paleoweathering conditions and provenance. Geology, 23, 921-924.

Flint, J.J., 1974. Stream gradient as a function of order, magnitude, and discharge. Water Resources Research, 10, 969-973.

Garzanti, E., Andò, S., 2007. Heavy-mineral concentration in modern sands: implications for provenance interpretation. In: Mange, M.A., Wright, D.T. (Eds.), Heavy Minerals in Use. Elsevier, Amsterdam, Developments in Sedimentology Series 58, pp.517-545.

Garzanti, E., Vezzoli, G., 2003. A classification of metamorphic grains in sands based on their composition and grade. Journal of Sedimentary Research, 73, 830-837.

Garzanti, E., Vermeesch, P., Padoan, M., Resentini, A., Vezzoli, G., Andò, S., 2014. Provenance of passive-margin sand (southern Africa). The Journal of Geology, 122, 17-42.

Haley, B.A., Klinkhammer, G.P., McManus, J., 2004. Rare earth elements in pore waters of marine sediments. Geochimica Cosmochimica Acta, 68,1265-1279.

Harnois, L., 1988. The CIW index: a new chemical index of weathering. Sedimentary Geology, 55, 319-322.

Hay, W.W., 1998. Detrital sediment fluxes from continents to oceans. Chemical Geology, 145, 287-323.

Holisticos, 2012. Environmental impact study for the rehabilitation and expansion of the Cambambe hydroelectric power plant. https://www.miga.org/documents/Angola_Cambambe_HPP_EIS.pdf

Korup, O., Schlunegger, F., 2009. Rock-type control on erosion-induced uplift, eastern Swiss alps. Earth and Planetary Science Letters, 278, 278-285.

Hubert, J.F., 1962. A zircon-tourmaline-rutile maturity index and the interdependence of the composition of heavy minerals assemblages with the gross composition and texture of sandstones. Journal of Sedimentary Petrology 32:440-450.

National Directorate of Water, 2005. A rapid water resources and water use assessment for Angola, Final Report. Ministry of Energy and Water Affairs, Republic of Angola, National Water Sector Management Project, Activity C, 307 p.

Nesbitt, H.W., Young, G.M., 1982. Early Proterozoic climates and plate motions inferred from major element chemistry of lutites. Nature, 299, 715-717.

Parker, A., 1970. An index of weathering for silicate rocks. Geological Magazine, 107, 501-504.

Shahzad, F., Gloaguen, R., 2011. TecDEM: a MATLAB based toolbox for tectonic geomorphology, part 1: drainage network pre-processing and stream profile analysis. Computers & Geosciences, 37, 250-260.

Appendix Figure A1

Click here to download high resolution image

River	Area km²	Length km	Elevation mean m	k_{sn}	θ
Mebridege	19071	290	589	121	0.13
Dande	11446	285	621	141	0.29
Longa	23031	310	888	106	0.09
Queve	22815	300	1360	114	0.11
Catumbela	16533	240	1321	107	-0.06
Coporolo	15239	220	908	94	0.21
Bero	10476	210	718	121	0.31
Cunene	113835	1050	1286	66	-0.02

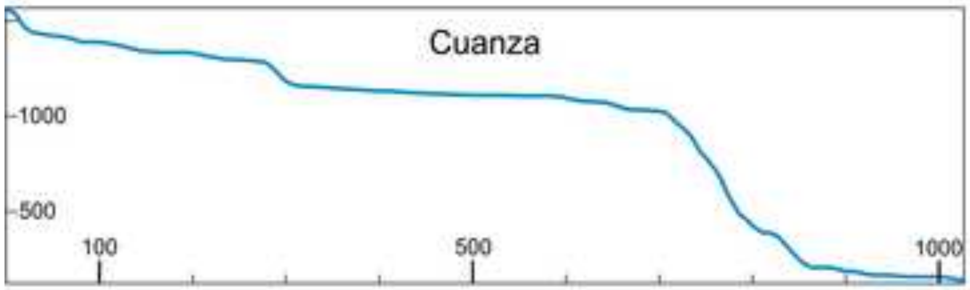

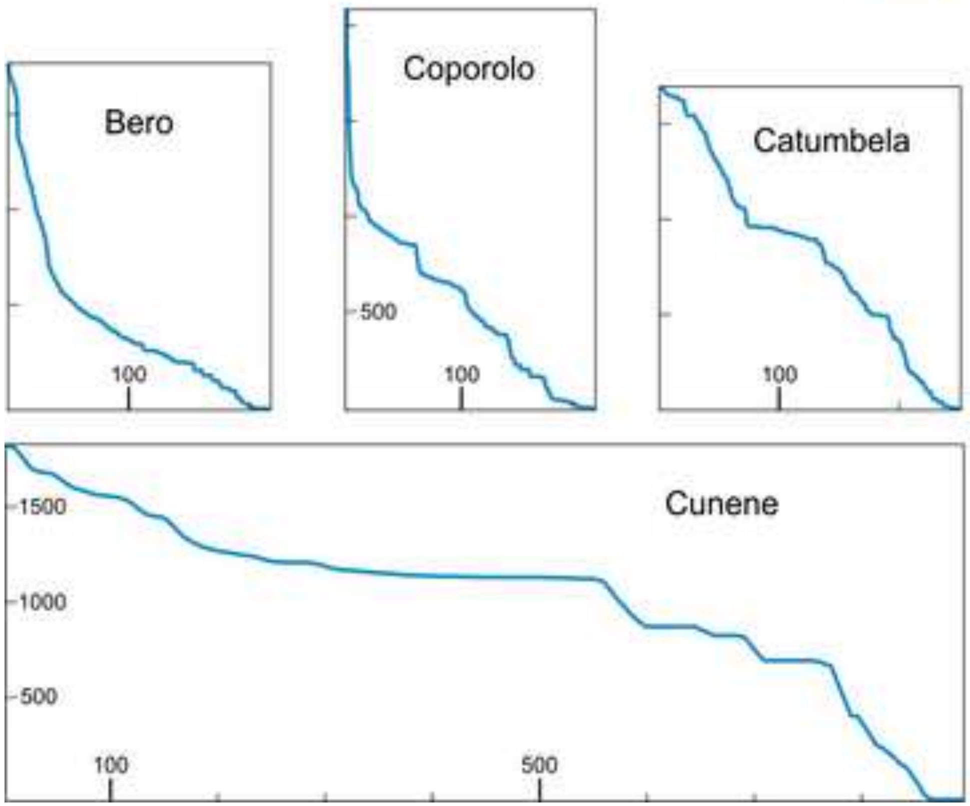

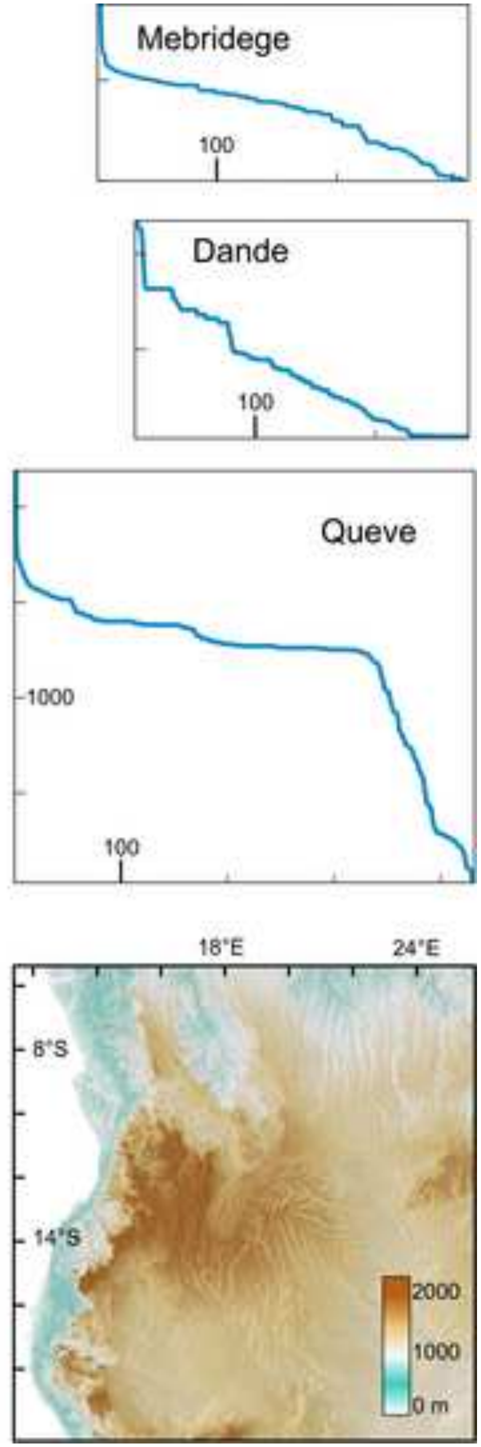

Appendix Table A1

Table A1

Sample	River / Desert	Site	Facies	Country	Collected by	Year	Latitude	Longitude
S4053	Loussoni	St. Paul	river sand	Congo	M.Orlando	2009	S 04 28	E 12 12
S0162		Pointe Noire	beach sand	Congo	D. Dell'Era	1997	S 04 48	E 11 50
S0161	Loémé	Djeno	river sand	Congo	D. Dell'Era	1997	S 04 54	E 11 56
S3533	Congo	Brazzaville	river sand	Congo	F.Bolognesi	2005	S 4 17	E 15 17
S5114	Congo	Kinshasa	river sand	Congo	P.Vermesch	2016	S 04 19 32	E 15 13 42
S5115	Congo	Boma	river sand	Congo	P.Vermesch	2016	S 05 51 58	E 13 00 14
S4899	Congo	Soyo	estuary sand	Angola	E.Garzanti	2015	S 06 07 52	E 12 22 25
S4898	Congo	Soyo estuary	estuary sand	Angola	E.Garzanti	2015	S 06 07 09	E 12 21 32
S4901		Quimtomba	beach sand	Angola	E.Garzanti	2015	S 06 15 00	E 12 20 46
S4902		Quifuma	beach sand	Angola	E.Garzanti	2015	S 06 23 30	E 12 25 37
S4904	Luculu	Quivanda	estuary sand	Angola	E.Garzanti	2015	S 06 41 15	E 12 34 52
S4903		Quivanda	beach sand	Angola	E.Garzanti	2015	S 06 41 17	E 12 34 49
S4905		Mbua-Moyo	beach sand	Angola	E.Garzanti	2015	S 06 51 42	E 12 44 32
S4897	Mebridege	Cassa de Telha	river sand	Angola	E.Garzanti	2015	S 07 08 24	E 12 58 58
S4906		N'Zeto	beach sand	Angola	E.Garzanti	2015	S 07 13 42	E 12 51 14
S4907		Pidi mouth	beach sand	Angola	E.Garzanti	2015	S 07 18 02	E 12 53 03
S4908		Musserra	beach sand	Angola	E.Garzanti	2015	S 07 34 51	E 13 00 16
S4895	Sembo	Musserra	river sand	Angola	E.Garzanti	2015	S 07 39 35	E 13 11 26
S4894	Loge	Porta Freitas Morna	river sand	Angola	E.Garzanti	2015	S 07 43 56	E 13 19 56
S4909		Ambriz	beach sand	Angola	E.Garzanti	2015	S 07 50 58	E 13 06 17
S4893	Onzo	Tabi	river sand	Angola	E.Garzanti	2015	S 08 09 47	E 13 25 31
S4892	Lifune	Conde Loca	river sand	Angola	E.Garzanti	2015	S 08 23 18	E 13 28 16
S4910		Barra do Dande	beach sand	Angola	E.Garzanti	2015	S 08 28 04	E 13 22 58
S4891	Dande	Caxito	river sand	Angola	E.Garzanti	2015	S 08 36 23	E 13 33 33
S4911	Bengo	Quifangondo	estuary sand	Angola	E.Garzanti	2015	S 08 43 48	E 13 26 17
S4912		Cacuaco	beach sand	Angola	E.Garzanti	2015	S 08 46 24	E 13 22 15
S4652		Ilha de Luanda	beach sand	Angola	R.Giardini	2013	S 8 47	E 13 14E
S3764		Mussulo	beach sand	Angola	M.Orlando	2008	S 8 59	E 13 02
S4913		Palmeirinhas	beach sand	Angola	E.Garzanti	2015	S 09 07 16	E 13 00 57
S4914		Barra do Cuanza	estuary sand	Angola	E.Garzanti	2015	S 09 20 24	E 13 09 02
S4915	Cuanza	Barra do Cuanza	river sand	Angola	E.Garzanti	2015	S 09 19 22	E 13 09 45
S3765		Cabo Ledo	beach sand	Angola	M.Orlando	2008	S 9 40	E 13 13
S4916		Sao Braz	beach sand	Angola	E.Garzanti	2015	S 09 58 27	E 13 19 31
S4917	Longa	Calamba	river sand	Angola	E.Garzanti	2015	S 10 11 50	E 13 31 16
S4918		Porto Amboim	beach sand	Angola	E.Garzanti	2015	S 10 42 36	E 13 46 30
S4919		Sumbe	beach sand	Angola	E.Garzanti	2015	S 11 09 47	E 13 50 19
S4920		Quicombo	beach sand	Angola	P.Dinis	2015	S 11 19 05	E 13 48 55
S4921		Candunga	beach sand	Angola	P.Dinis	2015	S 11 44 24	E 13 47 39
S4922	Queve	Cachoeira	river sand	Angola	E.Garzanti	2015	S 10 59 19	E 14 05 45
S4923		Carimba	beach sand	Angola	E.Garzanti	2015	S 11 04 35	E 13 51 20
S4924	Cambongo	Sumbe	river sand	Angola	E.Garzanti	2015	S 11 11 56	E 13 50 47
S4925	Quicombo	Quicombo	river sand	Angola	E.Garzanti	2015	S 11 19 18	E 13 50 25
S4926	Tapado	Chitonde	river sand	Angola	E.Garzanti	2015	S 11 48 38	E 13 56 47
S4927	Balombo	Canjala	river sand	Angola	E.Garzanti	2015	S 11 59 45	E 13 59 45
S4928		Egito Praia	beach sand	Angola	E.Garzanti	2015	S 11 57 37	E 13 45 42
S4929	Culango	Culango	river sand	Angola	E.Garzanti	2015	S 12 18 04	E 13 49 54
S4930		Praia Sousa	beach sand	Angola	P.Dinis	2015	S 11 36 36	E 13 47 06
S4934		Lobito spit	beach sand	Angola	E.Garzanti	2015	S 12 18 58	E 13 34 52
S4865		Lobito spit	beach sand	Angola	P.Dinis	2014	S 12 19 14	E 13 34 45
S4863		Lobito spit	beach sand	Angola	P.Dinis	2014	S 12 20 19	E 13 33 04
S4864		Lobito spit	beach sand	Angola	P.Dinis	2014	S 12 20 22	E 13 33 06
S4862		Catumbela N	beach sand	Angola	P.Dinis	2014	S 12 24 51	E 13 29 42
PB.AC		Catumbela mouth	beach sand	Angola	P.Dinis	2014	S 12 26 14	E 13 28 58
S4861		Catumbela mouth	beach sand	Angola	P.Dinis	2014	S 12 27 02	E 13 28 33
S4655	Catumbela	Praia Bebe	beach placer	Angola	A. Pereira	2013	S 12 27 00	E 13 28 30
S5118	Cubal da Hanha	Vista Alegre	river sand	Angola	J.Huvi	2017	S 12 49 44	E 13 59 14
CAV	Catumbela	Fazenda Santo Antonio	river sand	Angola	P.Dinis	2014	S 12 30 17	E 13 46 54
S5116	Calumbolo	Supua	river sand	Angola	J.Huvi	2017	S 12 27 00	E 13 46 06
S5117	Capilongo	Capilongo	river sand	Angola	J.Huvi	2017	S 12 27 50	E 13 36 22
S4933	Catumbela	Catumbela	river sand	Angola	E.Garzanti	2015	S 12 26 27	E 13 33 03
S4860	Catumbela	Catumbela	river sand	Angola	P.Dinis	2014	S 12 27 00	E 13 34 32
S4859		Catumbela airport	beach sand	Angola	P.Dinis	2014	S 12 30 17	E 13 28 56
S4932	Cavaco	Benguela	river sand	Angola	E.Garzanti	2015	S 12 34 00	E 13 25 04
S4931		Benguela	beach sand	Angola	E.Garzanti	2015	S 12 34 45	E 13 23 40
S4935		Baia Farta	beach sand	Angola	E.Garzanti	2015	S 12 35 51	E 13 12 15
S4858		Baia Farta	beach sand	Angola	P.Dinis	2014	S 12 36 57	E 13 11 26
S4857		Canucua	beach sand	Angola	P.Dinis	2014	S 12 47 53	E 12 59 14
S4856		Saco NE	beach sand	Angola	P.Dinis	2014	S 12 51 25	E 12 57 03

S4855		Saco N	beach sand	Angola	P.Dinis	2014	S 12 51 42	E 12 56 18
S4854		Saco SE	beach sand	Angola	P.Dinis	2014	S 12 52 30	E 12 57 16
S4853		Saco S	beach sand	Angola	P.Dinis	2014	S 12 52 46	E 12 56 39
S4852	Coporolo	Santa Tereza	beach sand	Angola	P.Dinis	2014	S 12 54 01	E 13 05 20
S4936	Coporolo	Dombe Grande	river sand	Angola	E.Garzanti	2015	S 12 55 01	E 13 06 20
S4937		Cuio	beach sand	Angola	E.Garzanti	2015	S 12 58 58	E 12 58 43
S4938		Equimina	beach sand	Angola	E.Garzanti	2015	S 13 11 49	E 12 46 54
S4939		Baia Binga	beach sand	Angola	E.Garzanti	2015	S 13 20 19	E 12 39 06
S4940	Cangala	Santa Maria	river sand	Angola	E.Garzanti	2015	S 13 33 33	E 12 38 28
S4941		Lucira	beach sand	Angola	E.Garzanti	2015	S 13 51 58	E 12 31 14
S4942	Carujamba	Lucira	river sand	Angola	E.Garzanti	2015	S 13 59 19	E 12 31 01
S4943	*(low outer berm)*	Inamangando	beach sand	Angola	E.Garzanti	2015	S 14 02 33	E 12 23 09
S4944	*(high inner berm)*	Inamangando	beach sand	Angola	E.Garzanti	2015	S 14 02 34	E 12 23 10
S4945	Inamangando	Inamangando	river sand	Angola	E.Garzanti	2015	S 14 03 04	E 12 25 38
S4946		Baia das Salinas	beach sand	Angola	E.Garzanti	2015	S 14 11 18	E 12 20 38
S4947	Bentiaba	Bentiaba	river sand	Angola	E.Garzanti	2015	S 14 16 05	E 12 22 46
S4948		Bentiaba	beach sand	Angola	E.Garzanti	2015	S 14 17 23	E 12 22 11
P4948		Bentiaba	beach placer	Angola	E.Garzanti	2015	S 14 17 23	E 12 22 11
S4949		Chapeu Armado	beach sand	Angola	E.Garzanti	2015	S 14 26 55	E 12 20 38
S4950		Mariquita	beach sand	Angola	E.Garzanti	2015	S 14 45 41	E 12 17 04
S4951	Giraul	Giraul	river sand	Angola	E.Garzanti	2015	S 15 04 30	E 12 09 18
S4952	Bero	Namibe	river sand	Angola	E.Garzanti	2015	S 15 09 54	E 12 10 05
S4953		Namibe	beach sand	Angola	E.Garzanti	2015	S 15 11 32	E 12 08 50
Moçamedes Desert								
S4954		Subida Grande	beach sand	Angola	E.Garzanti	2015	S 15 25 21	E 12 01 54
S4802	*(fossil dune)*	Nonguai	fossil dune	Angola	P.Dinis	2014	S 15 45 57	E 12 04 40
S4955	Curoca	Curoca mouth	river sand	Angola	E.Garzanti	2015	S 15 43 53	E 11 55 24
S4956		Curoca mouth	beach sand	Angola	E.Garzanti	2015	S 15 43 56	E 11 54 38
S4804		Tombua	beach sand	Angola	P.Dinis	2014	S 15 47 54	E 11 51 18
S4805	*(outer spit)*	Tombua	beach sand	Angola	P.Dinis	2014	S 15 47 20	E 11 49 08
S4774		Tombua	eolian dune	Angola	E.Baptista	2014	S 15 47 56	E 11 51 54
S4957		Vanesa	beach sand	Angola	E.Garzanti	2015	S 15 57 09	E 11 46 06
S4961		Cova dos Medos	eolian dune	Angola	E.Garzanti	2015	S 16 01 24	E 11 48 47
S4958		Vanesinha	beach sand	Angola	E.Garzanti	2015	S 16 09 25	E 11 47 36
S4959		Praia do Navio	beach sand	Angola	E.Garzanti	2015	S 16 16 23	E 11 48 35
S4960		Praia do Navio	eolian dune	Angola	P.Vermeesch	2015	S 16 16 25	E 11 48 44
S5058		Riscos	beach sand	Angola	A.Sampaio	2016	S 16 30 00	E 11 49 21
S5059		Riscos	eolian dune	Angola	A.Sampaio	2016	S 16 30 00	E 11 49 21
S5057		Saco dos Tigres	beach sand	Angola	A.Sampaio	2016	S 16 48 27	E 11 48 13
S5055		Praia dos Esponjas	beach sand	Angola	A.Sampaio	2016	S 17 05	E 11 44 40
S5056		Praia dos Esponjas	eolian dune	Angola	A.Sampaio	2016	S 17 05	E 11 44 40
S5054		Foz do Cunene	eolian dune	Angola	A.Sampaio	2016	S 17 15 24	E 11 45 18
S5053		Foz do Cunene	beach sand	Angola	A.Sampaio	2016	S 17 15 24	E 11 45 18
Cunene catchment								
S5050	Caculuvar	Techango	river sand	Angola	A.Trindade	2016	S 16 38 15	E 14 54 16
S5049	Mucope	Techiulo	river sand	Angola	A.Trindade	2016	S 16 31 46	E 14 52 22
S3931	Cunene	Ruacana	river sand	Namibia	L.Ciceri	2008	S 17 24 30	E 14 13
S3934	Omuhongo	Oryeheke	river sand	Namibia	L.Ciceri	2008	S 16 59 20	E 13 22 10
S4775	Cunene	Epupa Falls	river sand	Namibia	F.Vermeesch	2014	S 17 00	E 13 15
S5052	Cunene	Foz do Cunene	estuary sand	Angola	A.Sampaio	2016	S 17 15 24	E 11 45 18
OFFSHORE CORE TOP SAMPLES			**Depth (m)**		**Corer**			
1004	Meteor M6/6	GeoB1004-3	-31	Congo mouth	Giant box corer	1988	S 06 05 58	E 12 07 39
1001	Meteor M6/6	GeoB1001-1	-45	Congo mouth	Giant box corer	1988	S 05 51 58	E 11 58 20
1011	Meteor M6/6	GeoB1011_2	-73	Tabado mouth	Giant box corer	1988	S 11 48 14	E 13 39 41
1012/1	Meteor M6/6	GeoB1012_1	-99	Tabado mouth	Giant box corer	1988	S 11 48 33	E 13 35 27
1012/2	Meteor M6/6	GeoB1012_2	-99	Tabado mouth	Giant box corer	1988	S 11 48 33	E 13 35 27
1013	Meteor M6/6	GeoB1013_2	-250	Tabado mouth	Giant box corer	1988	S 11 47 55	E 13 26 47
2/2 5-7	ODP Leg 175	1078 A	-438	Balombo mouth	Piston corer	1997	S 11 55 13	E 13 24 08
3/1 15-17	ODP Leg 175	1078 A	-438	Balombo mouth	Piston corer	1997	S 11 55 13	E 13 24 08
1/2 105-106	DSDP Leg 40	365	-3040	Cuanza volcanic ridge	Rotary core barrel	1975	S 11 39 06	E 11 53 43
1/6 65-67	DSDP Leg 40	365	-3040	Cuanza volcanic ridge	Rotary core barrel	1975	S 11 39 06	E 11 53 43
4918	Meteor M41/1	GeoB4918_5	-1339	Coporolo mouth	Gravity corer	1998	S 12 50 24	E 12 41 48
1/1 89-91	ODP Leg 175	1080 A	-2766	Baia dos Tigres	Piston corer	1997	S 16 33 35	E 10 49 12
2/4 31-33	ODP Leg 175	1080 A	-2766	Baia dos Tigres	Piston corer	1997	S 16 33 35	E 10 49 12
1/6 65-67	ODP Leg 175	1080 B	-2768	Baia dos Tigres	Piston corer	1997	S 16 33 36	E 10 49 12
1019	Meteor M6/6	GeoB1019-3	-75	Cunene mouth	Giant box corer	1988	S 17 10 29	E 11 38 50
1020	Meteor M6/6	GeoB1020-1	-110	Cunene mouth	Giant box corer	1988	S 17 10 07	E 11 32 53
1021	Meteor M6/6	GeoB1021-3	-173	Cunene mouth	Giant box corer	1988	S 17 10 34	E 11 24 00
1022	Meteor M6/6	GeoB1022-2	-551	Cunene mouth	Giant box corer	1988	S 17 10 24	E 11 17 53
1704	Meteor 20/2	GeoB1704-1	-399	Walvis Ridge	Giant box corer	1992	S 19 24 24	E 11 36 42
1705	Meteor 20/2	GeoB1705-1	-642	Walvis Ridge	Gravity corer	1992	S 19 30 18	E 11 23 54

Appendix Table A2

Click here to download Table: Table A2 Angola Rivers.pdf

Table A2

River	Area	Length	Perimeter	Elevation mean	Elevation max	Annual water discharge mean	Annual water discharge mean spec.	Annual water discharge max spec.	Annual water discharge min spec.	Precipitation	Sdm.load	Sdm.yield	Erosion
	km^2	*km*	*km*	*m a.s.l.*	*m a.s.l.*	*m^3/s*	*l/s km^2*	*l/s km^2*	*q*	*mm/a*	*ton/a*	*ton/km2 a*	*mm/a*
Congo	4014500	4700	11895	955	1548	41000	8.7	11.6	5.5	1375	60000000	15	0.006
Luculu	1449	95	185	151	315	8	5.6	6.0	4.7	836			
Mebridege	19071	290	890	589	1295	124	6.5	11.4	3.5	974			
Sembo	2093	125	250	284	734	7	3.3	4.4	2.6	550			
Loge	12819	230	581	531	1281	53	4.1	10.4	1.9	612			
Onzo	2942	130	324	359	913	7	2.4	2.8	2.0	415			
Lifune	3019	150	334	376	1133	9	2.9	4.5	2.4	513			
Dande	11446	285	649	621	1474	59	5.2	10.0	2.4	832			
Bengo	11089	300	663	483	1530	44	3.9	7.4	1.5	883			
Cuanza	150446	965	2702	1200	1964	1064	7.1	14.2	1.6	1188	618500	4	0.0016
Longa	23031	310	791	888	2099	138	6.0	9.1	3.3	991			
Queve	22815	300	899	1360	2575	213	9.4	16.3	2.6	1131			
Cambongo	2309	310	286	867	2260	14	5.9	10.9	2.6	763			
Quicombo	5512	50	434	1081	2545	40	7.2	15.6	0.9	965			
Tapado	1617	40	190	582	1583	7	4.1	7.4	2.3	745			
Balombo	4414	200	451	1186	2609	42	9.6	18.4	2.8	1100			
Culango	2881	120	266	949	2142	13	4.3	8.4	2.3	883			
Catumbela	16533	240	748	1321	2570	149	9.0	17.3	1.8	1182			
Cavaco	4398	120	313	738	1570	19	4.4	6.8	1.6	751			
Coporolo	15239	220	667	908	2406	70	4.6	9.2	1.1	846			
Cangala	363	60	115	547	827	0.3	0.8	1.1	0.4	312			
Carujamba	2931	160	305	664	1230	5	1.8	3.8	0.2	560			
Inamangando	1859	145	263	623	1477	2	1.1	3.0	0.1	479			
Bentiaba	6935	210	472	873	2325	12	1.8	3.7	0.2	648			
Giraul	4709	190	393	615	2322	4	0.8	2.5	0.1	409			
Bero	10476	210	588	718	2094	5	0.5	1.5	0.1	364			
Curoca	19338	324	849	762	1864	4	0.2	0.9	0.0	238			
Cunene	113835	1050	2390	1286	2484	290	2.5	13.7	0.0	704	8700000	76	0.029

Appendix Table A3

Table A3

Click here to download Table: Table A3 Angola PT.pdf

River	Site	Sample	Operator	GSZ (mm)	Q	KF	P	Lv	Lc	Lh	Lp	Lms	Lmv	Lmf	Lmb	Lu	mica	HM	total	Q	F	L	**MI***	**MI**	Lm	Lv	Ls	Qp/Q	P/F	Mic/F	Vm/V	Mb/M
RIVERS & BEACHES IN THE CONGO																																
Loussoni	St. Paul	S4053	G.Vezzoli	325	99	0	0	0	0	0	1	0	0	0	0	0	0	0	100.0	99	0	1	n.d.	100	n.d.	n.d.	n.d.	8	n.d.	n.d.	n.d.	n.d.
	Pointe Noire	S0162	G.Vezzoli	510	99	1	0	0	0	0	0	0	0	0	0	0	0	0	100.0	99	1	0	n.d.	n.d.	n.d.	n.d.	n.d.	4	n.d.	100	n.d.	n.d.
Loémé	Djeno	S0161	G.Vezzoli	220	99	0	0	0	0	0	0	0	0	0	0	0	0	1	100.0	100	0	0	n.d.	n.d.	n.d.	n.d.	n.d.	2	n.d.	n.d.	n.d.	n.d.
Congo	Brazzaville	S3533	G.Vezzoli	240	97	2	0	0	0	0	0	0	0	0	0	0	0	0	100.0	97	2	0	n.d.	n.d.	n.d.	n.d.	n.d.	2	0	38	n.d.	n.d.
Congo	Kinshasa	S5114	G.Vezzoli	160	98	1	0	0	0	0	0	0	0	0	0	0	0	1	100.0	99	1	0	n.d.	n.d.	n.d.	n.d.	n.d.	2	n.d.	n.d.	n.d.	n.d.
Congo	Boma	S5115	G.Vezzoli	125	97	1	1	0	0	0	0	0	0	0	0	0	0	1	100.0	99	1	0	n.d.	n.d.	n.d.	n.d.	n.d.	1	40	75	n.d.	n.d.
Congo	Soyo	S4899	G.Vezzoli	175	98	1	1	0	0	0	0	0	0	0	0	0	0	0	100.0	98	2	0	n.d.	n.d.	n.d.	n.d.	n.d.	1	57	0	n.d.	n.d.
Congo	Soyo estuary	S4898	A.Resentini	180	98	1	1	0	0	0	0	0	0	0	0	0	0	0	100.0	99	1	0	n.d.	n.d.	n.d.	n.d.	n.d.	3	40	40	n.d.	n.d.
BEACHES & SHELF IN NORTHERN ANGOLA																																
-31 m inner shelf offshore of Congo mouth		1004-3	G.Vezzoli	200	82	5	3	0	0	0	0	0	0	0	0	0	0	10	100.0	91	9	0	n.d.	n.d.	n.d.	n.d.	n.d.	1	38	25	n.d.	n.d.
	Quimtomba	S4901	G.Vezzoli	630	97	1	1	0	0	0	0	0	0	0	0	0	0	0	100.0	98	2	0	n.d.	n.d.	n.d.	n.d.	n.d.	4	43	57	n.d.	n.d.
	Quifuma	S4902	A.Resentini	345	95	3	1	0	0	0	0	0	0	0	0	0	0	1	100.0	96	4	0	n.d.	n.d.	n.d.	n.d.	n.d.	4	31	17	n.d.	n.d.
	Quivanda	S4903	A.Resentini	350	88	6	3	0	0	0	0	0	0	0	0	0	0	3	100.0	91	9	0	n.d.	n.d.	n.d.	n.d.	n.d.	10	35	20	n.d.	n.d.
	Mbua-Moyo	S4905	A.Resentini	380	90	5	4	0	0	0	0	0	0	0	0	0	0	2	100.0	91	9	0	n.d.	n.d.	n.d.	n.d.	n.d.	9	43	18	n.d.	n.d.
	Pidi mouth	S4907	A.Resentini	245	77	9	3	0	0	0	0	0	0	0	0	0	0	10	100.0	86	14	0	n.d.	n.d.	n.d.	n.d.	n.d.	8	27	8	n.d.	n.d.
	Musserra	S4908	G.Vezzoli	325	72	6	6	1	0	0	0	0	0	0	0	0	0	15	100.0	85	14	2	n.d.	n.d.	13	63	25	5	49	13	n.d.	n.d.
	Ambriz	S4909	A.Resentini	330	82	5	3	0	1	0	0	0	0	0	0	0	0	9	100.0	90	9	1	n.d.	n.d.	n.d.	n.d.	n.d.	3	39	23	n.d.	n.d.
	Barra do Dande	S4910	G.Vezzoli	460	82	9	3	0	0	0	0	0	0	1	0	0	0	4	100.0	86	13	1	425	309	50	0	50	7	26	60	n.d.	0
	Cacuaco	S4912	A.Resentini	120	92	4	1	0	1	0	0	0	0	0	0	0	1	1	100.0	94	4	2	n.d.	n.d.	17	0	83	4	20	36	n.d.	n.d.
RIVERS IN NORTHERN ANGOLA																																
Luculu	Quivanda	S4904	A.Resentini	370	86	4	5	0	0	0	0	0	0	0	0	0	0	5	100.0	91	9	0	n.d.	n.d.	n.d.	n.d.	n.d.	4	53	34	n.d.	n.d.
Mebridege	Cassa de Telha	S4897	A.Resentini	345	93	3	3	0	0	0	0	1	0	1	0	0	0	0	100.0	93	6	1	183	122	60	20	20	20	55	6	n.d.	0
Sembo	Musserra	S4895	A.Resentini	750	77	14	8	0	0	0	0	0	0	0	0	0	0	0	100.0	78	22	0	n.d.	n.d.	n.d.	n.d.	n.d.	35	38	19	n.d.	n.d.
Loge	Porta Freitas Morna	S4894	A.Resentini	305	76	6	8	0	0	0	0	0	0	0	0	0	0	10	100.0	84	15	0	n.d.	n.d.	n.d.	n.d.	n.d.	12	55	9	n.d.	n.d.
Onzo	Tabi	S4893	A.Resentini	480	81	7	6	0	0	0	0	0	0	0	0	0	0	6	100.0	86	14	0	325	325	n.d.	n.d.	n.d.	4	43	19	n.d.	13
Lifune	Conde Loca	S4892	A.Resentini	345	87	5	1	0	0	0	0	0	0	0	0	0	2	5	100.0	93	7	0	n.d.	n.d.	n.d.	n.d.	n.d.	7	21	27	n.d.	n.d.
Dande	Caxito	S4891	A.Resentini	150	80	8	6	0	0	0	0	0	0	1	0	0	4	2	100.0	85	14	2	275	275	100	0	0	4	42	27	n.d.	0
Bengo	Quifangondo	S4911	A.Resentini	135	82	6	5	0	4	0	0	0	0	0	0	0	0	4	100.0	85	11	4	n.d.	n.d.	0	0	100	6	45	27	n.d.	n.d.
CUANZA & CUANZA LITTORAL CELL																																
	Ilha de Luanda	S4652	G.Vezzoli	570	81	10	7	0	0	0	0	0	0	0	0	0	0	0	100.0	81	18	1	n.d.	143	0	25	75	17	42	35	n.d.	n.d.
	Mussulo	S3764	G.Vezzoli	550	83	13	4	0	0	0	0	0	0	0	0	0	0	0	100.0	83	17	0	n.d.	n.d.	n.d.	n.d.	n.d.	23	24	44	n.d.	n.d.
	Palmeirinhas	S4913	A.Resentini	560	82	10	7	0	0	0	0	0	0	0	0	0	0	1	100.0	83	17	0	n.d.	n.d.	n.d.	n.d.	n.d.	19	40	20	n.d.	n.d.
	Barra do Cuanza	S4914	A.Resentini	530	79	12	8	0	1	0	0	0	0	0	0	0	0	1	100.0	79	20	1	n.d.	n.d.	13	38	50	22	41	21	n.d.	n.d.
Cuanza	Barra do Cuanza	S4915	A.Resentini	260	87	5	6	0	1	0	0	0	0	0	0	0	0	0	100.0	87	12	1	n.d.	n.d.	0	0	100	7	54	25	n.d.	n.d.
BEACHES & SHELF IN CENTRAL ANGOLA																																
	Cabo Ledo	S3765	G.Vezzoli	360	69	14	8	1	1	0	0	0	0	0	0	0	0	7	100.0	74	24	2	n.d.	140	0	60	40	20	37	26	n.d.	n.d.
	Sao Braz	S4916	A.Resentini	205	67	14	13	0	2	0	0	0	0	0	0	0	0	3	100.0	70	28	3	n.d.	n.d.	6	0	94	14	48	29	n.d.	n.d.
	Porto Amboim	S4918	A.Resentini	430	72	11	11	0	0	0	0	0	0	0	0	0	0	6	100.0	76	23	1	n.d.	n.d.	n.d.	n.d.	n.d.	26	52	17	n.d.	n.d.
	Carimba	S4923	A.Resentini	350	71	8	10	0	0	0	0	0	0	0	1	0	0	9	100.0	78	21	1	325	260	60	20	20	22	55	20	n.d.	100
	Praia Sousa	S4930	A.Resentini	720	75	14	9	0	1	0	0	0	0	0	0	0	0	2	100.0	77	23	1	n.d.	n.d.	n.d.	n.d.	n.d.	24	38	30	n.d.	n.d.
	Egito Praia	S4928	A.Resentini	650	70	14	13	0	0	0	0	0	0	0	0	0	0	2	100.0	72	28	1	n.d.	n.d.	n.d.	n.d.	n.d.	14	47	23	n.d.	n.d.
-73 m shelf offshore of Tapado mouth		1011	G.Vezzoli	90	40	26	24	0	1	0	0	1	0	0	0	0	2	6	100.0	44	54	2	n.d.	n.d.	20	0	80	2	48	21	n.d.	n.d.
-99 m shelf offshore of Tapado mouth		1012/2	G.Vezzoli	115	47	26	17	0	2	0	0	0	0	0	0	0	0	7	100.0	51	46	3	n.d.	n.d.	13	0	88	9	40	19	n.d.	n.d.
RIVERS IN CENTRAL ANGOLA																																
Longa	Calamba	S4917	A.Resentini	130	82	6	6	1	2	0	0	0	0	0	0	0	0	3	100.0	84	13	3	n.d.	75	9	27	64	6	51	27	n.d.	n.d.
Queve	Cachoeira	S4922	A.Resentini	350	73	16	9	0	0	0	0	0	0	0	0	0	1	1	100.0	74	26	0	n.d.	n.d.	n.d.	n.d.	n.d.	25	34	34	n.d.	n.d.
Cambongo	Sumbe	S4924	A.Resentini	335	68	13	14	2	0	0	0	0	0	0	0	0	1	2	100.0	71	27	2	425	283	14	86	0	21	52	18	n.d.	25
Quicombo	Quicombo	S4925	A.Resentini	260	60	21	10	0	1	0	0	0	0	1	1	0	2	5	100.0	65	33	2	340	340	67	0	33	26	33	28	n.d.	40
Tapado	Chitonde	S4926	A.Resentini	500	56	27	16	0	0	0	0	0	0	0	0	0	1	0	100.0	57	43	0	n.d.	n.d.	n.d.	n.d.	n.d.	37	37	22	n.d.	n.d.
Balombo	Canjala	S4927	A.Resentini	190	53	26	19	0	0	0	0	0	0	0	0	0	1	0	100.0	53	46	1	n.d.	n.d.	n.d.	n.d.	n.d.	22	42	31	n.d.	n.d.
Culango	Culango	S4929	A.Resentini	355	57	23	18	0	0	0	0	0	0	0	0	0	1	1	100.0	58	42	0	n.d.	n.d.	n.d.	n.d.	n.d.	13	43	31	n.d.	n.d.
COPOROLO, CATUMBELA & LITTORAL CELLS																																
	Lobito spit	S4863	A.Resentini	280	52	16	16	0	0	0	0	0	0	0	1	0	2	14	100.0	61	38	1	420	420	n.d.	n.d.	n.d.	11	49	22	n.d.	100
	Catumbela N	S4862	A.Resentini	310	70	12	10	0	0	0	0	0	0	0	1	0	1	6	100.0	75	23	2	327	327	93	7	0	11	45	29	n.d.	82
Catumbela mouth	Praia Bebe	S4655	G.Vezzoli	690	50	10	17	0	0	0	0	0	0	0	0	0	1	22	100.0	64	35	1	363	322	n.d.	n.d.	n.d.	15	63	14	n.d.	50
Cubal da Hanha	Vista Alegre	S5118	G.Vezzoli	290	57	20	19	0	0	0	0	0	0	0	0	0	0	3	100.0	59	41	0	n.d.	325	n.d.	n.d.	n.d.	5	49	23	n.d.	n.d.
Calumbolo	Supua	S5116	G.Vezzoli	750	53	16	24	1	0	0	0	0	0	0	0	0	3	3	100.0	56	43	1	363	290	33	67	0	40	60	12	n.d.	19
Capilongo	Capilongo	S5117	G.Vezzoli	670	39	9	34	1	1	0	1	0	0	2	0	0	7	5	100.0	44	49	7	413	333	38	22	40	32	78	11	n.d.	4
Catumbela	Catumbela	S4860	A.Resentini	590	65	13	9	0	0	0	0	0	0	0	0	0	1	11	100.0	74	25	1	n.d.	n.d.	n.d.	n.d.	n.d.	15	40	35	n.d.	n.d.
Catumbela	Catumbela	S4933	A.Resentini	335	72	16	9	0	0	0	0	0	0	0	0	0	0	1	100.0	73	26	1	317	158	n.d.	n.d.	n.d.	22	36	31	n.d.	42
	Catumbela airport	S4859	A.Resentini	330	48	24	23	0	0	0	0	0	0	0	0	0	2	3	100.0	50	49	1	283	283	n.d.	n.d.	n.d.	8	49	26	n.d.	75
Cavaco	Benguela	S4932	A.Resentini	315	43	26	24	0	0	0	0	0	0	0	1	0	1	3	100.0	45	53	2	350	300	71	14	14	7	48	32	n.d.	83
	Benguela	S4931	A.Resentini	340	64	11	18	0	2	0	0	0	0	0	1	0	1	4	100.0	68	30	3	260	260	28	6	67	16	63	22	n.d.	70
	Baia Farta	S4858	A.Resentini	340	70	13	11	0	0	0	0	0	0	0	0	0	0	6	100.0	75	25	0	n.d.	200	n.d.	n.d.	n.d.	13	46	15	n.d.	n.d.
	Camucua	S4857	A.Resentini	340	63	25	11	0	0	0	0	0	0	0	0	0	0	1	100.0	64	36	0	n.d.	n.d.	n.d.	n.d.	n.d.	28	30	21	n.d.	n.d.
	Saco S	S4853	A.Resentini	610	63	20	16	0	0	0	0	0	0	0	0	0	0	1	100.0	64	36	0	n.d.	n.d.	n.d.	n.d.	n.d.	22	44	18	n.d.	n.d.
Coporolo	Santa Tereza	S4852	A.Resentini	330	61	23	15	0	0	0	0	0	0	0	0	0	0	1	100.0	62	38	0	300	300	n.d.	n.d.	n.d.	22	39	34	n.d.	13
Coporolo	Dombe Grande	S4936	A.Resentini	340	62	18	17	0	0	0	0	0	0	0	0	0	1	2	100.0	64	36	0	n.d.	n.d.	n.d.	n.d.	n.d.	13	49	26	n.d.	n.d.
BEACHES IN SOUTHERN ANGOLA																																
	Cuio	S4937	A.Resentini	350	45	15	29	0	2	0	0	0	0	0	1	0	0	8	100.0	49	47	3	363	363	41	5	55	21	65	7	n.d.	63
	Equimina	S4938	A.Resentini	335	40	13	21	0	0	0	0	0	0	1	1	0	0	23	100.0	53	44	3	289	289	100	0	0	11	62	15	n.d.	61
	Baia Binga	S4939	A.Resentini	445	52	13	14	0	1	0	0	0	0	0	1	0	0	20	100.0	65	33	2	380	380	40	0	60	5	51	15	n.d.	80
	Lucira	S4941	A.Resentini	390	44	12	36	0	0	0	0	0	0	2	1	0	0	5	100.0	46	50	4	295	295	88	4	8	43	75	13	n.d.	30
low outer berm	Inamangando	S4943	G.Vezzoli	400	49	20	19	0	0	0	0	0	1	0	0	0	0	11	100.0	54	44	2	338	338	55	45	0	41	48	29	n.d.	58
high inner berm	Inamangando	S4944	G.Vezzoli	340	51	19	22	0	0	0	0	0	0	0	0	0	0	7	100.0	55	44	1	240	200	n.d.	n.d.	n.d.	24	53	20	n.d.	30
	Baia das Salinas	S4946	G.Vezzoli	415	57	13	25	0	0	0	0	0	1	0	0	0	1	4	100.0	60	39	1	340	309	n.d.	n.d.	n.d.	34	66	11	n.d.	80
	Bentiaba	S4948	G.Vezzoli	520	50	20	22	0	0	0	0	0	1	0	0	0	0	7	100.0	54	44	1	229	178	25	50	25	44	53	17	n.d.	50
	Chapeu Armado	S4949	G.Vezzoli	355	58	26	14	1	0	0	0	0	0	0	0	0	0	0	100.0	57	40	3	320	188	0	40	60	24	35	36	n.d.	0
	Mariquita	S4950	A.Resentini	670	59	20	19	0	0	0	0	0	0	0	0	0	0	1	100.0	59	40	1	350	300	63	13	25	24	49	12	n.d.	42
	Namibe	S4953	G.Vezzoli	325	47	12	27	0	0	0	0	1	1	1	1	0	0	10	100.0	53	43	4	383	358	83	8	8	11	70	3	n.d.	50
RIVERS IN SOUTHERN ANGOLA																																
Cangala	Santa Maria	S4940	A.Resentini	240	59	13	25	0	0	0	0	0	0	0	1	0	0	2	100.0	60	39	1	267	267	88	13	0	17	65	14	n.d.	67
Carujamba	Lucira	S4942	A.Resentini	490	48	21	29	0	0	0	0	0	0	0	0	0	0	2	100.0	49	51	0	n.d.	n.d.	n.d.	n.d.	n.d.	32	58	18	n.d.	n.d.
Inamangando	Inamangando	S4945	A.Resentini	335	52	18	22	0	0	0	0	0	1	1	1	0	0	5	100.0	54	42	4	275	259	73	9	18	24	55	15	n.d.	41
Bentiaba	Bentiaba	S4947	A.Resentini	350	52	19	28	0	0	0	0	0	0	0	0	0	0	1	100.0	52	47	1	317	317	n.d.	n.d.	n.d.	30	60	12	n.d.	42
Giraul	Giraul	S4951	A.Resentini	325	53	17	23	0	0	0	0	0	0	1	0	0	0	5	100.0	56	43	1	250	250	n.d.	n.d.	n.d.	25	57	6	n.d.	6
Bero	Namibe	S4952	G.Vezzoli	230	42	16	32	0	0	0	1	0	0	2	0	0	1	5	100.0	45	51	4	350	311	67	4	29	12	67	7	n.d.	19
CUNENE RIVER SYSTEM																																
Cunene	Matala	S4773	G.Vezzoli	230	75	19	6	0	0	0	0	0	0	0	0	0	0	0	100.0	75	25	0	n.d.	n.d.	n.d.	n.d.	n.d.	2	24	7	n.d.	n.d.
Mucope	Techiulo	S5049	A.Resentini	230	99	1	0	0	0	0	0	0	0	0	0	0	0	0	100.0	99	1	0	n.d.	n.d.	n.d.	n.d.	n.d.	5	0	25	n.d.	n.d.
Caculuvar	Techango	S5050	A.Resentini	470	99	1	0	0	0	0	0	0	0	0	0	0	0	0	100.0	99	1	0	n.d.	n.d.	n.d.	n.d.	n.d.	8	25	25	n.d.	n.d.
Caculuvar confluence	Omutele	S5051	A.Resentini	540	83	11	7	0	0	0	0	0	0	0	0	0	0	0	100.0	83	17	0	n.d.	n.d.	n.d.	n.d.	n.d.	14	38	19	n.d.	n.d.
Cunene	Ruacana	S3931	G.Vezzoli	130	79	12	4	1	1	0	1	0	0	0	0	0	0	1	100.0	80	17	3	n.d.	38.5	5	18	77	6	25	20	n.d.	n.d.
Ehomba	Ehomba	S3932	G.Vezzoli	120	80	11	2	1	1	0	4	0	0	0	0	0	0	1	100.0	80	14	6	n.d.	45.5	8	15	78	7	17	16	n.d.	n.d.
Ondoto	Chitado	S3933	G.Vezzoli	170	70	12	8	0	0	0	4	2	1	1	0	0	1	1	100.0	71	21	8	214	50.6	29	8	63	36	41	22	n.d.	21
Omuhongo	Etengua	S3935	G.Vezzoli	290	56	28	12	0	0	0	0	0	0	1	0	0	1	1	100.0	58	41	1	415	415	n.d.	n.d.	n.d.	34	31	31	n.d.	12
Omuhongo	Oryeheke	S3934	G.Vezzoli	370	43	25	26	0	0	0	1	0	0	1	0	0	1	2	100.0	45	53	3	319	213	61	0	39	47	51	17	n.d.	19
Cunene	Epupa Falls	S4775	G.Vezzoli	330	54	13	26	1	0	0	1	1	0	1	0	0	0	3	100.0	56	40	4	295	151	46	25	29	33	68	13	n.d.	17
Otjinjange	Van Zyl's Pass	S3936	G.Vezzoli	220	58	11	11	0	1	0	0	0	1	4	2	0	3	9	100.0	65	25	10	383	362	81	5	14	28	49	19	n.d.	35
Marienfluss	Otyoyonoka	S3937	G.Vezzoli	115	49	13	11	0	0	0	0	0	1	3	1	0	3	20	100.0	64	30	6	436	436	94	6	0	32	47	22	n.d.	44
Cunene	Foz do Cunene	S5052	G.Vezzoli	325	57	12	20	1	0	0	0	1	1	0	0	0	0	6	100.0	61	34	4	256	171	37	50	13	18	63	11	80	34
ORANGE LITTORAL CELL ONSHORE																																
	Subida Grande	S4954	G.Vezzoli	285	75	7	11	3	0	0	0	1	1	1	0	0	0	1	100.0	76	18	6	277	144	33	59	9	7	63	7	58	35
fossil dune	Nonguai	S4802	A.Resentini	335	70	16	12	0	0	0	0	0	0	1	0	0	1	0	100.0	71	28	1	300	300	88	0	13	6	44	13	n.d.	13
Curoca	Curoca mouth	S4955	A.Resentini	320	62	6	16	3	0	0	0	0	1	1	0	0	0	12	100.0	70	24	5	200	80	20	80	0	7	74	11	100	33
	Curoca mouth	S4956	A.Resentini	345	69	7	13	2	0	0	0	1	0	0	0	0	0	7	100.0	74	22	4	200	83.3	25	58	17	10	65	5	100	20
outer spit	Tombua	S4805	A.Resentini	295	73	11	12	2	0	0	0	0	0	0	0	0	0	3	100.0	75	23	2	450	164	0	100	0	9	53	5	100	50
eolian dune	Tombua	S4774	G.Vezzoli	270	74	4	11	5	0	0	0	0	0	0	0	0	0	4	100.0	78	16	6	383	63.9	10	84	6	11	73	9	80	25
	Vanesa	S4957	A.Resentini	290	70	10	14	1	0	0	0	0	0	0	0	0	0	4	100.0	73	25	2	n.d.	28.6	8	83	8	9	59	18	100	n.d.
eolian dune	Cova dos Medos	S4961	G.Vezzoli	255	35	4	10	4	0	0	1	0	1	0	0	0	0	44	100.0	62	25	13	213	73.9	15	70	15	13	71	15	100	44
	Vanesinha	S4958	G.Vezzoli	300	60	5	11	2	1	0	0	1	0	0	0	0	0	19	100.0	74	20	6	233	111	19	53	28	9	67	12	88	17
	Praia do Navio	S4959	A.Resentini	355	64	7	14	4	0	0	0	0	0	0	0	0	0	12	100.0	72	24	4	n.d.	68.8	0	100	0	12	68	11	100	n.d.
eolian dune	Praia do Navio	S4960	A.Resentini	215	24	2	7	2	0	0	0	0	0	0	1	0	0	64	100.0	66	25	9	300	92.3	33	67	0	13	79	6	100	100
eolian dune	Riscos	S5059	G.Vezzoli	325	73	8	14	2	0	0	1	0	0	0	0	0	0	2	100.0	75	22	3	371	163	14	59	27	8	64	15	100	14
	Riscos	S5058	A.Resentini	165	57	8	16	1	0	0	0	0	0	0	0	0	0	17	100.0	69	29	2	n.d.	66.7	17	67	17	3	67	4	100	n.d.
	Saco dos Tigres	S5057	G.Vezzoli	345	74	9	13	2	0	0	0	0	0	1	0	0	0	1	100.0	75	22	3	260	108	28	72	0	14	59	15	100	10
eolian dune	Praia dos Esponjas	S5056	A.Resentini	325	65	12	17	2	1	0	0	0	0	0	0	0	0	4	100.0	67	30	3	n.d.	0	0	75	25	10	59	15	100	n.d.
	Praia dos Esponjas	S5055	G.Vezzoli	330	65	14	15	3	0	0	0	0	1	1	0	0	0	1	100.0	66	29	5	270	108	28	66	6	11	52	12	67	40
eolian dune	Foz do Cunene	S5054	G.Vezzoli	200	63	13	15	2	0	0	0	1	0	1	0	0	0	5	100.0	66	29	4	220	105	32	52	17	11	54	16	88	5
	Foz do Cunene	S5053	G.Vezzoli	339	57	9	13	3	0	0	1	1	1	0	0	0	0	15	100.0	67	26	7	192	100	25	57	18	8	59	17	78	35
ORANGE LITTORAL CELL OFFSHORE																																
-110 m outer shelf offshore of Cunene mouth		1020	G.Vezzoli	70	68	7	14	1	0	0	1	2	1	1	0	0	0	6	100.0	72	22	6	150	90	39	17	44	4	66	11	n.d.	8
-173 m outer shelf offshore of Cunene mouth		1021	G.Vezzoli	85	69	8	13	1	1	0	1	1	1	0	0	0	1	5	100.0	73	22	5	143	76.9	21	29	50	4	62	10	n.d.	21

Table A4

River	Site	Sample	GSZ class (mm)	%finer	%class	%coarser	method	Operator	tHMcounted	total grains	HM %weight	tHM %weight	zircon	tourmaline	rutile	Ti oxides	titanite	apatite	epidote group	epidote in RF	garnet	staurolite	andalusite	kyanite	sillimanite	amphibole	oxy-hornblende	amphibole in RF	clinopyroxene	clinopyroxene in RF	enstatite	hypersthene	olivine	spinel	others		HCI	MMI	ZTR	% transparent	% opaques	% Fe oxides	% Ti oxides	% turbid HM	% rock fragments	% soils & turbid	% glauc./phosp./sulph.	% chlorite	% biotite	% carbonates	% light minerals	
RIVERS & BEACHES IN THE CONGO																																																				
Loussoni	St. Paul	S4053	32-355	0.0%	76%	24%	Fleet	M.Limonta	69	228	0.04	0.01	39.1	34.8	2.9	0.0	0.0	4.3	2.9	0.0	8.7	5.8	0.0	1.4	0.0	0.0	0.0	0.0	0.0	0.0	0.0	0.0	0.0	0.0	0.0	100.0	n.d.	50	77	30%	2%	0%	0%	0%	2%	63%	0%	0%	0%	0%	3%	100%
	Pointe Noire	S0162	32-355	0.2%	77%	23%	Point	M.Limonta	299	498	0.5	0.3	26.1	24.7	15.7	0.3	0.0	0.0	0.7	0.0	0.0	13.4	0.3	18.1	0.7	0.0	0.0	0.0	0.0	0.0	0.0	0.0	0.0	0.0	0.0	100.0	n.d.	51	67	60%	26%	1%	3%	0%	0%	8%	0%	0%	0%	0%	1%	100%
Loémé	Djeno	S0161	32-355	0.1%	79%	21%	Area	M.Padoan	240	632	1.2	0.5	36.7	20.4	13.8	0.4	0.0	0.0	7.9	0.0	0.0	10.0	0.8	10.0	0.0	0.0	0.0	0.0	0.0	0.0	0.0	0.0	0.0	0.0	0.0	100.0	n.d.	50	71	38%	42%	2%	2%	1%	0%	14%	0%	0%	0%	0%	2%	100%
Congo	Brazzaville	S3533	63-250	0.05%	40%	60%	Area	M.Padoan	211	853	0.05	0.01	19.9	25.6	3.8	1.9	0.0	0.0	13.7	0.0	3.8	17.1	0.9	8.5	0.0	3.8	0.0	0.0	0.0	0.0	0.0	0.0	0.0	0.0	0.9	100.0	22	50	49	25%	70%	1%	0%	4%	0%	0%	0%	0%	0%	0%	1%	100%
Congo	Kinshasa	S5114	>15	0.7%	99%	0%	Point	M.Limonta	244	886	0.77	0.21	60.2	10.7	7.0	0.0	0.0	0.0	5.7	0.0	1.6	9.8	0.0	2.5	0.0	1.6	0.0	0.0	0.4	0.0	0.0	0.0	0.0	0.0	0.4	100.0	n.d.	50	78	28%	71%	0%	0%	0%	0%	1%	0%	0%	0%	0%	0%	100%
Congo	Boma	S5115	>15	0.4%	100%	0%	Point	M.Limonta	217	452	0.53	0.25	16.1	23.0	4.6	0.0	0.5	0.0	19.8	0.5	1.8	15.2	0.0	9.7	3.2	5.1	0.0	0.0	0.0	0.0	0.0	0.5	0.0	0.0	0.0	100.0	3	56	44	48%	44%	0%	0%	1%	1%	6%	0%	0%	0%	0%	0%	100%
Congo	Soyo	S4899	<500	0%	100%	0.4%	Point	M.Limonta	207	302	0.4	0.3	11.1	19.8	4.8	0.0	0.5	0.5	8.2	0.0	2.9	8.7	0.0	32.9	0.5	10.1	0.0	0.0	0.0	0.0	0.0	0.0	0.0	0.0	0.0	100.0	5	51	36	69%	21%	0%	1%	0%	0%	9%	0%	0%	0%	0%	1%	100%
Congo	Soyo estuary	S4898	<500	0%	97%	3%	Point	M.Limonta	208	572	0.3	0.1	9.1	29.8	8.2	0.0	1.0	1.0	19.2	0.0	2.4	5.3	1.0	6.7	3.4	13.0	0.0	0.0	0.0	0.0	0.0	0.0	0.0	0.0	0.0	100.0	5	60	47	36%	23%	1%	2%	0%	0%	35%	0%	1%	2%	0%	0%	100%
BEACHES & SHELF IN NORTHERN ANGOLA																																																				
-31 m inner shelf offshore	Congo mouth	1004	>15	0%	100%	0%	Point	M.Limonta	210	458	6.6	3.0	8.6	1.4	8.6	0.0	0.0	1.0	28.6	0.0	22.9	0.5	0.0	7.6	1.9	18.6	0.0	0.0	0.5	0.0	0.0	0.0	0.0	0.0	0.0	100.0	14	60	19	46%	45%	5%	0%	0%	0%	3%	0%	0%	0%	0%	0%	100%
	Quimtomba	S4901	<500	0%	78%	22%	Point	M.Padoan	219	378	2.2	1.3	3.7	4.6	4.6	0.0	0.0	0.9	30.6	0.5	13.2	8.7	0.0	17.4	0.0	16.0	0.0	0.0	0.0	0.0	0.0	0.0	0.0	0.0	0.0	100.0	3	50	13	58%	33%	0%	0%	0%	3%	5%	0%	0%	1%	0%	0%	100%
	Quifuma	S4902	<500	0%	76%	24%	Point	M.Padoan	205	361	1.5	0.8	0.5	2.0	2.9	0.0	0.5	0.0	39.0	0.0	12.7	4.9	0.0	15.1	0.0	22.4	0.0	0.0	0.0	0.0	0.0	0.0	0.0	0.0	0.0	100.0	7	50	5	57%	30%	0%	0%	0%	1%	9%	0%	0%	2%	0%	0%	100%
	Quivanda	S4903	<500	0%	88%	12%	Point	M.Padoan	245	308	3.9	3.1	0.8	2.0	0.8	0.0	0.0	0.0	30.2	0.0	23.7	0.4	0.8	9.0	0.0	32.2	0.0	0.0	0.0	0.0	0.0	0.0	0.0	0.0	0.0	100.0	7	50	4	80%	9%	0%	0%	1%	2%	6%	0%	0%	2%	0%	0%	100%
	Mbua-Moyo	S4905	<500	0%	94%	6%	Point	M.Padoan	210	242	4.1	3.6	1.0	0.5	1.9	0.0	1.4	1.4	45.7	0.0	18.6	1.0	0.0	5.7	0.0	22.9	0.0	0.0	0.0	0.0	0.0	0.0	0.0	0.0	0.0	100.0	9	50	3	87%	9%	0%	0%	0%	0%	2%	0%	0%	1%	0%	0%	100%
	N'Zeto	S4906	<500	0%	65%	35%	Point	M.Padoan	251	263	5.4	5.2	1.6	0.0	0.8	0.0	0.4	0.4	35.9	0.0	14.7	0.0	0.0	7.6	0.0	38.6	0.0	0.0	0.0	0.0	0.0	0.0	0.0	0.0	0.0	100.0	9	50	2	95%	3%	0%	0%	0%	0%	0%	0%	0%	0%	0%	0%	100%
	Pidi mouth	S4907	<500	0%	81%	19%	Point	M.Padoan	202	225	4.3	3.8	1.0	0.5	0.5	0.0	1.5	1.0	55.4	2.5	7.9	0.5	0.0	2.0	0.0	26.7	0.0	0.5	0.0	0.0	0.0	0.0	0.0	0.0	0.0	100.0	6	50	2	90%	8%	0%	0%	0%	0%	1%	0%	0%	0%	0%	0%	100%
	Musserra	S4908	<500	0%	89%	11%	Point	M.Padoan	244	272	7.1	6.3	2.0	0.0	0.8	0.0	2.0	1.2	57.4	0.0	16.8	0.0	0.0	2.0	0.0	17.6	0.0	0.0	0.0	0.0	0.0	0.0	0.0	0.0	0.0	100.0	10	50	3	90%	10%	0%	0%	0%	0%	0%	0%	0%	0%	0%	0%	100%
	Ambriz	S4909	<500	0%	96%	4%	Point	M.Padoan	216	236	9.1	8.3	0.5	1.9	1.4	0.0	3.7	0.9	33.8	0.0	39.8	0.0	0.0	9.7	0.0	8.3	0.0	0.0	0.0	0.0	0.0	0.0	0.0	0.0	0.0	100.0	0	50	4	92%	7%	0%	0%	0%	0%	0%	0%	0%	0%	1%	0%	100%
	Barra do Dande	S4910	<500	0%	84%	16%	Point	M.Limonta	210	276	7.4	5.6	3.3	1.9	2.4	0.0	0.5	0.0	31.9	0.0	29.0	0.0	0.0	6.7	0.5	19.5	0.0	0.0	4.3	0.0	0.0	0.0	0.0	0.0	0.0	100.0	17	53	8	76%	20%	0%	0%	0%	0%	4%	0%	0%	0%	0%	0%	100%
	Cacuaco	S4912	<500	0%	97%	3%	Point	M.Padoan	221	343	1.5	1.0	1.8	5.0	2.7	0.0	1.8	1.4	52.9	0.0	0.5	3.2	0.0	4.1	0.0	26.7	0.0	0.0	0.0	0.0	0.0	0.0	0.0	0.0	0.0	100.0	8	50	10	64%	19%	0%	1%	0%	2%	6%	0%	0%	6%	0%	1%	100%
RIVERS IN NORTHERN ANGOLA																																																				
Luculu	Quivanda	S4904	15-500	1.7%	83%	16%	Point	M.Padoan	292	349	6.1	5.1	2.1	2.4	2.1	0.0	1.4	0.0	30.1	0.0	32.9	1.7	0.0	14.7	0.0	12.7	0.0	0.0	0.0	0.0	0.0	0.0	0.0	0.0	0.0	100.0	4	50	7	84%	14%	0%	0%	0%	0%	2%	0%	0%	0%	0%	0%	100%
Mebridege	Cassa de Telha	S4897	15-500	0%	67%	33%	Fleet	M.Padoan	278	929	0.1	0.03	5.4	3.2	0.0	1.4	2.2	3.6	6.8	1.4	1.1	0.0	0.0	3.2	0.0	62.9	0.0	7.6	1.1	0.0	0.0	0.0	0.0	0.0	0.0	100.0	9	50	9	30%	19%	0%	0%	2%	19%	27%	0%	0%	1%	0%	2%	100%
Sembo	Musserra	S4895	<500	0%	9%	91%	Point	M.Padoan	217	245	2.7	2.4	0.9	1.4	0.0	0.0	0.0	0.0	19.8	0.9	2.3	0.0	0.0	1.4	0.0	72.4	0.0	0.0	0.9	0.0	0.0	0.0	0.0	0.0	0.0	100.0	0	n.d.	2	89%	2%	0%	0%	0%	2%	1%	0%	0%	4%	0%	1%	100%
Loge	Porta Freitas Morna	S4894	15-500	0%	78%	22%	Point	M.Padoan	254	265	7.0	6.7	0.8	0.0	0.0	0.0	0.8	1.2	69.3	0.8	1.6	0.0	0.0	0.0	0.0	25.6	0.0	0.0	0.0	0.0	0.0	0.0	0.0	0.0	0.0	100.0	1	n.d.	1	96%	2%	0%	0%	0%	0%	1%	0%	0%	0%	0%	0%	100%
Onzo	Tabi	S4893	<500	0%	38%	62%	Point	M.Limonta	215	232	8.1	7.5	0.0	0.0	1.4	0.0	0.0	0.0	26.0	0.5	7.4	0.0	0.0	5.6	0.0	56.7	0.0	0.0	2.3	0.0	0.0	0.0	0.0	0.0	0.0	100.0	8	50	1	93%	2%	0%	0%	0%	1%	2%	0%	0%	1%	0%	2%	100%
Lifune	Conde Loca	S4892	15-500	0.7%	61%	38%	Point	M.Limonta	209	257	4.1	3.4	2.9	1.4	2.4	0.0	0.0	0.0	34.9	0.0	11.5	0.0	0.0	11.5	0.5	34.0	0.0	0.0	1.0	0.0	0.0	0.0	0.0	0.0	0.0	100.0	18	52	7	81%	12%	0%	0%	0%	0%	5%	0%	0%	0%	0%	0%	100%
Dande	Caxito	S4891	15-500	1.8%	96%	2%	Point	M.Padoan	200	302	2.5	1.6	2.0	2.0	1.5	0.0	1.0	0.0	47.5	0.0	6.0	0.0	0.0	3.5	0.0	35.5	0.0	0.0	0.0	0.0	0.0	1.0	0.0	0.0	0.0	100.0	16	50	6	66%	18%	0%	0%	0%	1%	3%	0%	0%	6%	0%	5%	100%
Bengo	Quifangondo	S4911	15-500	4.7%	69%	26%	Point	M.Padoan	253	350	2.3	1.7	2.8	1.2	2.4	0.0	0.4	0.4	30.4	0.0	13.0	1.2	0.0	10.3	0.0	36.8	0.0	0.0	0.0	0.0	0.0	1.2	0.0	0.0	0.0	100.0	11	50	6	72%	10%	0%	0%	0%	1%	5%	0%	0%	11%	0%	0%	100%
CUANZA & CUANZA LITTORAL CELL																																																				
	Ilha de Luanda	S4652	32-355	0%	2%	98%	Point	M.Limonta	226	300	5.3	4.0	1.8	0.0	0.0	0.0	0.4	0.0	40.3	4.4	3.1	0.9	0.4	2.7	0.9	20.8	0.0	0.0	24.3	0.0	0.0	0.0	0.0	0.0	0.0	100.0	8	59	2	75%	15%	0%	0%	1%	0%	8%	0%	0%	1%	0%	0%	100%
	Mussulo	S3764	32-355	0%	20%	80%	Fleet	M.Limonta	117	168	1.2	0.8	1.7	0.9	0.0	0.0	0.9	0.0	49.6	3.4	0.9	0.0	1.7	0.9	0.0	26.5	0.0	0.0	12.0	0.0	0.0	0.0	0.0	0.0	1.7	100.0	12	n.d.	3	70%	16%	1%	0%	1%	1%	12%	0%	0%	1%	0%	0%	100%
	Palmeirinhas	S4913	<500	0%	60%	40%	Point	M.Limonta	225	362	2.3	1.4	7.6	0.0	0.0	0.0	1.3	2.7	51.1	0.9	4.9	2.7	0.0	2.2	0.0	14.7	0.0	0.0	12.0	0.0	0.0	0.0	0.0	0.0	0.0	100.0	1	50	8	62%	30%	0%	0%	1%	1%	6%	0%	0%	0%	0%	0%	100%
	Barra do Cuanza	S4914	<500	0%	64%	36%	Point	M.Limonta	219	269	1.6	1.3	4.6	0.0	0.0	0.0	0.5	4.1	53.4	0.5	2.7	0.5	0.0	0.0	0.0	25.1	0.0	0.0	7.3	0.9	0.0	0.0	0.5	0.0	0.0	100.0	6	n.d.	5	81%	12%	2%	0%	0%	0%	4%	0%	0%	0%	0%	0%	100%
Cuanza	Barra do Cuanza	S4915	15-500	0%	98%	2%	Point	M.Limonta	205	334	1.0	0.6	9.3	6.3	2.0	0.0	0.0	0.5	50.7	1.0	4.9	0.0	0.5	2.0	0.5	15.1	0.0	0.0	7.3	0.0	0.0	0.0	0.0	0.0	0.0	100.0	10	58	18	61%	31%	1%	0%	0%	0%	6%	0%	0%	1%	0%	0%	100%
BEACHES & SHELF IN CENTRAL ANGOLA																																																				
	Cabo Ledo	S3765	32-355	0%	60%	40%	Area	M.Limonta	204	295	12.7	8.8	6.9	0.5	0.0	0.0	1.0	3.9	54.9	0.5	2.5	0.0	0.0	1.0	0.0	14.7	0.0	0.0	7.4	0.0	0.0	0.0	0.0	0.0	6.9	100.0	3	n.d.	7	69%	28%	0%	0%	0%	0%	2%	0%	0%	0%	0%	0%	100%
	Sao Braz	S4916	<500	0%	94%	6%	Point	M.Limonta	219	265	4.1	3.4	3.2	0.5	0.0	0.0	0.0	4.6	65.8	0.5	0.9	0.0	0.0	0.5	0.5	21.0	0.0	0.0	2.3	0.0	0.0	0.5	0.0	0.0	0.0	100.0	4	n.d.	4	83%	10%	0%	0%	0%	0%	6%	0%	0%	0%	0%	0%	100%
	Porto Amboim	S4918	<500	0%	59%	41%	Point	M.Limonta	212	273	10.5	8.1	5.2	0.0	0.9	0.0	0.0	6.6	39.6	1.9	0.9	0.0	0.0	1.4	0.0	20.8	0.0	0.0	19.8	0.9	0.0	0.0	1.9	0.0	0.0	100.0	9	n.d.	6	78%	16%	0%	0%	0%	1%	4%	0%	0%	0%	0%	0%	100%
	Carimba	S4923	<500	0%	60%	40%	Point	M.Limonta	202	296	11.6	7.9	10.9	0.5	0.0	0.0	1.0	3.5	47.0	1.5	1.0	0.5	0.0	0.5	0.0	18.8	0.0	0.0	14.9	0.0	0.0	0.0	0.0	0.0	0.0	100.0	11	n.d.	11	68%	28%	0%	0%	0%	0%	3%	0%	0%	0%	0%	1%	100%
	Sumbe	S4919	<500	0%	64%	36%	Point	M.Limonta	200	288	3.6	2.5	11.0	0.5	0.0	0.0	0.0	6.0	56.5	0.5	0.5	0.0	0.0	0.0	0.0	17.5	0.0	0.0	7.5	0.0	0.0	0.0	0.0	0.0	0.0	100.0	2	n.d.	12	69%	27%	0%	0%	0%	1%	2%	0%	0%	0%	0%	0%	100%
	Quicombo	S4920	<500	0%	70%	30%	Point	M.Limonta	202	283	5.9	4.2	13.9	0.0	0.0	0.0	0.5	0.5	60.9	0.0	0.5	0.0	0.0	0.0	0.0	12.4	0.0	0.0	10.4	0.0	0.0	1.0	0.0	0.0	0.0	100.0	3	n.d.	14	71%	24%	0%	0%	0%	0%	4%	0%	0%	0%	0%	0%	100%
	Praia Sousa	S4930	<500	0%	32%	68%	Point	M.Limonta	206	299	2.0	1.4	2.4	0.0	0.0	0.0	0.0	0.0	58.7	1.9	0.0	0.0	0.0	0.0	0.5	23.3	0.0	0.0	13.1	0.0	0.0	0.0	0.0	0.0	0.0	100.0	1	n.d.	2	69%	16%	0%	0%	0%	1%	14%	0%	0%	0%	0%	0%	100%
	Candunga	S4921	<500	0%	28%	72%	Point	M.Limonta	203	275	6.4	4.7	8.9	0.0	0.0	0.0	0.5	0.0	51.2	3.0	0.5	0.0	0.0	0.0	0.0	12.8	0.0	1.0	18.7	3.4	0.0	0.0	0.0	0.0	0.0	100.0	8	n.d.	9	74%	17%	0%	0%	0%	1%	8%	0%	0%	0%	0%	0%	100%
	Egito Praia	S4928	<500	0%	50%	50%	Point	M.Limonta	205	281	1.7	1.2	0.0	0.0	0.0	0.0	0.0	0.0	41.5	2.9	0.5	0.0	0.0	0.0	0.0	23.9	0.0	1.0	27.3	2.9	0.0	0.0	0.0	0.0	0.0	100.0	5	n.d.	0	73%	7%	0%	1%	1%	1%	17%	0%	0%	0%	0%	0%	100%
-73 m shelf offshore	Tapado mouth	1011	>15	19.1%	81%	0%	Point	M.Limonta	205	225	3.2	2.9	2.0	0.5	0.5	0.0	0.5	1.5	63.9	1.5	0.0	0.0	0.0	0.0	0.0	26.3	0.0	0.0	3.4	0.0	0.0	0.0	0.0	0.0	0.0	100.0	9	n.d.	3	91%	2%	1%	1%	0%	0%	3%	0%	0%	0%	0%	1%	100%
-99 m shelf offshore	Tapado mouth	1012/1	>15	11.6%	88%	0%	Raman	M.Limonta	283	296	4.9	4.5	1.8	0.0	0.0	0.0	2.1	2.5	79.5	0.4	0.0	0.0	0.0	0.0	0.0	13.1	0.0	0.0	0.7	0.0	0.0	0.0	0.0	0.0	0.0	100.0	2	n.d.	2	92%	3%	0%	0%	0%	0%	3%	0%	0%	2%	0%	0%	100%
-99 m shelf offshore	Tapado mouth	1012/2	>15	9.1%	91%	0%	Point	M.Limonta	223	236	4.0	3.8	3.6	0.0	0.0	0.4	0.4	1.8	70.0	1.3	0.0	0.0	0.0	0.0	0.4	20.2	0.0	0.0	1.8	0.0	0.0	0.0	0.0	0.0	0.0	100.0	7	n.d.	4	94%	3%	0%	0%	1%	0%	1%	0%	0%	0%	0%	0%	100%
-250 m slope offshore	Tapado mouth	1013	>15	40.2%	60%	0%	Point	M.Limonta	211	228	6.1	5.6	1.9	0.9	0.0	0.0	0.0	1.9	79.6	0.0	0.5	0.0	0.0	0.0	0.5	14.7	0.0	0.0	0.0	0.0	0.0	0.0	0.0	0.0	0.0	100.0	3	n.d.	3	93%	1%	0%	1%	0%	0%	3%	0%	0%	2%	0%	0%	100%
-3040 m south of Cuanza seamount chain		1/2 105-10	> 5	99.3%	0.3%	0.4%	Raman	M.Limonta	14	61	14.0	3.2	7	0	0	0	0	7	64	0	0	0	0	0	0	21	0	0	0	0	0	0	0	0	0	100.0	n.d.	n.d.	7	23%	0%	49%	0%	0%	0%	3%	11%	0%	5%	0%	8%	100%
RIVERS IN CENTRAL ANGOLA																																																				
Longa	Calamba	S4917	15-500	1.3%	68%	30%	Point	M.Padoan	229	278	3.0	2.5	7.4	0.4	0.0	0.0	0.9	0.0	84.7	0.0	0.4	0.4	0.0	0.0	0.0	5.7	0.0	0.0	0.0	0.0	0.0	0.0	0.0	0.0	0.0	100.0	0	n.d.	8	82%	17%	0%	0%	0%	0%	0%	0%	0%	0%	0%	0%	100%
Queve	Cachoeira	S4922	15-500	0%	80%	20%	Point	M.Limonta	208	327	0.8	0.5	1.0	0.0	0.0	0.0	0.5	1.0	40.9	2.4	1.9	0.0	0.0	0.5	1.0	51.0	0.0	0.0	0.0	0.0	0.0	0.0	0.0	0.0	0.0	100.0	4	n.d.	1	64%	8%	2%	2%	0%	1%	13%	0%	0%	12%	0%	1%	100%
Cambongo	Sumbe	S4924	15-500	0.4%	79%	20%	Point	M.Limonta	207	281	2.9	2.1	22.2	0.0	0.0	0.0	0.0	1.0	48.8	1.9	1.4	0.0	0.0	0.5	0.0	18.4	0.0	0.0	4.8	0.5	0.0	0.5	0.0	0.0	0.0	100.0	7	n.d.	22	74%	17%	1%	2%	0%	1%	5%	0%	0%	0%	0%	0%	100%
Quicombo	Quicombo	S4925	15-500	1.4%	55%	43%	Point	M.Limonta	210	318	6.1	4.0	10.0	0.0	0.0	0.0	0.5	5.2	63.3	0.5	2.9	0.0	0.0	0.0	0.0	14.8	0.0	0.5	2.4	0.0	0.0	0.0	0.0	0.0	0.0	100.0	10	n.d.	10	66%	25%	0%	1%	0%	0%	6%	0%	0%	2%	0%	0%	100%
Tapado	Chitonde	S4926	15-500	0%	34%	66%	Point	M.Padoan	220	338	1.0	0.6	3.2	0.0	0.0	0.0	0.0	0.5	56.8	21.4	0.9	0.0	0.0	0.0	0.0	16.4	0.0	0.9	0.0	0.0	0.0	0.0	0.0	0.0	0.0	100.0	0	n.d.	3	65%	5%	0%	0%	0%	19%	6%	0%	0%	4%	0%	1%	100%
Balombo	Canjala	S4927	15-500	0.9%	90%	9%	Point	M.Limonta	210	317	2.0	1.3	7.6	0.0	0.0	0.0	0.0	0.0	86.7	1.9	0.0	0.0	0.0	0.0	0.0	2.9	0.0	0.0	1.0	0.0	0.0	0.0	0.0	0.0	0.0	100.0	11	n.d.	8	66%	17%	1%	2%	0%	1%	12%	0%	0%	1%	0%	0%	100%
Culango	Culango	S4929	15-500	0.3%	31%	69%	Point	M.Padoan	209	339	2.2	1.4	13.9	0.0	0.0	0.0	0.5	0.5	58.4	12.4	0.0	0.0	0.0	0.0	0.0	14.4	0.0	0.0	0.0	0.0	0.0	0.0	0.0	0.0	0.0	100.0	2	n.d.	14	62%	19%	0%	0%	0%	15%	4%	0%	0%	1%	0%	0%	100%
COPOROLO, CATUMBELA & LITTORAL CELLS																																																				
	Lobito spit	S4863	<500	0%	64%	36%	Point	M.Limonta	208	306	18.6	12.6	4.8	0.5	0.0	0.0	0.5	0.5	65.9	3.4	1.9	0.0	0.0	0.0	0.0	13.0	0.0	0.0	9.1	0.5	0.0	0.0	0.0	0.0	0.0	100.0	9	n.d.	5	68%	29%	0%	0%	1%	0%	2%	0%	0%	0%	0%	0%	100%
	Lobito spit	S4934	<500	0%	73%	27%	Point	M.Limonta	204	266	7.2	5.5	5.9	0.0	0.0	0.0	0.0	0.5	51.5	6.4	0.0	0.0	0.0	0.0	0.0	25.0	0.0	0.5	10.3	0.0	0.0	0.0	0.0	0.0	0.0	100.0	7	n.d.	6	77%	19%	0%	0%	0%	0%	3%	0%	0%	0%	0%	0%	100%
	Catumbela N	S4862	<500	0%	58%	42%	Point	M.Limonta	219	352	5.7	3.6	1.8	0.0	0.5	0.0	0.5	0.0	56.6	4.1	0.0	0.0	0.0	0.0	0.0	17.8	0.0	0.5	15.1	2.3	0.0	0.9	0.0	0.0	0.0	100.0	7	n.d.	2	62%	30%	0%	0%	0%	1%	7%	0%	0%	0%	0%	0%	100%
Catumbela mouth	Praia Bebe	S4655	32-355	0%	100%	0%	Area	M.Padoan	109	5056	87.7	1.9	26.6	0.0	0.0	0.0	0.9	0.0	36.7	0.9	0.0	1.8	0.0	1.8	0.0	11.0	0.0	0.9	19.3	0.0	0.0	0.0	0.0	0.0	0.0	100.0	28	50	27	2%	90%	0%	0%	0%	1%	0%	0%	0%	0%	0%	6%	100%
Cubal da Hanha	Vista Alegre	S5118	32-500	18%	70%	12%	Point	M.Limonta	202	271	3.7	2.8	16.8	0.0	0.0	0.0	0.5	0.0	46.5	2.5	0.5	0.0	0.0	0.0	0.0	33.2	0.0	0.0	0.0	0.0	0.0	0.0	0.0	0.0	0.0	100.0	9	n.d.	17	75%	15%	2%	1%	0%	0%	7%	0%	0%	1%	0%	0%	100%
Calumbolo	Supua	S5116	32-500	2%	28%	70%	Point	M.Limonta	207	253	6.2	5.1	0.5	0.0	0.5	0.0	0.0	0.5	80.2	3.9	0.0	0.0	0.0	0.0	0.0	13.0	0.5	0.0	1.0	0.0	0.0	0.0	0.0	0.0	0.0	100.0	6	n.d.	1	82%	2%	0%	2%	0%	0%	4%	0%	0%	9%	1%	0%	100%
Capilongo	Capilongo	S5117	32-500	1%	42%	57%	Point	M.Limonta	217	386	4.9	2.8	0.0	0.0	0.0	0.0	0.9	4.6	41.5	4.1	0.0	0.0	0.0	0.0	0.0	6.0	0.0	0.0	33.6	9.2	0.0	0.0	0.0	0.0	0.0	100.0	0	n.d.	0	56%	3%	0%	2%	0%	5%	7%	0%	0%	25%	1%	1%	100%
Catumbela	Catumbela	S4860	15-500	0.2%	23%	77%	Point	M.Limonta	208	737	18.5	5.2	5.3	0.5	0.5	0.0	1.4	0.5	47.6	1.4	0.0	0.0	0.0	0.0	0.0	15.4	0.0	0.0	21.6	0.0	0.0	0.5	5.3	0.0	0.0	100.0	5	n.d.	6	28%	59%	0%	0%	0%	0%	12%	0%	0%	1%	0%	0%	100%
Catumbela	Catumbela	S4933	15-500	0%	48%	52%	Point	M.Limonta	213	330	1.3	0.8	1.9	0.5	0.0	0.0	0.0	0.0	61.0	8.5	0.0	0.0	0.0	0.0	0.0	19.7	0.0	1.9	5.2	1.4	0.0	0.0	0.0	0.0	0.0	100.0	5	n.d.	2	65%	5%	0%	0%	1%	5%	19%	0%	0%	6%	0%	0%	100%
	Catumbela airport	S4859	bulk	0%	100%	0%	Point	M.Limonta	218	274	2.0	1.6	1.8	0.0	0.0	0.0	1.4	0.5	64.7	4.1	0.0	0.0	0.0	0.0	0.0	25.7	0.0	0.5	1.4	0.0	0.0	0.0	0.0	0.0	0.0	100.0	13	n.d.	2	80%	2%	0%	6%	0%	4%	5%	0%	0%	4%	0%	0%	100%
Cavaco	Benguela	S4932	15-500	0%	42%	58%	Point	M.Padoan	245	335	1.8	1.3	0.8	0.0	0.0	0.0	0.8	2.4	60.8	10.6	0.0	0.0	0.0	0.0	0.0	22.9	0.0	1.6	0.0	0.0	0.0	0.0	0.0	0.0	0.0	100.0	2	n.d.	1	73%	4%	0%	0%	0%	13%	2%	0%	0%	7%	0%	0%	100%
	Benguela	S4931	<500	0%	67%	33%	Point	M.Padoan	234	285	6.7	5.5	1.3	0.0	0.4	0.0	3.0	3.0	63.2	7.7	0.0	0.0	0.0	0.0	0.0	15.8	0.0	1.7	3.0	0.4	0.0	0.4	0.0	0.0	0.0	100.0	0	n.d.	2	82%	9%	0%	0%	1%	5%	1%	0%	0%	1%	0%	1%	100%
-1339 m c'tl rise offshore	Coporolo mouth	4918	> 5	90%	1%	9%	Raman	M.Limonta	209	258	3.8	3.1	0.5	0.0	0.0	0.0	2.9	1.9	78.5	0.0	1.4	0.0	0.0	0.0	0.0	14.8	0.0	0.0	0.0	0.0	0.0	0.0	0.0	0.0	0.0	100.0	0	n.d.	0	81%	0%	0%	3%	0%	0%	7%	0%	0%	3%	0%	5%	100%
	Baia Farta	S4858	bulk	0%	100%	0%	Point	S.Andò	200	239	4.4	3.7	1.0	0.0	0.0	0.0	1.0	0.5	71.5	9.0	0.5	0.0	0.0	0.0	1.0	15.5	0.0	0.0	0.0	0.0	0.0	0.0	0.0	0.0	0.0	100.0	4	n.d.	1	84%	9%	0%	1%	0%	5%	0%	0%	0%	0%	0%	1%	100%
	Baia Farta	S4935	<500	0%	58%	42%	Point	M.Padoan	229	325	2.4	1.7	0.0	0.0	0.0	0.0	2.2	0.4	47.6	17.0	0.4	0.0	0.0	0.0	0.0	27.9	0.0	0.9	2.6	0.0	0.0	0.9	0.0	0.0	0.0	100.0	1	n.d.	0	70%	4%	0%	0%	2%	21%	1%	0%	0%	0%	0%	1%	100%
	Camucua	S4857	<500	0%	22%	78%	Point	M.Limonta	224	279	1.8	1.5	2.2	0.0	0.0	0.0	0.4	0.9	67.0	8.5	0.4	0.0	0.0	0.0	0.0	16.5	0.0	1.3	2.2	0.0	0.0	0.0	0.0	0.0	0.4	100.0	7	n.d.	2	80%	15%	0%	0%	0%	2%	2%	0%	0%	0%	0%	0%	100%
	Saco S	S4853	<500	0%	14%	86%	Point	M.Padoan	237	327	2.1	1.5	0.4	0.4	0.0	0.0	1.7	0.4	48.5	19.8	0.4	0.0	0.0	0.0	0.0	24.9	0.4	1.7	0.8	0.4	0.0	0.0	0.0	0.0	0.0	100.0	4	n.d.	1	72%	3%	0%	0%	0%	19%	3%	0%	0%	1%	0%	1%	100%
Coporolo	Santa Tereza	S4852	15-500	0%	23%	77%	Point	M.Limonta	202	291	1.0	0.7	0.5	0.5	0.0	0.0	0.0	0.0	53.0	13.9	0.0	0.0	0.0	0.0	0.0	26.2	0.0	1.5	3.0	1.0	0.0	0.5	0.0	0.0	0.0	100.0	2	n.d.	1	69%	3%	1%	0%	0%	6%	16%	0%	0%	3%	0%	0%	100%
Coporolo	Dombe Grande	S4936	15-500	0.5%	78%	21%	Point	M.Padoan	227	294	2.5	1.9	3.1	0.0	0.0	0.4	0.4	0.0	57.3	9.3	0.4	0.0	0.4	0.0	0.0	27.3	0.0	0.4	0.4	0.0	0.0	0.4	0.0	0.0	0.0	100.0	2	n.d.	3	77%	9%	0%	0%	0%	9%	3%	0%	0%	0%	0%	1%	100%
BEACHES IN SOUTHERN ANGOLA																																																				
	Cuio	S4937	<500	0%	86%	14%	Point	M.Padoan	212	291	11.5	8.4	0.9	0.0	0.0	0.0	1.9	0.0	59.4	15.6	0.5	0.0	0.0	0.0	0.0	20.8	0.0	0.9	0.0	0.0	0.0	0.0	0.0	0.0	0.0	100.0	0	n.d.	1	73%	4%	0%	0%	2%	20%	0%	0%	0%	0%	0%	0%	100%
	Equimina	S4938	<500	0%	45%	55%	Point	M.Padoan	214	513	20.9	8.7	13.6	0.0	0.0	0.0	1.4	1.9	42.1	23.8	2.3	0.0	0.0	0.0	0.0	12.6	0.0	2.3	0.0	0.0	0.0	0.0	0.0	0.0	0.0	100.0	10	n.d.	14	42%	44%	0%	0%	1%	11%	1%	0%	0%	2%	0%	0%	100%
	Baia Binga	S4939	<500	0%	76%	24%	Point	M.Padoan	249	273	10.8	9.8	0.0	0.0	0.4	0.0	0.8	1.2	43.0	2.0	0.8	0.0	0.0	0.0	0.0	51.4	0.0	0.4	0.0	0.0	0.0	0.0	0.0	0.0	0.0	100.0	1	n.d.	0	91%	4%	0%	0%	0%	3%	1%	0%	0%	0%	0%	0%	100%
	Lucira	S4941	<500	0%	59%	41%	Point	M.Padoan	212	362	6.0	3.5	0.0	0.0	1.4	0.0	1.9	2.4	41.5	35.4	0.9	0.0	0.0	0.0	0.0	9.0	0.0	7.5	0.0	0.0	0.0	0.0	0.0	0.0	0.0	100.0	2	n.d.	1	59%	7%	0%	0%	1%	30%	2%	0%	0%	2%	0%	0%	100%
low outer berm	Inamangando	S4943	<500	0%	53%	47%	Area	M.Padoan	253	982	20.9	5.4	9.1	1.2	1.6	0.0	3.2	1.2	46.6	19.8	0.8	0.0	0.0	0.0	0.0	16.2	0.0	0.4	0.0	0.0	0.0	0.0	0.0	0.0	0.0	100.0	0	n.d.	12	26%	68%	0%	0%	0%	5%	2%	0%	0%	0%	0%	0%	100%
high inner berm	Inamangando	S4944	<500	0%	78%	22%	Point	M.Padoan	229	353	8.2	5.3	1.3	0.0	0.0	0.0	1.3	0.0	45.4	14.4	0.4	0.0	0.0	0.0	0.0	34.1	0.0	1.3	0.0	0.0	0.0	1.7	0.0	0.0	0.0	100.0	5	n.d.	1	65%	25%	0%	0%	0%	8%	1%	0%	0%	0%	0%	0%	100%
	Baia das Salinas	S4946	<500	0%	43%	57%	Point	M.Padoan	204	251	6.4	5.2	0.5	0.0	0.0	0.0	2.0	1.0	34.8	16.2	0.0	0.0	0.0	0.0	0.0	43.6	0.0	2.0	0.0	0.0	0.0	0.0	0.0	0.0	0.0	100.0	5	n.d.	0	81%	7%	0%	0%	0%	10%	1%	0%	0%	1%	0%	0%	100%
	Bentiaba	S4948	<500	0%	42%	58%	Point	M.Padoan	210	349	7.4	4.5	1.4	0.0	1.9	0.0	1.4	0.0	38.1	27.1	0.5	0.0	0.0	0.0	0.0	22.4	0.0	6.7	0.5	0.0	0.0	0.0	0.0	0.0	0.0	100.0	4	n.d.	3	60%	21%	0%	0%	0%	18%	1%	0%	0%	0%	0%	0%	100%
	Chapeu Armado	S4949	<500	0%	79%	21%	Point	M.Padoan	217	526	1.5	0.6	18.9	0.0	4.6	0.0	6.5	3.7	34.6	11.1	8.3	0.0	0.0	0.0	0.0	8.8	0.0	0.9	1.4	0.9	0.0	0.5	0.0	0.0	0.0	100.0	11	n.d.	24	41%	33%	0%	0%	0%	21%	2%	0%	0%	1%	1%	1%	100%
	Mariquita	S4950	<500	0%	19%	81%	Point	M.Padoan	227	476	1.5	0.7	0.0	0.0	1.3	0.0	0.0	0.0	21.6	18.9	1.8	0.0	0.0	0.0	0.0	32.6	0.0	12.8	10.6	0.4	0.0	0.0	0.0	0.0	0.0	100.0	1	n.d.	1	48%	3%	0%	0%	3%	45%	0%	0%	0%	0%	0%	1%	100%
	Namibe	S4953	<500	0%	96%	4%	Point	S.Andò	204	278	13.4	9.8	0.0	0.0	0.0	0.0	2.0	0.5	23.5	4.9	1.5	0.0	0.0	0.0	0.0	43.6	0.0	5.4	8.8	0.0	1.5	7.4	1.0	0.0	0.0	100.0	14	n.d.	0	73%	10%	1%	1%	2%	10%	0%	0%	0%	1%	0%	1%	100%
RIVERS IN SOUTHERN ANGOLA																																																				
Cangala	Santa Maria	S4940	15-500	0.3%	64%	36%	Point	M.Padoan	248	354	3.4	2.4	0.4	0.0	0.0	0.0	1.2	0.8	58.5	17.3	0.0	0.0	0.0	0.0	0.0	20.6	0.0	1.2	0.0	0.0	0.0	0.0	0.0	0.0	0.0	100.0	6	n.d.	0	70%	6%	0%	0%	1%	19%	1%	0%	0%	2%	0%	0%	100%
Carujamba	Lucira	S4942	<500	0%	34%	66%	Point	M.Padoan	246	292	2.2	1.8	0.4	0.0	0.0	0.0	0.8	0.0	39.0	24.4	0.0	0.0	0.0	0.0	0.0	32.5	0.0	2.8	0.0	0.0	0.0	0.0	0.0	0.0	0.0	100.0	2	n.d.	0	84%	1%	0%	0%	0%	13%	0%	0%	0%	1%	0%	1%	100%
Inamangando	Inamangando	S4945	15-500	0.2%	63%	37%	Point	M.Padoan	209	274	3.8	2.9	1.4	0.0	0.0	0.0	2.9	0.0	48.3	29.7	0.0	0.0	0.0	0.0	0.0	16.7	0.0	1.0	0.0	0.0	0.0	0.0	0.0	0.0	0.0	100.0	17	n.d.	1	76%	5%	0%	0%	0%	16%	0%	0%	0%	1%	0%	1%	100%
Bentiaba	Bentiaba	S4947	15-500	0%	37%	63%	Point	M.Padoan	208	256	4.4	3.5	0.0	0.0	0.0	0.0	0.5	1.9	57.2	4.3	0.0	0.0	0.0	0.0	0.0	32.2	0.0	3.4	0.5	0.0	0.0	0.0	0.0	0.0	0.0	100.0	16	n.d.	0	81%	7%	0%	0%	0%	10%	0%	0%	0%	1%	0%	1%	100%
Giraul	Giraul	S4951	15-500	0%	23%	77%	Point	M.Padoan	224	316	4.8	3.4	0.9	0.0	0.0	0.0	1.3	0.4	32.1	9.8	2.7	0.0	0.0	0.0	0.0	46.4	0.0	5.4	0.4	0.0	0.0	0.4	0.0	0.0	0.0	100.0	7	n.d.	1	71%	18%	0%	0%	2%	8%	1%	0%	0%	1%	0%	0%	100%
Bero	Namibe	S4952	15-500	0%	42%	58%	Point	M.Padoan	223	362	4.5	2.8	0.0	0.0	0.0	0.0	0.0	0.9	10.8	10.3	0.4	0.0	0.0	0.0	0.4	45.7	0.0	14.8	8.1	1.3	0.0	7.2	0.0	0.0	0.0	100.0	5	n.d.	0	62%	6%	0%	0%	2%	27%	3%	0%	0%	0%	0%	1%	100%
CUNENE RIVER SYSTEM																																																				
Cunene	Matala	S4773	15-500	2.2%	69%	29%	Point	S.Andò	200	349	0.4	0.2	88.5	1.0	3.0	0.0	2.0	0.5	2.0	0.0	0.0	0.5	0.0	0.5	0.0	1.0	0.0	0.0	1.0	0.0	0.0	0.0	0.0	0.0	0.0	100.0	n.d.	n.d.	93	57%	27%	5%	1%	1%	0%	5%	0%	1%	0%	0%	3%	100%
Mucope	Techiulo	S5049	15-500	1.9%	91%	8%	Point	M.Padoan	213	478	0.1	0.1	50.2	23.5	4.2	0.9	0.0	1.4	7.5	0.5	0.0	5.2	3.8	1.9	0.0	0.9	0.0	0.0	0.0	0.0	0.0	0.0	0.0	0.0	0.0	100.0	n.d.	50	78	45%	48%	0%	1%	0%	2%	3%	0%	0%	0%	0%	1%	100%
Caculuvar	Techango	S5050	15-500	0.4%	55%	45%	Area	M.Padoan	234	1375	0.1	0.0	47.9	7.7	3.8	0.0	0.0	1.7	23.5	1.3	1.7	2.6	6.8	1.3	0.0	1.3	0.0	0.4	0.0	0.0	0.0	0.0	0.0	0.0	0.0	100.0	n.d.	50	59	17%	73%	0%	0%	0%	4%	6%	0%	0%	1%	0%	0%	100%
Caculuvar confluence	Omutele	S5051	15-500	0.5%	61%	38%	Area	M.Padoan	264	582	0.2	0.1	30.7	1.5	1.1	0.4	0.0	0.4	48.1	10.2	0.8	1.1	0.4	0.8	0.0	3.8	0.0	0.0	0.0	0.0	0.0	0.8	0.0	0.0	0.0	100.0	0	50	33	45%	44%	0%	0%	2%	3%	5%	0%	0%	0%	0%	0%	100%
Cunene	Ruacana	S3931	32-500	0%	100%	0%	Area	M.Padoan	212	424	1.6	0.8	1.9	1.9	0.9	2.4	0.0	1.4	32.1	0.0	1.4	0.0	0.9	0.0	2.4	54.7	0.0	0.0	0.0	0.0	0.0	0.0	0.0	0.0	0.0	100.0	16	86	5	50%	25%	1%	0%	20%	0%	0%	0%	0%	1%	0%	3%	100%
Ehomba	Ehomba	S3932	32-500	0.1%	97%	3%	Area	M.Padoan	129	678	0.9	0.2	21.7	5.4	5.4	10.1	0.0	0.0	27.1	0.0	3.9	0.0	0.0	0.8	0.0	25.6	0.0	0.0	0.0	0.0	0.0	0.0	0.0	0.0	0.0	100.0	34	n.d.	33	19%	42%	4%	0%	29%	0%	0%	0%	0%	0%	0%	5%	100%
Ondoto	Chitado	S3933	32-500	0.1%	86%	14%	Area	M.Padoan	201	484	4.3	1.8	7.0	1.0	3.0	2.0	0.0	0.0	51.7	0.0	4.5	0.0	0.0	0.0	0.5	30.3	0.0	0.0	0.0	0.0	0.0	0.0	0.0	0.0	0.0	100.0	34	n.d.	11	42%	31%	0%	0%	22%	0%	0%	0%	0%	1%	0%	5%	100%
Omuhongo	Etengua	S3935	32-500	0.0%	27%	73%	Area	M.Padoan	200	352	3.3	1.9	5.0	0.0	0.5	0.0	0.0	0.0	83.0	0.0	1.5	0.0	0.0	0.0	1.5	8.5	0.0	0.0	0.0	0.0	0.0	0.0	0.0	0.0	0.0	100.0	22	n.d.	6	57%	15%	1%	0%	26%	0%	0%	0%	0%	0%	0%	1%	100%
Omuhongo	Oryeheke	S3934	32-500	0.0%	75%	25%	Area	M.Padoan	254	438	7.5	4.3	5.1	0.0	0.0	0.0	0.0	0.4	62.6	0.0	1.6	0.0	0.0	0.0	0.8	26.4	0.0	0.0	3.1	0.0	0.0	0.0	0.0	0.0	0.0	100.0	26	n.d.	5	58%	22%	0%	0%	18%	0%	0%	0%	0%	1%	0%	1%	100%
Cunene	Epupa Falls	S4775	15-500	0.3%	52%	48%	Point	S.Andò	200	320	6.8	4.3	0.5	0.0	0.0	0.0	0.5	4.0	20.5	6.5	0.5	0.0	0.5	0.0	0.0	35.5	2.5	5.5	12.5	1.5	0.0	8.5	0.5	0.0	0.5	100.0	38	n.d.	1	63%	16%	1%	1%	1%	12%	5%	0%	0%	1%	0%	0%	100%
Otjinjange	Van Zyl's Pass	S3936	32-500	0.07%	98%	2%	Area	M.Padoan	215	292	17.0	12.5	0.5	0.5	0.0	0.0	0.0	0.0	31.6	0.0	0.5	0.0	0.0	0.0	0.5	66.5	0.0	0.0	0.0	0.0	0.0	0.0	0.0	0.0	0.0	100.0	4	n.d.	1	74%	11%	0%	0%	12%	0%	0%	0%	1%	1%	0%	1%	100%
Marienfluss	Otyoyonoka	S3937	32-500	0.6%	64%	36%	Area	M.Padoan	217	276	22.3	17.5	1.4	0.0	0.0	0.0	0.0	0.0	23.0	0.0	0.5	0.0	0.0	0.0	1.4	73.7	0.0	0.0	0.0	0.0	0.0	0.0	0.0	0.0	0.0	100.0	0	n.d.	1	79%	8%	0%	0%	5%	0%	0%	0%	0%	6%	0%	2%	100%
Cunene	Foz do Cunene	S5052	15-500	0%	95%	5%	Point	S.Andò	216	285	5.4	4.1	0.5	0.0	0.5	0.0	1.9	0.9	13.9	5.6	10.2	4.2	0.9	0.0	0.5	28.7	0.5	3.7	19.9	2.8	0.0	5.6	0.0	0.0	0.0	100.0	9	54	1	76%	8%	2%	1%	0%	11%	0%	1%	0%	1%	0%	0%	100%
ORANGE LITTORAL CELL ONSHORE																																																				
	Subida Grande	S4954	<500	0%	99%	0.8%	Point	S.Andò	210	306	3.1	2.2	0.5	1.9	0.0	0.0	1.4	0.5	15.7	1.9	9.5	2.4	0.5	0.0	0.0	22.9	0.0	1.4	34.8	1.4	0.0	4.3	0.0	0.0	1.0	100.0	26	50	2	69%	5%	1%	1%	0%	16%	1%	4%	0%	0%	3%	1%	100%
fossil dune	Nonguai	S4802	<500	0%	97%	3%	Point	M.Padoan	223	434	0.2	0.1	8.5	24.7	1.3	0.0	1.8	1.3	7.6	1.3	23.3	26.9	0.0	1.3	0.0	1.8	0.0	0.0	0.0	0.0	0.0	0.0	0.0	0.0	0.0	100.0	n.d.	50	35	51%	26%	0%	1%	0%	15%	5%	0%	0%	0%	0%	1%	100%
Curoca	Curoca mouth	S4955	15-500	0.1%	98%	2%	Point	M.Padoan	1342	2056	13.1	8.5	4.6	1.6	0.4	0.0	0.4	0.8	16.6	2.4	27.8	2.1	0.0	0.0	0.0	6.7	0.2	0.2	31.4	1.7	0.0	3.0	0.0	0.0	0.0	100.0	10	50	7	65%	26%	0%	0%	1%	6%	1%	0%	0%	0%	0%	2%	100%
	Curoca mouth	S4956	<500	0%	95%	5%	Point	M.Padoan	200	329	10.4	6.3	3.0	3.5	0.0	0.0	1.0	0.0	12.5	2.5	43.5	5.5	0.0	0.0	0.0	11.5	0.0	1.0	11.5	0.0	0.0	4.5	0.0	0.0	0.0	100.0	14	50	7	61%	25%	0%	0%	3%	8%	3%	0%	0%	0%	0%	1%	100%
outer spit	Tombua	S4805	<500	0%	97%	3%	Point	M.Padoan	892	1285	2.8	1.9	1.2	3.6	0.6	0.0	0.0	0.7	13.8	2.8	22.6	2.5	0.0	0.0	0.4	18.2	0.0	4.4	25.2	0.4	0.0	3.6	0.0	0.0	0.0	100.0	16	58	5	69%	12%	0%	0%	2%	11%	3%	0%	0%	0%	0%	2%	100%
eolian dune	Tombua	S4774	bulk	0%	100%	0%	Point	S.Andò	206	298	5.4	3.7	0.0	2.4	1.5	0.0	1.5	0.0	8.7	1.9	24.3	3.4	0.0	0.0	0.0	12.1	0.0	0.5	39.3	2.9	0.0	1.0	0.5	0.0	0.0	100.0	1	50	4	69%	6%	3%	1%	1%	7%	4%	8%	0%	0%	0%	0%	100%
	Vanesa	S4957	<500	0%	97%	3%	Point	M.Padoan	798	1229	4.0	2.6	2.0	3.1	0.5	0.0	0.0	0.1	10.9	2.6	42.9	6.6	0.0	0.5	0.0	11.4	0.0	2.9	12.7	0.0	0.0	3.8	0.0	0.0	0.0	100.0	15	50	6	65%	13%	0%	0%	3%	15%	3%	0%	0%	0%	0%	1%	100%
eolian dune	Cova dos Medos	S4961	<500	0%	98%	2%	Point	M.Padoan	212	305	18.5	12.9	2.4	1.4	0.5	0.0	0.0	0.0	10.8	2.8	39.2	5.2	0.0	0.0	0.0	12.7	0.0	1.4	19.3	0.5	0.0	3.8	0.0	0.0	0.0	100.0	4	50	4	70%	12%	0%	0%	1%	14%	2%	0%	0%	0%	0%	1%	100%
	Vanesinha	S4958	<500	0%	97%	3%	Point	S.Andò	768	974	14.5	11.5	0.1	1.0	0.0	0.0	0.3	0.5	5.2	4.7	68.4	3.8	0.0	0.0	0.3	6.3	0.0	0.8	7.2	0.0	0.0	1.6	0.0	0.0	0.0	100.0	20	53	1	79%	11%	1%	1%	0%	7%	1%	0%	0%	0%	0%	0%	100%
	Praia do Navio	S4959	<500	0%	99%	0.6%	Point	M.Padoan	764	1131	15.2	10.3	3.3	1.4	0.0	0.0	0.0	0.7	11.1	1.3	52.7	8.4	0.0	0.0	0.5	8.0	0.3	0.4	8.9	0.5	0.0	2.5	0.0	0.0	0.0	100.0	24	53	5	68%	19%	0%	0%	2%	7%	3%	0%	0%	0%	0%	1%	100%
eolian dune	Praia do Navio	S4960	<500	0%	99%	1%	Point	M.Padoan	771	1435	49.8	26.8	6.5	0.9	1.0	0.0	0.0	1.0	5.8	0.3	61.7	3.8	0.0	0.0	0.3	6.1	0.0	0.3	10.9	0.0	0.0	1.3	0.0	0.1	0.0	100.0	10	53	8	54%	38%	0%	0%	1%	3%	1%	0%	0%	0%	0%	3%	100%
eolian dune	Riscos	S5059	<500	0%	100%	0.4%	Point	S.Andò	201	257	2.5	1.9	3.0	1.0	0.0	0.5	1.5	0.0	11.9	1.0	41.8	3.0	0.0	0.0	0.5	8.5	0.0	0.5	21.4	3.5	0.0	2.0	0.0	0.0	0.0	100.0	18	57	4	78%	12%	2%	1%	0%	5%	1%	###	0%	0%	0%	0%	100%
	Riscos	S5058	<500	0%	100%	0.1%	Point	M.Padoan	480	649	11.3	8.4	3.1	1.7	0.6	0.0	0.0	0.6	12.9	1.7	21.3	2.3	0.0	0.0	0.0	8.3	0.0	0.2	42.9	1.5	0.0	2.9	0.0	0.0	0.0	100.0	5	50	5	74%	16%	0%	0%	2%	6%	1%	0%	0%	0%	0%	1%	100%
	Saco dos Tigres	S5057	<500	0%	99%	1%	Point	S.Andò	201	303	3.7	2.5	0.5	2.0	0.0	0.0	2.5	0.5	6.5	1.5	46.3	1.5	0.0	0.0	0.0	10.9	0.0	0.0	20.4	2.0	0.0	5.5	0.0	0.0	0.0	100.0	9	n.d.	2	66%	24%	0%	0%	0%	8%	0%	###	0%	0%	1%	0%	100%
eolian dune	Praia dos Esponjas	S5056	<500	0%	40%	60%	Point	S.Andò	348	474	2.7	2.0	1.7	0.0	0.0	0.0	0.6	2.6	12.4	5.2	7.5	1.1	0.0	0.0	0.0	17.0	0.3	0.3	40.8	2.0	0.0	8.3	0.0	0.0	0.3	100.0	12	50	2	73%	14%	1%	0%	0%	7%	1%	###	1%	1%	1%	0%	100%
	Praia dos Esponjas	S5055	<500	0%	82%	18%	Point	M.Padoan	214	341	2.1	1.3	0.5	2.3	0.5	0.0	1.9	2.3	10.7	6.5	7.5	2.8	0.0	1.4	0.0	21.5	0.0	2.8	36.9	0.5	0.0	1.9	0.0	0.0	0.0	100.0	17	50	3	63%	7%	0%	0%	4%	25%	1%	0%	0%	0%	0%	0%	100%
eolian dune	Foz do Cunene	S5054	<500	0%	100%	0%	Point	S.Andò	200	264	4.9	3.7	0.0	1.0	0.0	0.0	2.0	0.0	15.5	3.0	12.5	1.5	0.0	0.0	0.0	17.0	0.5	2.5	36.0	2.5	0.0	6.0	0.0	0.0	0.0	100.0	21	n.d.	1	76%	15%	1%	1%	0%	5%	2%	###	0%	0%	0%	1%	100%
	Foz do Cunene	S5053	<500	0%	44%	56%	Point	S.Andò	203	348	17.7	10.3	0.0	0.5	0.0	0.0	1.5	0.5	12.3	6.4	23.2	0.5	0.0	0.0	0.0	16.3	1.0	1.0	33.5	0.0	0.5	3.0	0.0	0.0	0.0	100.0	26	n.d.	0	58%	33%	1%	1%	0%	5%	0%	###	0%	1%	0%	1%	100%
ORANGE LITTORAL CELL OFFSHORE																																																				
-2766 m c'tl rise offshore	Baia dos Tigres	1/1 89-91	> 5	91%	9%	0%	Raman	M.Limonta	199	339	*1.6*	*0.9*	2.5	1.5	0.0	1.0	3.0	0.5	14.9	0.0	1.0	0.0	0.0	0.0	0.0	7.9	0.0	0.0	64.4	0.0	3.0	0.0	0.0	0.0	0.5	100.0	0	n.d.	4	54%	5%	0%	1%	0%	0%	27%	1%	0%	8%	0%	5%	100%
-2768 m c'tl rise offshore	Baia dos Tigres	2/4 31-33	> 5	92%	8%	0%	Raman	M.Limonta	198	374	*1.0*	*0.5*	3.0	0.0	0.0	1.0	4.0	5.0	20.5	0.0	7.5	0.5	1.0	1.0	0.0	19.0	0.0	0.0	36.5	0.0	0.0	0.0	0.0	0.0	1.0	100.0	0	n.d.	3	52%	2%	2%	2%	0%	2%	23%	2%	0%	10%	1%	4%	100%
-2766 m c'tl rise offshore	Baia dos Tigres	1/6 65-67	> 5	92%	8%	0%	Raman	M.Limonta	205	424	1.0	0.5	2.9	1.5	2.0	0.0	2.4	2.9	21.5	0.0	1.5	0.0	0.0	0.0	0.0	18.5	0.0	0.0	42.9	0.0	2.0	0.0	0.0	0.0	2.0	100.0	0	n.d.	6	48%	1%	1%	2%	0%	0%	28%	0%	0%	14%	2%	4%	100%
-75 m shelf offshore	Cunene mouth	1019	>15	46%	54%	0%	Raman	M.Limonta	200	257	*7.3*	*5.7*	0.5	0.5	1.0	0.5	4.5	2.0	10.0	0.0	1.5	0.0	0.5	0.0	0.0	11.0	0.0	0.0	66.5	0.0	0.0	0.5	0.0	0.0	1.0	100.0	0	n.d.	2	78%	1%	0%	0%	0%	0%	11%	0%	0%	5%	0%	4%	100%
-110 m outer shelf offshore	Cunene mouth	1020	>15	29%	71%	0%	Raman	M.Limonta	201	256	8.6	6.7	1.5	0.5	0.5	0.5	2.5	4.0	10.9	0.0	6.0	0.5	0.0	0.0	0.0	10.9	0.0	0.0	62.2	0.0	0.0	0.0	0.0	0.0	0.0	100.0	0	n.d.	2	79%	1%	0%	0%	0%	1%	15%	1%	0%	2%	0%	1%	100%
-173 m outer shelf offshore	Cunene mouth	1021	>15	15%	85%	0%	Raman	M.Limonta	203	248	5.9	4.8	0.0	0.0	2.0	1.0	2.5	2.0	13.8	0.0	1.5	0.0	0.0	0.0	0.5	6.9	0.0	0.0	70.0	0.0	0.0	0.0	0.0	0.0	0.0	100.0	n.d.	n.d.	2	82%	1%	0%	0%	0%	0%	10%	1%	0%	3%	0%	3%	100%
-551 m slope offshore of	Cunene mouth	1022	>15	3%	97%	0%	Raman	M.Limonta	198	244	*0.8*	*0.7*	2.5	1.5	1.5	0.0	2.0	2.0	17.2	0.0	5.1	1.0	0.5	0.0	1.0	5.1	0.0	0.0	60.6	0.0	0.0	0.0	0.0	0.0	0.0	100.0	n.d.	70	6	81%	2%	0%	0%	0%	0%	11%	1%	0%	2%	0%	3%	100%
-399 m continental slope on	Walvis Ridge	1704	>15	70%	30%	0%	Raman	M.Limonta	208	274	*0.3*	*0.2*	0.5	0.0	0.0	0.0	3.4	1.4	14.9	0.0	1.4	0.0	0.0	0.0	0.0	9.6	0.0	0.0	68.8	0.0	0.0	0.0	0.0	0.0	0.0	100.0	2	n.d.	0	76%	1%	0%	0%	0%	0%	8%	###	2%	4%	8%	1%	100%
-642 m continental slope on	Walvis Ridge	1705	>15	74%	26%	0%	Raman	M.Limonta	164	203	*1.0*	*0.8*	1.2	0.0	0.0	3.7	1.2	0.0	20.7	0.0	3.0	0.0	0.6	0.0	0.0	17.7	0.0	0.0	51.8	0.0	0.0	0.0	0.0	0.0	0.0	100.0	10	n.d.	1	81%	0%	0%	1%	0%	1%	11%	0%	0%	3%	0%	1%	100%

Appendix Table A5
Click here to download Table: Table A5 Angola TXT.pdf

Table A5

River	Site	Sample	Q	F	L	Clinopyroxene					Orthopyroxene					Amphibole					Epidote					Staurolite					Garnet					Kyanite					Andalusite					Apatite					Zircon		Tourmaline		Rutile		Titanite		Total				
						Unweathered	Corroded	Etched	Deeply etched	Skeletal	Unweathered	Corroded	Etched	Deeply etched	Skeletal	Unweathered	Corroded	Etched	Deeply etched	Skeletal	Unweathered	Corroded	Etched	Deeply etched	Skeletal	Unweathered	Corroded	Etched	Deeply etched	Skeletal	Unweathered	Corroded	Etched	Deeply etched	Skeletal	Unweathered	Corroded	Etched	Deeply etched	Skeletal	Unweathered	Corroded	Etched	Deeply etched	Skeletal	Unweathered	Corroded	Etched	Deeply etched	Skeletal	Unweathered	Corroded	Unweathered	Corroded	Unweathered	Corroded	Unweathered	Corroded	Unweathered	Corroded	Etched	Deeply etched	Skeletal
OPERATOR 1: Marta Padoan																																																															
Loussoni	St. Paul	S4053	99	0	1	n.d.	n.d.	n.d.	n.d.	n.d.	n.d.	n.d.	n.d.	n.d.	n.d.	n.d.	n.d.	n.d.	n.d.	n.d.	n.d.	n.d.	n.d.	n.d.	n.d.	25%	63%	13%	0%	0%	40%	60%	0%	0%	0%	n.d.	n.d.	n.d.	n.d.	n.d.	n.d.	n.d.	n.d.	n.d.	n.d.	n.d.	n.d.	n.d.	n.d.	n.d.	90%	10%	43%	57%	n.d.	n.d.	n.d.	n.d.	46%	51%	3%	0%	0%
	Pointe Noire	S0162	99	1	0	n.d.	n.d.	n.d.	n.d.	n.d.	n.d.	n.d.	n.d.	n.d.	n.d.	30%	70%	0%	0%	0%	n.d.	n.d.	n.d.	n.d.	n.d.	25%	54%	21%	0%	0%	n.d.	n.d.	n.d.	n.d.	n.d.	59%	41%	0%	0%	0%	n.d.	n.d.	n.d.	n.d.	n.d.	n.d.	n.d.	n.d.	n.d.	n.d.	91%	9%	65%	35%	71%	29%	n.d.	n.d.	62%	33%	4%	0%	0%
Loémé	Djeno	S0161	100	0	0	n.d.	n.d.	n.d.	n.d.	n.d.	n.d.	n.d.	n.d.	n.d.	n.d.	75%	0%	25%	0%	0%	86%	14%	0%	0%	0%	36%	59%	0%	0%	5%	n.d.	n.d.	n.d.	n.d.	n.d.	55%	45%	0%	0%	0%	n.d.	n.d.	n.d.	n.d.	n.d.	n.d.	n.d.	n.d.	n.d.	n.d.	100%	0%	83%	17%	93%	7%	n.d.	n.d.	79%	20%	1%	0%	1%
Congo	Brazzaville	S3533	97	2	0	n.d.	n.d.	n.d.	n.d.	n.d.	n.d.	n.d.	n.d.	n.d.	n.d.	22%	28%	50%	0%	0%	68%	28%	4%	0%	0%	50%	44%	6%	0%	0%	71%	29%	0%	0%	0%	71%	29%	0%	0%	0%	n.d.	n.d.	n.d.	n.d.	n.d.	n.d.	n.d.	n.d.	n.d.	n.d.	100%	0%	87%	13%	71%	29%	n.d.	n.d.	67%	25%	8%	0%	0%
Congo	Soyo	S4899	98	1	0	n.d.	n.d.	n.d.	n.d.	n.d.	n.d.	n.d.	n.d.	n.d.	n.d.	31%	38%	31%	0%	0%	88%	13%	0%	0%	0%	45%	55%	0%	0%	0%	33%	67%	0%	0%	0%	66%	34%	0%	0%	0%	n.d.	n.d.	n.d.	n.d.	n.d.	n.d.	n.d.	n.d.	n.d.	n.d.	n.d.	n.d.	82%	18%	100%	0%	n.d.	n.d.	62%	34%	4%	0%	0%
Congo	Soyo estuary	S4898	99	1	0	n.d.	n.d.	n.d.	n.d.	n.d.	n.d.	n.d.	n.d.	n.d.	n.d.	19%	21%	52%	2%	5%	39%	45%	11%	0%	5%	25%	50%	25%	0%	0%	50%	25%	25%	0%	0%	55%	45%	0%	0%	0%	n.d.	n.d.	n.d.	n.d.	n.d.	n.d.	n.d.	n.d.	n.d.	n.d.	n.d.	n.d.	46%	54%	n.d.	n.d.	n.d.	n.d.	35%	37%	24%	1%	3%
	Quimtomba	S4901	98	2	0	n.d.	n.d.	n.d.	n.d.	n.d.	n.d.	n.d.	n.d.	n.d.	n.d.	25%	28%	41%	6%	0%	67%	23%	8%	0%	2%	67%	33%	0%	0%	0%	72%	28%	0%	0%	0%	74%	22%	4%	0%	0%	n.d.	n.d.	n.d.	n.d.	n.d.	n.d.	n.d.	n.d.	n.d.	n.d.	100%	0%	n.d.	n.d.	100%	0%	n.d.	n.d.	63%	24%	12%	1%	1%
	Quifuma	S4902	96	4	0	n.d.	n.d.	n.d.	n.d.	n.d.	n.d.	n.d.	n.d.	n.d.	n.d.	36%	27%	30%	3%	3%	37%	49%	10%	2%	2%	33%	67%	0%	0%	0%	46%	46%	8%	0%	0%	46%	43%	11%	0%	0%	n.d.	n.d.	n.d.	n.d.	n.d.	n.d.	n.d.	n.d.	n.d.	n.d.	n.d.	n.d.	n.d.	n.d.	100%	0%	n.d.	n.d.	41%	43%	13%	1%	1%
Luculu	Quivanda	S4904	91	9	0	n.d.	n.d.	n.d.	n.d.	n.d.	n.d.	n.d.	n.d.	n.d.	n.d.	42%	58%	0%	0%	0%	62%	38%	0%	0%	0%	40%	60%	0%	0%	0%	64%	36%	0%	0%	0%	100%	0%	0%	0%	0%	n.d.	n.d.	n.d.	n.d.	n.d.	n.d.	n.d.	n.d.	n.d.	n.d.	100%	0%	n.d.	n.d.	n.d.	n.d.	n.d.	n.d.	65%	35%	0%	0%	0%
	Quivanda	S4903	91	9	0	n.d.	n.d.	n.d.	n.d.	n.d.	n.d.	n.d.	n.d.	n.d.	n.d.	48%	30%	18%	3%	0%	36%	58%	6%	0%	0%	n.d.	n.d.	n.d.	n.d.	n.d.	70%	30%	0%	0%	0%	100%	0%	0%	0%	0%	n.d.	n.d.	n.d.	n.d.	n.d.	n.d.	n.d.	n.d.	n.d.	n.d.	n.d.	n.d.	n.d.	n.d.	n.d.	n.d.	n.d.	n.d.	57%	35%	7%	1%	0%
	Mbua-Moyo	S4905	91	9	0	n.d.	n.d.	n.d.	n.d.	n.d.	n.d.	n.d.	n.d.	n.d.	n.d.	38%	27%	27%	8%	0%	53%	36%	6%	6%	0%	n.d.	n.d.	n.d.	n.d.	n.d.	62%	38%	0%	0%	0%	50%	50%	0%	0%	0%	n.d.	n.d.	n.d.	n.d.	n.d.	n.d.	n.d.	n.d.	n.d.	n.d.	n.d.	n.d.	n.d.	n.d.	n.d.	n.d.	n.d.	n.d.	53%	33%	10%	5%	0%
Mebridege	Cassa de Telha	S4897	93	6	1	n.d.	n.d.	n.d.	n.d.	n.d.	n.d.	n.d.	n.d.	n.d.	n.d.	42%	29%	25%	3%	1%	21%	79%	0%	0%	0%	n.d.	n.d.	n.d.	n.d.	n.d.	n.d.	n.d.	n.d.	n.d.	n.d.	71%	29%	0%	0%	0%	n.d.	n.d.	n.d.	n.d.	n.d.	100%	0%	0%	0%	0%	100%	0%	38%	63%	n.d.	n.d.	67%	33%	46%	32%	19%	2%	1%
	N'Zeto	S4906	n.d	n.d.	n.d.	n.d.	n.d.	n.d.	n.d.	n.d.	n.d.	n.d.	n.d.	n.d.	n.d.	20%	49%	24%	4%	3%	32%	56%	10%	1%	0%	n.d.	n.d.	n.d.	n.d.	n.d.	39%	45%	15%	0%	0%	71%	0%	29%	0%	0%	n.d.	n.d.	n.d.	n.d.	n.d.	n.d.	n.d.	n.d.	n.d.	n.d.	n.d.	n.d.	n.d.	n.d.	n.d.	n.d.	n.d.	n.d.	33%	47%	17%	2%	1%
	Pidi mouth	S4907	86	14	0	n.d.	n.d.	n.d.	n.d.	n.d.	n.d.	n.d.	n.d.	n.d.	n.d.	38%	23%	38%	0%	0%	71%	24%	5%	0%	0%	n.d.	n.d.	n.d.	n.d.	n.d.	79%	21%	0%	0%	0%	n.d.	n.d.	n.d.	n.d.	n.d.	n.d.	n.d.	n.d.	n.d.	n.d.	n.d.	n.d.	n.d.	n.d.	n.d.	n.d.	n.d.	n.d.	n.d.	n.d.	n.d.	n.d.	n.d.	64%	23%	14%	0%	0%
	Musserra	S4908	85	14	2	n.d.	n.d.	n.d.	n.d.	n.d.	n.d.	n.d.	n.d.	n.d.	n.d.	42%	29%	24%	5%	0%	70%	26%	3%	1%	0%	n.d.	n.d.	n.d.	n.d.	n.d.	63%	34%	3%	0%	0%	n.d.	n.d.	n.d.	n.d.	n.d.	n.d.	n.d.	n.d.	n.d.	n.d.	n.d.	n.d.	n.d.	n.d.	n.d.	n.d.	n.d.	n.d.	n.d.	n.d.	n.d.	80%	20%	65%	27%	7%	2%	0%
Sembo	Musserra	S4895	78	22	0	50%	0%	25%	25%	0%	n.d.	n.d.	n.d.	n.d.	n.d.	22%	23%	45%	6%	4%	50%	42%	8%	0%	0%	n.d.	n.d.	n.d.	n.d.	n.d.	0%	100%	0%	0%	0%	n.d.	n.d.	n.d.	n.d.	n.d.	n.d.	n.d.	n.d.	n.d.	n.d.	n.d.	n.d.	n.d.	n.d.	n.d.	n.d.	n.d.	n.d.	n.d.	n.d.	n.d.	n.d.	n.d.	30%	27%	35%	5%	3%
Loge	Porta Freitas Morna	S4894	84	15	0	n.d.	n.d.	n.d.	n.d.	n.d.	n.d.	n.d.	n.d.	n.d.	n.d.	31%	25%	44%	0%	0%	53%	44%	4%	0%	0%	n.d.	n.d.	n.d.	n.d.	n.d.	n.d.	n.d.	n.d.	n.d.	n.d.	n.d.	n.d.	n.d.	n.d.	n.d.	n.d.	n.d.	n.d.	n.d.	n.d.	n.d.	n.d.	n.d.	n.d.	n.d.	n.d.	n.d.	n.d.	n.d.	n.d.	n.d.	n.d.	n.d.	47%	37%	16%	0%	0%
	Ambriz	S4909	90	9	1	n.d.	n.d.	n.d.	n.d.	n.d.	n.d.	n.d.	n.d.	n.d.	n.d.	69%	8%	23%	0%	0%	56%	39%	6%	0%	0%	n.d.	n.d.	n.d.	n.d.	n.d.	66%	34%	0%	0%	0%	67%	27%	7%	0%	0%	n.d.	n.d.	n.d.	n.d.	n.d.	n.d.	n.d.	n.d.	n.d.	n.d.	n.d.	n.d.	n.d.	n.d.	n.d.	n.d.	20%	80%	63%	33%	4%	0%	0%
Onzo	Tabi	S4893	86	14	0	11%	0%	11%	56%	22%	n.d.	n.d.	n.d.	n.d.	n.d.	24%	26%	38%	10%	1%	52%	41%	7%	0%	0%	n.d.	n.d.	n.d.	n.d.	n.d.	48%	45%	7%	0%	0%	27%	64%	9%	0%	0%	n.d.	n.d.	n.d.	n.d.	n.d.	n.d.	n.d.	n.d.	n.d.	n.d.	n.d.	n.d.	n.d.	n.d.	n.d.	n.d.	n.d.	n.d.	33%	35%	23%	8%	2%
Lifune	Conde Loca	S4892	93	7	0	29%	14%	29%	14%	14%	n.d.	n.d.	n.d.	n.d.	n.d.	11%	23%	45%	14%	8%	38%	42%	18%	0%	2%	n.d.	n.d.	n.d.	n.d.	n.d.	61%	28%	11%	0%	0%	38%	35%	21%	6%	0%	n.d.	n.d.	n.d.	n.d.	n.d.	n.d.	n.d.	n.d.	n.d.	n.d.	n.d.	n.d.	n.d.	n.d.	100%	0%	n.d.	n.d.	33%	30%	27%	6%	4%
	Barra do Dande	S4910	86	13	1	33%	28%	22%	6%	11%	n.d.	n.d.	n.d.	n.d.	n.d.	31%	44%	22%	2%	0%	56%	26%	16%	2%	0%	n.d.	n.d.	n.d.	n.d.	n.d.	71%	29%	0%	0%	0%	61%	39%	0%	0%	0%	n.d.	n.d.	n.d.	n.d.	n.d.	n.d.	n.d.	n.d.	n.d.	n.d.	n.d.	n.d.	100%	0%	100%	0%	n.d.	n.d.	55%	30%	12%	1%	1%
Dande	Caxito	S4891	85	14	2	n.d.	n.d.	n.d.	n.d.	n.d.	n.d.	n.d.	n.d.	n.d.	n.d.	19%	20%	50%	11%	0%	44%	49%	4%	3%	0%	n.d.	n.d.	n.d.	n.d.	n.d.	55%	45%	0%	0%	0%	67%	33%	0%	0%	0%	n.d.	n.d.	n.d.	n.d.	n.d.	n.d.	n.d.	n.d.	n.d.	n.d.	n.d.	n.d.	n.d.	n.d.	n.d.	n.d.	n.d.	n.d.	38%	35%	22%	6%	0%
Bengo	Quifangondo	S4911	84	11	5	n.d.	n.d.	n.d.	n.d.	n.d.	n.d.	n.d.	n.d.	n.d.	n.d.	38%	37%	23%	3%	0%	49%	49%	3%	0%	0%	n.d.	n.d.	n.d.	n.d.	n.d.	46%	54%	0%	0%	0%	73%	27%	0%	0%	0%	n.d.	n.d.	n.d.	n.d.	n.d.	n.d.	n.d.	n.d.	n.d.	n.d.	n.d.	n.d.	n.d.	n.d.	100%	0%	n.d.	n.d.	48%	41%	10%	1%	0%
	Cacuaco	S4912	94	4	2	n.d.	n.d.	n.d.	n.d.	n.d.	n.d.	n.d.	n.d.	n.d.	n.d.	25%	17%	47%	11%	0%	65%	30%	5%	0%	0%	60%	20%	20%	0%	0%	n.d.	n.d.	n.d.	n.d.	n.d.	100%	0%	0%	0%	0%	n.d.	n.d.	n.d.	n.d.	n.d.	n.d.	n.d.	n.d.	n.d.	n.d.	100%	0%	63%	38%	100%	0%	75%	25%	57%	23%	17%	3%	0%
	Ilha de Luanda	S4652	81	17	1	n.d.	n.d.	n.d.	n.d.	n.d.	n.d.	n.d.	n.d.	n.d.	n.d.	n.d.	n.d.	n.d.	n.d.	n.d.	40%	60%	0%	0%	0%	n.d.	n.d.	n.d.	n.d.	n.d.	n.d.	n.d.	n.d.	n.d.	n.d.	n.d.	n.d.	n.d.	n.d.	n.d.	n.d.	n.d.	n.d.	n.d.	n.d.	n.d.	n.d.	n.d.	n.d.	n.d.	n.d.	n.d.	n.d.	n.d.	n.d.	n.d.	n.d.	n.d.	36%	55%	9%	0%	0%
	Mussulo	S3764	83	17	0	14%	57%	21%	7%	0%	n.d.	n.d.	n.d.	n.d.	n.d.	20%	40%	33%	7%	0%	10%	60%	30%	0%	0%	n.d.	n.d.	n.d.	n.d.	n.d.	n.d.	n.d.	n.d.	n.d.	n.d.	n.d.	n.d.	n.d.	n.d.	n.d.	n.d.	n.d.	n.d.	n.d.	n.d.	n.d.	n.d.	n.d.	n.d.	n.d.	n.d.	n.d.	n.d.	n.d.	n.d.	n.d.	n.d.	n.d.	14%	55%	27%	3%	0%
	Palmeirinhas	S4913	83	17	0	47%	35%	18%	0%	0%	n.d.	n.d.	n.d.	n.d.	n.d.	67%	0%	33%	0%	0%	55%	43%	2%	0%	0%	n.d.	n.d.	n.d.	n.d.	n.d.	57%	43%	0%	0%	0%	n.d.	n.d.	n.d.	n.d.	n.d.	n.d.	n.d.	n.d.	n.d.	n.d.	n.d.	n.d.	n.d.	n.d.	n.d.	100%	0%	n.d.	n.d.	n.d.	n.d.	n.d.	n.d.	60%	33%	7%	0%	0%
	Barra do Cuanza	S4914	79	19	2	36%	43%	21%	0%	0%	n.d.	n.d.	n.d.	n.d.	n.d.	53%	44%	3%	0%	0%	59%	41%	0%	0%	0%	n.d.	n.d.	n.d.	n.d.	n.d.	100%	0%	0%	0%	0%	n.d.	n.d.	n.d.	n.d.	n.d.	n.d.	n.d.	n.d.	n.d.	n.d.	n.d.	n.d.	n.d.	n.d.	n.d.	90%	10%	n.d.	n.d.	n.d.	n.d.	n.d.	n.d.	57%	40%	4%	0%	0%
Cuanza	Barra do Cuanza	S4915	86	12	2	n.d.	n.d.	n.d.	n.d.	n.d.	n.d.	n.d.	n.d.	n.d.	n.d.	50%	36%	14%	0%	0%	31%	66%	2%	0%	2%	n.d.	n.d.	n.d.	n.d.	n.d.	89%	11%	0%	0%	0%	50%	40%	0%	10%	0%	n.d.	n.d.	n.d.	n.d.	n.d.	n.d.	n.d.	n.d.	n.d.	n.d.	89%	11%	50%	50%	n.d.	n.d.	n.d.	n.d.	48%	46%	5%	1%	1%
	Cabo Ledo	S3765	72	23	5	20%	20%	60%	0%	0%	n.d.	n.d.	n.d.	n.d.	n.d.	11%	56%	28%	0%	6%	23%	63%	15%	0%	0%	n.d.	n.d.	n.d.	n.d.	n.d.	25%	75%	0%	0%	0%	20%	73%	0%	0%	7%	n.d.	n.d.	n.d.	n.d.	n.d.	25%	75%	0%	0%	0%	96%	4%	n.d.	n.d.	n.d.	n.d.	n.d.	n.d.	33%	51%	14%	0%	1%
	Sao Braz	S4916	65	26	9	38%	25%	13%	25%	0%	n.d.	n.d.	n.d.	n.d.	n.d.	33%	50%	10%	7%	0%	57%	40%	2%	0%	0%	n.d.	n.d.	n.d.	n.d.	n.d.	n.d.	n.d.	n.d.	n.d.	n.d.	n.d.	n.d.	n.d.	n.d.	n.d.	n.d.	n.d.	n.d.	n.d.	n.d.	57%	43%	0%	0%	0%	83%	17%	n.d.	n.d.	n.d.	n.d.	n.d.	n.d.	53%	39%	5%	4%	0%
Longa	Calamba	S4917	84	13	3	n.d.	n.d.	n.d.	n.d.	n.d.	n.d.	n.d.	n.d.	n.d.	n.d.	20%	70%	10%	0%	0%	67%	31%	1%	0%	0%	n.d.	n.d.	n.d.	n.d.	n.d.	n.d.	n.d.	n.d.	n.d.	n.d.	n.d.	n.d.	n.d.	n.d.	n.d.	n.d.	n.d.	n.d.	n.d.	n.d.	n.d.	n.d.	n.d.	n.d.	n.d.	100%	0%	n.d.	n.d.	n.d.	n.d.	n.d.	n.d.	66%	32%	2%	0%	0%
	Porto Amboim	S4918	76	23	1	34%	66%	0%	0%	0%	n.d.	n.d.	n.d.	n.d.	n.d.	41%	41%	12%	6%	0%	67%	33%	0%	0%	0%	n.d.	n.d.	n.d.	n.d.	n.d.	13%	88%	0%	0%	0%	n.d.	n.d.	n.d.	n.d.	n.d.	n.d.	n.d.	n.d.	n.d.	n.d.	n.d.	n.d.	n.d.	n.d.	n.d.	100%	0%	n.d.	n.d.	n.d.	n.d.	n.d.	n.d.	49%	48%	2%	1%	0%
Queve	Cachoeira	S4922	74	26	0	n.d.	n.d.	n.d.	n.d.	n.d.	n.d.	n.d.	n.d.	n.d.	n.d.	22%	27%	47%	3%	1%	18%	66%	16%	0%	0%	n.d.	n.d.	n.d.	n.d.	n.d.	100%	0%	0%	0%	0%	n.d.	n.d.	n.d.	n.d.	n.d.	n.d.	n.d.	n.d.	n.d.	n.d.	n.d.	n.d.	n.d.	n.d.	n.d.	n.d.	n.d.	n.d.	n.d.	n.d.	n.d.	n.d.	n.d.	22%	41%	34%	2%	1%
	Carimba	S4923	77	20	2	24%	47%	24%	5%	0%	n.d.	n.d.	n.d.	n.d.	n.d.	50%	46%	4%	0%	0%	37%	60%	3%	0%	0%	n.d.	n.d.	n.d.	n.d.	n.d.	45%	55%	0%	0%	0%	75%	25%	0%	0%	0%	n.d.	n.d.	n.d.	n.d.	n.d.	n.d.	n.d.	n.d.	n.d.	n.d.	100%	0%	n.d.	n.d.	n.d.	n.d.	n.d.	n.d.	43%	48%	8%	1%	0%
	Sumbe	S4919	n.d	n.d.	n.d.	25%	55%	10%	5%	5%	n.d.	n.d.	n.d.	n.d.	n.d.	15%	45%	27%	6%	6%	32%	61%	7%	0%	0%	n.d.	n.d.	n.d.	n.d.	n.d.	n.d.	n.d.	n.d.	n.d.	n.d.	n.d.	n.d.	n.d.	n.d.	n.d.	50%	50%	0%	0%	0%	n.d.	n.d.	n.d.	n.d.	n.d.	80%	20%	n.d.	n.d.	n.d.	n.d.	25%	75%	31%	54%	11%	2%	2%
Cambongo	Sumbe	S4924	71	27	2	19%	31%	35%	15%	0%	n.d.	n.d.	n.d.	n.d.	n.d.	3%	21%	59%	12%	6%	30%	56%	13%	0%	1%	n.d.	n.d.	n.d.	n.d.	n.d.	n.d.	n.d.	n.d.	n.d.	n.d.	n.d.	n.d.	n.d.	n.d.	n.d.	n.d.	n.d.	n.d.	n.d.	n.d.	n.d.	n.d.	n.d.	n.d.	n.d.	90%	10%	n.d.	n.d.	n.d.	n.d.	n.d.	n.d.	33%	40%	22%	4%	2%
Quicombo	Quicombo	S4925	65	33	2	25%	50%	25%	0%	0%	n.d.	n.d.	n.d.	n.d.	n.d.	10%	42%	39%	10%	0%	21%	72%	7%	0%	0%	n.d.	n.d.	n.d.	n.d.	n.d.	100%	0%	0%	0%	0%	n.d.	n.d.	n.d.	n.d.	n.d.	50%	0%	50%	0%	0%	83%	0%	17%	0%	0%	87%	13%	n.d.	n.d.	n.d.	n.d.	n.d.	n.d.	30%	55%	13%	2%	0%
	Quicombo	S4920	n.d	n.d.	n.d.	35%	40%	20%	5%	0%	n.d.	n.d.	n.d.	n.d.	n.d.	12%	38%	38%	8%	4%	40%	52%	8%	0%	1%	n.d.	n.d.	n.d.	n.d.	n.d.	n.d.	n.d.	n.d.	n.d.	n.d.	n.d.	n.d.	n.d.	n.d.	n.d.	n.d.	n.d.	n.d.	n.d.	n.d.	n.d.	n.d.	n.d.	n.d.	n.d.	88%	13%	n.d.	n.d.	n.d.	n.d.	n.d.	n.d.	36%	46%	14%	2%	1%
	Praia Sousa	S4930	76	23	1	35%	59%	0%	6%	0%	n.d.	n.d.	n.d.	n.d.	n.d.	54%	46%	0%	0%	0%	45%	50%	5%	0%	0%	n.d.	n.d.	n.d.	n.d.	n.d.	n.d.	n.d.	n.d.	n.d.	n.d.	n.d.	n.d.	n.d.	n.d.	n.d.	n.d.	n.d.	n.d.	n.d.	n.d.	n.d.	n.d.	n.d.	n.d.	n.d.	100%	0%	n.d.	n.d.	n.d.	n.d.	n.d.	n.d.	49%	48%	3%	1%	0%
	Candunga	S4921	n.d	n.d.	n.d.	0%	63%	29%	8%	0%	n.d.	n.d.	n.d.	n.d.	n.d.	13%	61%	26%	0%	0%	32%	64%	4%	0%	0%	n.d.	n.d.	n.d.	n.d.	n.d.	n.d.	n.d.	n.d.	n.d.	n.d.	n.d.	n.d.	n.d.	n.d.	n.d.	n.d.	n.d.	n.d.	n.d.	n.d.	n.d.	n.d.	n.d.	n.d.	n.d.	100%	0%	n.d.	n.d.	n.d.	n.d.	n.d.	n.d.	25%	60%	13%	2%	0%
Tapado	Chitonde	S4926	57	43	0	n.d.	n.d.	n.d.	n.d.	n.d.	n.d.	n.d.	n.d.	n.d.	n.d.	10%	45%	45%	0%	0%	23%	64%	13%	0%	0%	n.d.	n.d.	n.d.	n.d.	n.d.	n.d.	n.d.	n.d.	n.d.	n.d.	n.d.	n.d.	n.d.	n.d.	n.d.	n.d.	n.d.	n.d.	n.d.	n.d.	n.d.	n.d.	n.d.	n.d.	n.d.	83%	17%	n.d.	n.d.	n.d.	n.d.	n.d.	n.d.	23%	58%	19%	0%	0%
Balombo	Canjala	S4927	53	46	1	n.d.	n.d.	n.d.	n.d.	n.d.	n.d.	n.d.	n.d.	n.d.	n.d.	14%	57%	29%	0%	0%	27%	68%	5%	0%	0%	n.d.	n.d.	n.d.	n.d.	n.d.	n.d.	n.d.	n.d.	n.d.	n.d.	n.d.	n.d.	n.d.	n.d.	n.d.	n.d.	n.d.	n.d.	n.d.	n.d.	n.d.	n.d.	n.d.	n.d.	n.d.	92%	8%	n.d.	n.d.	n.d.	n.d.	n.d.	n.d.	32%	62%	6%	0%	0%
	Egito Praia	S4928	69	27	4	52%	35%	13%	0%	0%	n.d.	n.d.	n.d.	n.d.	n.d.	42%	44%	14%	0%	0%	24%	76%	0%	0%	0%	n.d.	n.d.	n.d.	n.d.	n.d.	n.d.	n.d.	n.d.	n.d.	n.d.	n.d.	n.d.	n.d.	n.d.	n.d.	n.d.	n.d.	n.d.	n.d.	n.d.	n.d.	n.d.	n.d.	n.d.	n.d.	n.d.	n.d.	n.d.	n.d.	n.d.	n.d.	n.d.	n.d.	40%	51%	10%	0%	0%
Culango	Culango	S4929	58	42	0	n.d.	n.d.	n.d.	n.d.	n.d.	n.d.	n.d.	n.d.	n.d.	n.d.	10%	24%	48%	10%	7%	32%	51%	15%	0%	2%	n.d.	n.d.	n.d.	n.d.	n.d.	n.d.	n.d.	n.d.	n.d.	n.d.	n.d.	n.d.	n.d.	n.d.	n.d.	n.d.	n.d.	n.d.	n.d.	n.d.	n.d.	n.d.	n.d.	n.d.	n.d.	92%	8%	n.d.	n.d.	n.d.	n.d.	n.d.	n.d.	37%	41%	18%	2%	2%
	Lobito spit	S4934	n.d	n.d.	n.d.	24%	41%	16%	8%	11%	n.d.	n.d.	n.d.	n.d.	n.d.	4%	28%	64%	0%	4%	26%	62%	11%	0%	1%	n.d.	n.d.	n.d.	n.d.	n.d.	n.d.	n.d.	n.d.	n.d.	n.d.	n.d.	n.d.	n.d.	n.d.	n.d.	n.d.	n.d.	n.d.	n.d.	n.d.	n.d.	n.d.	n.d.	n.d.	n.d.	78%	22%	n.d.	n.d.	n.d.	n.d.	n.d.	n.d.	26%	50%	19%	2%	3%
	Lobito spit	S4863	61	38	1	65%	24%	6%	6%	0%	n.d.	n.d.	n.d.	n.d.	n.d.	17%	42%	38%	4%	0%	41%	48%	7%	3%	1%	n.d.	n.d.	n.d.	n.d.	n.d.	n.d.	n.d.	n.d.	n.d.	n.d.	n.d.	n.d.	n.d.	n.d.	n.d.	n.d.	n.d.	n.d.	n.d.	n.d.	n.d.	n.d.	n.d.	n.d.	n.d.	100%	0%	n.d.	n.d.	n.d.	n.d.	n.d.	n.d.	46%	39%	11%	4%	1%
	Catumbela N	S4862	75	23	2	57%	23%	14%	3%	3%	n.d.	n.d.	n.d.	n.d.	n.d.	23%	60%	17%	0%	0%	47%	51%	3%	0%	0%	n.d.	n.d.	n.d.	n.d.	n.d.	n.d.	n.d.	n.d.	n.d.	n.d.	n.d.	n.d.	n.d.	n.d.	n.d.	n.d.	n.d.	n.d.	n.d.	n.d.	n.d.	n.d.	n.d.	n.d.	n.d.	100%	0%	n.d.	n.d.	n.d.	n.d.	n.d.	n.d.	44%	44%	9%	2%	1%
Catumbela mouth	Praia Bebe	S4655	64	35	1	38%	38%	19%	0%	6%	n.d.	n.d.	n.d.	n.d.	n.d.	25%	42%	33%	0%	0%	28%	56%	11%	0%	6%	n.d.	n.d.	n.d.	n.d.	n.d.	n.d.	n.d.	n.d.	n.d.	n.d.	n.d.	n.d.	n.d.	n.d.	n.d.	n.d.	n.d.	n.d.	n.d.	n.d.	n.d.	n.d.	n.d.	n.d.	n.d.	96%	4%	n.d.	n.d.	n.d.	n.d.	n.d.	n.d.	50%	35%	11%	0%	3%
Catumbela	Catumbela	S4933	73	26	1	13%	52%	35%	0%	0%	n.d.	n.d.	n.d.	n.d.	n.d.	28%	53%	18%	3%	0%	47%	36%	16%	0%	2%	n.d.	n.d.	n.d.	n.d.	n.d.	n.d.	n.d.	n.d.	n.d.	n.d.	n.d.	n.d.	n.d.	n.d.	n.d.	n.d.	n.d.	n.d.	n.d.	n.d.	n.d.	n.d.	n.d.	n.d.	n.d.	n.d.	n.d.	n.d.	n.d.	n.d.	n.d.	n.d.	n.d.	34%	45%	20%	1%	1%
Catumbela	Catumbela	S4860	74	25	1	59%	25%	16%	0%	0%	n.d.	n.d.	n.d.	n.d.	n.d.	37%	42%	16%	3%	3%	54%	40%	6%	0%	0%	n.d.	n.d.	n.d.	n.d.	n.d.	n.d.	n.d.	n.d.	n.d.	n.d.	n.d.	n.d.	n.d.	n.d.	n.d.	n.d.	n.d.	n.d.	n.d.	n.d.	n.d.	n.d.	n.d.	n.d.	n.d.	100%	0%	n.d.	n.d.	n.d.	n.d.	n.d.	n.d.	53%	35%	11%	1%	1%
Cavaco	Benguela	S4932	45	53	2	n.d.	n.d.	n.d.	n.d.	n.d.	n.d.	n.d.	n.d.	n.d.	n.d.	32%	47%	17%	4%	0%	49%	50%	2%	0%	0%	n.d.	n.d.	n.d.	n.d.	n.d.	n.d.	n.d.	n.d.	n.d.	n.d.	n.d.	n.d.	n.d.	n.d.	n.d.	n.d.	n.d.	n.d.	n.d.	n.d.	n.d.	n.d.	n.d.	n.d.	n.d.	n.d.	n.d.	n.d.	n.d.	n.d.	n.d.	n.d.	n.d.	45%	48%	6%	1%	0%
	Benguela	S4931	66	29	4	29%	43%	29%	0%	0%	n.d.	n.d.	n.d.	n.d.	n.d.	28%	38%	34%	0%	0%	50%	46%	3%	1%	0%	n.d.	n.d.	n.d.	n.d.	n.d.	n.d.	n.d.	n.d.	n.d.	n.d.	n.d.	n.d.	n.d.	n.d.	n.d.	n.d.	n.d.	n.d.	n.d.	n.d.	n.d.	n.d.	n.d.	n.d.	n.d.	n.d.	n.d.	n.d.	n.d.	n.d.	n.d.	100%	0%	48%	42%	9%	1%	0%
	Baia Farta	S4935	n.d	n.d.	n.d.	0%	100%	0%	0%	0%	n.d.	n.d.	n.d.	n.d.	n.d.	12%	44%	23%	19%	2%	19%	79%	1%	0%	1%	n.d.	n.d.	n.d.	n.d.	n.d.	n.d.	n.d.	n.d.	n.d.	n.d.	n.d.	n.d.	n.d.	n.d.	n.d.	n.d.	n.d.	n.d.	n.d.	n.d.	n.d.	n.d.	n.d.	n.d.	n.d.	n.d.	n.d.	n.d.	n.d.	n.d.	n.d.	n.d.	n.d.	15%	66%	10%	7%	1%
	Saco S	S4853	64	36	0	n.d.	n.d.	n.d.	n.d.	n.d.	n.d.	n.d.	n.d.	n.d.	n.d.	32%	42%	21%	5%	0%	39%	57%	4%	0%	0%	n.d.	n.d.	n.d.	n.d.	n.d.	n.d.	n.d.	n.d.	n.d.	n.d.	n.d.	n.d.	n.d.	n.d.	n.d.	n.d.	n.d.	n.d.	n.d.	n.d.	n.d.	n.d.	n.d.	n.d.	n.d.	n.d.	n.d.	n.d.	n.d.	n.d.	n.d.	50%	50%	36%	52%	10%	2%	0%
Coporolo	Dombe Grande	S4936	64	36	0	n.d.	n.d.	n.d.	n.d.	n.d.	n.d.	n.d.	n.d.	n.d.	n.d.	28%	33%	35%	4%	0%	36%	59%	4%	0%	0%	n.d.	n.d.	n.d.	n.d.	n.d.	n.d.	n.d.	n.d.	n.d.	n.d.	n.d.	n.d.	n.d.	n.d.	n.d.	n.d.	n.d.	n.d.	n.d.	n.d.	n.d.	n.d.	n.d.	n.d.	n.d.	100%	0%	n.d.	n.d.	n.d.	n.d.	n.d.	n.d.	36%	49%	15%	1%	0%
Coporolo	Santa Tereza	S4852	62	38	0	0%	0%	75%	25%	0%	n.d.	n.d.	n.d.	n.d.	n.d.	17%	47%	36%	0%	0%	41%	57%	2%	0%	0%	n.d.	n.d.	n.d.	n.d.	n.d.	n.d.	n.d.	n.d.	n.d.	n.d.	n.d.	n.d.	n.d.	n.d.	n.d.	n.d.	n.d.	n.d.	n.d.	n.d.	n.d.	n.d.	n.d.	n.d.	n.d.	n.d.	n.d.	n.d.	n.d.	n.d.	n.d.	n.d.	n.d.	29%	48%	22%	1%	0%
	Cuio	S4937	49	47	4	n.d.	n.d.	n.d.	n.d.	n.d.	n.d.	n.d.	n.d.	n.d.	n.d.	43%	38%	19%	0%	0%	57%	40%	3%	0%	0%	n.d.	n.d.	n.d.	n.d.	n.d.	n.d.	n.d.	n.d.	n.d.	n.d.	n.d.	n.d.	n.d.	n.d.	n.d.	n.d.	n.d.	n.d.	n.d.	n.d.	n.d.	n.d.	n.d.	n.d.	n.d.	n.d.	n.d.	n.d.	n.d.	n.d.	n.d.	n.d.	n.d.	56%	38%	6%	0%	0%
	Equimina	S4938	53	44	3	n.d.	n.d.	n.d.	n.d.	n.d.	n.d.	n.d.	n.d.	n.d.	n.d.	23%	58%	19%	0%	0%	20%	76%	4%	0%	0%	n.d.	n.d.	n.d.	n.d.	n.d.	75%	25%	0%	0%	0%	n.d.	n.d.	n.d.	n.d.	n.d.	n.d.	n.d.	n.d.	n.d.	n.d.	n.d.	n.d.	n.d.	n.d.	n.d.	96%	4%	n.d.	n.d.	n.d.	n.d.	n.d.	n.d.	35%	60%	6%	0%	0%
	Baia Binga	S4939	65	33	2	n.d.	n.d.	n.d.	n.d.	n.d.	n.d.	n.d.	n.d.	n.d.	n.d.	61%	35%	4%	0%	0%	51%	49%	0%	0%	0%	n.d.	n.d.	n.d.	n.d.	n.d.	n.d.	n.d.	n.d.	n.d.	n.d.	n.d.	n.d.	n.d.	n.d.	n.d.	n.d.	n.d.	n.d.	n.d.	n.d.	n.d.	n.d.	n.d.	n.d.	n.d.	n.d.	n.d.	n.d.	n.d.	n.d.	n.d.	n.d.	n.d.	56%	42%	2%	0%	0%
Cangala	Santa Maria	S4940	60	39	1	n.d.	n.d.	n.d.	n.d.	n.d.	n.d.	n.d.	n.d.	n.d.	n.d.	16%	20%	39%	10%	16%	14%	73%	13%	0%	1%	n.d.	n.d.	n.d.	n.d.	n.d.	n.d.	n.d.	n.d.	n.d.	n.d.	n.d.	n.d.	n.d.	n.d.	n.d.	n.d.	n.d.	n.d.	n.d.	n.d.	n.d.	n.d.	n.d.	n.d.	n.d.	n.d.	n.d.	n.d.	n.d.	n.d.	n.d.	n.d.	n.d.	15%	59%	19%	3%	5%
	Lucira	S4941	46	50	4	n.d.	n.d.	n.d.	n.d.	n.d.	n.d.	n.d.	n.d.	n.d.	n.d.	13%	63%	25%	0%	0%	17%	79%	4%	0%	0%	n.d.	n.d.	n.d.	n.d.	n.d.	n.d.	n.d.	n.d.	n.d.	n.d.	n.d.	n.d.	n.d.	n.d.	n.d.	n.d.	n.d.	n.d.	n.d.	n.d.	n.d.	n.d.	n.d.	n.d.	n.d.	n.d.	n.d.	n.d.	n.d.	n.d.	n.d.	n.d.	n.d.	18%	74%	8%	0%	0%
Carujamba	Lucira	S4942	49	51	0	n.d.	n.d.	n.d.	n.d.	n.d.	n.d.	n.d.	n.d.	n.d.	n.d.	8%	35%	48%	8%	1%	13%	65%	15%	2%	5%	n.d.	n.d.	n.d.	n.d.	n.d.	n.d.	n.d.	n.d.	n.d.	n.d.	n.d.	n.d.	n.d.	n.d.	n.d.	n.d.	n.d.	n.d.	n.d.	n.d.	n.d.	n.d.	n.d.	n.d.	n.d.	n.d.	n.d.	n.d.	n.d.	n.d.	n.d.	n.d.	n.d.	11%	51%	30%	5%	3%
(outer berm)	Inamangando	S4943	54	44	2	n.d.	n.d.	n.d.	n.d.	n.d.	n.d.	n.d.	n.d.	n.d.	n.d.	42%	33%	25%	0%	0%	33%	67%	0%	0%	0%	n.d.	n.d.	n.d.	n.d.	n.d.	n.d.	n.d.	n.d.	n.d.	n.d.	n.d.	n.d.	n.d.	n.d.	n.d.	n.d.	n.d.	n.d.	n.d.	n.d.	n.d.	n.d.	n.d.	n.d.	n.d.	100%	0%	n.d.	n.d.	n.d.	n.d.	80%	20%	45%	49%	5%	0%	0%
(inner berm)	Inamangando	S4944	55	44	1	n.d.	n.d.	n.d.	n.d.	n.d.	n.d.	n.d.	n.d.	n.d.	n.d.	17%	65%	17%	0%	0%	15%	83%	2%	0%	0%	n.d.	n.d.	n.d.	n.d.	n.d.	n.d.	n.d.	n.d.	n.d.	n.d.	n.d.	n.d.	n.d.	n.d.	n.d.	n.d.	n.d.	n.d.	n.d.	n.d.	n.d.	n.d.	n.d.	n.d.	n.d.	n.d.	n.d.	n.d.	n.d.	n.d.	n.d.	n.d.	n.d.	18%	73%	8%	0%	0%
Inamangando	Inamangando	S4945	54	42	4	n.d.	n.d.	n.d.	n.d.	n.d.	n.d.	n.d.	n.d.	n.d.	n.d.	21%	53%	26%	0%	0%	16%	76%	8%	0%	0%	n.d.	n.d.	n.d.	n.d.	n.d.	n.d.	n.d.	n.d.	n.d.	n.d.	n.d.	n.d.	n.d.	n.d.	n.d.	n.d.	n.d.	n.d.	n.d.	n.d.	n.d.	n.d.	n.d.	n.d.	n.d.	n.d.	n.d.	n.d.	n.d.	n.d.	n.d.	25%	75%	19%	69%	13%	0%	0%
	Baia das Salinas	S4946	60	39	1	n.d.	n.d.	n.d.	n.d.	n.d.	n.d.	n.d.	n.d.	n.d.	n.d.	25%	48%	28%	0%	0%	23%	70%	7%	0%	0%	n.d.	n.d.	n.d.	n.d.	n.d.	n.d.	n.d.	n.d.	n.d.	n.d.	n.d.	n.d.	n.d.	n.d.	n.d.	n.d.	n.d.	n.d.	n.d.	n.d.	n.d.	n.d.	n.d.	n.d.	n.d.	n.d.	n.d.	n.d.	n.d.	n.d.	n.d.	50%	50%	25%	58%	17%	0%	0%
Bentiaba	Bentiaba	S4947	52	47	1	n.d.	n.d.	n.d.	n.d.	n.d.	n.d.	n.d.	n.d.	n.d.	n.d.	36%	32%	28%	4%	0%	16%	78%	7%	0%	0%	n.d.	n.d.	n.d.	n.d.	n.d.	n.d.	n.d.	n.d.	n.d.	n.d.	n.d.	n.d.	n.d.	n.d.	n.d.	n.d.	n.d.	n.d.	n.d.	n.d.	n.d.	n.d.	n.d.	n.d.	n.d.	n.d.	n.d.	n.d.	n.d.	n.d.	n.d.	n.d.	n.d.	23%	61%	14%	1%	0%
	Bentiaba	S4948	54	44	1	n.d.	n.d.	n.d.	n.d.	n.d.	n.d.	n.d.	n.d.	n.d.	n.d.	51%	31%	17%	0%	0%	33%	64%	3%	0%	0%	n.d.	n.d.	n.d.	n.d.	n.d.	n.d.	n.d.	n.d.	n.d.	n.d.	n.d.	n.d.	n.d.	n.d.	n.d.	n.d.	n.d.	n.d.	n.d.	n.d.	n.d.	n.d.	n.d.	n.d.	n.d.	n.d.	n.d.	n.d.	n.d.	25%	75%	n.d.	n.d.	41%	51%	7%	0%	0%
	Chapeu Armado	S4949	57	40	3	n.d.	n.d.	n.d.	n.d.	n.d.	n.d.	n.d.	n.d.	n.d.	n.d.	14%	50%	36%	0%	0%	36%	64%	0%	0%	0%	n.d.	n.d.	n.d.	n.d.	n.d.	65%	35%	0%	0%	0%	n.d.	n.d.	n.d.	n.d.	n.d.	n.d.	n.d.	n.d.	n.d.	n.d.	n.d.	n.d.	n.d.	n.d.	n.d.	92%	8%	n.d.	n.d.	43%	57%	55%	45%	52%	43%	4%	0%	0%
	Mariquita	S4950	59	40	1	83%	0%	17%	0%	0%	n.d.	n.d.	n.d.	n.d.	n.d.	22%	78%	0%	0%	0%	38%	63%	0%	0%	0%	n.d.	n.d.	n.d.	n.d.	n.d.	n.d.	n.d.	n.d.	n.d.	n.d.	n.d.	n.d.	n.d.	n.d.	n.d.	n.d.	n.d.	n.d.	n.d.	n.d.	n.d.	n.d.	n.d.	n.d.	n.d.	n.d.	n.d.	n.d.	n.d.	n.d.	n.d.	n.d.	n.d.	35%	62%	3%	0%	0%
Giraul	Giraul	S4951	56	43	1	n.d.	n.d.	n.d.	n.d.	n.d.	n.d.	n.d.	n.d.	n.d.	n.d.	21%	51%	25%	3%	0%	17%	82%	2%	0%	0%	n.d.	n.d.	n.d.	n.d.	n.d.	0%	100%	0%	0%	0%	n.d.	n.d.	n.d.	n.d.	n.d.	n.d.	n.d.	n.d.	n.d.	n.d.	n.d.	n.d.	n.d.	n.d.	n.d.	n.d.	n.d.	n.d.	n.d.	n.d.	n.d.	n.d.	n.d.	19%	64%	15%	2%	0%
Bero	Namibe	S4952	45	51	4	29%	41%	29%	0%	0%	42%	8%	42%	0%	8%	13%	64%	21%	0%	1%	21%	79%	0%	0%	0%	n.d.	n.d.	n.d.	n.d.	n.d.	n.d.	n.d.	n.d.	n.d.	n.d.	n.d.	n.d.	n.d.	n.d.	n.d.	n.d.	n.d.	n.d.	n.d.	n.d.	n.d.	n.d.	n.d.	n.d.	n.d.	n.d.	n.d.	n.d.	n.d.	n.d.	n.d.	n.d.	n.d.	20%	58%	21%	0%	2%
fossil dune	Nonguai	S4802	71	28	1	n.d.	n.d.	n.d.	n.d.	n.d.	n.d.	n.d.	n.d.	n.d.	n.d.	n.d.	n.d.	n.d.	n.d.	n.d.	64%	36%	0%	0%	0%	32%	63%	5%	0%	0%	49%	46%	5%	0%	0%	n.d.	n.d.	n.d.	n.d.	n.d.	n.d.	n.d.	n.d.	n.d.	n.d.	n.d.	n.d.	n.d.	n.d.	n.d.	n.d.	n.d.	n.d.	n.d.	n.d.	n.d.	n.d.	n.d.	47%	47%	5%	0%	0%
Curoca	Curoca mouth	S4955	70	24	5	53%	27%	13%	0%	7%	25%	75%	0%	0%	0%	18%	27%	55%	0%	0%	29%	68%	4%	0%	0%	n.d.	n.d.	n.d.	n.d.	n.d.	64%	36%	0%	0%	0%	n.d.	n.d.	n.d.	n.d.	n.d.	n.d.	n.d.	n.d.	n.d.	n.d.	n.d.	n.d.	n.d.	n.d.	n.d.	n.d.	n.d.	n.d.	n.d.	n.d.	n.d.	n.d.	n.d.	50%	42%	8%	0%	1%
	Curoca mouth	S4956	74	22	4	n.d.	n.d.	n.d.	n.d.	n.d.	n.d.	n.d.	n.d.	n.d.	n.d.	0%	100%	0%	0%	0%	n.d.	n.d.	n.d.	n.d.	n.d.	100%	0%	0%	0%	0%	75%	25%	0%	0%	0%	n.d.	n.d.	n.d.	n.d.	n.d.	n.d.	n.d.	n.d.	n.d.	n.d.	n.d.	n.d.	n.d.	n.d.	n.d.	n.d.	n.d.	n.d.	n.d.	n.d.	n.d.	n.d.	n.d.	63%	38%	0%	0%	0%
(outer spit)	Tombua	S4805	75	23	2	0%	93%	7%	0%	0%	0%	75%	25%	0%	0%	13%	81%	6%	0%	0%	14%	71%	0%	0%	14%	17%	83%	0%	0%	0%	61%	39%	0%	0%	0%	n.d.	n.d.	n.d.	n.d.	n.d.	n.d.	n.d.	n.d.	n.d.	n.d.	n.d.	n.d.	n.d.	n.d.	n.d.	n.d.	n.d.	n.d.	n.d.	n.d.	n.d.	n.d.	n.d.	29%	66%	4%	0%	1%
eolian dune	Tombua	S4774	78	16	6	8%	77%	15%	0%	0%	n.d.	n.d.	n.d.	n.d.	n.d.	0%	100%	0%	0%	0%	0%	100%	0%	0%	0%	n.d.	n.d.	n.d.	n.d.	n.d.	18%	82%	0%	0%	0%	n.d.	n.d.	n.d.	n.d.	n.d.	n.d.	n.d.	n.d.	n.d.	n.d.	n.d.	n.d.	n.d.	n.d.	n.d.	n.d.	n.d.	n.d.	n.d.	n.d.	n.d.	n.d.	n.d.	9%	87%	4%	0%	0%
Moçamedes beach	Vanesa	S4957	73	25	2	n.d.	n.d.	n.d.	n.d.	n.d.	n.d.	n.d.	n.d.	n.d.	n.d.	n.d.	n.d.	n.d.	n.d.	n.d.	14%	86%	0%	0%	0%	20%	80%	0%	0%	0%	13%	88%	0%	0%	0%	n.d.	n.d.	n.d.	n.d.	n.d.	n.d.	n.d.	n.d.	n.d.	n.d.	n.d.	n.d.	n.d.	n.d.	n.d.	n.d.	n.d.	n.d.	n.d.	n.d.	n.d.	n.d.	n.d.	22%	78%	0%	0%	0%
Moçamedes dune	Cova dos Medos	S4961	62	25	13	86%	14%	0%	0%	0%	n.d.	n.d.	n.d.	n.d.	n.d.	90%	10%	0%	0%	0%	n.d.	n.d.	n.d.	n.d.	n.d.	100%	0%	0%	0%	0%	89%	11%	0%	0%	0%	n.d.	n.d.	n.d.	n.d.	n.d.	n.d.	n.d.	n.d.	n.d.	n.d.	n.d.	n.d.	n.d.	n.d.	n.d.	n.d.	n.d.	n.d.	n.d.	n.d.	n.d.	n.d.	n.d.	89%	11%	0%	0%	0%
Moçamedes beach	Vanesinha	S4958	74	20	6	n.d.	n.d.	n.d.	n.d.	n.d.	n.d.	n.d.	n.d.	n.d.	n.d.	n.d.	n.d.	n.d.	n.d.	n.d.	n.d.	n.d.	n.d.	n.d.	n.d.	n.d.	n.d.	n.d.	n.d.	n.d.	100%	0%	0%	0%	0%	n.d.	n.d.	n.d.	n.d.	n.d.	n.d.	n.d.	n.d.	n.d.	n.d.	n.d.	n.d.	n.d.	n.d.	n.d.	n.d.	n.d.	n.d.	n.d.	n.d.	n.d.	n.d.	n.d.	94%	0%	6%	0%	0%
Moçamedes dune	Praia do Navio	S4960	66	25	9	89%	11%	0%	0%	0%	n.d.	n.d.	n.d.	n.d.	n.d.	n.d.	n.d.	n.d.	n.d.	n.d.	75%	25%	0%	0%	0%	33%	67%	0%	0%	0%	80%	20%	0%	0%	0%	n.d.	n.d.	n.d.	n.d.	n.d.	n.d.	n.d.	n.d.	n.d.	n.d.	n.d.	n.d.	n.d.	n.d.	n.d.	71%	29%	n.d.	n.d.	n.d.	n.d.	n.d.	n.d.	75%	24%	1%	0%	0%
Moçamedes beach	Praia do Navio	S4959	72	24	4	n.d.	n.d.	n.d.	n.d.	n.d.	n.d.	n.d.	n.d.	n.d.	n.d.	0%	100%	0%	0%	0%	20%	80%	0%	0%	0%	40%	60%	0%	0%	0%	58%	42%	0%	0%	0%	n.d.	n.d.	n.d.	n.d.	n.d.	n.d.	n.d.	n.d.	n.d.	n.d.	n.d.	n.d.	n.d.	n.d.	n.d.	n.d.	n.d.	n.d.	n.d.	n.d.	n.d.	n.d.	n.d.	47%	53%	0%	0%	0%
Moçamedes dune	Riscos	S5059	75	22	3	n.d.	n.d.	n.d.	n.d.	n.d.	n.d.	n.d.	n.d.	n.d.	n.d.	n.d.	n.d.	n.d.	n.d.	n.d.	n.d.	n.d.	n.d.	n.d.	n.d.	n.d.	n.d.	n.d.	n.d.	n.d.	89%	11%	0%	0%	0%	n.d.	n.d.	n.d.	n.d.	n.d.	n.d.	n.d.	n.d.	n.d.	n.d.	n.d.	n.d.	n.d.	n.d.	n.d.	n.d.	n.d.	n.d.	n.d.	n.d.	n.d.	n.d.	n.d.	88%	12%	0%	0%	0%
Moçamedes beach	Riscos	S5058	69	29	2	16%	74%	11%	0%	0%	n.d.	n.d.	n.d.	n.d.	n.d.	50%	38%	13%	0%	0%	29%	71%	0%	0%	0%	25%	75%	0%	0%	0%	77%	23%	0%	0%	0%	n.d.	n.d.	n.d.	n.d.	n.d.	n.d.	n.d.	n.d.	n.d.	n.d.	n.d.	n.d.	n.d.	n.d.	n.d.	n.d.	n.d.	n.d.	n.d.	n.d.	n.d.	n.d.	n.d.	51%	44%	5%	0%	0%
Moçamedes beach	Saco dos Tigres	S5057	75	22	3	n.d.	n.d.	n.d.	n.d.	n.d.	n.d.	n.d.	n.d.	n.d.	n.d.	n.d.	n.d.	n.d.	n.d.	n.d.	n.d.	n.d.	n.d.	n.d.	n.d.	n.d.	n.d.	n.d.	n.d.	n.d.	96%	4%	0%	0%	0%	n.d.	n.d.	n.d.	n.d.	n.d.	n.d.	n.d.	n.d.	n.d.	n.d.	n.d.	n.d.	n.d.	n.d.	n.d.	n.d.	n.d.	n.d.	n.d.	n.d.	n.d.	n.d.	n.d.	93%	7%	0%	0%	0%
Moçamedes dune	Praia dos Esponjas	S5056	67	30	3	50%	38%	13%	0%	0%	57%	43%	0%	0%	0%	45%	55%	0%	0%	0%	25%	75%	0%	0%	0%	n.d.	n.d.	n.d.	n.d.	n.d.	60%	40%	0%	0%	0%	n.d.	n.d.	n.d.	n.d.	n.d.	n.d.	n.d.	n.d.	n.d.	n.d.	n.d.	n.d.	n.d.	n.d.	n.d.	n.d.	n.d.	n.d.	n.d.	n.d.	n.d.	n.d.	n.d.	47%	52%	2%	0%	0%
Moçamedes beach	Praia dos Esponjas	S5055	66	29	5	17%	50%	17%	17%	0%	50%	0%	50%	0%	0%	20%	26%	43%	9%	3%	27%	55%	9%	9%	0%	60%	0%	40%	0%	0%	82%	18%	0%	0%	0%	n.d.	n.d.	n.d.	n.d.	n.d.	n.d.	n.d.	n.d.	n.d.	n.d.	n.d.	n.d.	n.d.	n.d.	n.d.	n.d.	n.d.	n.d.	n.d.	n.d.	n.d.	50%	50%	38%	28%	27%	6%	1%
Moçamedes dune	Foz do Cunene	S5054	66	29	4	59%	35%	6%	0%	0%	75%	0%	25%	0%	0%	67%	33%	0%	0%	0%	48%	52%	0%	0%	0%	n.d.	n.d.	n.d.	n.d.	n.d.	86%	14%	0%	0%	0%	n.d.	n.d.	n.d.	n.d.	n.d.	n.d.	n.d.	n.d.	n.d.	n.d.	n.d.	n.d.	n.d.	n.d.	n.d.	n.d.	n.d.	n.d.	n.d.	n.d.	n.d.	n.d.	n.d.	63%	33%	4%	0%	0%
Moçamedes beach	Foz do Cunene	S5053	67	26	7	53%	47%	0%	0%	0%	80%	0%	20%	0%	0%	57%	43%	0%	0%	0%	25%	75%	0%	0%	0%	n.d.	n.d.	n.d.	n.d.	n.d.	86%	14%	0%	0%	0%	n.d.	n.d.	n.d.	n.d.	n.d.	n.d.	n.d.	n.d.	n.d.	n.d.	n.d.	n.d.	n.d.	n.d.	n.d.	n.d.	n.d.	n.d.	n.d.	n.d.	n.d.	n.d.	n.d.	56%	43%	1%	0%	0%
Cunene	Foz do Cunene	S5052	61	34	4	53%	47%	0%	0%	0%	29%	71%	0%	0%	0%	24%	76%	0%	0%	0%	26%	74%	0%	0%	0%	n.d.	n.d.	n.d.	n.d.	n.d.	86%	14%	0%	0%	0%	n.d.	n.d.	n.d.	n.d.	n.d.	n.d.	n.d.	n.d.	n.d.	n.d.	n.d.	n.d.	n.d.	n.d.	n.d.	n.d.	n.d.	n.d.	n.d.	n.d.	n.d.	50%	50%	35%	65%	0%	0%	0%
Marienfluss	Otyoyonoka	S3937	64	30	6	n.d.	n.d.	n.d.	n.d.	n.d.	n.d.	n.d.	n.d.	n.d.	n.d.	55%	21%	22%	0%	2%	80%	20%	0%	0%	0%	n.d.	n.d.	n.d.	n.d.	n.d.	n.d.	n.d.	n.d.	n.d.	n.d.	n.d.	n.d.	n.d.	n.d.	n.d.	n.d.	n.d.	n.d.	n.d.	n.d.	n.d.	n.d.	n.d.	n.d.	n.d.	n.d.	n.d.	n.d.	n.d.	n.d.	n.d.	n.d.	n.d.	61%	21%	17%	0%	2%
Otjinjange	Van Zyl's Pass	S3936	65	25	10	n.d.	n.d.	n.d.	n.d.	n.d.	n.d.	n.d.	n.d.	n.d.	n.d.	24%	21%	38%	0%	17%	77%	22%	2%	0%	0%	n.d.	n.d.	n.d.	n.d.	n.d.	n.d.	n.d.	n.d.	n.d.	n.d.	n.d.	n.d.	n.d.	n.d.	n.d.	n.d.	n.d.	n.d.	n.d.	n.d.	n.d.	n.d.	n.d.	n.d.	n.d.	n.d.	n.d.	n.d.	n.d.	n.d.	n.d.	n.d.	n.d.	42%	21%	26%	0%	12%
Omuhongo	Oryeheke	S3934	45	53	3	33%	33%	33%	0%	0%	n.d.	n.d.	n.d.	n.d.	n.d.	36%	28%	30%	0%	7%	50%	49%	1%	0%	0%	n.d.	n.d.	n.d.	n.d.	n.d.	50%	50%	0%	0%	0%	n.d.	n.d.	n.d.	n.d.	n.d.	n.d.	n.d.	n.d.	n.d.	n.d.	n.d.	n.d.	n.d.	n.d.	n.d.	100%	0%	n.d.	n.d.	n.d.	n.d.	n.d.	n.d.	49%	40%	9%	0%	2%
Omuhongo	Etengua	S3935	58	41	1	n.d.	n.d.	n.d.	n.d.	n.d.	n.d.	n.d.	n.d.	n.d.	n.d.	35%	41%	0%	0%	24%	40%	60%	1%	0%	0%	n.d.	n.d.	n.d.	n.d.	n.d.	n.d.	n.d.	n.d.	n.d.	n.d.	n.d.	n.d.	n.d.	n.d.	n.d.	n.d.	n.d.	n.d.	n.d.	n.d.	n.d.	n.d.	n.d.	n.d.	n.d.	100%	0%	n.d.	n.d.	n.d.	n.d.	n.d.	n.d.	43%	54%	1%	0%	2%
Ondoto	Chitado	S3933	71	21	8	n.d.	n.d.	n.d.	n.d.	n.d.	n.d.	n.d.	n.d.	n.d.	n.d.	22%	37%	29%	0%	12%	51%	48%	1%	0%	0%	n.d.	n.d.	n.d.	n.d.	n.d.	88%	13%	0%	0%	0%	n.d.	n.d.	n.d.	n.d.	n.d.	n.d.	n.d.	n.d.	n.d.	n.d.	n.d.	n.d.	n.d.	n.d.	n.d.	100%	0%	n.d.	n.d.	100%	0%	n.d.	n.d.	48%	38%	10%	0%	4%
Cunene tributary	Ehomba	S3932	80	14	6	n.d.	n.d.	n.d.	n.d.	n.d.	n.d.	n.d.	n.d.	n.d.	n.d.	16%	34%	44%	0%	6%	74%	26%	0%	0%	0%	n.d.	n.d.	n.d.	n.d.	n.d.	40%	60%	0%	0%	0%	n.d.	n.d.	n.d.	n.d.	n.d.	n.d.	n.d.	n.d.	n.d.	n.d.	n.d.	n.d.	n.d.	n.d.	n.d.	100%	0%	75%	25%	67%	33%	n.d.	n.d.	60%	24%	14%	0%	2%
Cunene	Ruacana	S3931	80	17	3	n.d.	n.d.	n.d.	n.d.	n.d.	n.d.	n.d.	n.d.	n.d.	n.d.	18%	33%	39%	0%	11%	38%	46%	14%	0%	2%	n.d.	n.d.	n.d.	n.d.	n.d.	n.d.	n.d.	n.d.	n.d.	n.d.	n.d.	n.d.	n.d.	n.d.	n.d.	n.d.	n.d.	n.d.	n.d.	n.d.	n.d.	n.d.	n.d.	n.d.	n.d.	n.d.	n.d.	n.d.	n.d.	n.d.	n.d.	n.d.	n.d.	28%	37%	28%	0%	7%
Caculuvar	Omutele	S5051	83	17	0	n.d.	n.d.	n.d.	n.d.	n.d.	n.d.	n.d.	n.d.	n.d.	n.d.	20%	30%	20%	10%	20%	24%	62%	13%	0%	1%	n.d.	n.d.	n.d.	n.d.	n.d.	n.d.	n.d.	n.d.	n.d.	n.d.	n.d.	n.d.	n.d.	n.d.	n.d.	n.d.	n.d.	n.d.	n.d.	n.d.	n.d.	n.d.	n.d.	n.d.	n.d.	92%	8%	n.d.	n.d.	n.d.	n.d.	n.d.	n.d.	44%	43%	9%	0%	2%
Caculuvar	Techango	S5050	99	1	0	n.d.	n.d.	n.d.	n.d.	n.d.	n.d.	n.d.	n.d.	n.d.	n.d.	n.d.	n.d.	n.d.	n.d.	n.d.	28%	72%	0%	0%	0%	25%	75%	0%	0%	0%	75%	25%	0%	0%	0%	n.d.	n.d.	n.d.	n.d.	n.d.	38%	62%	0%	0%	0%	n.d.	n.d.	n.d.	n.d.	n.d.	91%	9%	29%	71%	71%	29%	n.d.	n.d.	61%	39%	0%	0%	0%
Mucope	Techiulo	S5049	99	1	0	n.d.	n.d.	n.d.	n.d.	n.d.	n.d.	n.d.	n.d.	n.d.	n.d.	n.d.	n.d.	n.d.	n.d.	n.d.	10%	80%	10%	0%	0%	50%	50%	0%	0%	0%	n.d.	n.d.	n.d.	n.d.	n.d.	n.d.	n.d.	n.d.	n.d.	n.d.	n.d.	n.d.	n.d.	n.d.	n.d.	n.d.	n.d.	n.d.	n.d.	n.d.	85%	15%	69%	31%	n.d.	n.d.	n.d.	n.d.	68%	31%	1%	0%	0%
OPERATOR 2: Sergio Andò																																																															
	Baia Farta	S4858	75	25	0	n.d.	n.d.	n.d.	n.d.	n.d.	n.d.	n.d.	n.d.	n.d.	n.d.	60%	40%	0%	0%	0%	38%	62%	0%	0%	0%	n.d.	n.d.	n.d.	n.d.	n.d.	n.d.	n.d.	n.d.	n.d.	n.d.	n.d.	n.d.	n.d.	n.d.	n.d.	n.d.	n.d.	n.d.	n.d.	n.d.	n.d.	n.d.	n.d.	n.d.	n.d.	n.d.	n.d.	n.d.	n.d.	n.d.	n.d.	n.d.	n.d.	45%	55%	0%	0%	0%
	Namibe	S4953	53	43	4	47%	40%	13%	0%	0%	31%	63%	6%	0%	0%	34%	65%	2%	0%	0%	24%	76%	0%	0%	0%	n.d.	n.d.	n.d.	n.d.	n.d.	n.d.	n.d.	n.d.	n.d.	n.d.	n.d.	n.d.	n.d.	n.d.	n.d.	n.d.	n.d.	n.d.	n.d.	n.d.	n.d.	n.d.	n.d.	n.d.	n.d.	n.d.	n.d.	n.d.	n.d.	n.d.	n.d.	75%	25%	33%	64%	3%	0%	0%
	Subida Grande	S4954	76	18	6	20%	80%	0%	0%	0%	60%	40%	0%	0%	0%	25%	75%	0%	0%	0%	8%	92%	0%	0%	0%	n.d.	n.d.	n.d.	n.d.	n.d.	100%	0%	0%	0%	0%	n.d.	n.d.	n.d.	n.d.	n.d.	n.d.	n.d.	n.d.	n.d.	n.d.	n.d.	n.d.	n.d.	n.d.	n.d.	n.d.	n.d.	n.d.	n.d.	n.d.	n.d.	n.d.	n.d.	40%	60%	0%	0%	0%
OPERATOR 3: Mara Limonta																																																															
Loussoni	St. Paul	S4053	99	0	1	n.d.	n.d.	n.d.	n.d.	n.d.	n.d.	n.d.	n.d.	n.d.	n.d.	n.d.	n.d.	n.d.	n.d.	n.d.	n.d.	n.d.	n.d.	n.d.	n.d.	0%	100%	0%	0%	0%	33%	67%	0%	0%	0%	n.d.	n.d.	n.d.	n.d.	n.d.	n.d.	n.d.	n.d.	n.d.	n.d.	n.d.	n.d.	n.d.	n.d.	n.d.	46%	54%	50%	50%	n.d.	n.d.	n.d.	n.d.	38%	63%	0%	0%	0%
	Pointe Noire	S0162	99	1	0	n.d.	n.d.	n.d.	n.d.	n.d.	n.d.	n.d.	n.d.	n.d.	n.d.	n.d.	n.d.	n.d.	n.d.	n.d.	n.d.	n.d.	n.d.	n.d.	n.d.	48%	53%	0%	0%	0%	n.d.	n.d.	n.d.	n.d.	n.d.	59%	41%	0%	0%	0%	n.d.	n.d.	n.d.	n.d.	n.d.	n.d.	n.d.	n.d.	n.d.	n.d.	43%	57%	73%	27%	70%	30%	n.d.	n.d.	57%	43%	0%	0%	0%
Congo	Kinshasa	S5114	99	1	0	n.d.	n.d.	n.d.	n.d.	n.d.	n.d.	n.d.	n.d.	n.d.	n.d.	n.d.	n.d.	n.d.	n.d.	n.d.	29%	71%	0%	0%	0%	33%	67%	0%	0%	0%	25%	75%	0%	0%	0%	33%	67%	0%	0%	0%	n.d.	n.d.	n.d.	n.d.	n.d.	n.d.	n.d.	n.d.	n.d.	n.d.	44%	56%	91%	9%	82%	18%	n.d.	n.d.	46%	54%	0%	0%	0%
Congo	Boma	S5115	99	1	0	n.d.	n.d.	n.d.	n.d.	n.d.	n.d.	n.d.	n.d.	n.d.	n.d.	64%	36%	0%	0%	0%	33%	67%	0%	0%	0%	42%	58%	0%	0%	0%	25%	75%	0%	0%	0%	33%	67%	0%	0%	0%	n.d.	n.d.	n.d.	n.d.	n.d.	n.d.	n.d.	n.d.	n.d.	n.d.	46%	54%	100%	0%	40%	60%	n.d.	n.d.	44%	55%	1%	0%	0%
Congo	Soyo	S4899	98	2	0	n.d.	n.d.	n.d.	n.d.	n.d.	n.d.	n.d.	n.d.	n.d.	n.d.	n.d.	n.d.	n.d.	n.d.	n.d.	13%	88%	0%	0%	0%	22%	78%	0%	0%	0%	67%	33%	0%	0%	0%	44%	56%	0%	0%	0%	n.d.	n.d.	n.d.	n.d.	n.d.	n.d.	n.d.	n.d.	n.d.	n.d.	86%	14%	88%	12%	50%	50%	n.d.	n.d.	52%	48%	0%	0%	0%
Congo	Soyo estuary	S4898	99	1	0	n.d.	n.d.	n.d.	n.d.	n.d.	n.d.	n.d.	n.d.	n.d.	n.d.	81%	19%	0%	0%	0%	40%	60%	0%	0%	0%	45%	55%	0%	0%	0%	n.d.	n.d.	n.d.	n.d.	n.d.	57%	43%	0%	0%	0%	n.d.	n.d.	n.d.	n.d.	n.d.	n.d.	n.d.	n.d.	n.d.	n.d.	44%	56%	91%	9%	53%	47%	n.d.	n.d.	60%	40%	0%	0%	0%
-31 m inner shelf offshore Congo mouth		1004	91	9	0	n.d.	n.d.	n.d.	n.d.	n.d.	n.d.	n.d.	n.d.	n.d.	n.d.	84%	16%	0%	0%	0%	20%	80%	0%	0%	0%	n.d.	n.d.	n.d.	n.d.	n.d.	26%	74%	0%	0%	0%	38%	63%	0%	0%	0%	n.d.	n.d.	n.d.	n.d.	n.d.	n.d.	n.d.	n.d.	n.d.	n.d.	50%	50%	n.d.	n.d.	61%	39%	n.d.	n.d.	41%	59%	0%	0%	0%
Onzo	Tabi	S4893	86	14	0	0%	60%	40%	0%	0%	n.d.	n.d.	n.d.	n.d.	n.d.	89%	11%	0%	0%	0%	54%	46%	0%	0%	0%	n.d.	n.d.	n.d.	n.d.	n.d.	63%	38%	0%	0%	0%	83%	17%	0%	0%	0%	n.d.	n.d.	n.d.	n.d.	n.d.	n.d.	n.d.	n.d.	n.d.	n.d.	n.d.	n.d.	n.d.	n.d.	n.d.	n.d.	n.d.	n.d.	76%	23%	1%	0%	0%
Lifune	Conde Loca	S4892	93	7	0	n.d.	n.d.	n.d.	n.d.	n.d.	n.d.	n.d.	n.d.	n.d.	n.d.	81%	19%	0%	0%	0%	40%	60%	0%	0%	0%	n.d.	n.d.	n.d.	n.d.	n.d.	38%	63%	0%	0%	0%	42%	58%	0%	0%	0%	n.d.	n.d.	n.d.	n.d.	n.d.	n.d.	n.d.	n.d.	n.d.	n.d.	83%	17%	n.d.	n.d.	100%	0%	n.d.	n.d.	56%	43%	0%	0%	0%
	Barra do Dande	S4910	86	13	1	56%	44%	0%	0%	0%	n.d.	n.d.	n.d.	n.d.	n.d.	56%	44%	0%	0%	0%	25%	75%	0%	0%	0%	n.d.	n.d.	n.d.	n.d.	n.d.	23%	77%	0%	0%	0%	29%	71%	0%	0%	0%	n.d.	n.d.	n.d.	n.d.	n.d.	n.d.	n.d.	n.d.	n.d.	n.d.	43%	57%	75%	25%	60%	40%	n.d.	n.d.	34%	66%	0%	0%	0%
	Ilha de Luanda	S4652	81	18	1	21%	79%	0%	0%	0%	n.d.	n.d.	n.d.	n.d.	n.d.	81%	19%	0%	0%	0%	13%	87%	0%	0%	0%	n.d.	n.d.	n.d.	n.d.	n.d.	0%	100%	0%	0%	0%	40%	60%	0%	0%	0%	n.d.	n.d.	n.d.	n.d.	n.d.	n.d.	n.d.	n.d.	n.d.	n.d.	40%	60%	n.d.	n.d.	n.d.	n.d.	n.d.	n.d.	29%	71%	0%	0%	0%
	Mussulo	S3764	83	17	0	79%	14%	7%	0%	0%	n.d.	n.d.	n.d.	n.d.	n.d.	81%	16%	3%	0%	0%	7%	93%	0%	0%	0%	n.d.	n.d.	n.d.	n.d.	n.d.	n.d.	n.d.	n.d.	n.d.	n.d.	n.d.	n.d.	n.d.	n.d.	n.d.	n.d.	n.d.	n.d.	n.d.	n.d.	n.d.	n.d.	n.d.	n.d.	n.d.	n.d.	n.d.	n.d.	n.d.	n.d.	n.d.	n.d.	n.d.	39%	59%	2%	0%	0%
	Palmeirinhas	S4913	83	17	0	48%	52%	0%	0%	0%	n.d.	n.d.	n.d.	n.d.	n.d.	78%	22%	0%	0%	0%	15%	85%	0%	0%	0%	0%	100%	0%	0%	0%	18%	82%	0%	0%	0%	33%	67%	0%	0%	0%	n.d.	n.d.	n.d.	n.d.	n.d.	n.d.	n.d.	n.d.	n.d.	n.d.	65%	35%	n.d.	n.d.	n.d.	n.d.	n.d.	n.d.	30%	70%	0%	0%	0%
	Barra do Cuanza	S4914	79	20	1	40%	60%	0%	0%	0%	n.d.	n.d.	n.d.	n.d.	n.d.	86%	14%	0%	0%	0%	18%	82%	0%	0%	0%	n.d.	n.d.	n.d.	n.d.	n.d.	17%	83%	0%	0%	0%	n.d.	n.d.	n.d.	n.d.	n.d.	n.d.	n.d.	n.d.	n.d.	n.d.	n.d.	n.d.	n.d.	n.d.	n.d.	60%	40%	n.d.	n.d.	n.d.	n.d.	n.d.	n.d.	37%	63%	0%	0%	0%
Cuanza	Barra do Cuanza	S4915	87	12	1	27%	60%	13%	0%	0%	n.d.	n.d.	n.d.	n.d.	n.d.	93%	7%	0%	0%	0%	47%	50%	3%	0%	0%	n.d.	n.d.	n.d.	n.d.	n.d.	30%	70%	0%	0%	0%	100%	0%	0%	0%	0%	n.d.	n.d.	n.d.	n.d.	n.d.	n.d.	n.d.	n.d.	n.d.	n.d.	32%	68%	100%	0%	75%	25%	n.d.	n.d.	58%	40%	3%	0%	0%
	Cabo Ledo	S3765	74	24	2	57%	43%	0%	0%	0%	n.d.	n.d.	n.d.	n.d.	n.d.	93%	7%	0%	0%	0%	25%	75%	0%	0%	0%	n.d.	n.d.	n.d.	n.d.	n.d.	40%	60%	0%	0%	0%	n.d.	n.d.	n.d.	n.d.	n.d.	n.d.	n.d.	n.d.	n.d.	n.d.	40%	60%	0%	0%	0%	57%	43%	n.d.	n.d.	n.d.	n.d.	n.d.	n.d.	41%	59%	0%	0%	0%
	Sao Braz	S4916	70	28	3	60%	40%	0%	0%	0%	n.d.	n.d.	n.d.	n.d.	n.d.	90%	10%	0%	0%	0%	20%	80%	0%	0%	0%	n.d.	n.d.	n.d.	n.d.	n.d.	n.d.	n.d.	n.d.	n.d.	n.d.	n.d.	n.d.	n.d.	n.d.	n.d.	n.d.	n.d.	n.d.	n.d.	n.d.	50%	50%	0%	0%	0%	83%	17%	n.d.	n.d.	n.d.	n.d.	n.d.	n.d.	38%	62%	0%	0%	0%
	Porto Amboim	S4918	76	23	1	24%	76%	0%	0%	0%	n.d.	n.d.	n.d.	n.d.	n.d.	87%	13%	0%	0%	0%	15%	85%	0%	0%	0%	n.d.	n.d.	n.d.	n.d.	n.d.	n.d.	n.d.	n.d.	n.d.	n.d.	n.d.	n.d.	n.d.	n.d.	n.d.	n.d.	n.d.	n.d.	n.d.	n.d.	n.d.	n.d.	n.d.	n.d.	n.d.	73%	27%	n.d.	n.d.	n.d.	n.d.	n.d.	n.d.	39%	61%	0%	0%	0%
Queve	Cachoeira	S4922	74	26	0	n.d.	n.d.	n.d.	n.d.	n.d.	n.d.	n.d.	n.d.	n.d.	n.d.	68%	32%	0%	0%	0%	18%	82%	0%	0%	0%	n.d.	n.d.	n.d.	n.d.	n.d.	0%	100%	0%	0%	0%	n.d.	n.d.	n.d.	n.d.	n.d.	n.d.	n.d.	n.d.	n.d.	n.d.	n.d.	n.d.	n.d.	n.d.	n.d.	n.d.	n.d.	n.d.	n.d.	n.d.	n.d.	n.d.	n.d.	45%	56%	0%	0%	0%
	Carimba	S4923	78	21	1	48%	52%	0%	0%	0%	n.d.	n.d.	n.d.	n.d.	n.d.	13%	88%	0%	0%	0%	24%	76%	0%	0%	0%	n.d.	n.d.	n.d.	n.d.	n.d.	n.d.	n.d.	n.d.	n.d.	n.d.	n.d.	n.d.	n.d.	n.d.	n.d.	n.d.	n.d.	n.d.	n.d.	n.d.	n.d.	n.d.	n.d.	n.d.	n.d.	73%	27%	n.d.	n.d.	n.d.	n.d.	n.d.	n.d.	32%	68%	0%	0%	0%
	Sumbe	S4919	n.d	n.d.	n.d.	38%	62%	0%	0%	0%	n.d.	n.d.	n.d.	n.d.	n.d.	87%	13%	0%	0%	0%	13%	87%	0%	0%	0%	n.d.	n.d.	n.d.	n.d.	n.d.	n.d.	n.d.	n.d.	n.d.	n.d.	n.d.	n.d.	n.d.	n.d.	n.d.	n.d.	n.d.	n.d.	n.d.	n.d.	30%	70%	0%	0%	0%	68%	32%	n.d.	n.d.	n.d.	n.d.	n.d.	n.d.	34%	66%	0%	0%	0%
Cambongo	Sumbe	S4924	71	27	2	73%	18%	9%	0%	0%	n.d.	n.d.	n.d.	n.d.	n.d.	92%	8%	0%	0%	0%	29%	70%	1%	0%	0%	n.d.	n.d.	n.d.	n.d.	n.d.	75%	25%	0%	0%	0%	n.d.	n.d.	n.d.	n.d.	n.d.	n.d.	n.d.	n.d.	n.d.	n.d.	n.d.	n.d.	n.d.	n.d.	n.d.	85%	15%	n.d.	n.d.	n.d.	n.d.	n.d.	n.d.	59%	40%	1%	0%	0%
Quicombo	Quicombo	S4925	65	33	2	20%	80%	0%	0%	0%	n.d.	n.d.	n.d.	n.d.	n.d.	93%	7%	0%	0%	0%	17%	83%	0%	0%	0%	n.d.	n.d.	n.d.	n.d.	n.d.	20%	80%	0%	0%	0%	n.d.	n.d.	n.d.	n.d.	n.d.	n.d.	n.d.	n.d.	n.d.	n.d.	18%	82%	0%	0%	0%	67%	33%	n.d.	n.d.	n.d.	n.d.	n.d.	n.d.	33%	67%	0%	0%	0%
	Quicombo	S4920	n.d	n.d.	n.d.	70%	30%	0%	0%	0%	n.d.	n.d.	n.d.	n.d.	n.d.	100%	0%	0%	0%	0%	22%	78%	0%	0%	0%	n.d.	n.d.	n.d.	n.d.	n.d.	n.d.	n.d.	n.d.	n.d.	n.d.	n.d.	n.d.	n.d.	n.d.	n.d.	n.d.	n.d.	n.d.	n.d.	n.d.	n.d.	n.d.	n.d.	n.d.	n.d.	79%	21%	n.d.	n.d.	n.d.	n.d.	n.d.	n.d.	44%	56%	0%	0%	0%
	Praia Sousa	S4930	76	23	1	85%	11%	4%	0%	0%	n.d.	n.d.	n.d.	n.d.	n.d.	100%	0%	0%	0%	0%	26%	74%	0%	0%	0%	n.d.	n.d.	n.d.	n.d.	n.d.	n.d.	n.d.	n.d.	n.d.	n.d.	n.d.	n.d.	n.d.	n.d.	n.d.	n.d.	n.d.	n.d.	n.d.	n.d.	n.d.	n.d.	n.d.	n.d.	n.d.	75%	25%	n.d.	n.d.	n.d.	n.d.	n.d.	n.d.	52%	48%	0%	0%	0%
	Candunga	S4921	n.d	n.d.	n.d.	53%	47%	0%	0%	0%	n.d.	n.d.	n.d.	n.d.	n.d.	77%	23%	0%	0%	0%	12%	88%	0%	0%	0%	n.d.	n.d.	n.d.	n.d.	n.d.	n.d.	n.d.	n.d.	n.d.	n.d.	n.d.	n.d.	n.d.	n.d.	n.d.	n.d.	n.d.	n.d.	n.d.	n.d.	n.d.	n.d.	n.d.	n.d.	n.d.	72%	28%	n.d.	n.d.	n.d.	n.d.	n.d.	n.d.	35%	65%	0%	0%	0%
-73 m shelf offshore Tapado mouth		1011	44	54	2	57%	43%	0%	0%	0%	n.d.	n.d.	n.d.	n.d.	n.d.	85%	15%	0%	0%	0%	30%	70%	0%	0%	0%	n.d.	n.d.	n.d.	n.d.	n.d.	n.d.	n.d.	n.d.	n.d.	n.d.	n.d.	n.d.	n.d.	n.d.	n.d.	n.d.	n.d.	n.d.	n.d.	n.d.	n.d.	n.d.	n.d.	n.d.	n.d.	50%	50%	n.d.	n.d.	n.d.	n.d.	n.d.	n.d.	47%	53%	0%	0%	0%
-99 m shelf offshore Tapado mouth		1012/1	n.d	n.d.	n.d.	n.d.	n.d.	n.d.	n.d.	n.d.	n.d.	n.d.	n.d.	n.d.	n.d.	89%	11%	0%	0%	0%	30%	70%	0%	0%	0%	n.d.	n.d.	n.d.	n.d.	n.d.	n.d.	n.d.	n.d.	n.d.	n.d.	n.d.	n.d.	n.d.	n.d.	n.d.	n.d.	n.d.	n.d.	n.d.	n.d.	50%	50%	0%	0%	0%	20%	80%	n.d.	n.d.	n.d.	n.d.	n.d.	n.d.	38%	62%	0%	0%	0%
-99 m shelf offshore Tapado mouth		1012/2	51	46	3	75%	25%	0%	0%	0%	n.d.	n.d.	n.d.	n.d.	n.d.	92%	8%	0%	0%	0%	35%	65%	0%	0%	0%	n.d.	n.d.	n.d.	n.d.	n.d.	n.d.	n.d.	n.d.	n.d.	n.d.	n.d.	n.d.	n.d.	n.d.	n.d.	n.d.	n.d.	n.d.	n.d.	n.d.	50%	50%	0%	0%	0%	75%	25%	n.d.	n.d.	n.d.	n.d.	n.d.	n.d.	48%	52%	0%	0%	0%
-250 m slope offshore Tapado mouth		1013	n.d	n.d.	n.d.	n.d.	n.d.	n.d.	n.d.	n.d.	n.d.	n.d.	n.d.	n.d.	n.d.	94%	6%	0%	0%	0%	33%	67%	0%	0%	0%	n.d.	n.d.	n.d.	n.d.	n.d.	n.d.	n.d.	n.d.	n.d.	n.d.	n.d.	n.d.	n.d.	n.d.	n.d.	n.d.	n.d.	n.d.	n.d.	n.d.	100%	0%	0%	0%	0%	50%	50%	n.d.	n.d.	n.d.	n.d.	n.d.	n.d.	44%	56%	0%	0%	0%
Balombo	Canjala	S4927	53	46	1	n.d.	n.d.	n.d.	n.d.	n.d.	n.d.	n.d.	n.d.	n.d.	n.d.	100%	0%	0%	0%	0%	10%	90%	0%	0%	0%	n.d.	n.d.	n.d.	n.d.	n.d.	n.d.	n.d.	n.d.	n.d.	n.d.	n.d.	n.d.	n.d.	n.d.	n.d.	n.d.	n.d.	n.d.	n.d.	n.d.	n.d.	n.d.	n.d.	n.d.	n.d.	100%	0%	n.d.	n.d.	n.d.	n.d.	n.d.	n.d.	20%	80%	0%	0%	0%
	Egito Praia	S4928	72	28	1	65%	35%	0%	0%	0%	n.d.	n.d.	n.d.	n.d.	n.d.	83%	17%	0%	0%	0%	7%	93%	0%	0%	0%	n.d.	n.d.	n.d.	n.d.	n.d.	n.d.	n.d.	n.d.	n.d.	n.d.	n.d.	n.d.	n.d.	n.d.	n.d.	n.d.	n.d.	n.d.	n.d.	n.d.	n.d.	n.d.	n.d.	n.d.	n.d.	n.d.	n.d.	n.d.	n.d.	n.d.	n.d.	n.d.	n.d.	44%	56%	0%	0%	0%
	Lobito spit	S4934	n.d	n.d.	n.d.	81%	19%	0%	0%	0%	n.d.	n.d.	n.d.	n.d.	n.d.	87%	13%	0%	0%	0%	71%	29%	0%	0%	0%	n.d.	n.d.	n.d.	n.d.	n.d.	n.d.	n.d.	n.d.	n.d.	n.d.	n.d.	n.d.	n.d.	n.d.	n.d.	n.d.	n.d.	n.d.	n.d.	n.d.	n.d.	n.d.	n.d.	n.d.	n.d.	100%	0%	n.d.	n.d.	n.d.	n.d.	n.d.	n.d.	78%	22%	0%	0%	0%
	Lobito spit	S4863	61	38	1	75%	25%	0%	0%	0%	n.d.	n.d.	n.d.	n.d.	n.d.	73%	27%	0%	0%	0%	27%	73%	0%	0%	0%	n.d.	n.d.	n.d.	n.d.	n.d.	50%	50%	0%	0%	0%	n.d.	n.d.	n.d.	n.d.	n.d.	n.d.	n.d.	n.d.	n.d.	n.d.	n.d.	n.d.	n.d.	n.d.	n.d.	90%	10%	n.d.	n.d.	n.d.	n.d.	n.d.	n.d.	41%	59%	0%	0%	0%
	Catumbela N	S4862	75	23	2	79%	21%	0%	0%	0%	n.d.	n.d.	n.d.	n.d.	n.d.	76%	24%	0%	0%	0%	15%	85%	0%	0%	0%	n.d.	n.d.	n.d.	n.d.	n.d.	n.d.	n.d.	n.d.	n.d.	n.d.	n.d.	n.d.	n.d.	n.d.	n.d.	n.d.	n.d.	n.d.	n.d.	n.d.	n.d.	n.d.	n.d.	n.d.	n.d.	50%	50%	n.d.	n.d.	n.d.	n.d.	n.d.	n.d.	39%	60%	0%	0%	0%
Cubal da Hanha	Vista Alegre	S5118	59	41	0	n.d.	n.d.	n.d.	n.d.	n.d.	n.d.	n.d.	n.d.	n.d.	n.d.	49%	51%	0%	0%	0%	12%	88%	0%	0%	0%	n.d.	n.d.	n.d.	n.d.	n.d.	n.d.	n.d.	n.d.	n.d.	n.d.	n.d.	n.d.	n.d.	n.d.	n.d.	n.d.	n.d.	n.d.	n.d.	n.d.	n.d.	n.d.	n.d.	n.d.	n.d.	n.d.	n.d.	94%	6%	n.d.	n.d.	n.d.	n.d.	39%	61%	0%	0%	0%
Calumbolo	Supua	S5116	56	43	1	n.d.	n.d.	n.d.	n.d.	n.d.	n.d.	n.d.	n.d.	n.d.	n.d.	61%	39%	0%	0%	0%	28%	72%	0%	0%	0%	n.d.	n.d.	n.d.	n.d.	n.d.	n.d.	n.d.	n.d.	n.d.	n.d.	n.d.	n.d.	n.d.	n.d.	n.d.	n.d.	n.d.	n.d.	n.d.	n.d.	n.d.	n.d.	n.d.	n.d.	n.d.	n.d.	n.d.	n.d.	n.d.	n.d.	n.d.	n.d.	n.d.	33%	67%	0%	0%	0%
Capilongo	Capilongo	S5117	44	49	7	42%	55%	3%	0%	0%	n.d.	n.d.	n.d.	n.d.	n.d.	85%	15%	0%	0%	0%	56%	44%	0%	0%	0%	n.d.	n.d.	n.d.	n.d.	n.d.	n.d.	n.d.	n.d.	n.d.	n.d.	n.d.	n.d.	n.d.	n.d.	n.d.	n.d.	n.d.	n.d.	n.d.	n.d.	40%	60%	0%	0%	0%	n.d.	n.d.	n.d.	n.d.	n.d.	n.d.	n.d.	n.d.	52%	47%	1%	0%	0%
Catumbela	Catumbela	S4933	73	26	1	18%	82%	0%	0%	0%	n.d.	n.d.	n.d.	n.d.	n.d.	79%	21%	0%	0%	0%	28%	72%	0%	0%	0%	n.d.	n.d.	n.d.	n.d.	n.d.	n.d.	n.d.	n.d.	n.d.	n.d.	n.d.	n.d.	n.d.	n.d.	n.d.	n.d.	n.d.	n.d.	n.d.	n.d.	n.d.	n.d.	n.d.	n.d.	n.d.	100%	0%	n.d.	n.d.	n.d.	n.d.	n.d.	n.d.	40%	60%	0%	0%	0%
Catumbela	Catumbela	S4860	74	25	1	50%	50%	0%	0%	0%	n.d.	n.d.	n.d.	n.d.	n.d.	73%	27%	0%	0%	0%	14%	86%	0%	0%	0%	n.d.	n.d.	n.d.	n.d.	n.d.	n.d.	n.d.	n.d.	n.d.	n.d.	n.d.	n.d.	n.d.	n.d.	n.d.	n.d.	n.d.	n.d.	n.d.	n.d.	n.d.	n.d.	n.d.	n.d.	n.d.	82%	18%	n.d.	n.d.	n.d.	n.d.	n.d.	n.d.	37%	63%	0%	0%	0%
	Catumbela airport	S4859	50	49	1	n.d.	n.d.	n.d.	n.d.	n.d.	n.d.	n.d.	n.d.	n.d.	n.d.	56%	42%	2%	0%	0%	7%	93%	0%	0%	0%	n.d.	n.d.	n.d.	n.d.	n.d.	n.d.	n.d.	n.d.	n.d.	n.d.	n.d.	n.d.	n.d.	n.d.	n.d.	n.d.	n.d.	n.d.	n.d.	n.d.	n.d.	n.d.	n.d.	n.d.	n.d.	50%	50%	n.d.	n.d.	n.d.	n.d.	n.d.	n.d.	19%	81%	1%	0%	0%
	Camucua	S4857	64	36	0	20%	80%	0%	0%	0%	n.d.	n.d.	n.d.	n.d.	n.d.	70%	30%	0%	0%	0%	5%	95%	0%	0%	0%	n.d.	n.d.	n.d.	n.d.	n.d.	n.d.	n.d.	n.d.	n.d.	n.d.	n.d.	n.d.	n.d.	n.d.	n.d.	n.d.	n.d.	n.d.	n.d.	n.d.	n.d.	n.d.	n.d.	n.d.	n.d.	75%	25%	n.d.	n.d.	n.d.	n.d.	n.d.	n.d.	18%	82%	0%	0%	0%
Coporolo	Santa Tereza	S4852	62	38	0	33%	67%	0%	0%	0%	n.d.	n.d.	n.d.	n.d.	n.d.	51%	49%	0%	0%	0%	10%	90%	0%	0%	0%	n.d.	n.d.	n.d.	n.d.	n.d.	n.d.	n.d.	n.d.	n.d.	n.d.	n.d.	n.d.	n.d.	n.d.	n.d.	n.d.	n.d.	n.d.	n.d.	n.d.	n.d.	n.d.	n.d.	n.d.	n.d.	n.d.	n.d.	n.d.	n.d.	n.d.	n.d.	n.d.	n.d.	25%	75%	0%	0%	0%
-75 m shelf offshore Cunene mouth		1019	n.d	n.d.	n.d.	83%	17%	0%	0%	0%	n.d.	n.d.	n.d.	n.d.	n.d.	73%	27%	0%	0%	0%	63%	37%	0%	0%	0%	n.d.	n.d.	n.d.	n.d.	n.d.	n.d.	n.d.	n.d.	n.d.	n.d.	n.d.	n.d.	n.d.	n.d.	n.d.	n.d.	n.d.	n.d.	n.d.	n.d.	50%	50%	0%	0%	0%	n.d.	n.d.	n.d.	n.d.	n.d.	n.d.	56%	44%	77%	23%	0%	0%	0%
-110 m outer shelf offshore Cunene mouth		1020	72	22	6	39%	61%	0%	0%	0%	n.d.	n.d.	n.d.	n.d.	n.d.	73%	27%	0%	0%	0%	27%	73%	0%	0%	0%	n.d.	n.d.	n.d.	n.d.	n.d.	75%	25%	0%	0%	0%	n.d.	n.d.	n.d.	n.d.	n.d.	n.d.	n.d.	n.d.	n.d.	n.d.	75%	25%	0%	0%	0%	n.d.	n.d.	n.d.	n.d.	n.d.	n.d.	20%	80%	45%	55%	0%	0%	0%
-173 m outer shelf offshore Cunene mouth		1021	73	22	5	63%	37%	0%	0%	0%	n.d.	n.d.	n.d.	n.d.	n.d.	92%	8%	0%	0%	0%	54%	46%	0%	0%	0%	n.d.	n.d.	n.d.	n.d.	n.d.	n.d.	n.d.	n.d.	n.d.	n.d.	n.d.	n.d.	n.d.	n.d.	n.d.	n.d.	n.d.	n.d.	n.d.	n.d.	25%	75%	0%	0%	0%	n.d.	n.d.	n.d.	n.d.	100%	0%	80%	20%	64%	36%	0%	0%	0%
-551 m slope offshore of Cunene mouth		1022	n.d	n.d.	n.d.	44%	56%	0%	0%	0%	n.d.	n.d.	n.d.	n.d.	n.d.	70%	30%	0%	0%	0%	35%	65%	0%	0%	0%	n.d.	n.d.	n.d.	n.d.	n.d.	60%	40%	0%	0%	0%	n.d.	n.d.	n.d.	n.d.	n.d.	n.d.	n.d.	n.d.	n.d.	n.d.	25%	75%	0%	0%	0%	20%	80%	n.d.	n.d.	n.d.	n.d.	25%	75%	43%	57%	0%	0%	0%
-399 m continental slope on Walvis Ridge		1704	n.d	n.d.	n.d.	92%	8%	0%	0%	0%	n.d.	n.d.	n.d.	n.d.	n.d.	100%	0%	0%	0%	0%	71%	29%	0%	0%	0%	n.d.	n.d.	n.d.	n.d.	n.d.	80%	20%	0%	0%	0%	n.d.	n.d.	n.d.	n.d.	n.d.	n.d.	n.d.	n.d.	n.d.	n.d.	60%	40%	0%	0%	0%	n.d.	n.d.	n.d.	n.d.	n.d.	n.d.	n.d.	n.d.	87%	13%	0%	0%	0%
-642 m continental slope on Walvis Ridge		1705	n.d	n.d.	n.d.	72%	27%	1%	0%	0%	n.d.	n.d.	n.d.	n.d.	n.d.	100%	0%	0%	0%	0%	29%	71%	0%	0%	0%	n.d.	n.d.	n.d.	n.d.	n.d.	n.d.	n.d.	n.d.	n.d.	n.d.	n.d.	n.d.	n.d.	n.d.	n.d.	n.d.	n.d.	n.d.	n.d.	n.d.	n.d.	n.d.	n.d.	n.d.	n.d.	n.d.	n.d.	n.d.	n.d.	n.d.	n.d.	57%	43%	69%	31%	0%	0%	0%

Appendix Table A6

Click here to download Table: Table A6 Angola CHI.pdf

Table A6

Sample	River	Site	Analysed class µm	Sieving	wt% finer	Analysed class wt%	wt% coarser	SiO_2 wt%	Al_2O_3 wt%	Fe_2O_3 wt%	MgO wt%	CaO wt%	Na_2O wt%	K_2O wt%	TiO_2 wt%	P_2O_5 wt%	MnO wt%	LOI wt%	Total wt%	Rb ppm	Cs ppm	Be ppm	Sr ppm	Ba ppm	Sc ppm	Y ppm	La ppm	Ce ppm	Pr ppm	Nd ppm	Sm ppm	Eu ppm	Gd ppm	Tb ppm	Dy ppm	Ho ppm	Er ppm	Tm ppm	Yb ppm	Lu ppm	Th ppm	U ppm
							M.D.L.	0.01	0.01	0.04	0.01	0.01	0.01	0.01	0.01	0.01	0.01	0.1	0.01	0.1	0.1	1	0.5	1	1	0.1	0.1	0.1	0.02	0.3	0.05	0.02	0.05	0.01	0.05	0.02	0.03	0.01	0.05	0.01	0.2	0.1
RIVERS & BEACHES OF THE CONGO																																										
S4053	Loussoni	St. Paul	63-2000	dry	0%	98%	2%	98.3	0.3	0.7	0.0	0.0	<0.01	0.0	0.1	0.02	<0.01	0.5	99.9	2	0	<1	4	19	<1	2	5	6	1	3	1	0.1	1	0.1	0	0.1	0	0.1	0	0.0	1	0
S 162		Point Noire	63-2000	wet	0%	99%	1%	98.2	0.5	0.2	0.0	0.2	<0.01	0.0	0.0	0.04	<0.01	0.8	99.9	1	<0.1	<1	13	27	<1	2	2	4	0	2	0	0.1	0	0.0	0	0.1	0	0.0	0	0.0	1	0
S0161	Loémé	Djeno	63-2000	dry	0%	99%	1%	99.0	0.2	0.1	0.0	0.0	0.0	0.0	0.2	0.02	<0.01	0.4	99.9	0	0	<1	2	6	<1	2	1	1	0	1	0	0.0	0	0.1	0	0.1	0	0.1	0	0.1	1	0
S 3533	Congo	Brazzaville	63-2000	dry	0%	100%	0%	98.5	0.3	0.2	0.1	0.1	0.0	0.1	0.1	0.02	<0.01	0.7	100.0	3	0	<1	7	38	<1	2	3	6	1	2	0	0.1	0	0.1	0	0.1	0	0.0	0	0.0	1	0
S 4898		Soyo estuary	63-2000	wet	0%	100%	0%	96.2	1.4	0.5	0.1	0.1	0.1	0.2	0.1	0.02	0.01	1.4	100.0	4	0	1	19	94	<1	2	3	5	1	2	0	0.1	0	0.1	0	0.1	0	0.0	0	0.0	1	0
S 4899		Soyo	63-2000	wet	0%	100%	0%	96.6	1.1	0.4	0.0	0.1	0.0	0.0	0.2	0.02	<0.01	1.7	100.0	1	<0.1	<1	6	15	<1	2	2	4	0	2	0	0.1	0	0.0	0	0.0	0	0.0	0	0.0	1	0
RIVERS OF NORTHERN ANGOLA																																										
S 4904	Luculu	Quivanda	63-2000	wet	1%	99%	0%	91.9	3.8	1.3	0.2	0.6	0.4	0.6	0.3	0.05	0.04	0.7	99.9	9	0	<1	86	242	4	10	9	19	2	8	2	0.3	1	0.3	2	0.4	1	0.2	1	0.2	3	1
S 4897	Mebridege	Cassa de Telha	63-2000	wet	0%	96%	4%	95.2	1.4	0.9	0.1	0.1	0.1	0.3	0.1	0.03	<0.01	1.9	100.0	6	<0.1	<1	14	68	<1	3	4	7	1	4	1	0.2	1	0.1	1	0.1	0	0.1	0	0.0	1	0
S 4894	Loge	Porta Freitas Morna	63-2000	wet	0%	100%	0%	84.7	7.0	1.7	0.4	1.9	1.5	0.9	0.2	0.02	0.02	1.6	99.9	15	<0.1	<1	307	501	7	7	12	24	3	12	2	0.6	2	0.3	1	0.3	1	0.1	1	0.1	2	0
S 4891	Dande	Caxito	63-2000	wet	2%	98%	0%	87.0	5.9	1.6	0.4	0.6	1.1	1.4	0.3	0.03	0.02	1.2	99.6	33	0	3	69	435	3	7	11	22	2	9	2	0.3	1	0.2	1	0.3	1	0.1	1	0.1	3	1
S 4911	Bengo	Quifangondo	63-2000	wet	3%	96%	1%	88.8	3.3	0.8	0.2	2.7	0.5	0.9	0.1	0.05	0.01	2.5	100.0	16	0	1	139	319	1	4	5	11	1	5	1	0.2	1	0.1	1	0.1	0	0.1	0	0.1	1	1
BEACHES OF NORTHERN ANGOLA																																										
S 4902		Quifuma	63-2000	wet	0%	100%	0%	94.9	1.6	0.8	0.1	0.9	0.2	0.3	0.1	0.07	<0.01	1.0	99.9	4	<0.1	<1	64	140	1	3	4	8	1	3	1	0.1	1	0.1	0	0.1	0	0.1	0	0.1	1	0
S 4905		Mbua-Moyo	63-2000	wet	0%	100%	0%	89.0	3.9	1.1	0.3	2.3	0.7	0.7	0.2	0.18	0.02	1.5	99.9	10	<0.1	<1	202	329	4	8	9	17	2	8	2	0.4	2	0.2	1	0.3	1	0.1	1	0.1	2	1
S 4906		N'Zeto	63-2000	wet	0%	100%	0%	85.5	4.8	1.1	0.4	3.2	1.1	0.8	0.1	0.31	0.02	2.4	99.9	11	<0.1	<1	271	482	4	8	8	15	2	7	1	0.4	1	0.2	1	0.3	1	0.1	1	0.1	1	2
S 4908		Musserra	63-2000	wet	0%	100%	0%	86.4	5.3	1.6	0.3	2.4	1.1	0.8	0.2	0.04	0.04	1.6	99.8	11	<0.1	<1	292	468	7	12	13	28	3	12	2	0.6	2	0.3	2	0.4	1	0.2	1	0.2	3	1
S 4909		Ambriz	63-2000	wet	0%	100%	0%	84.3	4.8	1.1	0.4	4.4	0.8	0.8	0.2	0.05	0.05	3.1	99.9	11	<0.1	<1	299	504	6	13	9	18	2	9	2	0.5	2	0.3	2	0.5	1	0.2	2	0.2	1	1
CUANZA & CUANZA LITTORAL CELL																																										
S4652		Ilha de Luanda	63-2000	dry	0%	100%	0%	90.1	3.6	0.8	0.1	1.6	0.6	1.8	0.1	0.05	<0.01	1.2	99.9	31	0	<1	116	642	<1	2	4	6	1	3	0	0.2	0	0.1	0	0.1	0	0.0	0	0.1	1	0
S3764		Mussulo	63-2000	dry	0%	100%	0%	88.9	4.3	0.9	0.1	1.6	0.7	2.3	0.0	0.06	<0.01	1.2	99.9	44	1	<1	116	776	<1	2	5	8	1	3	1	0.2	0	0.1	0	0.1	0	0.0	0	0.0	1	0
S 4915	Cuanza	Barra do Cuanza	63-2000	wet	0%	100%	0%	93.5	2.3	0.5	0.1	0.5	0.2	0.8	0.1	0.03	<0.01	1.8	100.0	16	<0.1	<1	41	283	<1	3	4	7	1	4	1	0.1	1	0.1	1	0.1	0	0.1	0	0.1	2	0
RIVERS OF CENTRAL ANGOLA																																										
S 4917	Longa	Calamba	63-2000	wet	4%	87%	8%	88.1	3.8	0.8	0.3	2.1	0.4	1.6	0.2	0.03	0.02	2.5	99.9	28	0	<1	92	482	3	7	12	24	3	10	2	0.3	1	0.2	1	0.2	1	0.1	1	0.1	5	1
S 4922	Queve	Cachoeira	63-2000	wet	0%	100%	0%	85.4	7.1	0.8	0.1	0.5	0.8	3.3	0.2	0.02	0.02	1.8	99.9	69	0	1	104	865	1	3	6	13	1	5	1	0.2	1	0.1	0	0.1	0	0.1	0	0.1	3	1
S 4925	Quicombo	Quicombo	63-2000	wet	1%	98%	1%	83.3	7.2	1.1	0.2	0.9	0.7	3.9	0.2	0.07	0.02	2.1	99.9	75	1	<1	103	1132	2	4	11	22	2	9	1	0.3	1	0.1	1	0.1	0	0.1	0	0.1	7	1
S 4927	Balombo	Canjala	63-2000	wet	0%	94%	5%	80.7	9.1	1.2	0.2	0.3	0.7	5.3	0.4	0.03	0.03	1.9	99.8	109	1	3	87	1329	3	4	12	27	3	9	1	0.3	1	0.2	1	0.2	1	0.1	1	0.1	9	2
BEACHES OF CENTRAL ANGOLA																																										
S 3765		Cabo Ledo	63-2000	wet	0%	100%	0%	76.9	5.7	2.4	0.6	6.0	0.8	2.2	0.5	0.18	0.05	4.3	99.8	42	0	<1	272	2811	8	12	15	34	4	15	3	0.6	2	0.3	2	0.4	1	0.2	1	0.2	13	2
S 4918		Port Amboim	63-2000	wet	0%	100%	0%	84.2	5.6	1.9	0.6	2.8	0.8	2.0	0.4	0.24	0.04	1.1	99.9	38	0	<1	192	658	7	11	17	39	5	18	3	0.8	3	0.4	2	0.4	1	0.2	1	0.2	11	2
S 4919		Sumbe	63-2000	wet	0%	100%	0%	84.3	6.3	1.5	0.3	1.9	0.8	3.1	0.3	0.12	0.03	1.2	99.8	62	0	<1	162	911	5	7	12	26	3	11	2	0.4	2	0.2	1	0.3	1	0.1	1	0.2	14	2
COPOROLO, CATUMBELA & LITTORAL CELLS																																										
S 4934		Lobito spit	63-2000	wet	0%	100%	0%	79.7	8.1	3.4	0.6	2.1	1.4	2.8	0.9	0.07	0.06	0.6	99.8	57	0	<1	243	870	10	14	35	74	8	30	5	0.8	4	0.5	3	0.5	2	0.2	2	0.3	15	2
S 4655	Catumbela	Praia Bebe	500-2000	dry	0%	30%	70%	80.5	6.7	5.2	0.7	1.8	1.2	2.1	1.0	0.05	0.06	0.5	99.8	42	0	1	179	771	7	6	12	22	3	10	2	0.5	2	0.2	1	0.3	1	0.1	1	0.1	3	1
S 4933	Catumbela	Catumbela	63-2000	wet	0%	98%	1%	87.2	6.1	0.9	0.2	0.7	0.8	2.7	0.2	0.03	0.02	1.2	99.9	56	1	<1	106	798	2	3	6	14	1	5	1	0.2	1	0.1	0	0.1	0	0.0	0	0.1	3	1
S 4932	Cavaco	Benguela	63-2000	wet	0%	90%	10%	82.3	9.3	0.7	0.1	1.2	1.7	3.4	0.1	0.04	0.01	0.9	99.8	63	0	<1	250	1159	1	3	10	18	2	6	1	0.5	1	0.1	0	0.1	0	0.0	0	0.1	2	0
S 4936	Coporolo	Dombe Grande	63-2000	wet	1%	99%	0%	82.5	8.8	0.8	0.1	0.8	1.2	4.0	0.2	0.02	0.02	1.4	99.9	87	1	<1	175	1059	2	4	8	17	2	6	1	0.2	1	0.2	1	0.2	0	0.1	0	0.1	3	1
RIVERS OF SOUTHERN ANGOLA																																										
S 4940	Cangala	Santa Maria	63-2000	wet	0%	100%	0%	79.0	11.1	1.0	0.2	1.4	2.4	3.7	0.2	0.04	0.02	0.7	99.9	74	1	<1	320	1168	3	6	16	27	3	11	2	0.5	1	0.2	1	0.2	1	0.1	1	0.1	3	1
S 4945	Inamangando	Inamangando	63-2000	wet	1%	96%	4%	79.6	10.2	1.4	0.3	1.9	2.0	3.0	0.2	0.06	0.02	1.2	99.8	59	1	<1	354	987	6	6	18	33	4	14	2	0.6	2	0.3	1	0.3	1	0.1	1	0.1	5	1
S 4947	Bentiaba	Bentiaba	63-2000	wet	0%	96%	3%	79.8	10.7	0.9	0.2	1.2	2.1	4.0	0.1	0.02	0.02	0.9	99.8	81	1	<1	278	1110	2	4	11	21	2	9	1	0.4	1	0.1	1	0.1	0	0.1	0	0.1	3	0
S 4951	Giraul	Giraul	63-2000	wet	1%	97%	2%	80.4	9.7	1.4	0.3	1.3	1.7	3.7	0.2	0.03	0.03	1.2	99.9	97	1	<1	255	878	3	6	14	25	3	12	2	0.5	2	0.2	1	0.2	1	0.1	1	0.1	11	1
S 4952	Bero	Namibe	63-2000	wet	0%	99%	1%	77.1	10.7	2.1	0.8	2.1	2.1	2.9	0.3	0.05	0.04	1.7	99.8	74	1	<1	320	916	5	8	15	25	3	12	2	0.7	2	0.3	1	0.4	1	0.1	1	0.1	3	1
BEACHES OF SOUTHERN ANGOLA																																										
S 4938		Equimina	63-2000	wet	0%	94%	5%	71.8	11.0	5.7	0.3	2.5	2.4	2.7	1.6	0.09	0.17	1.3	99.5	49	1	<1	358	906	7	29	66	140	16	61	9	1.2	7	0.9	5	1.2	3	0.5	4	0.6	31	4
S 4939		Baia Binga	63-2000	wet	0%	100%	0%	71.9	11.0	1.6	0.8	6.0	2.9	1.9	0.3	0.05	0.03	3.4	99.8	30	0	<1	449	703	8	15	17	42	6	26	5	1.0	4	0.6	3	0.7	2	0.2	1	0.2	3	1
S 4941		Lucira	63-2000	wet	0%	97%	3%	74.1	12.9	1.8	0.5	3.3	3.0	2.2	0.2	0.06	0.03	1.8	99.8	40	1	2	463	866	6	7	19	36	4	16	3	0.8	2	0.3	1	0.3	1	0.1	1	0.1	3	0
S 4943	*(low outer berm)*	Inamangando	63-2000	wet	0%	100%	0%	71.7	8.9	10.2	0.2	1.5	1.7	2.9	1.6	0.06	0.14	0.8	99.6	64	1	<1	279	904	6	36	123	253	29	100	15	1.2	11	1.3	7	1.3	4	0.5	3	0.5	48	3
S 4944	*(high inner berm)*	Inamangando	63-2000	wet	0%	99%	1%	78.2	10.1	2.0	0.3	2.0	1.9	3.4	0.3	0.04	0.04	1.5	99.8	70	1	<1	306	911	5	9	23	43	5	18	3	0.5	3	0.4	2	0.4	1	0.2	1	0.2	11	1
S 4948		Bentiaba	63-2000	wet	0%	100%	0%	80.6	9.3	1.5	0.3	1.9	1.8	2.8	0.3	0.03	0.03	1.3	99.9	59	1	2	322	845	4	7	15	29	4	12	2	0.5	2	0.2	1	0.3	1	0.1	1	0.1	5	0
S 4953		Namibe	63-2000	wet	0%	100%	0%	75.2	9.6	3.8	1.5	3.2	1.7	2.2	0.9	0.18	0.07	1.5	99.8	55	1	<1	351	657	11	14	17	36	5	19	3	1.0	3	0.5	3	0.6	2	0.2	2	0.2	4	1
CUNENE RIVER SYSTEM																																										
S 3931	Cunene	Ruacana	63-2000	dry	2%	98%	0%	89.1	4.7	0.7	0.2	0.6	0.4	2.7	0.2	0.02	0.01	n.d.	98.6	75	1	3	60	587	2	6	8	15	2	6	1	0.3	1	0.2	1	0.2	1	0.1	1	0.1	3	1
S 3934	Omuhongo	Oryeheke	63-2000	dry	0%	98%	2%	74.6	12.5	2.0	0.6	2.9	2.1	3.6	0.4	0.06	0.03	1.0	99.8	85	1	<1	237	1062	4	9	13	20	3	8	2	0.6	2	0.3	2	0.4	1	0.2	1	0.2	8	1
S 4775	Cunene	Epupa Falls	63-2000	wet	n.d.	n.d.	n.d.	75.8	11.6	2.6	0.8	2.9	2.0	2.4	0.7	0.05	0.04	1.1	99.9	54	1	<1	257	710	4	8	11	23	3	11	2	0.7	2	0.3	2	0.3	1	0.1	1	0.1	4	0
ORANGE LITTORAL CELL																																										
S 4955	Curoca	Curoca mouth	63-2000	wet	0%	100%	0%	79.5	6.5	4.0	1.0	3.1	1.2	1.3	1.0	0.78	0.13	1.4	99.8	40	1	<1	196	310	10	28	16	31	4	14	3	0.7	3	0.6	4	1.1	4	0.6	4	0.6	6	4
S 4774	Moçamedes dune	Tombua	63-2000	wet	0%	100%	0%	81.4	6.1	2.7	1.0	3.3	1.2	1.2	0.5	0.88	0.08	1.5	99.9	37	1	<1	188	222	7	22	15	30	3	13	3	0.6	3	0.5	3	0.7	2	0.4	3	0.4	4	4
S 4957	Moçamedes beach	Vanesa	63-2000	wet	0%	100%	0%	86.0	5.8	1.4	0.4	1.7	1.1	1.3	0.2	0.37	0.07	1.8	100.0	41	1	<1	129	285	4	14	8	17	2	7	2	0.4	2	0.4	2	0.6	2	0.3	2	0.3	2	2
S 4959	Moçamedes beach	Praia do Navio	63-2000	wet	0%	100%	0%	78.3	7.0	4.3	1.0	3.6	1.2	1.1	0.7	1.00	0.17	1.7	99.9	32	1	1	193	233	12	36	16	34	4	16	3	0.7	4	0.8	5	1.4	5	0.7	5	0.8	4	4
S 4960	Moçamedes dune	Praia do Navio	63-2000	wet	0%	100%	0%	48.5	11.0	24.9	2.3	4.0	0.7	0.6	5.1	0.85	0.98	0.5	99.4	17	1	5	183	122	56	159	40	86	10	38	8	1.1	10	2.8	23	6.2	23	3.7	28	4.4	22	8

Zr	Hf	V	Nb	Ta	Cr	Mo	W	Co	Ni	Ni	Cu	Ag	Au	Zn	Cd	Hg	Ga	Tl	Sn	Pb	As	Sb	Bi	Se	TOT/C	TOT/S	CIA	CIW	PIA	WIP	CIX	CIA/WIP	$\alpha^{Al}Mg$	$\alpha^{Al}Ca$	$\alpha^{Al}Na$	$\alpha^{Al}K$	$\alpha^{Al}Rb$	$\alpha^{Al}Sr$	$\alpha^{Al}Ba$	LaN/YbN	LaN/SmN	GdN/HoN	HoN/YbN	Eu/Eu*	Ce/Ce*	MREE/MREE*
						a.r.d.				a.r.d.	a.r.d.	a.r.d.	a.r.d.	a.r.d.	a.r.d.	a.r.d.		a.r.d.		a.r.d.	a.r.d.	a.r.d.	a.r.d.	a.r.d.																						
0.1	0.1	8	0.1	0.1	14	0.1	0.5	0.2	0.1	20	0.1	0.1	0.5	1	0.1	0.01	0.5	0.1	1	0.1	0.5	0.1	0.1	0.5	0.02	0.02																				
ppm	ppm	ppm	ppm	ppm	ppm	ppm	ppm	ppm	ppm	ppm	ppm	ppm	ppb	ppm	ppm	ppm	ppm	ppm	ppm	ppm	ppm	ppm	ppm	ppm	wt%	wt%																				
80	2	<8	3	0.2	< 14	0.7	2.0	0	<20	3	7	<0.1	<0.5	3	<0.1	<0.01	1	<0.1	<1	1	<0.5	<0.1	<0.1	<0.5	0.02	0.11	82	95	94	0.5	84	183	2.1	2.3	12.6	1.4	1.1	1.4	0.5	11.8	5.4	1.5	1.1	0.50	0.68	0.98
26	1	<8	2	<0.1	<14	0.1	1.2	0	<20	1	3	<0.1	<0.5	5	<0.1	<0.01	<0.5	<0.1	<1	1	1	<0.1	<0.1	<0.5	0.05	<0.02	n.d.	n.d.	n.d.	n.d.	n.d.	n.d.	3.7	0.6	n.d.	2.4	3.0	0.8	0.7	10.9	7.5	1.5	1.0	0.66	0.94	1.01
203	5	13	3	0.2	< 14	<0.1	<0.5	0	<20	1	1	<0.1	4	17	<0.1	<0.01	1	<0.1	<1	0	1	<0.1	<0.1	<0.5	<0.02	<0.02	91	97	97	0.2	86	423	1.3	2.2	4.0	3.4	2.7	1.9	1.1	1.3	3.1	0.6	0.6	0.61	0.87	0.66
70	2	9	2	0.1	< 14	<0.1	0.5	1	20	2	2	<0.1	<0.5	16	<0.1	<0.01	1	<0.1	<1	1	<0.5	<0.1	<0.1	<0.5	0.02	<0.02	63	78	71	1	72	54	1.0	1.4	3.9	0.7	0.7	1.1	0.3	6.8	3.7	1.6	0.7	0.52	0.97	0.95
42	1	<8	1	0.1	<14	<0.1	5.4	3	<20	1	4	<0.1	<0.5	11	<0.1	<0.01	1	<0.1	<1	1	<0.5	<0.1	<0.1	<0.5	0.05	<0.02	73	83	80	3	77	23.0	4.2	4.4	2.9	1.3	2.0	1.6	0.6	8.1	3.4	1.7	0.8	0.52	1.02	1.06
86	2	8	2	0.2	<14	0.2	<0.5	<0.2	<20	1	6	<0.1	<0.5	14	<0.1	<0.01	1	<0.1	<1	8	<0.5	<0.1	<0.1	<0.5	0.13	<0.02	90	92	92	1	94	147.4	5.6	4.6	12.8	7.3	6.9	4.3	2.8	5.2	4.2	1.7	0.5	0.69	1.01	0.86
439	10	21	10	0.6	<14	<0.1	0.6	1	<20	1	4	<0.1	<0.5	7	<0.1	<0.01	3	<0.1	<1	2	<0.5	<0.1	<0.1	<0.5	0.12	<0.02	62	69	65	11	74	5.9	3.2	1.6	2.2	1.3	2.7	1.0	0.6	5.1	3.8	0.9	0.8	0.73	0.96	0.96
35	1	8	2	0.1	<14	0.1	<0.5	1	<20	2	6	<0.1	<0.5	10	<0.1	<0.01	1	<0.1	<1	3	1	<0.1	<0.1	<0.5	0.07	<0.02	70	82	79	4	75	20	2.3	3.1	3.2	1.1	1.4	2.1	0.8	8.8	3.7	1.9	1.0	0.68	0.76	1.35
154	4	34	3	0.2	21	<0.1	<0.5	3	<20	2	6	<0.1	<0.5	10	<0.1	<0.01	7	<0.1	<1	3	<0.5	<0.1	<0.1	<0.5	0.05	<0.02	50	54	51	27	67	1.8	2.9	0.9	1.1	1.5	2.9	0.5	0.5	10.4	3.4	1.9	1.0	0.89	0.93	1.29
267	7	27	7	0.5	21	0.1	0.6	3	<20	4	147	<0.1	<0.5	2557	<0.1	<0.01	6	<0.1	<1	3	<0.5	<0.1	<0.1	<0.5	0.08	0.04	58	68	61	24	65	2.4	2.1	2.4	1.3	0.9	1.1	1.9	0.5	7.1	4.4	1.3	0.8	0.68	0.98	0.90
115	3	23	3	0.1	34	0.8	<0.5	1	<20	3	5	<0.1	<0.5	22	0.4	<0.01	3	<0.1	<1	3	1	0.2	<0.1	<0.5	0.57	<0.02	33	37	29	20	64	1.7	2.3	0.3	1.5	0.7	1.3	0.5	0.4	9.7	4.1	1.6	1.1	0.75	0.97	1.18
48	1	13	2	<0.1	<14	0.2	1.7	1	<20	1	2	<0.1	<0.5	6	<0.1	<0.01	1	<0.1	<1	1	3	<0.1	<0.1	<0.5	0.16	<0.02	42	46	41	7	72	6.4	2.7	0.4	1.8	1.2	2.3	0.5	0.4	9.3	4.4	1.6	1.2	0.68	1.00	1.15
174	4	22	4	0.3	<14	0.3	1.5	1	<20	1	1	<0.1	<0.5	7	0.3	<0.01	3	<0.1	<1	2	2	<0.1	<0.1	<0.5	0.27	<0.02	41	44	39	18	67	2.2	2.2	0.4	1.2	1.2	2.4	0.4	0.5	6.9	3.5	1.5	0.9	0.81	0.93	1.27
98	3	23	2	0.2	14	0.3	0.8	2	<20	2	1	<0.1	<0.5	7	0.5	<0.01	3	<0.1	<1	1	2	<0.1	<0.1	<0.5	0.43	<0.02	38	41	36	26	64	1.5	1.8	0.4	1.0	1.2	2.7	0.4	0.4	7.3	3.8	1.4	1.0	0.80	0.89	1.19
510	12	28	6	0.4	<14	<0.1	0.9	2	<20	1	1	<0.1	<0.5	3	<0.1	<0.01	5	<0.1	<1	1	1	<0.1	<0.1	<0.5	0.21	<0.02	44	47	43	24	67	1.8	2.5	0.6	1.1	1.3	2.9	0.4	0.4	6.7	3.5	1.5	0.9	0.77	0.99	1.06
167	4	19	5	0.3	<14	<0.1	<0.5	1	<20	1	1	<0.1	<0.5	4	<0.1	<0.01	3	<0.1	<1	1	1	<0.1	<0.1	<0.5	0.79	<0.02	32	34	30	26	69	1.2	1.9	0.3	1.4	1.2	2.8	0.3	0.4	3.9	3.0	1.1	0.9	0.88	0.95	1.08
40	1	8	2	0.1	< 14	0.8	1.3	0	<20	2	6	<0.1	1	4	<0.1	<0.01	3	<0.1	<1	3	1	<0.1	<0.1	<0.5	0.23	0.05	38	48	30	25	55	1.5	5.5	0.6	1.4	0.4	0.7	0.7	0.2	11.4	6.2	2.2	0.7	1.17	0.81	1.12
40	1	13	2	0.1	< 14	0.4	<0.5	1	<20	2	7	<0.1	1	4	<0.1	<0.01	6	<0.1	<1	2	2	<0.1	<0.1	<0.5	0.21	0.05	41	53	32	29	55	1.4	7.2	0.7	1.5	0.4	0.6	0.8	0.2	25.1	5.2	1.4	2.0	0.95	0.84	1.36
138	3	9	3	0.2	<14	0.2	<0.5	1	<20	1	4	<0.1	<0.5	27	<0.1	<0.01	2	<0.1	<1	8	1	<0.1	<0.1	<0.5	0.13	<0.02	54	69	57	10	66	5.3	4.0	1.3	2.9	0.6	0.9	1.3	0.3	6.1	4.1	1.6	0.6	0.46	0.98	0.88
423	10	14	4	0.3	<14	0.3	<0.5	1	<20	1	4	<0.1	<0.5	7	<0.1	<0.01	3	<0.1	2	3	1	0.2	<0.1	<0.5	0.49	<0.02	38	46	32	23	62	1.7	2.2	0.5	2.3	0.5	0.9	0.9	0.3	9.9	4.3	1.9	0.7	0.49	0.96	0.85
58	2	13	4	0.3	<14	0.1	<0.5	1	<20	1	3	<0.1	<0.5	9	<0.1	<0.01	5	<0.1	<1	4	1	<0.1	<0.1	<0.5	0.06	<0.02	55	77	63	37	59	1.5	9.0	4.0	2.1	0.4	0.6	1.5	0.3	12.8	5.0	1.6	0.9	0.95	1.09	0.95
150	4	21	17	0.6	<14	0.2	<0.5	1	<20	2	3	<0.1	<0.5	8	<0.1	<0.01	5	<0.1	<1	4	1	<0.1	<0.1	<0.5	0.18	<0.02	51	73	52	43	57	1.2	5.8	2.0	2.3	0.4	0.6	1.5	0.2	17.7	6.6	2.1	1.0	0.97	1.07	0.98
117	3	26	9	0.9	<14	0.1	0.9	3	<20	2	3	<0.1	<0.5	12	<0.1	<0.01	6	<0.1	<1	6	<0.5	<0.1	<0.1	<0.5	0.09	<0.02	55	84	67	52	57	1.1	8.7	6.8	3.1	0.3	0.5	2.3	0.3	13.6	5.3	1.8	0.9	0.62	1.08	0.88
528	13	50	37	1.3	55	0.6	0.9	3	<20	3	2	<0.1	<0.5	11	0.1	<0.01	5	<0.1	<1	2	4	0.1	<0.1	1	0.95	0.07	29	32	22	42	60	0.7	1.6	0.2	1.6	0.5	0.8	0.5	0.1	8.1	3.4	1.8	0.9	0.69	0.98	1.08
284	7	43	51	1.3	96	0.3	<0.5	3	<20	3	2	<0.1	<0.5	7	<0.1	<0.01	5	<0.1	<1	2	2	<0.1	<0.1	<0.5	0.22	<0.02	41	49	37	32	62	1.3	1.4	0.5	1.6	0.6	0.9	0.6	0.3	9.5	3.4	1.8	1.0	0.86	1.00	1.18
589	14	28	34	0.9	<14	0.2	0.7	2	<20	2	2	<0.1	<0.5	10	<0.1	<0.01	5	<0.1	<1	3	1	<0.1	<0.1	<0.5	0.22	<0.02	45	59	40	38	58	1.2	3.9	0.9	1.8	0.4	0.6	0.9	0.3	9.1	4.2	1.7	0.8	0.78	0.97	0.96
597	15	87	9	0.7	14	0.2	0.6	4	<20	3	3	<0.1	<0.5	9	<0.1	<0.01	8	<0.1	<1	3	2	<0.1	<0.1	<0.5	0.05	<0.02	47	58	46	43	61	1.1	2.2	1.0	1.4	0.6	0.9	0.7	0.4	14.7	4.6	2.1	0.9	0.57	0.99	0.90
90	3	162	5	0.4	75	0.7	<0.5	10	<20	8	10	<0.1	<0.5	11	<0.1	<0.01	9	<0.1	<1	3	<0.5	<0.1	<0.1	<0.5	<0.02	0.03	48	57	46	35	61	1.4	1.4	1.0	1.3	0.6	1.0	0.8	0.3	10.5	4.7	1.7	0.9	0.94	0.88	1.15
48	1	21	3	0.4	<14	<0.1	0.6	3	<20	2	4	<0.1	<0.5	6	<0.1	<0.01	5	<0.1	<1	3	1	<0.1	<0.1	<0.5	0.05	<0.02	54	72	57	32	59	1.7	4.0	2.3	1.9	0.5	0.7	1.3	0.3	12.6	4.3	1.7	1.0	0.89	1.07	1.09
61	1	15	2	<0.1	<14	<0.1	<0.5	1	<20	2	3	<0.1	<0.5	5	<0.1	<0.01	8	<0.1	<1	3	1	<0.1	<0.1	<0.5	0.05	<0.02	52	66	54	48	59	1.1	11.0	2.0	1.3	0.5	0.9	0.8	0.3	23.3	5.6	2.5	0.8	1.56	0.94	1.24
81	2	20	5	0.4	<14	0.1	8.5	1	<20	2	3	<0.1	<0.5	6	<0.1	<0.01	7	0.3	<1	3	1	<0.1	<0.1	<0.5	0.04	<0.02	53	72	56	48	58	1.1	10.3	2.8	1.7	0.4	0.6	1.1	0.3	13.4	4.1	1.6	1.2	0.67	1.07	1.12
126	3	19	13	0.8	<14	0.2	0.8	1	<20	2	2	<0.1	<0.5	6	<0.1	<0.01	10	<0.1	<1	3	<0.5	<0.1	<0.1	<0.5	0.05	<0.02	52	64	53	57	58	0.9	9.5	2.0	1.1	0.6	1.0	0.8	0.4	18.2	5.3	1.8	1.0	0.95	0.86	1.01
306	8	28	4	0.4	<14	<0.1	0.9	1	<20	2	3	<0.1	<0.5	8	<0.1	<0.01	10	<0.1	<1	3	<0.5	<0.1	<0.1	<0.5	0.06	<0.02	51	61	51	49	61	1.0	6.3	1.4	1.2	0.7	1.1	0.6	0.4	13.7	4.5	1.6	1.0	0.81	0.90	1.03
52	1	18	2	0.2	<14	<0.1	3.8	1	<20	1	3	<0.1	<0.5	7	<0.1	<0.01	9	<0.1	<1	3	<0.5	<0.1	<0.1	<0.5	0.05	<0.02	52	66	54	56	58	0.9	9.7	2.3	1.2	0.5	0.8	0.8	0.4	19.0	5.3	2.6	0.8	0.90	0.95	1.08
92	2	28	3	0.4	21	0.2	0.6	2	<20	3	5	<0.1	<0.5	6	<0.1	<0.01	8	<0.1	<1	4	<0.5	<0.1	<0.1	<0.5	0.03	<0.02	52	66	53	51	59	1.0	5.1	1.9	1.3	0.5	0.6	0.8	0.4	14.0	5.0	2.0	0.9	0.85	0.85	1.00
84	2	40	3	0.3	48	0.1	0.6	5	<20	8	7	<0.1	<0.5	11	<0.1	<0.01	9	<0.1	<1	3	1	<0.1	<0.1	<0.5	0.04	<0.02	51	60	52	51	62	1.0	2.1	1.3	1.2	0.8	0.9	0.7	0.4	10.6	4.5	1.5	1.1	1.08	0.83	1.31
2474	49	88	93	5.5	27	0.3	<0.5	3	<20	2	4	<0.1	<0.5	22	<0.1	<0.01	11	<0.1	2	5	<0.5	<0.1	<0.1	<0.5	0.07	<0.02	50	57	49	52	62	1.0	6.5	1.1	1.1	0.8	1.4	0.7	0.5	11.3	4.4	1.8	0.9	0.45	0.98	0.82
88	2	44	7	0.5	21	0.2	1.2	3	<20	2	3	<0.1	<0.5	6	<0.1	<0.01	10	<0.1	<1	2	1	<0.1	<0.1	<0.5	0.77	<0.02	38	41	37	60	62	0.6	2.2	0.5	0.9	1.2	2.3	0.5	0.6	9.2	2.0	1.7	1.5	0.65	0.96	1.41
71	2	35	3	0.2	14	0.2	<0.5	5	<20	4	5	<0.1	<0.5	12	<0.1	<0.01	13	<0.1	<1	5	1	<0.1	<0.1	<0.5	0.12	<0.02	50	54	49	55	64	0.9	4.3	1.0	1.0	1.2	2.1	0.6	0.6	23.7	4.3	2.1	1.5	1.06	0.90	1.34
685	16	171	33	2.0	68	0.1	1.1	4	<20	3	66	<0.1	<0.5	423	<0.1	<0.01	9	<0.1	2	5	1	<0.1	<0.1	<0.5	0.05	<0.02	51	63	52	44	60	1.2	7.2	1.5	1.3	0.6	0.9	0.7	0.4	25.3	5.0	2.4	1.1	0.28	0.98	0.76
168	5	39	6	0.4	14	0.1	7.4	2	<20	2	33	<0.1	<0.5	200	<0.1	<0.01	9	<0.1	<1	3	1	<0.1	<0.1	<0.5	0.11	<0.02	49	60	49	52	60	0.9	5.5	1.3	1.2	0.6	0.9	0.7	0.4	13.5	4.2	1.6	1.1	0.56	0.88	0.98
72	2	28	5	0.5	<14	0.1	1.0	2	<20	1	2	<0.1	1	5	<0.1	<0.01	9	<0.1	<1	3	<0.5	<0.1	<0.1	<0.5	0.08	<0.02	50	60	50	46	61	1.1	5.3	1.3	1.2	0.7	1.0	0.6	0.4	12.0	4.0	1.8	0.9	0.74	0.93	1.10
168	4	80	10	0.7	82	0.2	1.8	9	24	9	6	<0.1	<0.5	13	<0.1	<0.01	9	<0.1	1	4	2	<0.1	<0.1	<0.5	0.04	<0.02	48	54	47	46	65	1.0	1.0	0.8	1.3	0.9	1.1	0.6	0.6	6.9	3.0	1.7	1.0	0.88	0.91	1.39
71	2	21	6	0.4	41	<0.1	0.8	1	<20	2	2	<0.1	2	7	<0.1	<0.01	4	<0.1	<1	2	<0.5	<0.1	<0.1	<0.5	n.d.	n.d.	51	74	52	28	57	1.8	3.8	2.2	2.7	0.4	0.4	1.7	0.3	7.2	4.8	1.3	0.9	0.83	0.97	1.11
286	8	33	5	0.2	68	0.4	0.7	4	<20	8	7	<0.1	<0.5	9	<0.1	<0.01	11	0.1	<1	3	<0.5	<0.1	0.2	<0.5	0.05	0.08	50	59	50	59	63	0.9	3.2	1.1	1.4	0.7	0.9	1.2	0.5	8.7	4.6	1.3	1.1	1.08	0.80	1.17
106	3	51	6	0.4	41	<0.1	<0.5	6	<20	12	4	<0.1	<0.5	12	<0.1	<0.01	8	<0.1	<1	4	<0.5	<0.1	<0.1	<0.5	0.04	<0.02	51	58	52	48	66	1.1	2.2	1.0	1.4	1.0	1.4	1.0	0.6	8.8	3.5	1.5	1.1	1.12	0.95	1.33
785	19	83	11	0.8	89	0.2	2.5	7	<20	5	5	<0.1	2	12	<0.1	<0.01	7	<0.1	1	3	2	<0.1	<0.1	<0.5	0.13	<0.02	48	53	47	30	66	1.6	1.0	0.5	1.3	1.0	1.0	0.7	0.8	2.7	3.3	0.8	0.8	0.71	0.92	0.85
403	10	56	8	0.7	62	0.2	0.6	5	<20	7	7	<0.1	<0.5	11	<0.1	<0.01	6	<0.1	2	3	3	<0.1	<0.1	<0.5	0.17	0.03	46	51	45	29	66	1.6	0.9	0.5	1.2	1.1	1.0	0.7	1.1	3.9	3.4	1.1	0.8	0.69	0.99	0.99
55	2	22	6	0.6	21	0.2	<0.5	2	<20	3	4	<0.1	<0.5	6	<0.1	<0.01	5	<0.1	<1	2	3	<0.1	<0.1	<0.5	0.09	<0.02	52	60	53	25	64	2.1	2.3	0.9	1.3	0.9	0.9	1.0	0.8	2.5	3.4	0.8	0.8	0.73	0.95	0.91
265	7	70	8	0.6	62	0.4	<0.5	5	<20	5	6	<0.1	<0.5	11	<0.1	<0.01	7	<0.1	1	3	4	<0.1	<0.1	1	0.13	0.03	49	54	49	28	69	1.7	1.1	0.5	1.4	1.3	1.4	0.8	1.1	2.2	3.2	0.7	0.8	0.61	0.97	0.83
3106	77	380	56	5.9	281	0.7	2.6	27	26	12	10	<0.1	<0.5	29	0.1	<0.01	13	<0.1	9	5	3	0.1	0.1	<0.5	0.10	0.03	61	63	62	25	86	2.5	0.7	0.7	3.7	4.0	4.1	1.3	3.5	1.0	3.1	0.4	0.6	0.37	0.98	0.57

Appendix B

Click here to download Table: Appendix B Angola Zircon.xlsx

Sample S4899 | **Congo estuary @ Soyo** | 06°07'52" S | 12°22' 25" E | 96 grain analysed | 70 concordant ages

	concentrations			isotopic ratios						ages						discordance		preferred age	
grain	U [ppm]	Pb [ppm]	Th/U	Pb207/Pb206	2σ 76	Pb207/U235	2σ 75	Pb206/U238	2σ 68	age 206/238	2σ age 68	age 207/235	2σ age 75	age 207/206	2σ age 76	Δ 68-75 [%]	Δ 68-76 [%]	age	2σ age
X4899_G001	66.8	7.2	0.4933	0.06015	0.0026	0.83537	0.03496	0.10076	0.00256	618.9	15	616.6	23.2	609	93.4	0.4	1.6	618.9	15
X4899_G002	44.3	20.1	0.9887	0.12093	0.0036	6.03036	0.17956	0.3618	0.00868	1990.7	41	1980.2	33.4	1970	53	0.5	1.1	1970	53
X4899_G003	190.5	78.9	0.7495	0.12353	0.0033	5.9634	0.1596	0.35025	0.00786	1935.8	37.6	1970.5	30.4	2007.8	47.4	-1.8	-3.6	2007.8	47.4
X4899_G004	151.4	28.8	0.6165	0.07311	0.0022	1.71571	0.05118	0.17026	0.0039	1013.5	21.4	1014.4	24.2	1017	61	-0.1	-0.3	1013.5	21.4
X4899_G005	188.9	103.9	0.5412	0.23891	0.00608	16.31767	0.41926	0.49555	0.01096	2594.6	47.2	2895.6	32.2	3112.7	40.6	-10.4	-16.6		
X4899_G006	279	23.4	0.2793	0.05939	0.00184	0.68404	0.02094	0.08357	0.0019	517.4	11.4	529.2	15.8	581.4	67.2	-2.2	-11	517.4	11.4
X4899_G007				0.82317	0.0387	450.67239	48.01494	3.97218	0.4299										
X4899_G008	217.4	24.8	0.6058	0.06881	0.0021	0.97938	0.02936	0.10326	0.00234	633.5	13.6	693.3	19.2	893	63	-8.6	-29.1	633.5	13.6
X4899_G009	106.3	63	0.7073	0.17606	0.00468	11.93279	0.31998	0.49174	0.0112	2578.2	48.4	2599.1	32.8	2616.1	44.2	-0.8	-1.4	2616.1	44.2
X4899_G010	1148.8	102.1	0.8968	0.54374	0.01378	8.36508	0.2118	0.11162	0.00244	682.1	14.2	2271.4	30.4	4364.4	37.2	-70	-84.4		
X4899_G011	156.9	12.5	0.0071	0.05823	0.00204	0.69578	0.0238	0.08669	0.00204	535.9	12.2	536.3	17.6	538.4	76.6	-0.1	-0.5	535.9	12.2
X4899_G012	135.6	15.3	1.033	0.05771	0.00204	0.72619	0.02514	0.0913	0.00214	563.2	12.6	554.3	18.2	518.8	77.6	1.6	8.6	563.2	12.6
X4899_G013	131.6	72	1.3843	0.12932	0.00356	7.01963	0.19418	0.39383	0.00904	2140.6	41.8	2113.9	31.8	2088.7	48.4	1.3	2.5	2088.7	48.4
X4899_G014	94.8	9.5	0.6306	0.05868	0.00232	0.73287	0.02816	0.09061	0.00222	559.1	13.2	558.2	20	555.2	86.2	0.2	0.7	559.1	13.2
X4899_G015	16.6	8	0.7369	0.13699	0.00484	7.65947	0.27108	0.40566	0.01124	2195	51.6	2191.9	40.4	2189.5	61.4	0.1	0.3	2189.5	61.4
X4899_G016	79.4	8.8	0.4513	0.06046	0.00252	0.87318	0.03534	0.10478	0.00264	642.4	15.4	637.3	23	620.1	90	0.8	3.6	642.4	15.4
X4899_G017	43.1	4.6	0.3457	0.06011	0.00306	0.85741	0.0421	0.10349	0.00284	634.8	16.6	628.7	27.2	607.5	110	1	4.5	634.8	16.6
X4899_G018	260.8	139.5	0.6076	0.1814	0.00474	11.60226	0.3051	0.46404	0.01036	2457.4	45.6	2572.9	32.2	2665.7	43.2	-4.5	-7.8	2665.7	43.2
X4899_G019	273.1	154.9	0.801	0.1767	0.00452	11.35759	0.2925	0.46634	0.01022	2467.5	45	2552.9	31.4	2622.1	42.6	-3.3	-5.9	2622.1	42.6
X4899_G020	226.1	13.1	2.4728	0.3015	0.01016	1.66518	0.05134	0.04007	0.00106	253.3	6.6	995.4	27.2	3477.9	52.2	-74.6	-92.7		
X4899_G021	720.8	156.4	1.54	0.28769	0.0074	7.33331	0.18838	0.18494	0.00406	1093.9	22	2152.9	30.2	3405.2	40	-49.2	-67.9		
X4899_G022	307.9	37.2	0.1472	0.16054	0.00436	2.57032	0.06902	0.11616	0.0026	708.4	15	1292.2	25.8	2461.4	45.8	-45.2	-71.2		
X4899_G023	75.5	47.6	0.8969	0.18146	0.00488	12.51686	0.33934	0.50047	0.01146	2615.8	49.2	2644	33.2	2666.3	44.6	-1.1	-1.9	2666.3	44.6
X4899_G024	398.4	44.8	1.5353	0.05624	0.00172	0.62255	0.01888	0.08031	0.0018	498	10.8	491.4	14.8	461.9	67.8	1.3	7.8	498	10.8
X4899_G025	129.6	53.5	0.4224	0.13206	0.00362	6.8608	0.18856	0.37693	0.00858	2061.9	40.2	2093.6	31.6	2125.5	48	-1.5	-3	2125.5	48
X4899_G026	176.7	20.3	0.8925	0.06384	0.00214	0.84988	0.02788	0.09658	0.00224	594.3	13.2	624.6	19	736.3	71	-4.8	-19.3	594.3	13.2
X4899_G027	148.2	88.2	0.2682	0.26621	0.0069	21.10511	0.55156	0.57519	0.01282	2929.1	52.4	3143.4	33.2	3283.8	40.8	-6.8	-10.8	3283.8	40.8
X4899_G028	108.7	15.3	0.1153	0.0922	0.00298	1.85494	0.05886	0.14597	0.00346	878.3	19.4	1065.2	26.4	1471.5	61.4	-17.5	-40.3		
X4899_G029	214.6	46.6	0.3716	0.09458	0.00262	2.70771	0.0746	0.20771	0.00464	1216.6	24.8	1330.6	26.4	1519.7	52.2	-8.6	-19.9		
X4899_G030	55.7	14.7	0.7123	0.08946	0.00306	2.81427	0.09446	0.22823	0.00562	1325.2	29.4	1359.3	31.6	1414	65.4	-2.5	-6.3	1414	65.4
X4899_G031	241.1	22.4	0.1923	0.05673	0.00182	0.74133	0.02344	0.09481	0.00216	583.9	12.8	563.2	17	481.1	70.8	3.7	21.4	583.9	12.8
X4899_G032	895.9	167.1	0.4904	0.21105	0.00544	4.86304	0.12546	0.16717	0.00364	996.5	20.2	1795.9	28.4	2913.6	41.8	-44.5	-65.8		
X4899_G033	885.6	95.9	0.226	0.27058	0.0071	3.98233	0.10386	0.10678	0.00236	654	13.8	1630.6	27.8	3309.4	41.2	-59.9	-80.2		
X4899_G034	130	39.6	0.0233	0.1118	0.00306	4.86187	0.1331	0.3155	0.00708	1767.7	34.6	1795.7	29.8	1828.9	49.6	-1.6	-3.3	1828.9	49.6
X4899_G035	339.5	77.3	0.5411	0.07956	0.00218	2.26739	0.0618	0.20677	0.00458	1211.6	24.4	1202.2	24.8	1186.1	54.2	0.8	2.1	1186.1	54.2
X4899_G036	106.7	19.6	0.3745	0.0802	0.0025	1.92781	0.05908	0.1744	0.00404	1036.3	22.2	1090.8	26	1201.9	61.4	-5	-13.8	1036.3	22.2
X4899_G037	231.6	11.1	0.3655	0.04996	0.00194	0.32031	0.01214	0.04652	0.0011	293.1	6.8	282.1	11.2	193.1	90.2	3.9	51.8	293.1	6.8
X4899_G038	45.4	8.8	1.0742	0.07036	0.00286	1.49426	0.05894	0.15408	0.00396	923.8	22.2	928.1	29.2	938.9	83.4	-0.5	-1.6	923.8	22.2
X4899_G039	132	54.3	0.7044	0.12279	0.00334	5.95212	0.16168	0.35168	0.00788	1942.6	37.6	1968.9	30.6	1997.2	48.4	-1.3	-2.7	1997.2	48.4
X4899_G040	71.5	51.2	0.7458	0.19946	0.00536	15.51752	0.42008	0.56444	0.01286	2885	53	2847.6	33.6	2821.8	43.8	1.3	2.2	2821.8	43.8
X4899_G041	1026.7	74.8	0.7556	0.31737	0.00846	2.89234	0.07612	0.06612	0.00146	412.7	8.8	1379.9	26.2	3557.1	41	-70.1	-88.4		
X4899_G042	35.2	4.4	0.4933	0.06564	0.0032	1.06151	0.05	0.11732	0.00322	715.1	18.6	734.6	29.2	794.9	102.2	-2.6	-10	715.1	18.6
X4899_G043	90.9	55	1.1224	0.2685	0.00716	17.51734	0.469	0.47334	0.01072	2498.2	47	2963.6	33.6	3297.3	41.8	-15.7	-24.2		
X4899_G044				0.74766	0.0846				321.57934										
X4899_G045	30.8	21.7	0.9743	0.19701	0.00596	14.73197	0.45236	0.54251	0.0139	2793.9	58	2798.1	37.6	2801.6	49.4	-0.1	-0.3	2801.6	49.4
X4899_G046	70.3	12.5	0.5125	0.07391	0.0028	1.67535	0.06176	0.16446	0.0041	981.5	22.6	999.2	28.8	1039	76.4	-1.8	-5.5	981.5	22.6
X4899_G047	503.1	153	0.0293	0.11328	0.00302	4.91723	0.13084	0.31493	0.00692	1764.9	34	1805.2	29.2	1852.7	48.2	-2.2	-4.7	1852.7	48.2
X4899_G048	81	8.3	0.3744	0.05961	0.00274	0.81776	0.03644	0.09953	0.0026	611.7	15.2	606.8	24.2	589.4	99.6	0.8	3.8	611.7	15.2
X4899_G049	200.4	38.6	0.4363	0.09616	0.0028	2.36781	0.06824	0.17864	0.00406	1059.5	22.2	1232.9	26.4	1550.9	54.6	-14.1	-31.7	1059.5	22.2
X4899_G050	95.6	54	0.4761	0.16836	0.00468	11.45273	0.32008	0.49351	0.01142	2585.8	49.2	2560.7	33.8	2541.4	46.6	1	1.7	2541.4	46.6
X4899_G051	142.3	24.9	0.3189	0.07278	0.00232	1.71027	0.05354	0.1705	0.00396	1014.9	21.8	1012.4	25.2	1007.8	64.6	0.2	0.7	1014.9	21.8
X4899_G052	82.6	9.3	0.4314	0.06167	0.00266	0.90548	0.03786	0.10652	0.00272	652.5	15.8	654.7	24.2	662.7	92.4	-0.3	-1.5	652.5	15.8
X4899_G053	100.4	43	0.715	0.14454	0.00426	7.19678	0.21138	0.36122	0.00856	1988	40.6	2136.1	33.8	2282.3	50.8	-6.9	-12.9	2282.3	50.8
X4899_G054	66.8	8.8	0.81	0.06496	0.00312	1.00201	0.04662	0.1119	0.00304	683.8	17.6	704.8	28	773	101	-3	-11.5	683.8	17.6
X4899_G055	128	46.2	0.7034	0.1126	0.00332	4.81866	0.1408	0.31047	0.0072	1743	35.4	1788.2	31.6	1841.8	53.4	-2.5	-5.4	1841.8	53.4
X4899_G056	39.1	26.8	1.2681	0.18244	0.00554	12.62945	0.38666	0.50223	0.01264	2623.4	54.2	2652.4	37.2	2675.2	50.2	-1.1	-1.9	2675.2	50.2
X4899_G057	56.5	28.1	1.5875	0.11918	0.0037	5.7333	0.177	0.34901	0.00844	1929.9	40.4	1936.4	34	1944	55.6	-0.3	-0.7	1944	55.6
X4899_G058	103.9	16.8	0.531	0.09831	0.00324	1.99817	0.06416	0.14745	0.00352	886.7	19.8	1114.9	27.6	1592.3	61.6	-20.5	-44.3		
X4899_G059	20.6	4.5	0.6126	0.09568	0.0046	2.5785	0.11952	0.19552	0.00586	1151.2	31.6	1294.6	41.4	1541.5	90.4	-11.1	-25.3		
X4899_G060	132		1.7774	0.12632	0.00352	5.57696	0.15436	0.3203	0.0072	1791.2	35.2	1912.5	30.8	2047.4	49.2	-6.3	-12.5	2047.4	49.2
X4899_G061	21.7	9.2	0.7196	0.18168	0.00612	8.90974	0.29698	0.35578	0.00956	1962.1	45.4	2328.8	39.4	2668.3	55.8	-15.7	-26.5		
X4899_G062	143.9	56.8	0.542	0.11925	0.0033	5.76289	0.1584	0.3506	0.00784	1937.5	37.4	1940.9	30.8	1945	49.4	-0.2	-0.4	1945	49.4
X4899_G063	1834.1	187.4	0.5502	0.15154	0.00408	1.91999	0.05136	0.09192	0.00202	566.9	12	1088.1	23.2	2363.4	46	-47.9	-76		
X4899_G064	39.9	3.4	0.0344	0.06302	0.0033	0.7873	0.03974	0.09064	0.00254	559.3	15	589.6	26.6	708.9	111.4	-5.1	-21.1	559.3	15
X4899_G065	60.5	6	0.9035	0.05818	0.00326	0.65981	0.03562	0.08228	0.00236	509.7	14	514.5	25.4	536.5	122.6	-0.9	-5	509.7	14
X4899_G066	41.5	5.5	0.9814	0.06206	0.00302	0.91719	0.04314	0.10723	0.0029	656.6	16.8	660.9	27	676.2	104	-0.6	-2.9	656.6	16.8
X4899_G067	66.8	11.5	0.4921	0.07188	0.00272	1.57832	0.05824	0.15929	0.00396	952.8	22	961.7	28.2	982.5	77	-0.9	-3	952.8	22
X4899_G068	211.8	33.3	27.0992	0.56459	0.01568	12.64792	0.34352	0.16252	0.00376	970.8	20.8	2653.8	34	4419.4	40.6	-63.4	-78		
X4899_G069				0.19429	0.965	11.81268	56.03586	0.44109	1.09532										
X4899_G070				0.87093	0.05016			321.21115	371.21664										
X4899_G071	440.6	174.2	0.4713	0.12568	0.0034	6.19485	0.16634	0.3576	0.00786	1970.8	37.4	2003.7	30.4	2038.4	47.8	-1.6	-3.3	2038.4	47.8
X4899_G072	28.1	2.9	0.7729	0.05971	0.0045	0.74179	0.05366	0.09013	0.00306	556.3	18	563.4	35.8	593.1	163.4	-1.3	-6.2	556.3	18
X4899_G073	41.9	26	0.4696	0.1801	0.0052	13.14021	0.38082	0.52932	0.01256	2738.6	53	2689.8	35.2	2653.8	47.8	1.8	3.2	2653.8	47.8
X4899_G074	1067.4	382.9	0.0498	0.16724	0.00444	8.44591	0.22342	0.36638	0.00796	2012.3	37.6	2280.1	31.2	2530.2	44.6	-11.7	-20.5		
X4899_G075	77.1	12	0.3737	0.07072	0.0025	1.44298	0.04994	0.14802	0.00356	889.9	20	907	25.6	949.3	72.4	-1.9	-6.3	889.9	20
X4899_G076	239.1	19.6	0.4048	0.05627	0.00186	0.61139	0.01978	0.07883	0.0018	489.1	10.8	484.4	15.4	463	73.2	1	5.6	489.1	10.8
X4899_G077	37.9	4	0.2478	0.05958	0.00296	0.86805	0.04164	0.10571	0.00288	647.8	16.8	634.5	26.8	588.4	107.8	2.1	10.1	647.8	16.8
X4899_G078	101.2	18.5	0.5973	0.07096	0.0023	1.61293	0.0512	0.1649	0.00382	984	21.2	975.2	25	956.3	66.2	0.9	2.9	984	21.2
X4899_G079	44.7	18.5	0.5774	0.12577	0.00392	6.31534	0.19522	0.36428	0.0088	2002.4	41.6	2020.6	34.6	2039.7	55.2	-0.9	-1.8	2039.7	55.2
X4899_G080	51.8	4.2	0.0053	0.05838	0.00282	0.7168	0.03344	0.08908	0.00238	550.1	14	548.8	23.4	544.1	105.6	0.2	1.1	550.1	14
X4899_G081				0.14154	0.38658	49.26075	146.36184	2.52488	4.0963										
X4899_G082	27.7	12	0.8084	0.11766	0.00388	5.80246	0.18968	0.35778	0.00894	1971.6	42.4	1946.8	35.8	1921	59.2	1.3	2.6	1921	59.2
X4899_G083	238.3	25.1	0.1702	0.06099	0.00192	0.90956	0.02808	0.1082	0.00246	662.3	14.4	656.8	18.8	638.9	67.8	0.8	3.7	662.3	14.4
X4899_G084	164	13.8	0.2936	0.0567	0.00214	0.65061	0.0238	0.08325	0.00198	515.5	11.8	508.9	17.8	479.9	83.4	1.3	7.4	515.5	11.8
X4899_G085	363.2	32.6	0.5544	0.05909	0.00186	0.67277	0.0208	0.0826	0.00186	511.6	11	522.4	15.8	570.4	68.4	-2.1	-10.3	511.6	11
X4899_G086	295.6	49.5	0.0685	0.08055	0.00234	1.94045	0.05566	0.17476	0.0039	1038.3	21.4	1095.2	24.6	1210.5	57.2	-5.2	-14.2	1038.3	21.4
X4899_G087	846.5	196.5	0.2173	0.12477	0.00342	4.08287	0.11122	0.2374	0.00522	1373.2	27.2	1650.9	28.6	2025.5	48.6	-16.8	-32.2		
X4899_G088	228	93.4	0.6293	0.12067	0.00334	5.9031	0.16216	0.35491	0.00786	1958	37.4	1961.7	30.8	1966.2	49.4	-0.2	-0.4	1966.2	49.4
X4899_G089	24.9	4.3	0.4423	0.07072	0.00352	1.59921	0.07706	0.16406	0.00468	979.3	26	969.9	35.8	949.3	101.8	1	3.2	979.3	26
X4899_G090	82.6	8.9	0.2661	0.06241	0.00252	0.92123	0.03604	0.10709	0.00266	655.8	15.4	663	23	688.2	86.2	-1.1	-4.7	655.8	15.4
X4899_G091	130.8	33.3	0.4961	0.12681	0.00374	4.17498	0.12138	0.23884	0.00548	1380.7	28.6	1669.1	30.6	2054.2	52	-17.3	-32.8		
X4899_G092	150.2	56.1	0.5291	0.11758	0.00334	5.42337	0.15266	0.33461	0.00752	1860.7	36.4	1888.6	31	1919.8	51	-1.5	-3.1	1919.8	51
X4899_G093	410.6	37.4	0.3733	0.07436	0.0023	0.92081	0.02788	0.08983	0.00204	554.5	12	662.8	18.6	1051.3	62.4	-16.3	-47.3		
X4899_G094	73.5	6.5	0.3559	0.05681	0.00246	0.67311	0.02824	0.08596	0.00216	531.6	12.8	522.6	20.4	484.2	95.6	1.7	9.8	531.6	12.8
X4899_G095	122.1	23.3	0.6777	0.08616	0.00268	1.98242	0.06042	0.16693	0.00384	995.2	21.2	1109.5	26.2	1341.8	60	-10.3	-25.8	995.2	21.2
X4899_G096	33.2	6.9	0.444	0.08644	0.00354	2.30326	0.09176	0.19332	0.00516	1139.3	27.8	1213.3	34.6	1348	79	-6.1	-15.5		